NASA/CR-1999-209522

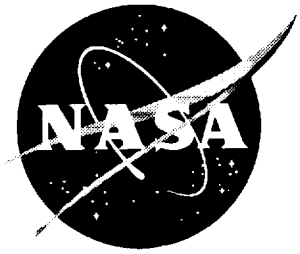

Investigation of Inner Loop Flight Control Strategies for High-Speed Research

Brett Newman and Ayman Kassem
Old Dominion University, Norfolk, Virginia

December 1999

The NASA STI Program Office . . . in Profile

Since its founding, NASA has been dedicated to the advancement of aeronautics and space science. The NASA Scientific and Technical Information (STI) Program Office plays a key part in helping NASA maintain this important role.

The NASA STI Program Office is operated by Langley Research Center, the lead center for NASA's scientific and technical information. The NASA STI Program Office provides access to the NASA STI Database, the largest collection of aeronautical and space science STI in the world. The Program Office is also NASA's institutional mechanism for disseminating the results of its research and development activities. These results are published by NASA in the NASA STI Report Series, which includes the following report types:

- TECHNICAL PUBLICATION. Reports of completed research or a major significant phase of research that present the results of NASA programs and include extensive data or theoretical analysis. Includes compilations of significant scientific and technical data and information deemed to be of continuing reference value. NASA counterpart of peer-reviewed formal professional papers, but having less stringent limitations on manuscript length and extent of graphic presentations.

- TECHNICAL MEMORANDUM. Scientific and technical findings that are preliminary or of specialized interest, e.g., quick release reports, working papers, and bibliographies that contain minimal annotation. Does not contain extensive analysis.

- CONTRACTOR REPORT. Scientific and technical findings by NASA-sponsored contractors and grantees.

- CONFERENCE PUBLICATION. Collected papers from scientific and technical conferences, symposia, seminars, or other meetings sponsored or co-sponsored by NASA.

- SPECIAL PUBLICATION. Scientific, technical, or historical information from NASA programs, projects, and missions, often concerned with subjects having substantial public interest.

- TECHNICAL TRANSLATION. English-language translations of foreign scientific and technical material pertinent to NASA's mission.

Specialized services that complement the STI Program Office's diverse offerings include creating custom thesauri, building customized databases, organizing and publishing research results . . . even providing videos.

For more information about the NASA STI Program Office, see the following:

- Access the NASA STI Program Home Page at ***http://www.sti.nasa.gov***

- Email your question via the Internet to help@sti.nasa.gov

- Fax your question to the NASA STI Help Desk at (301) 621-0134

- Telephone the NASA STI Help Desk at (301) 621-0390

- Write to:
  NASA STI Help Desk
  NASA Center for AeroSpace Information
  7121 Standard Drive
  Hanover, MD 21076-1320

NASA/CR-1999-209522

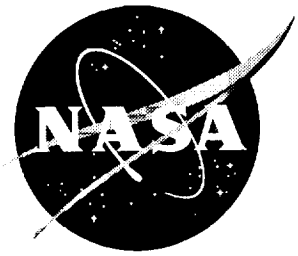

Investigation of Inner Loop Flight Control Strategies for High-Speed Research

Brett Newman and Ayman Kassem
Old Dominion University, Norfolk, Virginia

National Aeronautics and
Space Administration

Langley Research Center
Hampton, Virginia 23681-2199

Prepared for Langley Research Center
under Contract NAS1-19858

December 1999

Available from:

NASA Center for AeroSpace Information (CASI)
7121 Standard Drive
Hanover, MD 21076-1320
(301) 621-0390

National Technical Information Service (NTIS)
5285 Port Royal Road
Springfield, VA 22161-2171
(703) 605-6000

Table of Contents

List of Figures

List of Figures Continued

List of Figures Continued

List of Figures Continued

List of Tables

Section I
Introduction

This report describes the activities and findings conducted under contract NAS-19858-71 with NASA Langley Research Center. Subject matter is the investigation of suitable flight control design methodologies and solutions for large, flexible high-speed vehicles. Specifically, methodologies are to address the inner control loops used for stabilization and augmentation of a highly coupled airframe system possibly involving rigid-body motion, structural vibrations, unsteady aerodynamics, and actuator dynamics. The flight control strategies must address basic specifications/requirements,[1,2] or clearly display the design tradeoffs to the flight control engineer. Techniques considered in this body of work are primarily conventional-based[3] for two reasons. First, conventional-based schemes facilitate an understanding into the "physics" which leads to simple yet effective solutions that go a long way in implementation of a multiply redundant architecture requiring scheduling with flight condition and modification during test and development. Secondly, wisdom advises an assessment of the capabilities of less sophisticated, but highly successful techniques when tackling a new challenge (large flexible high-speed vehicles), before transitioning to more advanced design strategies.

The vehicle of interest is the High-Speed Civil Transport (HSCT).[4,5] This vehicle is projected to have a pitch divergence due to the relaxation of static stability at subsonic speeds. Further, significant interaction between rigid-body and aeroelastic degrees of freedom is expected. Characteristics of this sort will, by necessity, require a set of initial feedback loops to correct for these deficiencies and bring the closed-loop vehicle system back to a level which is acceptable to the pilot and passengers. Functions of this inner loop flight control system (FCS) for HSCT will be to 1) artificially supply the stability inherently lacking in the airframe, 2) augment the key pilot/passenger centered responses to obtain crisp, well damped behavior, and 3) suppress

aeroelastic motions in all responses, all with minimal FCS architecture. The objectives of the contract work are to explore the possibilities for such an inner loop FCS.

This work is heavily dependent upon the timely generation, by external sources, of representative airframe math models with the requisite fidelity. Section II presents several numerical models made available to the contractor, as well as an applicable model available in the literature archive.[6-8] The contracting agency supplied models originated from two independent sources, Boeing and Langley. The Boeing models are generated with internal code, whereas the Langley models are derived with the package Integrated Structures Aerodynamics and Controls (ISAC).[9] Comparisons of two similar models from the independent sources revealed significant discrepancies and concerns. Further, additional studies with one of these models conducted by other researchers have reported atypical features. At this time, the use of any and all aeroelastic airframe dynamic models should be treated with caution. In spite of this hurdle, one model was deemed sufficiently accurately for FCS studies.

The contract Statement of Work (see Appendix A) consisted of three distinct tasks contributing to the overall objective. These tasks include

1. Application of previous design milestones to HSCT,
2. Expanded consideration of Multi-Sensor/Single-Surface design strategies, and
3. Multi-Sensor/Multi-Surface design strategies.

These tasks are briefly outlined here before moving on to the dedicated chapters with detailed reporting of the activities.

Analysis/Synthesis of a conventional Single-Sensor/Single-Surface (SS/SS) FCS, using a vehicle model (SCRA[8]) which accurately represents the features of current HSCT configurations under study, indicates multiple conflicting constraints that can not be overcome with this architecture.[10] Studies of a Multi-Sensor/Single-Surface (MS/SS) arrangement shows improved potential for success, but still with undesirable features. Section III describes the first task of exercising these milestones on current aeroelastic models (Ref. H) of the HSCT for assessment of the baseline configuration. The previous SS/SS and MS/SS milestones have exploited

characteristics specific to the design model such as modal frequency distribution and modal input-output participation. These FCS have been adjusted and re-tuned for Ref. H specific data. Results indicate the control system design issues are strikingly similar to the previous investigations. Aeroelastic dynamics heavily influence the inner loop design and rate gyro placement is critical. Gain stabilization employing a single rate gyro does not appear feasible.

The second task reported on in Section IV is a more in-depth investigation of the MS/SS or blended sensor architecture. Rate gyro placement within a highly elastic vehicle directly influences the aeroelastic behavior and aeroelastic-rigid-body coupling in transfer functions involving that angular rate. Therefore, the capability, or lack thereof, to augment the vehicle rigid-body/aeroelastic dynamics is highly dependent upon sensor mounting location.[10,11] Seldom can multiple desirable features be obtained with a single sensor in a highly elastic vehicle. Blending of several sensors allows more design freedom to shape the composite feedback signal for effective control. Formal optimization search algorithms have been employed to assist the multiple sensor placement challenge. Formulation of cost functionals which capture the key desirable/undesirable FCS characteristics associated with fore and aft center line candidate sensor locations have been considered. The technique has demonstrated potential by converging to the "manually optimized" solution, as well as offering improvement beyond this manual design. Even still, several objectionable features persist and are shown to be inherent with the low pass/band pass implementation. Consideration of lag-lead and lead-lag filters for blending circumvents this problem.

Closed-loop systems with MS/SS architectures, although showing promise, also indicate drawbacks. Primarily, their inability to provide acceptable motions at the cockpit station. Section V describes this limitation as part of the third task which is to explore the advantages of using a Multi-Sensor/Multi-Surface (MS/MS) architecture for the inner loop FCS. The addition of a secondary but fully independent channel dedicated to aeroelastic suppression, which operates in harmony with the primary channel dedicated to rigid-body control, offers enormous potential for exploitation.[8] Studies have concentrated on existing surfaces already present in the Ref. H math

models, such as wing trailing edge devices. However, preliminary results indicate the trailing edge surfaces, coupled with the elevator, are not appropriate for the aeroelastic suppression function.

Section II
Aeroelastic Vehicle Modeling Issues

A. Model Description

Modeling of highly integrated HSCT class vehicles requires the flight dynamics engineer to return to the governing fundamental principles of rigid-body motion, structural vibrations, unsteady aerodynamics, etc. Revisiting these principles allows the relevant features to enter the early stages of the modeling process. The resulting models accurately capture the contributions from each discipline to the overall dynamic behavior, as well as the interaction between the disciplines. Refs. 12-15 describe such a process leading to nonlinear models, from which linear models can be extracted for use in control system design.

The linear models are represented in state space form as

$$\begin{aligned} \dot{x} &= Ax + Bu + B'\dot{u} + B''\ddot{u} \\ y &= Cx \end{aligned} \tag{1.1}$$

In general, the state vector x consists of the rigid-body positions and velocities, generalized coordinates originating from the structural vibrations, and variables representing the unsteady aerodynamic degrees of freedom. Focusing on the longitudinal dynamics leads to

$$x = \left[u \; w \; q \; \theta \; \ldots \dot{\eta}_i \ldots \; \ldots \eta_i \ldots \; \ldots z_i \ldots \right]^T \tag{1.2}$$

- u - forward speed
- w - downward speed
- q - pitch rate
- θ - pitch angle
- η_i - generalized coordinate for i^{th} aeroelastic mode
- z_i - i^{th} unsteady aerodynamic state

Control inputs are denoted by u where

$$u = \left[\delta_E \; \ldots \delta_{TEi} \ldots \right]^T \tag{1.3}$$

- δ_E - elevator deflection
- δ_{TEi} - i^{th} wing trailing edge symmetric deflection (TE1 is inboard most, TE4 is outboard most)

Finally, responses of interest y include measured pitch rates throughout the vehicle,

$$y = \left[\ldots q_{xs} \ldots \right]^T \tag{1.4}$$

q_{xs} - pitch rate at structural body location x_s

If unsteady aerodynamics are modeled, then surface deflection rates and accelerations become inputs leading to matrices B' and B" as indicated in Eq. (1.1). To circumvent this noncausal behavior, and to model the actuation hardware dynamics, 3rd order actuator models are considered as a "front end" to the airframe model. Fig. 1 illustrates this feature with the elevator surface actuator. From Fig. 1, the elevator actuator model is

$$\delta_E(s) = \frac{p}{s+p} \frac{\omega^2}{s^2+2\zeta\omega s+\omega^2} \delta_{E\,c}(s) \tag{1.5}$$

$$\begin{bmatrix} \dot{\delta}_E \\ \ddot{\delta}_E \\ \dddot{\delta}_E \end{bmatrix} = \begin{bmatrix} 0 & 1 & 0 \\ 0 & 0 & 1 \\ -p\omega^2 & -(p2\zeta\omega+\omega^2) & -(p+2\zeta\omega) \end{bmatrix} \begin{bmatrix} \delta_E \\ \dot{\delta}_E \\ \ddot{\delta}_E \end{bmatrix} + \begin{bmatrix} 0 \\ 0 \\ p\omega^2 \end{bmatrix} \delta_{E\,c}$$

$$\begin{bmatrix} \delta_E \\ \dot{\delta}_E \\ \ddot{\delta}_E \end{bmatrix} = \begin{bmatrix} 1\,0\,0 \\ 0\,1\,0 \\ 0\,0\,1 \end{bmatrix} \begin{bmatrix} \delta_E \\ \dot{\delta}_E \\ \ddot{\delta}_E \end{bmatrix}$$

Note G(s) represents the airframe transfer function matrix. Generalizing for all actuator hardware,

$$\begin{aligned} \dot{x}_a &= A_a x_a + B_a u_c \\ \begin{bmatrix} u \\ \dot{u} \\ \ddot{u} \end{bmatrix} &= \begin{bmatrix} C_a \\ C_a' \\ C_a'' \end{bmatrix} x_a \end{aligned} \tag{1.6}$$

which leads to the overall airframe-actuator model

$$\begin{aligned} \begin{bmatrix} \dot{x} \\ \dot{x}_a \end{bmatrix} &= \begin{bmatrix} A & \hat{A} \\ 0 & A_a \end{bmatrix} \begin{bmatrix} x \\ x_a \end{bmatrix} + \begin{bmatrix} 0 \\ B_a \end{bmatrix} u_c \\ y &= \begin{bmatrix} C\ 0 \end{bmatrix} \begin{bmatrix} x \\ x_a \end{bmatrix} \end{aligned} \tag{1.7}$$

$$\hat{A} = BC_a + B'C_a' + B''C_a''$$

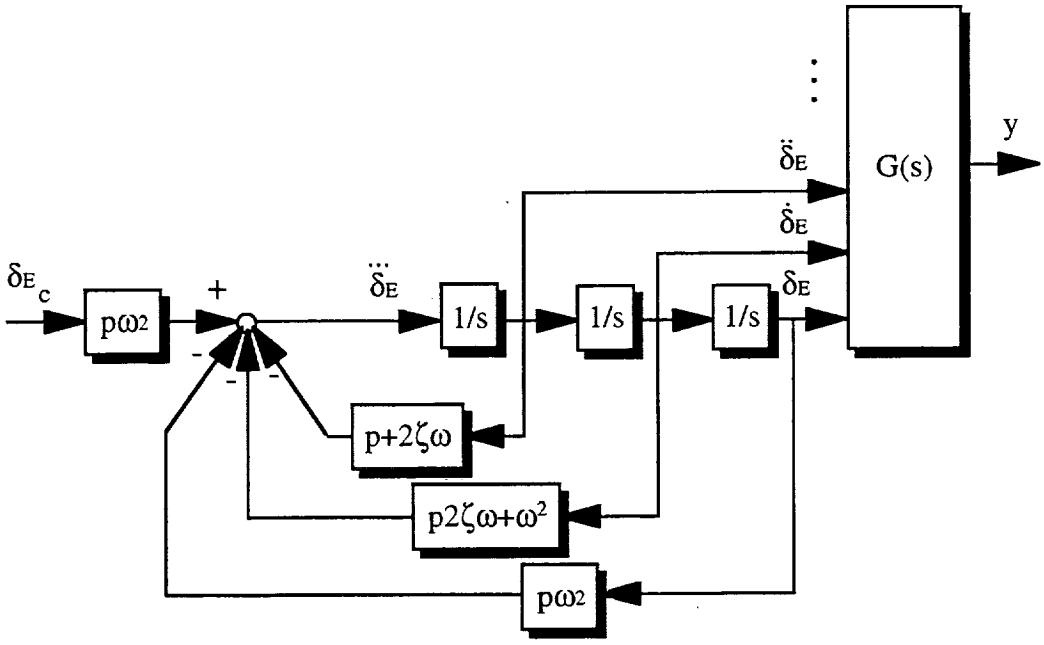

Figure 1. Overall Airframe-Actuator Model

Several numerical models of the type discussed here were made available by Boeing and Langley for the Ref. H HSCT.[6,7] The baseline configuration is shown in Fig. 2. The vehicle consists of a long slender fuselage with a highly swept cranked delta wing and conventional aft tail. In addition to this, a numerical model for the Supersonic Cruise Aircraft (SCRA) is available.[8] This configuration is shown in Fig. 3 and is quite similar to the Ref. H HSCT geometry making it applicable for inner loop flight control studies of HSCT class vehicles.

Appendix B describes one of the Boeing numerical models. Internal code at Boeing was used for development. This model contains the full set of rigid-body states, as well as 15 aeroelastic modes. However, the unsteady aerodynamic expansion included only the quadratic terms in s leading to no explicit unsteady aerodynamic states. The original model lacked representation of the actuator hardware as in Eq. (1.1). However, actuator models consistent with the Langley models were incorporated. The Appendix B model corresponds to the following flight condition.

Source: Boeing (Appendix B)		
Trim Condition: Wings-Level, Level, Rectilinear Flight, Initial Cruise Phase		
M = 0.95	h = 30,000 ft	W = 614,864 lbf (M1N)

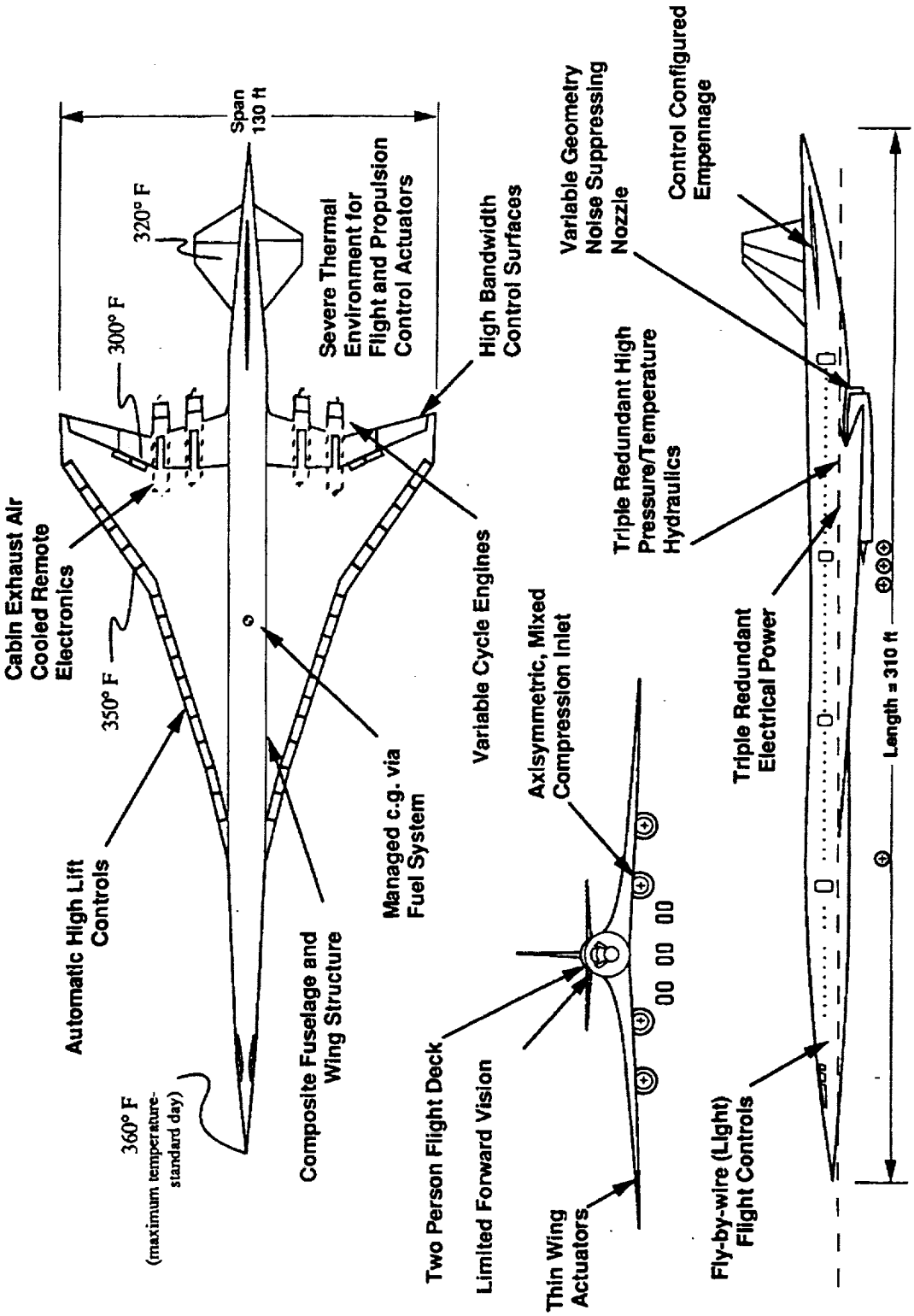

Figure 2. Ref. H HSCT Configuration

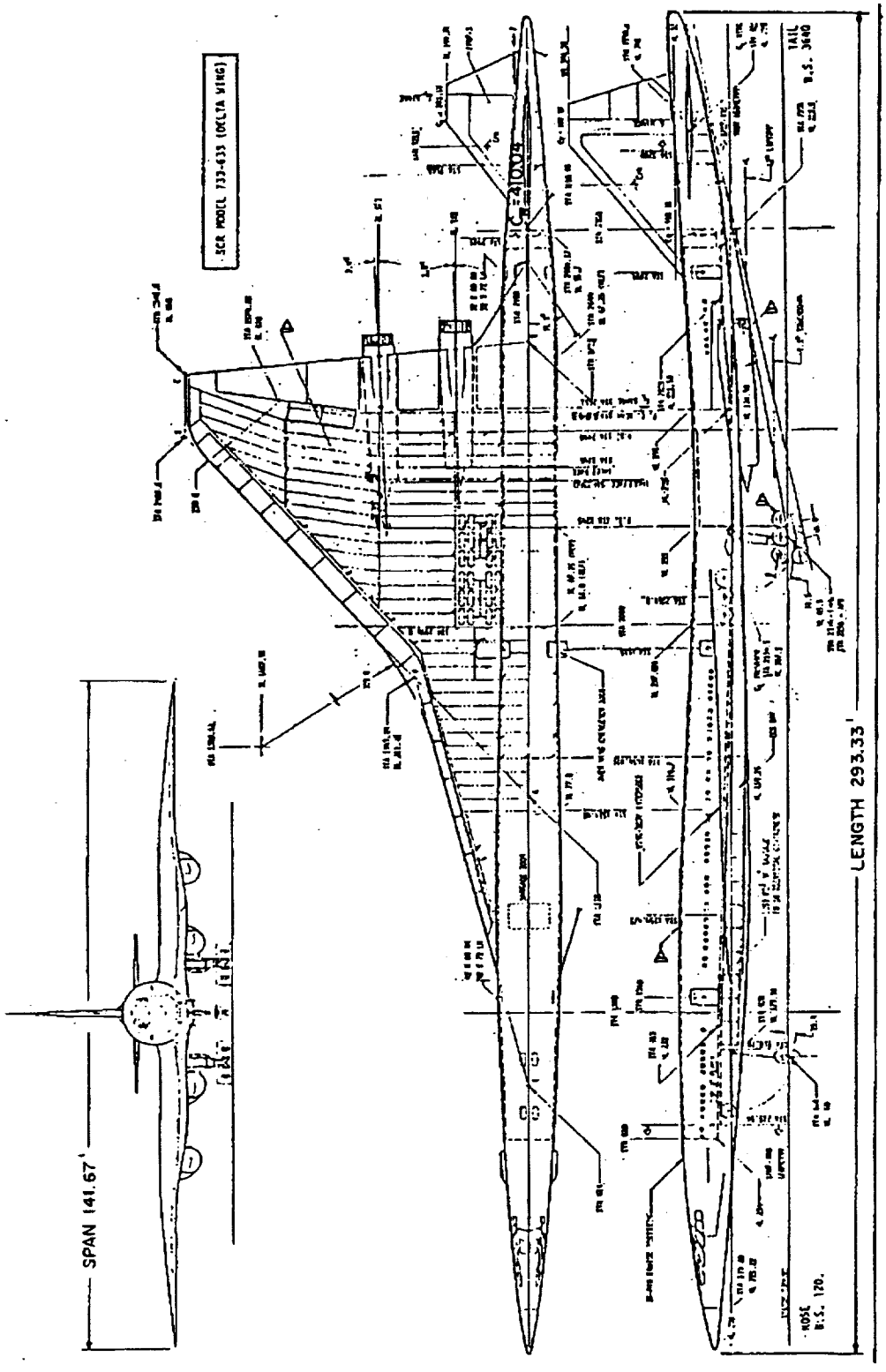

Figure 3. SCRA Configuration

Appendix C and D describe two Langley models generated with the Integrated Structures Aerodynamics and Controls (ISAC) package.[9] The original models lacked the rigid-body forward speed degree of freedom (i.e., essentially a short period approximation). However, the Appendix D model has been altered from the original. This model is an aggregate model using the forward speed degree of freedom stability and control derivatives from the Ref. H Cycle 1 Simulation[16] to augment the ISAC output. This procedure is discussed further in Section II-C. The Appendix C model was not altered in this way. Both models include 17 aeroelastic modes and 10 unsteady aerodynamic states. Also, the models were supplied as overall airframe-actuator packages. The relevant data is listed below.

Source:	Langley (Appendix C)	
Trim Condition:	Wings-Level, Level, Rectilinear Flight, Ascent Phase	
M = 0.88	h = 20,000 ft	W = 646,458 lbf (M5)

Source:	Langley (Appendix D)	
Trim Condition:	Wings-Level, Level, Rectilinear Flight, Final Cruise Phase	
M = 0.24	h = 0 ft	W = 384,862 (M3A)

One additional numerical model is given in Ref. 10, corresponding to the SCRA configuration. This model contains the full set of rigid-body states, along with 18 aeroelastic modes. No explicit unsteady aerodynamic states are present in the model. The model is a modified version of that found in Ref. 8. First, the raw model was awkward in that coupling existed at the $\dot{u}/\dot{w}/\dot{q}/\ddot{\eta}_i/\delta_E$ level. Elimination of this coupling by algebraic manipulation of the governing equations was implemented. Secondly, Ref. 8 indicated a discrepancy in the imbedded actuator model. To eliminate questions of validity, supplied actuator dynamics were residualized out of the model. Finally, the stability derivative M_w was adjusted to bring the static margin from 7.3% stable to 10% unstable. With the above qualifiers, the model represents the bare airframe, as in Eq. (1.1). The SCRA model corresponds to the following flight condition.

Source:	NASA-CR-172201 (Ref. 10)	
Trim Condition:	Wings-Level, Level, Rectilinear Flight, Ascent Phase	
M = 0.6	h = 6,500 ft	W = 730,000 lbf

B. Boeing/Langley Model Comparison

Modeling a highly elastic vehicle with unsteady air flow is a difficult task, and the current procedures for this are lacking in some respect. As wisdom should have it, initial analysis should compare/contrast similar models from independent sources to assess if they are in rough agreement, thereby invoking confidence in predictions of vehicle motions. On the other hand, if considerable differences do exist, the implication is to use caution when relying upon the model. Models in Appendix B and C are examined in this way. Although dissimilar flight conditions exist between these two models, the environment during the early stages of the contract did not allow comparison of identical flight conditions. Regardless, the trim conditions are considered to be close enough for first order assessment.

Table 1 lists the poles of the Boeing airframe-actuator model. At this high-speed, high-altitude condition, the HSCT inherent pitch instability has nearly disappeared as the aerodynamic center has shifted aft. Rigid-body modes consist of a faster, stable oscillatory mode and two extremely slow exponential modes, one stable, the other unstable. This distribution of poles is somewhat peculiar in that the real stable mode is not deeper into the left-half plane, so that as the aerodynamic center moves aft and the real unstable mode moves to the left and pairs off with this pole to form the short period mode, the frequency of oscillation is conventional (i.e., around 1 rad/s). Perhaps this change has already occurred and the distribution represents a conventional short period mode with a long period mode that has degenerated into a tuck instability. Examination of the M_u stability derivative and the eigenvectors supports this possibility. Aeroelastic mode frequencies include the 1st and 2nd mode values at 7.0 and 12.8 rad/s all the way up to a value of 43.7 rad/s for the 15th mode. Damping ratios for these aeroelastic modes are extremely light (i.e., on the order of 0.1 or sometimes considerably less), as expected.

Tables 2-6 contain the gain and zeros for measured pitch rate to elevator transfer functions at 5 locations along the fuselage centerline. Each set of factored numerators contain the rigid-body zeros $1/\tau_{\theta_1}$ and $1/\tau_{\theta_2}$, and a pair of zeros for every aeroelastic mode. The overriding feature that is apparent from these Tables relative to Table 1 is the "tight" aeroelastic dipoles (i.e., zero/pole

separation is small) for aft sensor locations (2,115 in, 2,525 in, and 3,157 in). At forward locations, the dipole structures degrade relative to the aft locations. This feature is more easily recognized graphically. Figs. 4-8 show the pole/zero distributions in the complex plane, while Figs. 9-13 display the corresponding frequency responses. Note in Fig. 6 how all aeroelastic zeros are virtually on top of the corresponding poles. In Fig. 11, this feature can be seen as a relatively smooth -20 db/dec magnitude plot in the 10-100 rad/s frequency range.

Transitioning to the Langley model, Tab. 7 lists the airframe-actuator poles. From Tab. 7, note the rigid-body modes consist of a stable oscillatory mode and one real neutrally stable mode. Recall this model does not have the forward speed degree of freedom, hence the pole at the origin. Since a strong oscillatory mode still exists after the "short period approximation" via ISAC, one can conclude that this mode is indeed the conventional short period, not the so-called 3rd oscillatory mode associated with relaxed static margins. The HSCT relaxed static stability feature is not present at this flight condition. Aeroelastic mode frequencies include the 1st and 2nd mode values at 7.7 and 15.6 rad/s all the way up to a value of 63.1 rad/s for the 17th mode. Damping ratios for these aeroelastic modes are extremely light (i.e., on the order of 0.1 or sometimes considerably less), as expected.

Tables 8-12 and Figs. 14-23 describe the pitch rate to elevator transfer function data for the Langley model which parallels the previous data for the Boeing model. The main feature to focus on here is that "tight" aeroelastic dipoles occur in an isolated fashion, not in a long sequence of many modes. Here, the magnitude frequency response plots indicate considerable dynamics in the aeroelastic frequency ranges. Further, as the sensor location is varied, the plots indicate that different aeroelastic modes are being sensed.

Table 1. Poles Of Boeing Appendix B Model			
Root Location (1/s)	Freq. (rad/s)	Damping (-)	Description
2.9822e-02	2.9822e-02	-1.0000e+00	Tuck Unstable
-3.6534e-02	3.6534e-02	1.0000e+00	Tuck Stable
-5.9134e-01+ 1.1896e+00i	1.3285e+00	4.4511e-01	Short Period
-5.9134e-01- 1.1896e+00i	1.3285e+00	4.4511e-01	Short Period
-3.5111e-01+ 7.0209e+00i	7.0297e+00	4.9947e-02	Aeroelastic 1
-3.5111e-01- 7.0209e+00i	7.0297e+00	4.9947e-02	Aeroelastic 1
-5.3373e-01+ 1.2806e+01i	1.2817e+01	4.1642e-02	Aeroelastic 2
-5.3373e-01- 1.2806e+01i	1.2817e+01	4.1642e-02	Aeroelastic 2
-1.4936e-01+ 1.4679e+01i	1.4680e+01	1.0174e-02	Aeroelastic 3
-1.4936e-01- 1.4679e+01i	1.4680e+01	1.0174e-02	Aeroelastic 3
-2.6817e-01+ 1.5759e+01i	1.5761e+01	1.7015e-02	Aeroelastic 4
-2.6817e-01- 1.5759e+01i	1.5761e+01	1.7015e-02	Aeroelastic 4
-2.4187e-01+ 1.6383e+01i	1.6385e+01	1.4762e-02	Aeroelastic 5
-2.4187e-01- 1.6383e+01i	1.6385e+01	1.4762e-02	Aeroelastic 5
-5.7167e-01+ 2.0059e+01i	2.0067e+01	2.8488e-02	Aeroelastic 6
-5.7167e-01- 2.0059e+01i	2.0067e+01	2.8488e-02	Aeroelastic 6
-2.4019e+00+ 2.0381e+01i	2.0522e+01	1.1704e-01	Aeroelastic 7
-2.4019e+00- 2.0381e+01i	2.0522e+01	1.1704e-01	Aeroelastic 7
-2.2000e+01	2.2000e+01	1.0000e+00	Elevator Actuator
-6.3930e-01+ 2.5915e+01i	2.5923e+01	2.4662e-02	Aeroelastic 8
-6.3930e-01- 2.5915e+01i	2.5923e+01	2.4662e-02	Aeroelastic 8
-1.8180e+00+ 3.1420e+01i	3.1473e+01	5.7763e-02	Aeroelastic 9
-1.8180e+00- 3.1420e+01i	3.1473e+01	5.7763e-02	Aeroelastic 9
-1.2665e+00+ 3.7844e+01i	3.7865e+01	3.3447e-02	Aeroelastic 10
-1.2665e+00- 3.7844e+01i	3.7865e+01	3.3447e-02	Aeroelastic 10
-2.7426e+00+ 3.7857e+01i	3.7956e+01	7.2257e-02	Aeroelastic 11
-2.7426e+00- 3.7857e+01i	3.7956e+01	7.2257e-02	Aeroelastic 11
-5.1396e-01+ 3.9994e+01i	3.9998e+01	1.2850e-02	Aeroelastic 12
-5.1396e-01- 3.9994e+01i	3.9998e+01	1.2850e-02	Aeroelastic 12
-5.2496e-01+ 4.1405e+01i	4.1408e+01	1.2678e-02	Aeroelastic 13
-5.2496e-01- 4.1405e+01i	4.1408e+01	1.2678e-02	Aeroelastic 13
-5.8376e-01+ 4.2330e+01i	4.2334e+01	1.3789e-02	Aeroelastic 14
-5.8376e-01- 4.2330e+01i	4.2334e+01	1.3789e-02	Aeroelastic 14
-4.5366e-01+ 4.3745e+01i	4.3747e+01	1.0370e-02	Aeroelastic 15
-4.5366e-01- 4.3745e+01i	4.3747e+01	1.0370e-02	Aeroelastic 15
-1.5556e+02+ 1.5556e+02i	2.2000e+02	7.0710e-01	Elevator Actuator
-1.5556e+02- 1.5556e+02i	2.2000e+02	7.0710e-01	Elevator Actuator

Table 2. Zeros Of Boeing Appendix B Model For 319 in Pitch Rate To Elevator Channel			
Gain = 1.6751e-01 rad/s/rad			
Root Location (1/s)	Freq. (rad/s)	Damping (-)	Description
0	0	-1.0000e+00	Pitch "Rate"
-9.6188e-03	9.6188e-03	1.0000e+00	Tau Theta 1
-5.8642e-01	5.8642e-01	1.0000e+00	Tau Theta 2
-1.2571e+00+ 7.0173e+00i	7.1290e+00	1.7634e-01	Aeroelastic 1
-1.2571e+00- 7.0173e+00i	7.1290e+00	1.7634e-01	Aeroelastic 1
-2.0863e-01+ 1.2904e+01i	1.2906e+01	1.6166e-02	Aeroelastic 2
-2.0863e-01- 1.2904e+01i	1.2906e+01	1.6166e-02	Aeroelastic 2
-1.5076e-01+ 1.4680e+01i	1.4681e+01	1.0269e-02	Aeroelastic 3
-1.5076e-01- 1.4680e+01i	1.4681e+01	1.0269e-02	Aeroelastic 3
-1.9468e-01+ 1.5642e+01i	1.5643e+01	1.2445e-02	Aeroelastic 4
-1.9468e-01- 1.5642e+01i	1.5643e+01	1.2445e-02	Aeroelastic 4
-3.3056e-01+ 1.6373e+01i	1.6376e+01	2.0186e-02	Aeroelastic 5
-3.3056e-01- 1.6373e+01i	1.6376e+01	2.0186e-02	Aeroelastic 5
-1.7261e+00+ 1.9798e+01i	1.9873e+01	8.6854e-02	Aeroelastic 6
-1.7261e+00- 1.9798e+01i	1.9873e+01	8.6854e-02	Aeroelastic 6
-7.1160e-01+ 2.0589e+01i	2.0601e+01	3.4541e-02	Aeroelastic 7
-7.1160e-01- 2.0589e+01i	2.0601e+01	3.4541e-02	Aeroelastic 7
-2.2495e+00+ 2.5994e+01i	2.6091e+01	8.6217e-02	Aeroelastic 8
-2.2495e+00- 2.5994e+01i	2.6091e+01	8.6217e-02	Aeroelastic 8
-1.6874e+00+ 3.1451e+01i	3.1496e+01	5.3576e-02	Aeroelastic 9
-1.6874e+00- 3.1451e+01i	3.1496e+01	5.3576e-02	Aeroelastic 9
-8.6767e-01+ 3.6919e+01i	3.6930e+01	2.3495e-02	Aeroelastic 10
-8.6767e-01- 3.6919e+01i	3.6930e+01	2.3495e-02	Aeroelastic 10
-3.0486e+00+ 3.8669e+01i	3.8789e+01	7.8594e-02	Aeroelastic 11
-3.0486e+00- 3.8669e+01i	3.8789e+01	7.8594e-02	Aeroelastic 11
-5.6945e-01+ 3.9911e+01i	3.9915e+01	1.4267e-02	Aeroelastic 12
-5.6945e-01- 3.9911e+01i	3.9915e+01	1.4267e-02	Aeroelastic 12
-6.4701e-01+ 4.1463e+01i	4.1468e+01	1.5603e-02	Aeroelastic 13
-6.4701e-01- 4.1463e+01i	4.1468e+01	1.5603e-02	Aeroelastic 13
-7.5046e-01+ 4.2345e+01i	4.2352e+01	1.7719e-02	Aeroelastic 14
-7.5046e-01- 4.2345e+01i	4.2352e+01	1.7719e-02	Aeroelastic 14
-4.6148e-01+ 4.3746e+01i	4.3749e+01	1.0548e-02	Aeroelastic 15
-4.6148e-01- 4.3746e+01i	4.3749e+01	1.0548e-02	Aeroelastic 15
-1.4154e+03	1.4154e+03	1.0000e+00	Noncausal Rate
2.0840e+03	2.0840e+03	-1.0000e+00	Noncausal Acceleration

Table 3. Zeros Of Boeing Appendix B Model For 778 in Pitch Rate To Elevator Channel			
Gain = -6.3496e-02 rad/s/rad			
Root Location (1/s)	Freq. (rad/s)	Damping (-)	Description
0	0	-1.0000e+00	Pitch "Rate"
-9.6210e-03	9.6210e-03	1.0000e+00	Tau Theta 1
-5.8122e-01	5.8122e-01	1.0000e+00	Tau Theta 2
-1.7018e+00+ 6.9512e+00i	7.1565e+00	2.3780e-01	Aeroelastic 1
-1.7018e+00- 6.9512e+00i	7.1565e+00	2.3780e-01	Aeroelastic 1
-1.2571e-01+ 1.2978e+01i	1.2979e+01	9.6862e-03	Aeroelastic 2
-1.2571e-01- 1.2978e+01i	1.2979e+01	9.6862e-03	Aeroelastic 2
-1.5132e-01+ 1.4681e+01i	1.4681e+01	1.0307e-02	Aeroelastic 3
-1.5132e-01- 1.4681e+01i	1.4681e+01	1.0307e-02	Aeroelastic 3
-1.7203e-01+ 1.5615e+01i	1.5616e+01	1.1016e-02	Aeroelastic 4
-1.7203e-01- 1.5615e+01i	1.5616e+01	1.1016e-02	Aeroelastic 4
-3.4564e-01+ 1.6367e+01i	1.6371e+01	2.1113e-02	Aeroelastic 5
-3.4564e-01- 1.6367e+01i	1.6371e+01	2.1113e-02	Aeroelastic 5
-1.6822e+00+ 1.9736e+01i	1.9808e+01	8.4924e-02	Aeroelastic 6
-1.6822e+00- 1.9736e+01i	1.9808e+01	8.4924e-02	Aeroelastic 6
-7.3628e-01+ 2.0631e+01i	2.0644e+01	3.5666e-02	Aeroelastic 7
-7.3628e-01- 2.0631e+01i	2.0644e+01	3.5666e-02	Aeroelastic 7
-1.8881e+00+ 2.5982e+01i	2.6050e+01	7.2479e-02	Aeroelastic 8
-1.8881e+00- 2.5982e+01i	2.6050e+01	7.2479e-02	Aeroelastic 8
-1.7566e+00+ 3.1423e+01i	3.1472e+01	5.5815e-02	Aeroelastic 9
-1.7566e+00- 3.1423e+01i	3.1472e+01	5.5815e-02	Aeroelastic 9
-1.1948e+00+ 3.7481e+01i	3.7500e+01	3.1860e-02	Aeroelastic 10
-1.1948e+00- 3.7481e+01i	3.7500e+01	3.1860e-02	Aeroelastic 10
-2.7036e+00+ 3.8173e+01i	3.8268e+01	7.0649e-02	Aeroelastic 11
-2.7036e+00- 3.8173e+01i	3.8268e+01	7.0649e-02	Aeroelastic 11
-5.2517e-01+ 3.9973e+01i	3.9977e+01	1.3137e-02	Aeroelastic 12
-5.2517e-01- 3.9973e+01i	3.9977e+01	1.3137e-02	Aeroelastic 12
-5.4532e-01+ 4.1413e+01i	4.1416e+01	1.3167e-02	Aeroelastic 13
-5.4532e-01- 4.1413e+01i	4.1416e+01	1.3167e-02	Aeroelastic 13
-6.0126e-01+ 4.2336e+01i	4.2340e+01	1.4201e-02	Aeroelastic 14
-6.0126e-01- 4.2336e+01i	4.2340e+01	1.4201e-02	Aeroelastic 14
-4.5406e-01+ 4.3745e+01i	4.3747e+01	1.0379e-02	Aeroelastic 15
-4.5406e-01- 4.3745e+01i	4.3747e+01	1.0379e-02	Aeroelastic 15
-3.0870e+02+ 2.7688e+03i	2.7860e+03	1.1080e-01	Noncausal Rate
-3.0870e+02- 2.7688e+03i	2.7860e+03	1.1080e-01	Noncausal Acceleration

Table 4. Zeros Of Boeing Appendix B Model For 2,115 in Pitch Rate To Elevator Channel			
Gain = 2.7205e-01 rad/s/rad			
Root Location (1/s)	Freq. (rad/s)	Damping (-)	Description
0	0	-1.0000e+00	Pitch "Rate"
-9.6149e-03	9.6149e-03	1.0000e+00	Tau Theta 1
-5.9588e-01	5.9588e-01	1.0000e+00	Tau Theta 2
-1.3902e-01+ 7.0062e+00i	7.0076e+00	1.9838e-02	Aeroelastic 1
-1.3902e-01- 7.0062e+00i	7.0076e+00	1.9838e-02	Aeroelastic 1
-5.6232e-01+ 1.2809e+01i	1.2821e+01	4.3859e-02	Aeroelastic 2
-5.6232e-01- 1.2809e+01i	1.2821e+01	4.3859e-02	Aeroelastic 2
-1.4931e-01+ 1.4679e+01i	1.4680e+01	1.0171e-02	Aeroelastic 3
-1.4931e-01- 1.4679e+01i	1.4680e+01	1.0171e-02	Aeroelastic 3
-2.8226e-01+ 1.5778e+01i	1.5780e+01	1.7887e-02	Aeroelastic 4
-2.8226e-01- 1.5778e+01i	1.5780e+01	1.7887e-02	Aeroelastic 4
-2.2266e-01+ 1.6386e+01i	1.6388e+01	1.3587e-02	Aeroelastic 5
-2.2266e-01- 1.6386e+01i	1.6388e+01	1.3587e-02	Aeroelastic 5
-5.3595e-01+ 2.0044e+01i	2.0051e+01	2.6729e-02	Aeroelastic 6
-5.3595e-01- 2.0044e+01i	2.0051e+01	2.6729e-02	Aeroelastic 6
-2.5712e+00+ 2.0415e+01i	2.0576e+01	1.2496e-01	Aeroelastic 7
-2.5712e+00- 2.0415e+01i	2.0576e+01	1.2496e-01	Aeroelastic 7
-6.4491e-01+ 2.5909e+01i	2.5917e+01	2.4884e-02	Aeroelastic 8
-6.4491e-01- 2.5909e+01i	2.5917e+01	2.4884e-02	Aeroelastic 8
-1.8735e+00+ 3.1469e+01i	3.1525e+01	5.9431e-02	Aeroelastic 9
-1.8735e+00- 3.1469e+01i	3.1525e+01	5.9431e-02	Aeroelastic 9
-1.2197e+00+ 3.7718e+01i	3.7737e+01	3.2322e-02	Aeroelastic 10
-1.2197e+00- 3.7718e+01i	3.7737e+01	3.2322e-02	Aeroelastic 10
-2.9273e+00+ 3.7953e+01i	3.8066e+01	7.6900e-02	Aeroelastic 11
-2.9273e+00- 3.7953e+01i	3.8066e+01	7.6900e-02	Aeroelastic 11
-5.2465e-01+ 3.9977e+01i	3.9981e+01	1.3123e-02	Aeroelastic 12
-5.2465e-01- 3.9977e+01i	3.9981e+01	1.3123e-02	Aeroelastic 12
-5.6081e-01+ 4.1426e+01i	4.1430e+01	1.3536e-02	Aeroelastic 13
-5.6081e-01- 4.1426e+01i	4.1430e+01	1.3536e-02	Aeroelastic 13
-6.3974e-01+ 4.2352e+01i	4.2357e+01	1.5104e-02	Aeroelastic 14
-6.3974e-01- 4.2352e+01i	4.2357e+01	1.5104e-02	Aeroelastic 14
-4.5727e-01+ 4.3747e+01i	4.3749e+01	1.0452e-02	Aeroelastic 15
-4.5727e-01- 4.3747e+01i	4.3749e+01	1.0452e-02	Aeroelastic 15
-9.2113e+02	9.2113e+02	1.0000e+00	Noncausal Rate
1.9753e+03	1.9753e+03	-1.0000e+00	Noncausal Acceleration

Table 5. Zeros Of Boeing Appendix B Model For 2,525 in Pitch Rate To Elevator Channel			
Gain = 4.8694e-01 rad/s/rad			
Root Location (1/s)	Freq. (rad/s)	Damping (-)	Description
0	0	-1.0000e+00	Pitch "Rate"
-9.6124e-03	9.6124e-03	1.0000e+00	Tau Theta 1
-6.0185e-01	6.0185e-01	1.0000e+00	Tau Theta 2
1.7056e-01+ 6.9474e+00i	6.9495e+00	-2.4544e-02	Aeroelastic 1
1.7056e-01- 6.9474e+00i	6.9495e+00	-2.4544e-02	Aeroelastic 1
-4.0933e-01+ 1.2819e+01i	1.2825e+01	3.1916e-02	Aeroelastic 2
-4.0933e-01- 1.2819e+01i	1.2825e+01	3.1916e-02	Aeroelastic 2
-1.4955e-01+ 1.4679e+01i	1.4680e+01	1.0188e-02	Aeroelastic 3
-1.4955e-01- 1.4679e+01i	1.4680e+01	1.0188e-02	Aeroelastic 3
-2.5227e-01+ 1.5737e+01i	1.5739e+01	1.6029e-02	Aeroelastic 4
-2.5227e-01- 1.5737e+01i	1.5739e+01	1.6029e-02	Aeroelastic 4
-2.5650e-01+ 1.6380e+01i	1.6382e+01	1.5657e-02	Aeroelastic 5
-2.5650e-01- 1.6380e+01i	1.6382e+01	1.5657e-02	Aeroelastic 5
-5.8119e-01+ 2.0087e+01i	2.0095e+01	2.8922e-02	Aeroelastic 6
-5.8119e-01- 2.0087e+01i	2.0095e+01	2.8922e-02	Aeroelastic 6
-2.3676e+00+ 2.0306e+01i	2.0444e+01	1.1581e-01	Aeroelastic 7
-2.3676e+00- 2.0306e+01i	2.0444e+01	1.1581e-01	Aeroelastic 7
-7.8283e-01+ 2.5967e+01i	2.5979e+01	3.0133e-02	Aeroelastic 8
-7.8283e-01- 2.5967e+01i	2.5979e+01	3.0133e-02	Aeroelastic 8
-2.0304e+00+ 3.1587e+01i	3.1652e+01	6.4147e-02	Aeroelastic 9
-2.0304e+00- 3.1587e+01i	3.1652e+01	6.4147e-02	Aeroelastic 9
-3.3703e+00+ 3.7651e+01i	3.7802e+01	8.9159e-02	Aeroelastic 10
-3.3703e+00- 3.7651e+01i	3.7802e+01	8.9159e-02	Aeroelastic 10
-1.0849e+00+ 3.8023e+01i	3.8038e+01	2.8520e-02	Aeroelastic 11
-1.0849e+00- 3.8023e+01i	3.8038e+01	2.8520e-02	Aeroelastic 11
-5.2799e-01+ 3.9983e+01i	3.9987e+01	1.3204e-02	Aeroelastic 12
-5.2799e-01- 3.9983e+01i	3.9987e+01	1.3204e-02	Aeroelastic 12
-6.5175e-01+ 4.1504e+01i	4.1509e+01	1.5701e-02	Aeroelastic 13
-6.5175e-01- 4.1504e+01i	4.1509e+01	1.5701e-02	Aeroelastic 13
-8.2270e-01+ 4.2370e+01i	4.2378e+01	1.9413e-02	Aeroelastic 14
-8.2270e-01- 4.2370e+01i	4.2378e+01	1.9413e-02	Aeroelastic 14
-4.6068e-01+ 4.3745e+01i	4.3748e+01	1.0530e-02	Aeroelastic 15
-4.6068e-01- 4.3745e+01i	4.3748e+01	1.0530e-02	Aeroelastic 15
-5.4261e+02	5.4261e+02	1.0000e+00	Noncausal Rate
1.8747e+03	1.8747e+03	-1.0000e+00	Noncausal Acceleration

Table 6. Zeros Of Boeing Appendix B Model For 3,157 in Pitch Rate To Elevator Channel			
Gain = 6.6562e-01 rad/s/rad			
Root Location (1/s)	Freq. (rad/s)	Damping (-)	Description
0	0	-1.0000e+00	Pitch "Rate"
-9.6010e-03	9.6010e-03	1.0000e+00	Tau Theta 1
-6.3307e-01	6.3307e-01	1.0000e+00	Tau Theta 2
1.1613e-01+ 7.0028e+00i	7.0038e+00	-1.6580e-02	Aeroelastic 1
1.1613e-01- 7.0028e+00i	7.0038e+00	-1.6580e-02	Aeroelastic 1
-2.7374e-01+ 1.2881e+01i	1.2884e+01	2.1247e-02	Aeroelastic 2
-2.7374e-01- 1.2881e+01i	1.2884e+01	2.1247e-02	Aeroelastic 2
-1.5066e-01+ 1.4680e+01i	1.4680e+01	1.0263e-02	Aeroelastic 3
-1.5066e-01- 1.4680e+01i	1.4680e+01	1.0263e-02	Aeroelastic 3
-2.0911e-01+ 1.5696e+01i	1.5697e+01	1.3321e-02	Aeroelastic 4
-2.0911e-01- 1.5696e+01i	1.5697e+01	1.3321e-02	Aeroelastic 4
-2.8144e-01+ 1.6368e+01i	1.6370e+01	1.7193e-02	Aeroelastic 5
-2.8144e-01- 1.6368e+01i	1.6370e+01	1.7193e-02	Aeroelastic 5
-4.7890e-01+ 1.9854e+01i	1.9859e+01	2.4115e-02	Aeroelastic 6
-4.7890e-01- 1.9854e+01i	1.9859e+01	2.4115e-02	Aeroelastic 6
-2.0048e+00+ 2.0588e+01i	2.0686e+01	9.6919e-02	Aeroelastic 7
-2.0048e+00- 2.0588e+01i	2.0686e+01	9.6919e-02	Aeroelastic 7
1.4099e-01+ 2.6032e+01i	2.6033e+01	-5.4159e-03	Aeroelastic 8
1.4099e-01- 2.6032e+01i	2.6033e+01	-5.4159e-03	Aeroelastic 8
-1.3343e+00+ 3.1172e+01i	3.1201e+01	4.2765e-02	Aeroelastic 9
-1.3343e+00- 3.1172e+01i	3.1201e+01	4.2765e-02	Aeroelastic 9
-1.2452e+00+ 3.7208e+01i	3.7229e+01	3.3448e-02	Aeroelastic 10
-1.2452e+00- 3.7208e+01i	3.7229e+01	3.3448e-02	Aeroelastic 10
-1.6783e+00+ 3.8801e+01i	3.8838e+01	4.3214e-02	Aeroelastic 11
-1.6783e+00- 3.8801e+01i	3.8838e+01	4.3214e-02	Aeroelastic 11
-5.8711e-01+ 3.9972e+01i	3.9977e+01	1.4686e-02	Aeroelastic 12
-5.8711e-01- 3.9972e+01i	3.9977e+01	1.4686e-02	Aeroelastic 12
-5.3092e-01+ 4.1379e+01i	4.1383e+01	1.2830e-02	Aeroelastic 13
-5.3092e-01- 4.1379e+01i	4.1383e+01	1.2830e-02	Aeroelastic 13
-5.1641e-01+ 4.2258e+01i	4.2261e+01	1.2219e-02	Aeroelastic 14
-5.1641e-01- 4.2258e+01i	4.2261e+01	1.2219e-02	Aeroelastic 14
-4.4073e-01+ 4.3733e+01i	4.3735e+01	1.0077e-02	Aeroelastic 15
-4.4073e-01- 4.3733e+01i	4.3735e+01	1.0077e-02	Aeroelastic 15
1.2888e+02	1.2888e+02	-1.0000e+00	Noncausal Rate
-5.5392e+03	5.5392e+03	1.0000e+00	Noncausal Acceleration

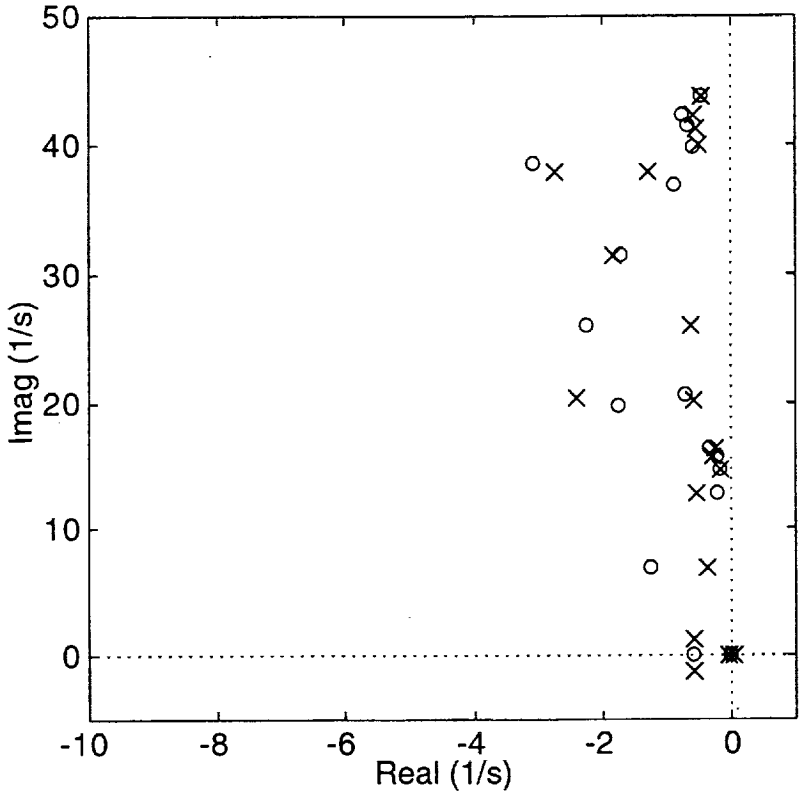

Figure 4. Pole-Zero Pattern Of Boeing Appendix B Model For 319 in Pitch Rate To Elevator Channel

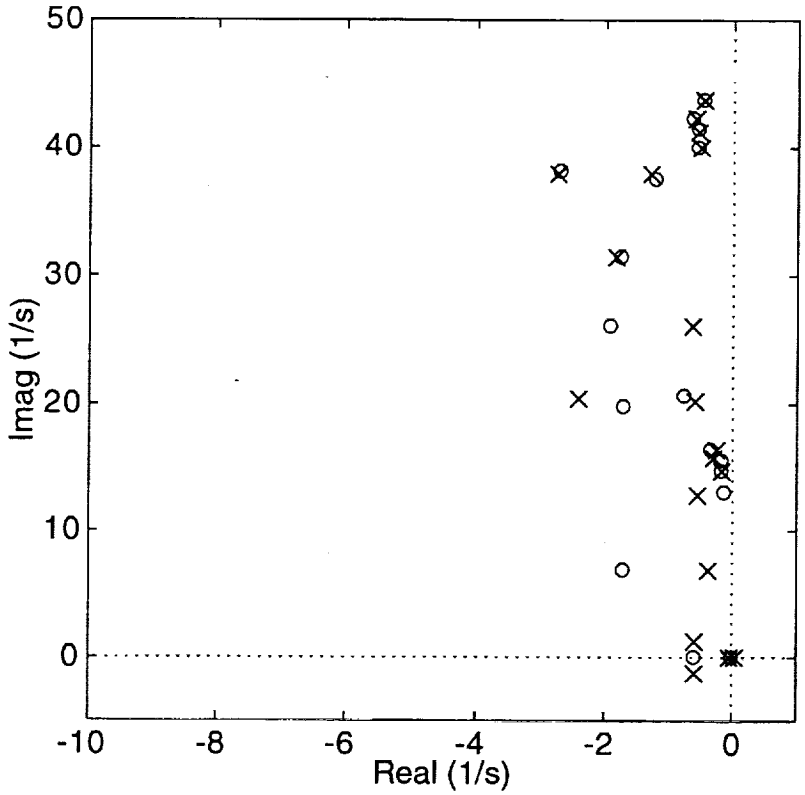

Figure 5. Pole-Zero Pattern Of Boeing Appendix B Model For 778 in Pitch Rate To Elevator Channel

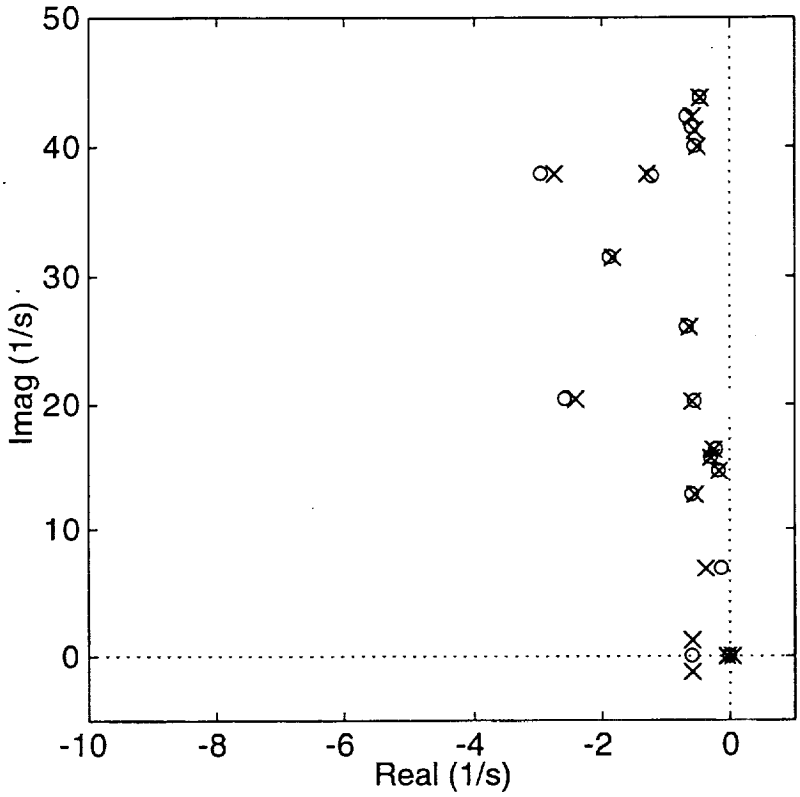

Figure 6. Pole-Zero Pattern Of Boeing Appendix B Model
For 2,115 in Pitch Rate To Elevator Channel

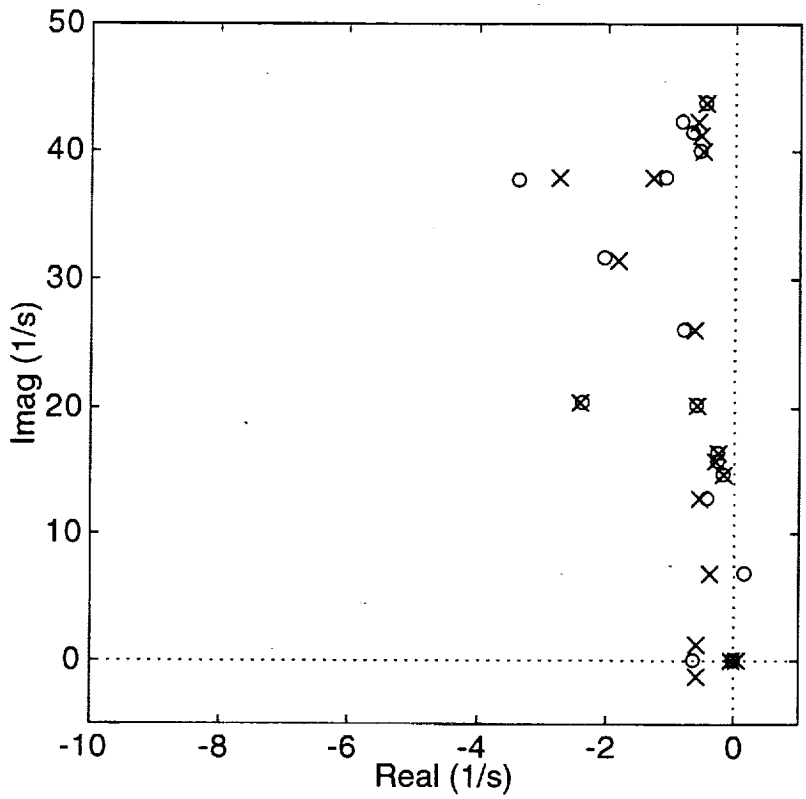

Figure 7. Pole-Zero Pattern Of Boeing Appendix B Model
For 2,525 in Pitch Rate To Elevator Channel

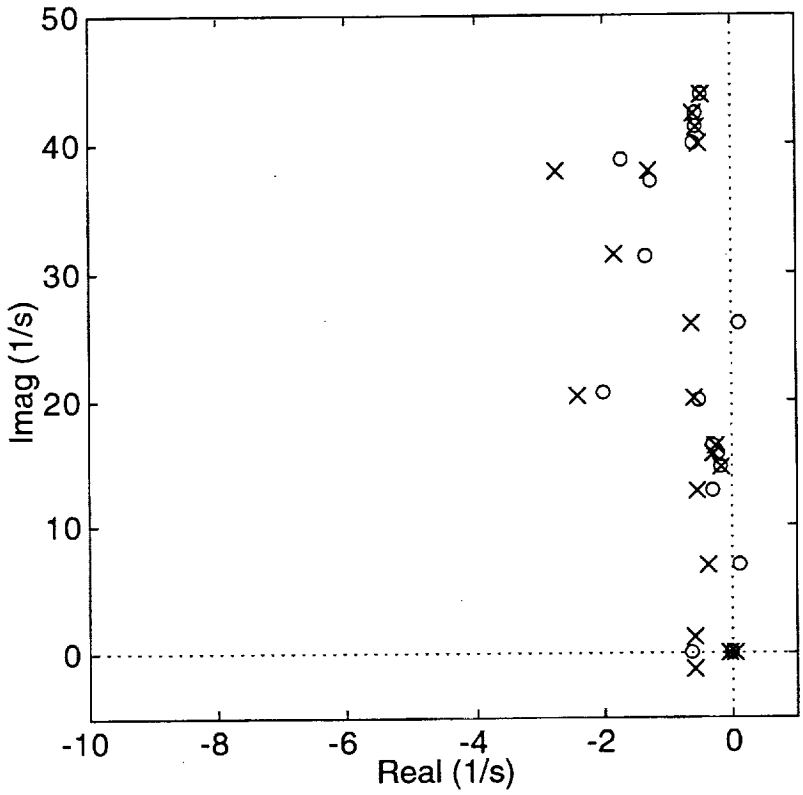

Figure 8. Pole-Zero Pattern Of Boeing Appendix B Model For 3,157 in Pitch Rate To Elevator Channel

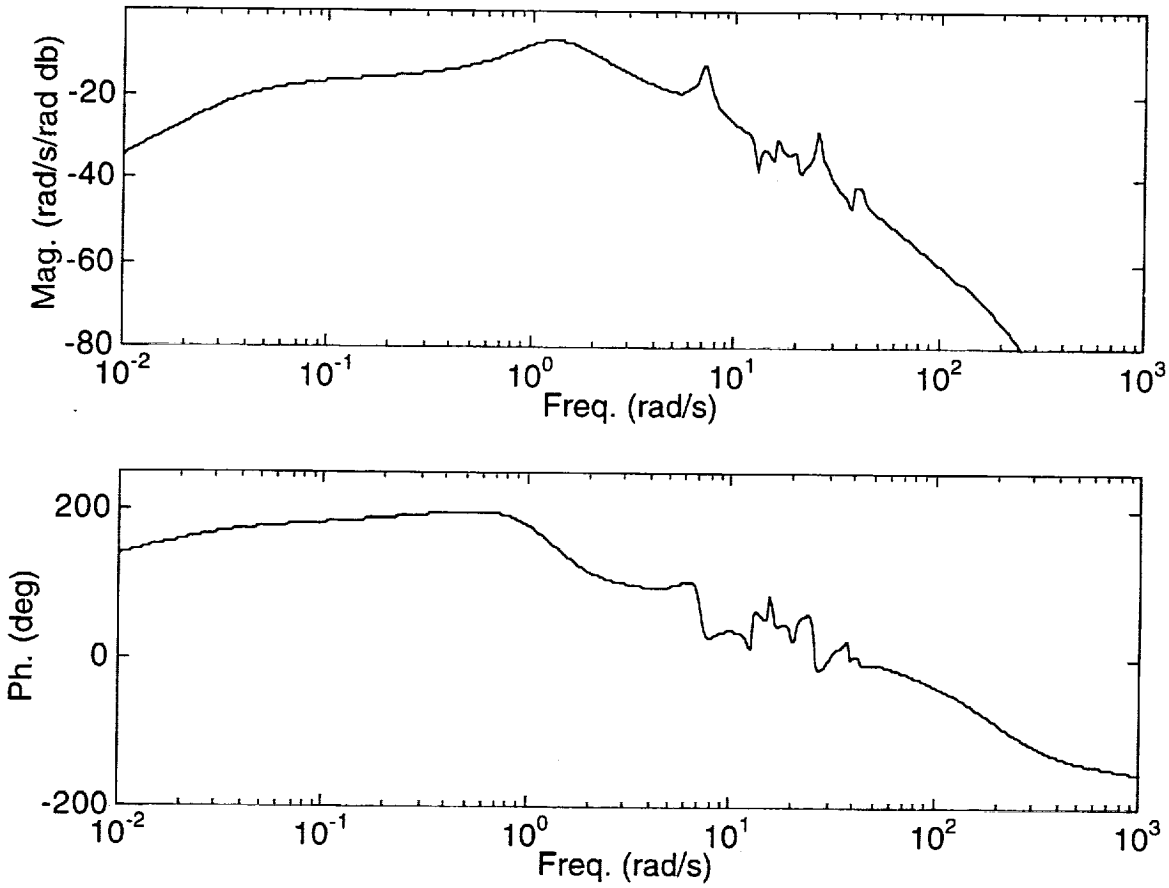

Figure 9. Frequency Response Of Boeing Appendix B Model
For 319 in Pitch Rate To Elevator Channel

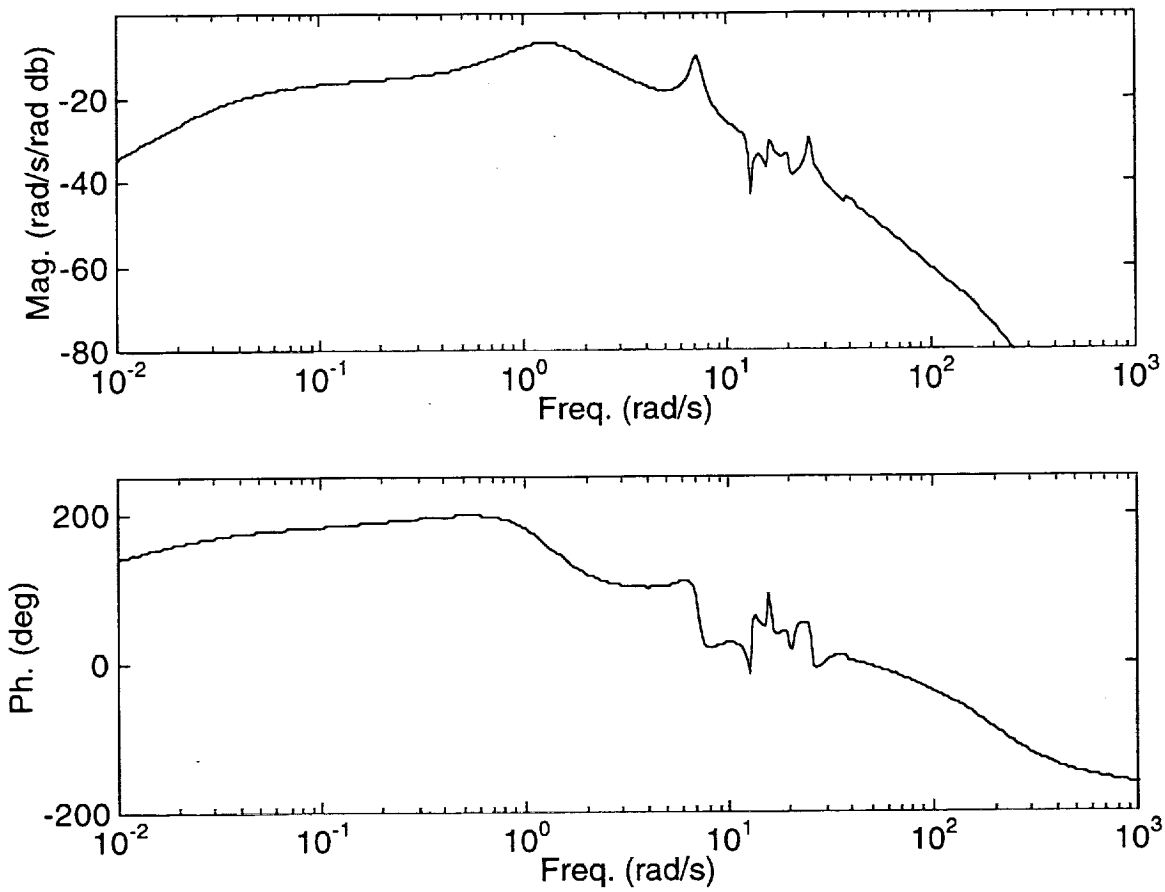

Figure 10. Frequency Response Of Boeing Appendix B Model
For 778 in Pitch Rate To Elevator Channel

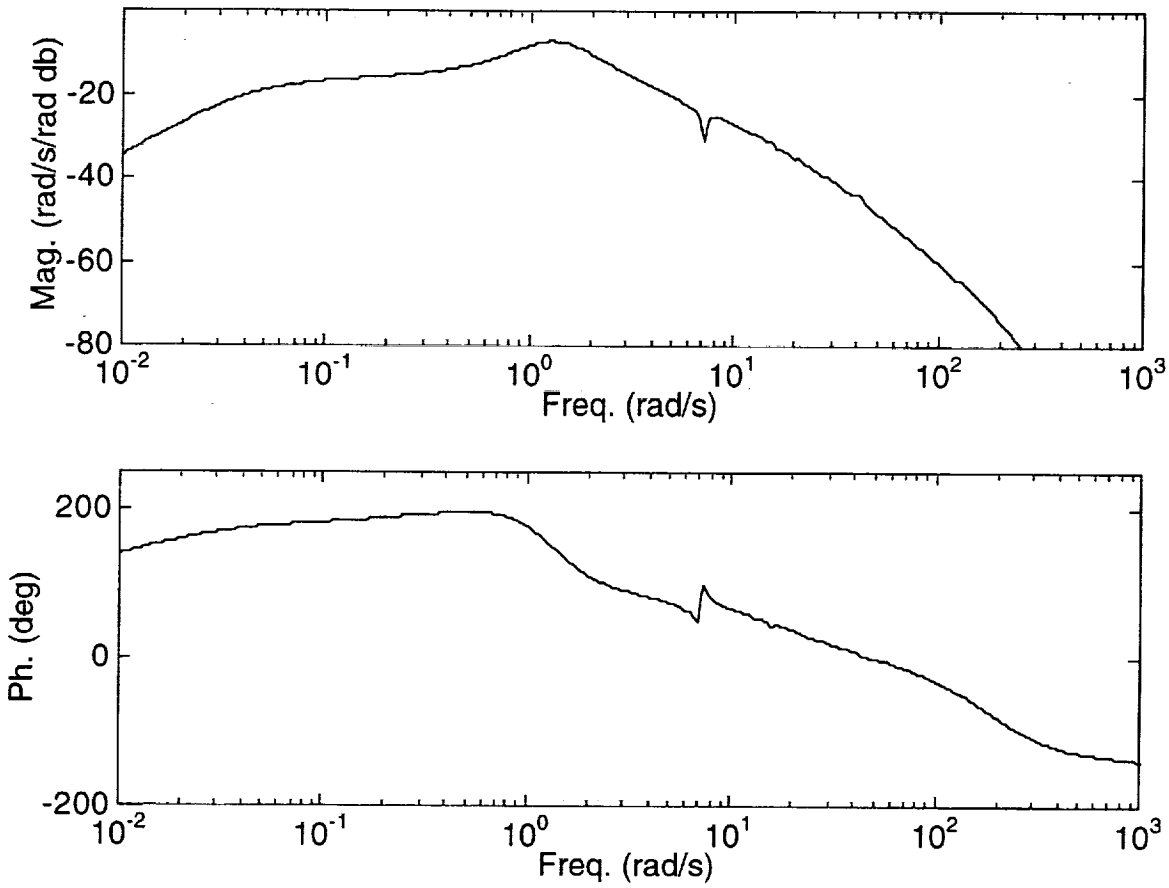

Figure 11. Frequency Response Of Boeing Appendix B Model
For 2,115 in Pitch Rate To Elevator Channel

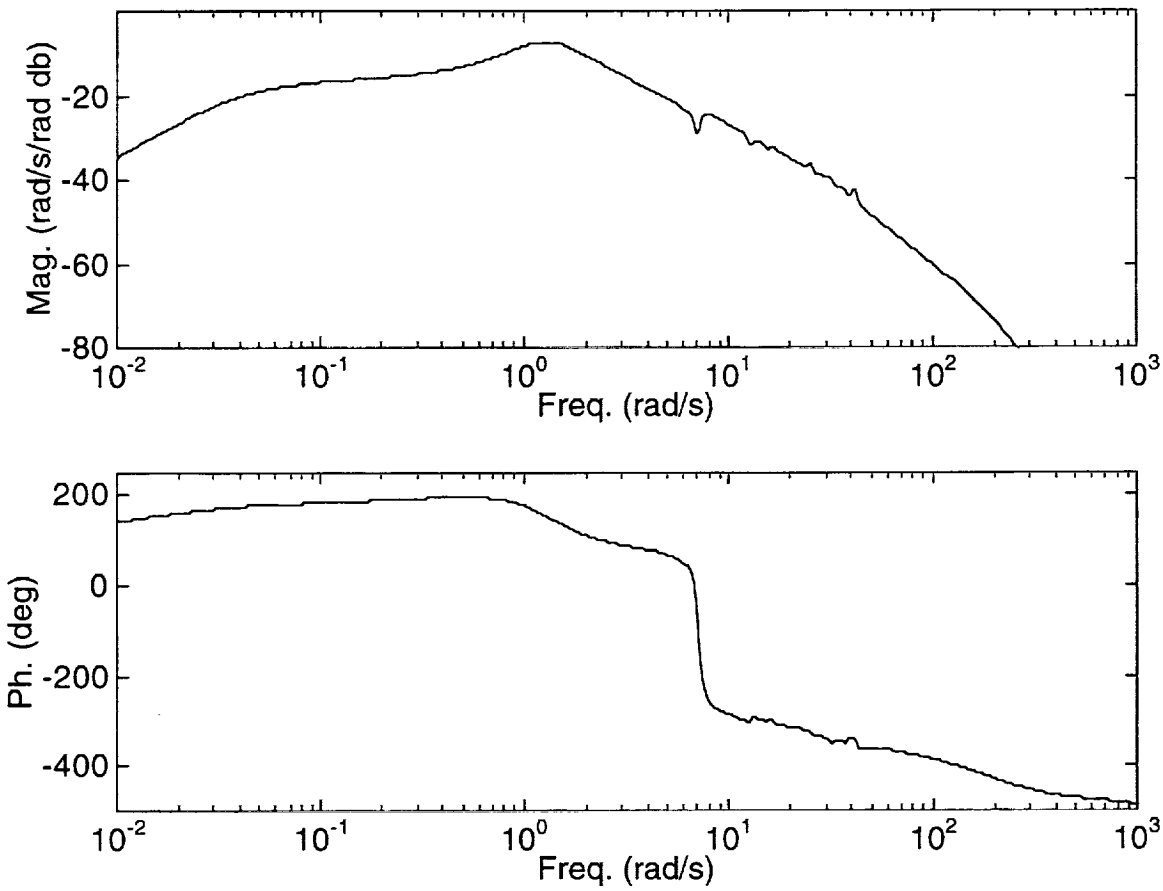

Figure 12. Frequency Response Of Boeing Appendix B Model
For 2,525 in Pitch Rate To Elevator Channel

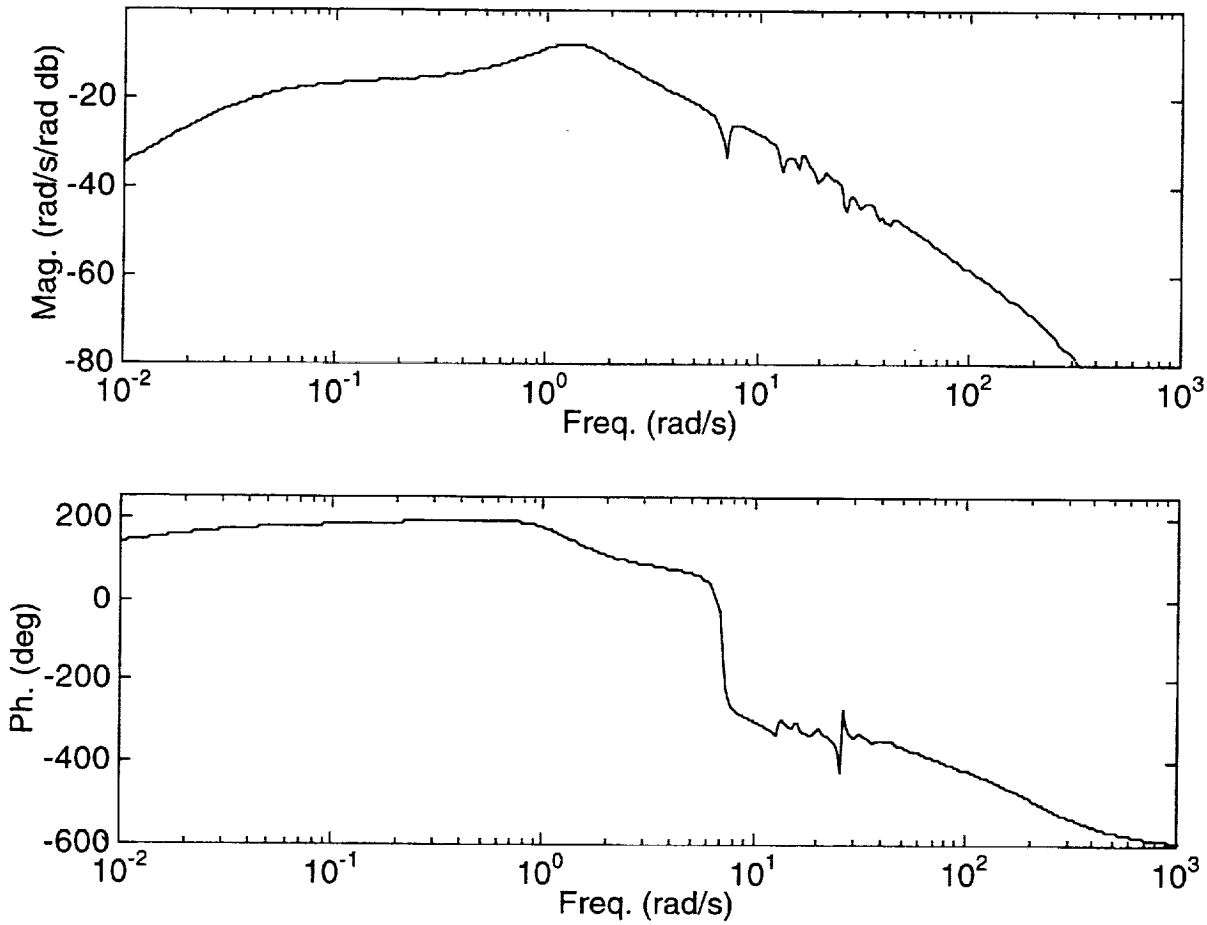

Figure 13. Frequency Response Of Boeing Appendix B Model
For 3,157 in Pitch Rate To Elevator Channel

Table 7. Poles Of Langley Appendix C Model			
Root Location (1/s)	Freq. (rad/s)	Damping (-)	Description
0	0	-1.0000e+00	Long Period Remnant
-6.6398e-01+ 1.6657e+00i	1.7932e+00	3.7028e-01	Short Period
-6.6398e-01- 1.6657e+00i	1.7932e+00	3.7028e-01	Short Period
-2.2755e+00	2.2755e+00	1.0000e+00	Unsteady Aero 1
-4.5517e+00	4.5517e+00	1.0000e+00	Unsteady Aero 2
-3.7179e-01+ 7.6920e+00i	7.7009e+00	4.8279e-02	Aeroelastic 1
-3.7179e-01- 7.6920e+00i	7.7009e+00	4.8279e-02	Aeroelastic 1
-1.0837e+00+ 1.5547e+01i	1.5585e+01	6.9536e-02	Aeroelastic 2
-1.0837e+00- 1.5547e+01i	1.5585e+01	6.9536e-02	Aeroelastic 2
-1.6395e+01	1.6395e+01	1.0000e+00	Unsteady Aero 3
-6.5794e-04+ 1.6855e+01i	1.6855e+01	3.9035e-05	Aeroelastic 3
-6.5794e-04- 1.6855e+01i	1.6855e+01	3.9035e-05	Aeroelastic 3
-6.2405e-01+ 1.8063e+01i	1.8074e+01	3.4528e-02	Aeroelastic 4
-6.2405e-01- 1.8063e+01i	1.8074e+01	3.4528e-02	Aeroelastic 4
-1.0123e-01+ 1.9385e+01i	1.9385e+01	5.2221e-03	Aeroelastic 5
-1.0123e-01- 1.9385e+01i	1.9385e+01	5.2221e-03	Aeroelastic 5
-3.1294e+00+ 2.1527e+01i	2.1753e+01	1.4386e-01	Aeroelastic 6
-3.1294e+00- 2.1527e+01i	2.1753e+01	1.4386e-01	Aeroelastic 6
-2.2000e+01	2.2000e+01	1.0000e+00	Elevator Actuator
-3.5439e-01+ 2.3358e+01i	2.3361e+01	1.5170e-02	Aeroelastic 7
-3.5439e-01- 2.3358e+01i	2.3361e+01	1.5170e-02	Aeroelastic 7
-2.6099e+01+ 1.0311e+00i	2.6120e+01	9.9922e-01	Unsteady Aero 4
-2.6099e+01- 1.0311e+00i	2.6120e+01	9.9922e-01	Unsteady Aero 5
-5.5033e-01+ 2.8147e+01i	2.8152e+01	1.9549e-02	Aeroelastic 8
-5.5033e-01- 2.8147e+01i	2.8152e+01	1.9549e-02	Aeroelastic 8
-3.2799e+01	3.2799e+01	1.0000e+00	Unsteady Aero 6
-8.4445e+00+ 3.3125e+01i	3.4184e+01	2.4703e-01	Aeroelastic 9
-8.4445e+00- 3.3125e+01i	3.4184e+01	2.4703e-01	Aeroelastic 9
-1.0298e+00+ 3.7226e+01i	3.7240e+01	2.7653e-02	Aeroelastic 10
-1.0298e+00- 3.7226e+01i	3.7240e+01	2.7653e-02	Aeroelastic 10
-9.1697e-01+ 3.8256e+01i	3.8267e+01	2.3962e-02	Aeroelastic 11
-9.1697e-01- 3.8256e+01i	3.8267e+01	2.3962e-02	Aeroelastic 11
-3.9221e+01	3.9221e+01	1.0000e+00	Unsteady Aero 7
-4.4741e+01	4.4741e+01	1.0000e+00	Unsteady Aero 8
-1.0188e+00+ 4.8602e+01i	4.8613e+01	2.0957e-02	Aeroelastic 12
-1.0188e+00- 4.8602e+01i	4.8613e+01	2.0957e-02	Aeroelastic 12
-4.7311e-01+ 4.9809e+01i	4.9811e+01	9.4981e-03	Aeroelastic 13
-4.7311e-01- 4.9809e+01i	4.9811e+01	9.4981e-03	Aeroelastic 13
-4.1768e-01+ 5.5466e+01i	5.5468e+01	7.5301e-03	Aeroelastic 14
-4.1768e-01- 5.5466e+01i	5.5468e+01	7.5301e-03	Aeroelastic 14
-1.6584e+00+ 5.6245e+01i	5.6270e+01	2.9472e-02	Aeroelastic 15
-1.6584e+00- 5.6245e+01i	5.6270e+01	2.9472e-02	Aeroelastic 15
-5.9895e+01	5.9895e+01	1.0000e+00	Unsteady Aero 9
-1.8456e-01+ 6.1086e+01i	6.1087e+01	3.0213e-03	Aeroelastic 16
-1.8456e-01- 6.1086e+01i	6.1087e+01	3.0213e-03	Aeroelastic 16
-6.1559e+00+ 6.2762e+01i	6.3063e+01	9.7614e-02	Aeroelastic 17
-6.1559e+00- 6.2762e+01i	6.3063e+01	9.7614e-02	Aeroelastic 17
-9.9206e+01	9.9206e+01	1.0000e+00	Unsteady Aero 10
-1.5556e+02+ 1.5556e+02i	2.2000e+02	7.0710e-01	Elevator Actuator
-1.5556e+02- 1.5556e+02i	2.2000e+02	7.0710e-01	Elevator Actuator

Table 8. Zeros Of Langley Appendix C Model For 319 in Pitch Rate To Elevator Channel			
Gain = -3.9047e+04 rad/s/rad			
Root Location (1/s)	Freq. (rad/s)	Damping (-)	Description
0	0	-1.0000e+00	Long Period Remnant
-5.9247e-01	5.9247e-01	1.0000e+00	Tau Theta 2
-2.2120e+00	2.2120e+00	1.0000e+00	Unsteady Aero 1
-5.1325e+00+ 8.9339e-01i	5.2097e+00	9.8519e-01	Unsteady Aero 2
-5.1325e+00- 8.9339e-01i	5.2097e+00	9.8519e-01	Aeroelastic 1
5.4243e+00	5.4243e+00	-1.0000e+00	Aeroelastic 1
1.1913e+01	1.1913e+01	-1.0000e+00	Aeroelastic 2
-8.2172e+00+ 9.2496e+00i	1.2372e+01	6.6415e-01	Aeroelastic 2
-8.2172e+00- 9.2496e+00i	1.2372e+01	6.6415e-01	Noncausal Rate
-5.8924e-01+ 1.6483e+01i	1.6493e+01	3.5726e-02	Aeroelastic 4
-5.8924e-01- 1.6483e+01i	1.6493e+01	3.5726e-02	Aeroelastic 4
7.5358e-03+ 1.6847e+01i	1.6847e+01	-4.4732e-04	Aeroelastic 3
7.5358e-03- 1.6847e+01i	1.6847e+01	-4.4732e-04	Aeroelastic 3
-1.7097e+01	1.7097e+01	1.0000e+00	Unsteady Aero 3
6.8133e-02+ 1.9432e+01i	1.9432e+01	-3.5062e-03	Aeroelastic 5
6.8133e-02- 1.9432e+01i	1.9432e+01	-3.5062e-03	Aeroelastic 5
3.9066e+00+ 1.9513e+01i	1.9900e+01	-1.9631e-01	Aeroelastic 8
3.9066e+00- 1.9513e+01i	1.9900e+01	-1.9631e-01	Aeroelastic 8
-2.7607e+00+ 2.2065e+01i	2.2237e+01	1.2415e-01	Aeroelastic 6
-2.7607e+00- 2.2065e+01i	2.2237e+01	1.2415e-01	Aeroelastic 6
-1.6394e-01+ 2.4311e+01i	2.4312e+01	6.7432e-03	Aeroelastic 7
-1.6394e-01- 2.4311e+01i	2.4312e+01	6.7432e-03	Aeroelastic 7
-2.0905e+01+ 1.4858e+01i	2.5647e+01	8.1509e-01	Unsteady Aero 4
-2.0905e+01- 1.4858e+01i	2.5647e+01	8.1509e-01	Unsteady Aero 5
-2.8893e+01	2.8893e+01	1.0000e+00	Unsteady Aero 6
-8.0596e+00+ 3.1974e+01i	3.2974e+01	2.4442e-01	Aeroelastic 9
-8.0596e+00- 3.1974e+01i	3.2974e+01	2.4442e-01	Aeroelastic 9
3.3601e+01	3.3601e+01	-1.0000e+00	Noncausal Acceleration
-3.3473e+00+ 3.3460e+01i	3.3627e+01	9.9541e-02	Aeroelastic 10
-3.3473e+00- 3.3460e+01i	3.3627e+01	9.9541e-02	Aeroelastic 10
-3.6607e+01+ 1.1028e+00i	3.6624e+01	9.9955e-01	Unsteady Aero 7
-3.6607e+01- 1.1028e+00i	3.6624e+01	9.9955e-01	Unsteady Aero 8
-1.3632e+00+ 3.7844e+01i	3.7868e+01	3.5999e-02	Aeroelastic 11
-1.3632e+00- 3.7844e+01i	3.7868e+01	3.5999e-02	Aeroelastic 11
7.8412e+00+ 3.7506e+01i	3.8317e+01	-2.0464e-01	Aeroelastic 13
7.8412e+00- 3.7506e+01i	3.8317e+01	-2.0464e-01	Aeroelastic 13
-1.1068e+00+ 4.8746e+01i	4.8759e+01	2.2700e-02	Aeroelastic 12
-1.1068e+00- 4.8746e+01i	4.8759e+01	2.2700e-02	Aeroelastic 12
-4.1280e-01+ 5.5171e+01i	5.5172e+01	7.4820e-03	Aeroelastic 14
-4.1280e-01- 5.5171e+01i	5.5172e+01	7.4820e-03	Aeroelastic 14
-1.4677e+00+ 5.6289e+01i	5.6308e+01	2.6066e-02	Aeroelastic 15
-1.4677e+00- 5.6289e+01i	5.6308e+01	2.6066e-02	Aeroelastic 15
-5.8229e+01	5.8229e+01	1.0000e+00	Unsteady Aero 9
-1.8979e-01+ 6.1174e+01i	6.1174e+01	3.1025e-03	Aeroelastic 16
-1.8979e-01- 6.1174e+01i	6.1174e+01	3.1025e-03	Aeroelastic 16
-5.5883e+00+ 6.5153e+01i	6.5393e+01	8.5458e-02	Aeroelastic 17
-5.5883e+00- 6.5153e+01i	6.5393e+01	8.5458e-02	Aeroelastic 17
9.0277e+01	9.0277e+01	-1.0000e+00	Unsteady Aero 10

Table 9. Zeros Of Langley Appendix C Model For 778 in Pitch Rate To Elevator Channel			
Gain = -3.0002e+04 rad/s/rad			
Root Location (1/s)	Freq. (rad/s)	Damping (-)	Description
0	0	-1.0000e+00	Long Period Remnant
-6.1608e-01	6.1608e-01	1.0000e+00	Tau Theta 2
-2.2150e+00	2.2150e+00	1.0000e+00	Unsteady Aero 1
-5.3828e+00+ 5.8472e-01i	5.4145e+00	9.9415e-01	Unsteady Aero 2
-5.3828e+00- 5.8472e-01i	5.4145e+00	9.9415e-01	Aeroelastic 1
6.0254e+00	6.0254e+00	-1.0000e+00	Aeroelastic 1
1.1268e+01	1.1268e+01	-1.0000e+00	Aeroelastic 2
-8.9740e+00+ 9.3435e+00i	1.2955e+01	6.9270e-01	Aeroelastic 2
-8.9740e+00- 9.3435e+00i	1.2955e+01	6.9270e-01	Noncausal Rate
-6.5832e-01+ 1.6398e+01i	1.6411e+01	4.0113e-02	Aeroelastic 4
-6.5832e-01- 1.6398e+01i	1.6411e+01	4.0113e-02	Aeroelastic 4
6.1091e-03+ 1.6847e+01i	1.6847e+01	-3.6261e-04	Aeroelastic 3
6.1091e-03- 1.6847e+01i	1.6847e+01	-3.6261e-04	Aeroelastic 3
7.2728e-02+ 1.9422e+01i	1.9422e+01	-3.7446e-03	Aeroelastic 5
7.2728e-02- 1.9422e+01i	1.9422e+01	-3.7446e-03	Aeroelastic 5
4.6870e+00+ 1.9411e+01i	1.9969e+01	-2.3471e-01	Aeroelastic 8
4.6870e+00- 1.9411e+01i	1.9969e+01	-2.3471e-01	Aeroelastic 8
-2.2057e+01	2.2057e+01	1.0000e+00	Unsteady Aero 3
-2.7513e+00+ 2.1928e+01i	2.2100e+01	1.2449e-01	Aeroelastic 6
-2.7513e+00- 2.1928e+01i	2.2100e+01	1.2449e-01	Aeroelastic 6
6.2303e-03+ 2.4383e+01i	2.4383e+01	-2.5552e-04	Aeroelastic 7
6.2303e-03- 2.4383e+01i	2.4383e+01	-2.5552e-04	Aeroelastic 7
-2.3211e+01+ 1.0317e+01i	2.5401e+01	9.1380e-01	Unsteady Aero 4
-2.3211e+01- 1.0317e+01i	2.5401e+01	9.1380e-01	Unsteady Aero 5
8.4858e+00+ 2.8813e+01i	3.0037e+01	-2.8251e-01	Unsteady Aero 6
8.4858e+00- 2.8813e+01i	3.0037e+01	-2.8251e-01	Noncausal Acceleration
-7.5645e+00+ 3.1676e+01i	3.2567e+01	2.3228e-01	Aeroelastic 9
-7.5645e+00- 3.1676e+01i	3.2567e+01	2.3228e-01	Aeroelastic 9
-3.9962e+00+ 3.5972e+01i	3.6193e+01	1.1041e-01	Aeroelastic 10
-3.9962e+00- 3.5972e+01i	3.6193e+01	1.1041e-01	Aeroelastic 10
-1.5286e+00+ 3.8051e+01i	3.8082e+01	4.0139e-02	Aeroelastic 11
-1.5286e+00- 3.8051e+01i	3.8082e+01	4.0139e-02	Aeroelastic 11
-3.9071e+01+ 5.6219e+00i	3.9473e+01	9.8981e-01	Unsteady Aero 7
-3.9071e+01- 5.6219e+00i	3.9473e+01	9.8981e-01	Unsteady Aero 8
-4.0767e+01	4.0767e+01	1.0000e+00	Unsteady Aero 9
-4.5276e+00+ 4.3970e+01i	4.4202e+01	1.0243e-01	Aeroelastic 13
-4.5276e+00- 4.3970e+01i	4.4202e+01	1.0243e-01	Aeroelastic 13
-1.0856e+00+ 4.8692e+01i	4.8704e+01	2.2290e-02	Aeroelastic 12
-1.0856e+00- 4.8692e+01i	4.8704e+01	2.2290e-02	Aeroelastic 12
-5.9652e-01+ 5.5121e+01i	5.5125e+01	1.0821e-02	Aeroelastic 14
-5.9652e-01- 5.5121e+01i	5.5125e+01	1.0821e-02	Aeroelastic 14
-1.3912e+00+ 5.6331e+01i	5.6348e+01	2.4689e-02	Aeroelastic 15
-1.3912e+00- 5.6331e+01i	5.6348e+01	2.4689e-02	Aeroelastic 15
-6.6529e-02+ 6.1180e+01i	6.1180e+01	1.0874e-03	Aeroelastic 16
-6.6529e-02- 6.1180e+01i	6.1180e+01	1.0874e-03	Aeroelastic 16
-3.5584e+00+ 6.3113e+01i	6.3213e+01	5.6292e-02	Aeroelastic 17
-3.5584e+00- 6.3113e+01i	6.3213e+01	5.6292e-02	Aeroelastic 17
-6.7604e+01	6.7604e+01	1.0000e+00	Unsteady Aero 10

Table 10. Zeros Of Langley Appendix C Model For 2,115 in Pitch Rate To Elevator Channel			
Gain = 1.0629e+04 rad/s/rad			
Root Location (1/s)	Freq. (rad/s)	Damping (-)	Description
0	0	-1.0000e+00	Long Period Remnant
-5.4398e-01	5.4398e-01	1.0000e+00	Tau Theta 2
-2.2173e+00	2.2173e+00	1.0000e+00	Unsteady Aero 1
-4.8276e+00	4.8276e+00	1.0000e+00	Unsteady Aero 2
3.4063e-01+ 5.7676e+00i	5.7776e+00	-5.8957e-02	Aeroelastic 1
3.4063e-01- 5.7676e+00i	5.7776e+00	-5.8957e-02	Aeroelastic 1
1.3975e+01	1.3975e+01	-1.0000e+00	Aeroelastic 2
-1.1762e+01+ 8.5312e+00i	1.4531e+01	8.0950e-01	Aeroelastic 2
-1.1762e+01- 8.5312e+00i	1.4531e+01	8.0950e-01	Unsteady Aero 2
-6.4042e-01+ 1.6822e+01i	1.6834e+01	3.8043e-02	Aeroelastic 4
-6.4042e-01- 1.6822e+01i	1.6834e+01	3.8043e-02	Aeroelastic 4
1.3090e-02+ 1.6853e+01i	1.6853e+01	-7.7670e-04	Aeroelastic 3
1.3090e-02- 1.6853e+01i	1.6853e+01	-7.7670e-04	Aeroelastic 3
-9.0321e-02+ 1.9434e+01i	1.9434e+01	4.6475e-03	Aeroelastic 5
-9.0321e-02- 1.9434e+01i	1.9434e+01	4.6475e-03	Aeroelastic 5
4.2390e+00+ 1.9224e+01i	1.9686e+01	-2.1533e-01	Noncausal Rate
4.2390e+00- 1.9224e+01i	1.9686e+01	-2.1533e-01	Noncausal Acceleration
-7.5631e-01+ 2.0772e+01i	2.0786e+01	3.6386e-02	Aeroelastic 7
-7.5631e-01- 2.0772e+01i	2.0786e+01	3.6386e-02	Aeroelastic 7
-2.1382e+01	2.1382e+01	1.0000e+00	Unsteady Aero 4
-2.4899e+00+ 2.2288e+01i	2.2427e+01	1.1102e-01	Aeroelastic 6
-2.4899e+00- 2.2288e+01i	2.2427e+01	1.1102e-01	Aeroelastic 6
-2.8239e-01+ 2.5379e+01i	2.5381e+01	1.1126e-02	Aeroelastic 8
-2.8239e-01- 2.5379e+01i	2.5381e+01	1.1126e-02	Aeroelastic 8
-1.1680e+00+ 3.3313e+01i	3.3333e+01	3.5041e-02	Aeroelastic 10
-1.1680e+00- 3.3313e+01i	3.3333e+01	3.5041e-02	Aeroelastic 10
-3.3916e+01	3.3916e+01	1.0000e+00	Unsteady Aero 5
-7.3553e+00+ 3.4098e+01i	3.4882e+01	2.1086e-01	Aeroelastic 9
-7.3553e+00- 3.4098e+01i	3.4882e+01	2.1086e-01	Aeroelastic 9
-3.4286e+01+ 1.1550e+01i	3.6180e+01	9.4767e-01	Unsteady Aero 6
-3.4286e+01- 1.1550e+01i	3.6180e+01	9.4767e-01	Unsteady Aero 7
-3.8270e+01	3.8270e+01	1.0000e+00	Unsteady Aero 8
-1.0582e+00+ 3.8333e+01i	3.8347e+01	2.7595e-02	Aeroelastic 11
-1.0582e+00- 3.8333e+01i	3.8347e+01	2.7595e-02	Aeroelastic 11
-4.6407e+01	4.6407e+01	1.0000e+00	Unsteady Aero 9
-1.1995e+00+ 4.8751e+01i	4.8766e+01	2.4597e-02	Aeroelastic 12
-1.1995e+00- 4.8751e+01i	4.8766e+01	2.4597e-02	Aeroelastic 12
-1.6505e-01+ 5.4365e+01i	5.4365e+01	3.0360e-03	Aeroelastic 13
-1.6505e-01- 5.4365e+01i	5.4365e+01	3.0360e-03	Aeroelastic 13
-8.2232e-01+ 5.6449e+01i	5.6455e+01	1.4566e-02	Aeroelastic 14
-8.2232e-01- 5.6449e+01i	5.6455e+01	1.4566e-02	Aeroelastic 14
-2.4569e-01+ 6.1336e+01i	6.1336e+01	4.0056e-03	Aeroelastic 16
-2.4569e-01- 6.1336e+01i	6.1336e+01	4.0056e-03	Aeroelastic 16
-1.0850e+00+ 6.3509e+01i	6.3519e+01	1.7082e-02	Aeroelastic 15
-1.0850e+00- 6.3509e+01i	6.3519e+01	1.7082e-02	Aeroelastic 15
-8.1470e+00+ 6.5886e+01i	6.6388e+01	1.2272e-01	Aeroelastic 17
-8.1470e+00- 6.5886e+01i	6.6388e+01	1.2272e-01	Aeroelastic 17
-6.6991e+01	6.6991e+01	1.0000e+00	Unsteady Aero 10

Table 11. Zeros Of Langley Appendix C Model For 2,525 in Pitch Rate To Elevator Channel			
Gain = -2.1164e+04 rad/s/rad			
Root Location (1/s)	Freq. (rad/s)	Damping (-)	Description
0	0	-1.0000e+00	Long Period Remnant
-5.0748e-01	5.0748e-01	1.0000e+00	Tau Theta 2
-2.2193e+00	2.2193e+00	1.0000e+00	Unsteady Aero 1
-4.7833e+00	4.7833e+00	1.0000e+00	Unsteady Aero 2
2.0185e-01+ 4.8141e+00i	4.8183e+00	-4.1893e-02	Aeroelastic 1
2.0185e-01- 4.8141e+00i	4.8183e+00	-4.1893e-02	Aeroelastic 1
-9.7248e-01+ 1.1729e+01i	1.1769e+01	8.2631e-02	Aeroelastic 2
-9.7248e-01- 1.1729e+01i	1.1769e+01	8.2631e-02	Aeroelastic 2
-1.8062e-04+ 1.6859e+01i	1.6859e+01	1.0714e-05	Aeroelastic 3
-1.8062e-04- 1.6859e+01i	1.6859e+01	1.0714e-05	Aeroelastic 3
-5.5810e-01+ 1.7749e+01i	1.7758e+01	3.1428e-02	Aeroelastic 4
-5.5810e-01- 1.7749e+01i	1.7758e+01	3.1428e-02	Aeroelastic 4
-1.0054e-01+ 1.9400e+01i	1.9401e+01	5.1822e-03	Aeroelastic 5
-1.0054e-01- 1.9400e+01i	1.9401e+01	5.1822e-03	Aeroelastic 5
-1.5929e+01+ 1.1237e+01i	1.9494e+01	8.1714e-01	Noncausal Rate
-1.5929e+01- 1.1237e+01i	1.9494e+01	8.1714e-01	Noncausal Acceleration
-1.9961e+01	1.9961e+01	1.0000e+00	Unsteady Aero 3
-3.1350e+00+ 2.1292e+01i	2.1522e+01	1.4567e-01	Aeroelastic 6
-3.1350e+00- 2.1292e+01i	2.1522e+01	1.4567e-01	Aeroelastic 6
-3.7192e-01+ 2.3357e+01i	2.3360e+01	1.5921e-02	Aeroelastic 7
-3.7192e-01- 2.3357e+01i	2.3360e+01	1.5921e-02	Aeroelastic 7
2.4878e+01+ 1.1402e+01i	2.7367e+01	-9.0907e-01	Unsteady Aero 4
2.4878e+01- 1.1402e+01i	2.7367e+01	-9.0907e-01	Unsteady Aero 5
-2.7865e+01	2.7865e+01	1.0000e+00	Unsteady Aero 6
-5.3162e-01+ 2.8026e+01i	2.8031e+01	1.8965e-02	Aeroelastic 8
-5.3162e-01- 2.8026e+01i	2.8031e+01	1.8965e-02	Aeroelastic 8
-5.2232e+00+ 3.3660e+01i	3.4063e+01	1.5334e-01	Aeroelastic 9
-5.2232e+00- 3.3660e+01i	3.4063e+01	1.5334e-01	Aeroelastic 9
2.6002e+00+ 3.6483e+01i	3.6576e+01	-7.1090e-02	Aeroelastic 10
2.6002e+00- 3.6483e+01i	3.6576e+01	-7.1090e-02	Aeroelastic 10
-3.7682e+01	3.7682e+01	1.0000e+00	Unsteady Aero 7
-1.1017e+00+ 3.8228e+01i	3.8244e+01	2.8807e-02	Aeroelastic 11
-1.1017e+00- 3.8228e+01i	3.8244e+01	2.8807e-02	Aeroelastic 11
-3.9698e+01+ 1.1981e+01i	4.1466e+01	9.5735e-01	Unsteady Aero 8
-3.9698e+01- 1.1981e+01i	4.1466e+01	9.5735e-01	Unsteady Aero 9
-4.6578e-01+ 4.9887e+01i	4.9889e+01	9.3363e-03	Aeroelastic 13
-4.6578e-01- 4.9887e+01i	4.9889e+01	9.3363e-03	Aeroelastic 13
2.4699e+00+ 5.1007e+01i	5.1066e+01	-4.8367e-02	Aeroelastic 12
2.4699e+00- 5.1007e+01i	5.1066e+01	-4.8367e-02	Aeroelastic 12
-2.9587e+01+ 4.6609e+01i	5.5207e+01	5.3593e-01	Aeroelastic 15
-2.9587e+01- 4.6609e+01i	5.5207e+01	5.3593e-01	Aeroelastic 15
-2.6015e-01+ 5.5480e+01i	5.5481e+01	4.6889e-03	Aeroelastic 14
-2.6015e-01- 5.5480e+01i	5.5481e+01	4.6889e-03	Aeroelastic 14
-1.5767e-01+ 6.1067e+01i	6.1068e+01	2.5818e-03	Aeroelastic 16
-1.5767e-01- 6.1067e+01i	6.1068e+01	2.5818e-03	Aeroelastic 16
-6.2815e+00+ 6.2538e+01i	6.2853e+01	9.9940e-02	Aeroelastic 17
-6.2815e+00- 6.2538e+01i	6.2853e+01	9.9940e-02	Aeroelastic 17
-6.5238e+01	6.5238e+01	1.0000e+00	Unsteady Aero 10

Table 12. Zeros Of Langley Appendix C Model For 3,157 in Pitch Rate To Elevator Channel			
Gain = -1.7268e+06 rad/s/rad			
Root Location (1/s)	Freq. (rad/s)	Damping (-)	Description
0	0	-1.0000e+00	Long Period Remnant
-2.9959e-01	2.9959e-01	1.0000e+00	Tau Theta 2
-2.2299e+00	2.2299e+00	1.0000e+00	Unsteady Aero 1
-4.6107e+00	4.6107e+00	1.0000e+00	Unsteady Aero 2
-2.5691e+00+ 4.4773e+00i	5.1620e+00	4.9769e-01	Aeroelastic 1
-2.5691e+00- 4.4773e+00i	5.1620e+00	4.9769e-01	Aeroelastic 1
3.0134e+00+ 4.2686e+00i	5.2251e+00	-5.7671e-01	Aeroelastic 2
3.0134e+00- 4.2686e+00i	5.2251e+00	-5.7671e-01	Aeroelastic 2
9.7752e+00+ 9.9692e+00i	1.3962e+01	-7.0012e-01	Noncausal Rate
9.7752e+00- 9.9692e+00i	1.3962e+01	-7.0012e-01	Noncausal Acceleration
-2.1867e-04+ 1.6858e+01i	1.6858e+01	1.2971e-05	Aeroelastic 3
-2.1867e-04- 1.6858e+01i	1.6858e+01	1.2971e-05	Aeroelastic 3
-1.5868e+01+ 5.9859e+00i	1.6960e+01	9.3564e-01	Unsteady Aero 3
-1.5868e+01- 5.9859e+00i	1.6960e+01	9.3564e-01	Unsteady Aero 4
-5.4668e-01+ 1.7976e+01i	1.7984e+01	3.0398e-02	Aeroelastic 4
-5.4668e-01- 1.7976e+01i	1.7984e+01	3.0398e-02	Aeroelastic 4
-1.8840e+01	1.8840e+01	1.0000e+00	Unsteady Aero 5
-2.0291e-01+ 1.9465e+01i	1.9466e+01	1.0424e-02	Aeroelastic 5
-2.0291e-01- 1.9465e+01i	1.9466e+01	1.0424e-02	Aeroelastic 5
-3.1819e+00+ 2.0016e+01i	2.0267e+01	1.5700e-01	Aeroelastic 6
-3.1819e+00- 2.0016e+01i	2.0267e+01	1.5700e-01	Aeroelastic 6
-9.2883e-01+ 2.3202e+01i	2.3221e+01	4.0000e-02	Aeroelastic 7
-9.2883e-01- 2.3202e+01i	2.3221e+01	4.0000e-02	Aeroelastic 7
-2.5133e+01	2.5133e+01	1.0000e+00	Unsteady Aero 6
-8.4607e-01+ 2.7478e+01i	2.7491e+01	3.0776e-02	Aeroelastic 8
-8.4607e-01- 2.7478e+01i	2.7491e+01	3.0776e-02	Aeroelastic 8
-6.8184e-01+ 3.1296e+01i	3.1303e+01	2.1782e-02	Aeroelastic 10
-6.8184e-01- 3.1296e+01i	3.1303e+01	2.1782e-02	Aeroelastic 10
-1.0021e+01+ 3.3156e+01i	3.4637e+01	2.8931e-01	Aeroelastic 9
-1.0021e+01- 3.3156e+01i	3.4637e+01	2.8931e-01	Aeroelastic 9
-3.6957e+01+ 1.4662e+00i	3.6986e+01	9.9921e-01	Unsteady Aero 7
-3.6957e+01- 1.4662e+00i	3.6986e+01	9.9921e-01	Unsteady Aero 8
-1.3359e+00+ 3.7891e+01i	3.7915e+01	3.5234e-02	Aeroelastic 11
-1.3359e+00- 3.7891e+01i	3.7915e+01	3.5234e-02	Aeroelastic 11
-4.3994e+00+ 4.2963e+01i	4.3187e+01	1.0187e-01	Aeroelastic 12
-4.3994e+00- 4.2963e+01i	4.3187e+01	1.0187e-01	Aeroelastic 12
-3.0716e-01+ 4.9059e+01i	4.9060e+01	6.2610e-03	Aeroelastic 13
-3.0716e-01- 4.9059e+01i	4.9060e+01	6.2610e-03	Aeroelastic 13
-5.1854e+01	5.1854e+01	1.0000e+00	Unsteady Aero 9
1.0266e-01+ 5.3739e+01i	5.3739e+01	-1.9104e-03	Aeroelastic 14
1.0266e-01- 5.3739e+01i	5.3739e+01	-1.9104e-03	Aeroelastic 14
-4.4628e-01+ 5.5929e+01i	5.5931e+01	7.9791e-03	Aeroelastic 15
-4.4628e-01- 5.5929e+01i	5.5931e+01	7.9791e-03	Aeroelastic 15
-2.9175e-02+ 6.1142e+01i	6.1142e+01	4.7718e-04	Aeroelastic 16
-2.9175e-02- 6.1142e+01i	6.1142e+01	4.7718e-04	Aeroelastic 16
-4.2451e+00+ 6.3687e+01i	6.3829e+01	6.6508e-02	Aeroelastic 17
-4.2451e+00- 6.3687e+01i	6.3829e+01	6.6508e-02	Aeroelastic 17
-7.6529e+01	7.6529e+01	1.0000e+00	Unsteady Aero 10

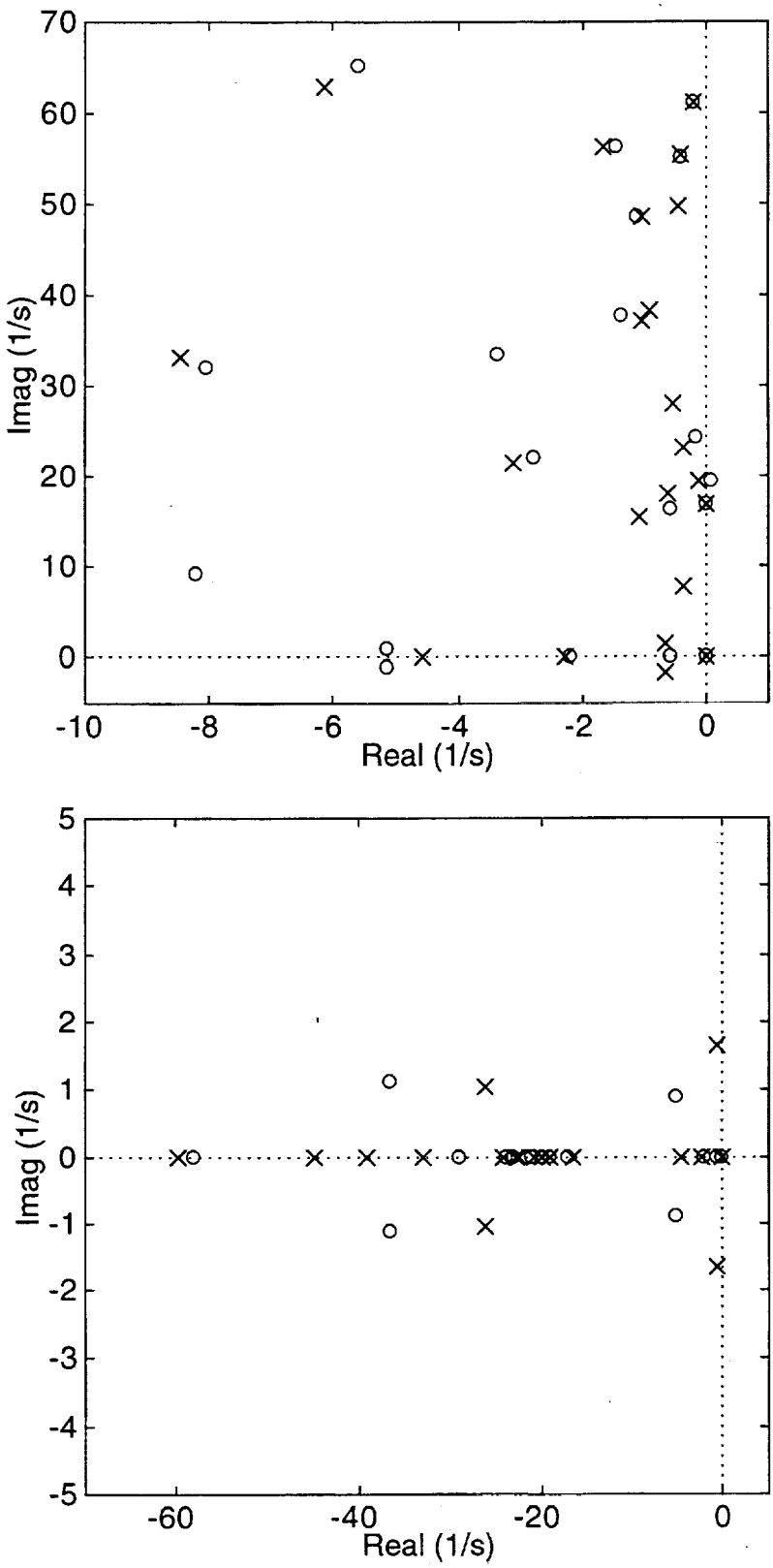

Figure 14. Pole-Zero Pattern Of Langley Appendix C Model For 319 in Pitch Rate To Elevator Channel

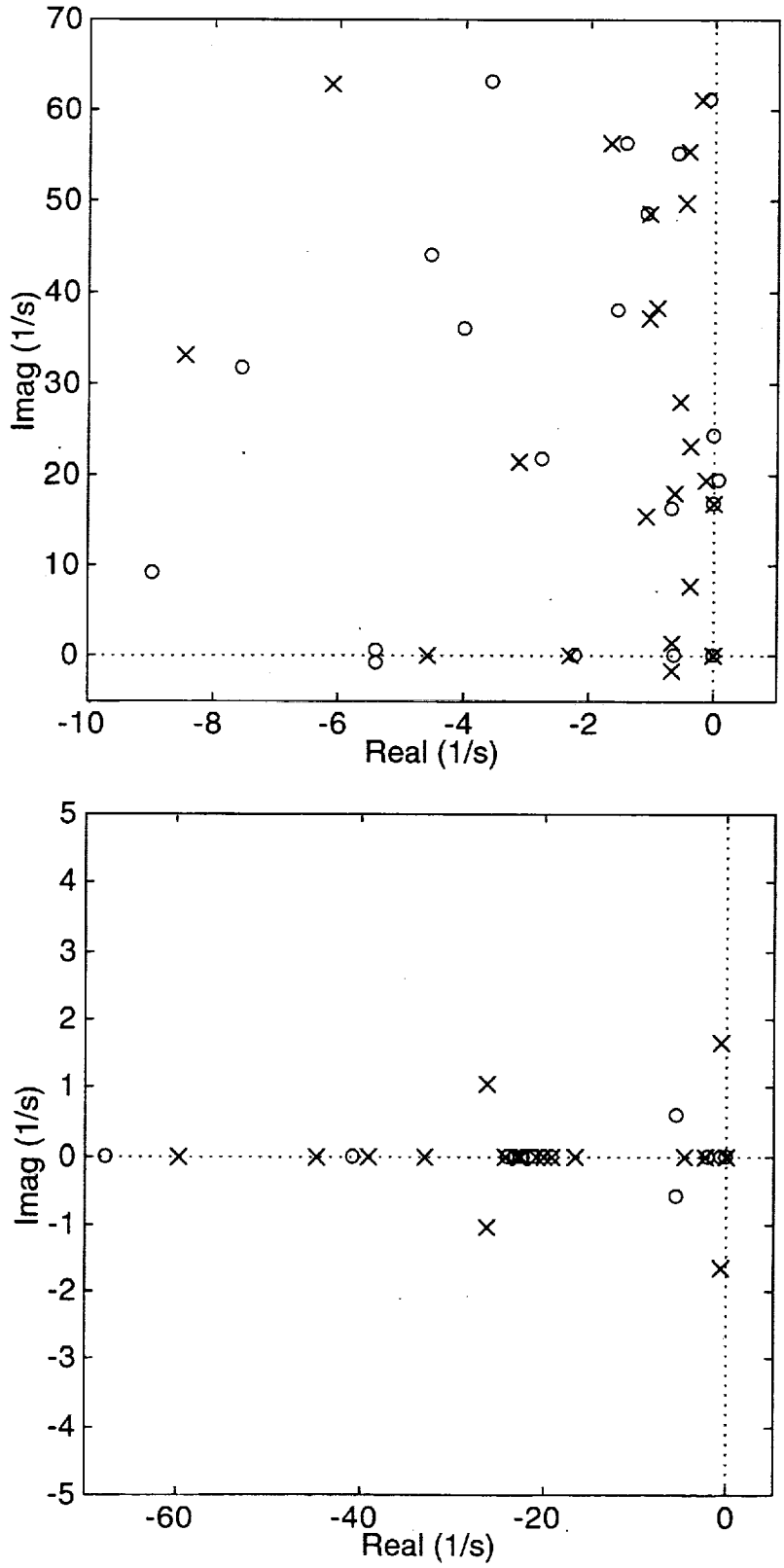

Figure 15. Pole-Zero Pattern Of Langley Appendix C Model For 778 in Pitch Rate To Elevator Channel

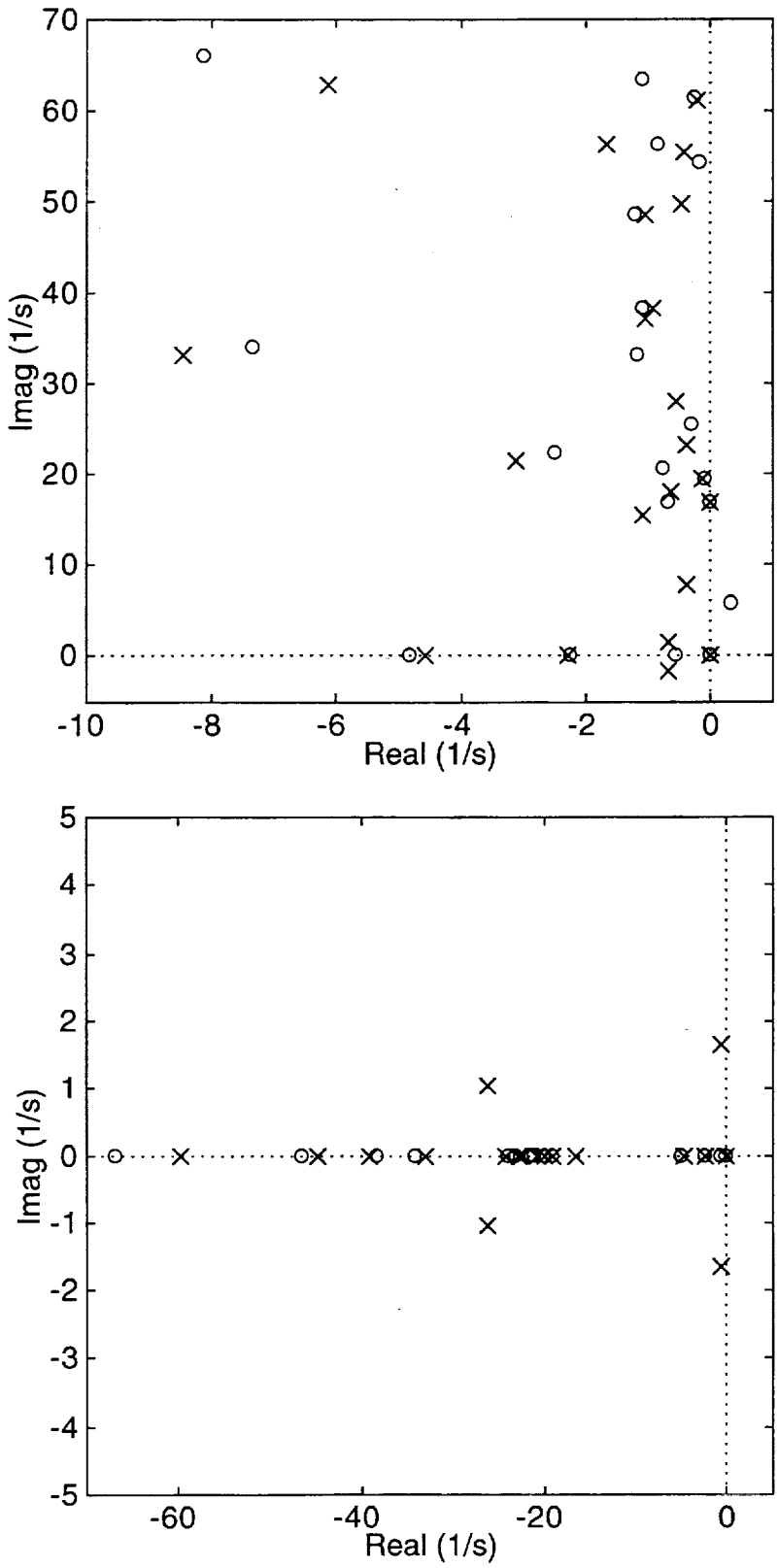

Figure 16. Pole-Zero Pattern Of Langley Appendix C Model For 2,115 in Pitch Rate To Elevator Channel

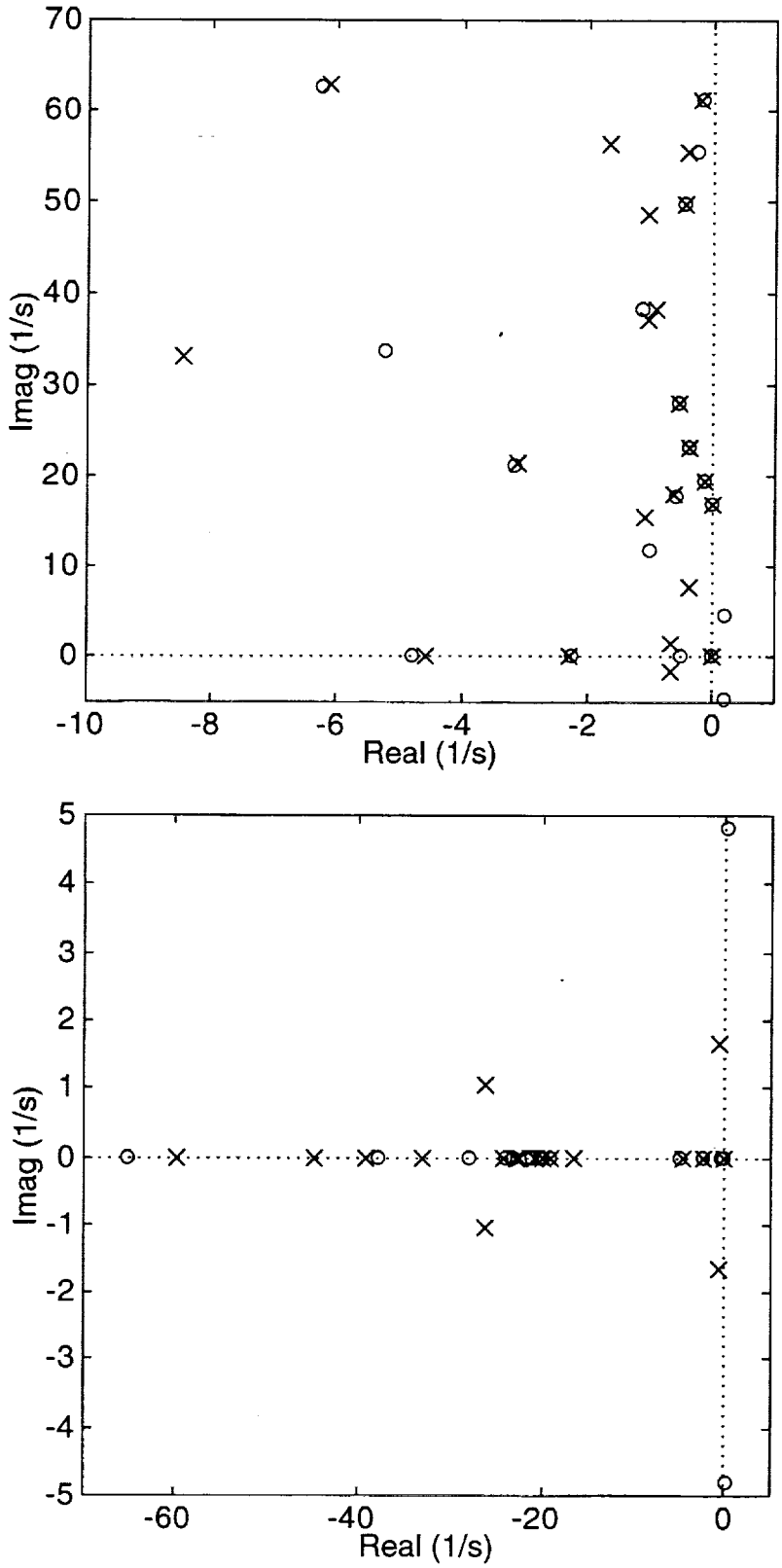

Figure 17. Pole-Zero Pattern Of Langley Appendix C Model For 2,525 in Pitch Rate To Elevator Channel

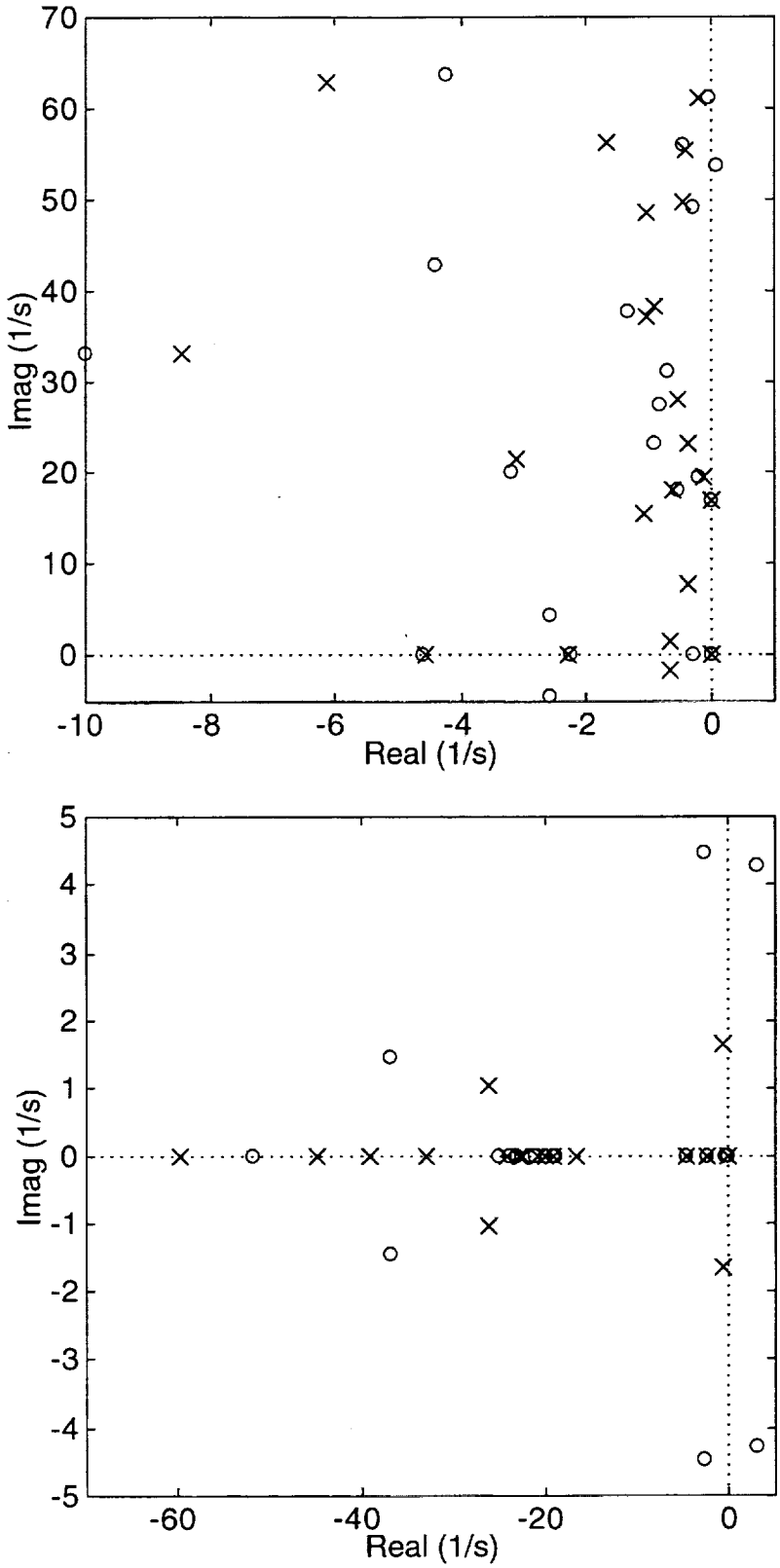

Figure 18. Pole-Zero Pattern Of Langley Appendix C Model For 3,157 in Pitch Rate To Elevator Channel

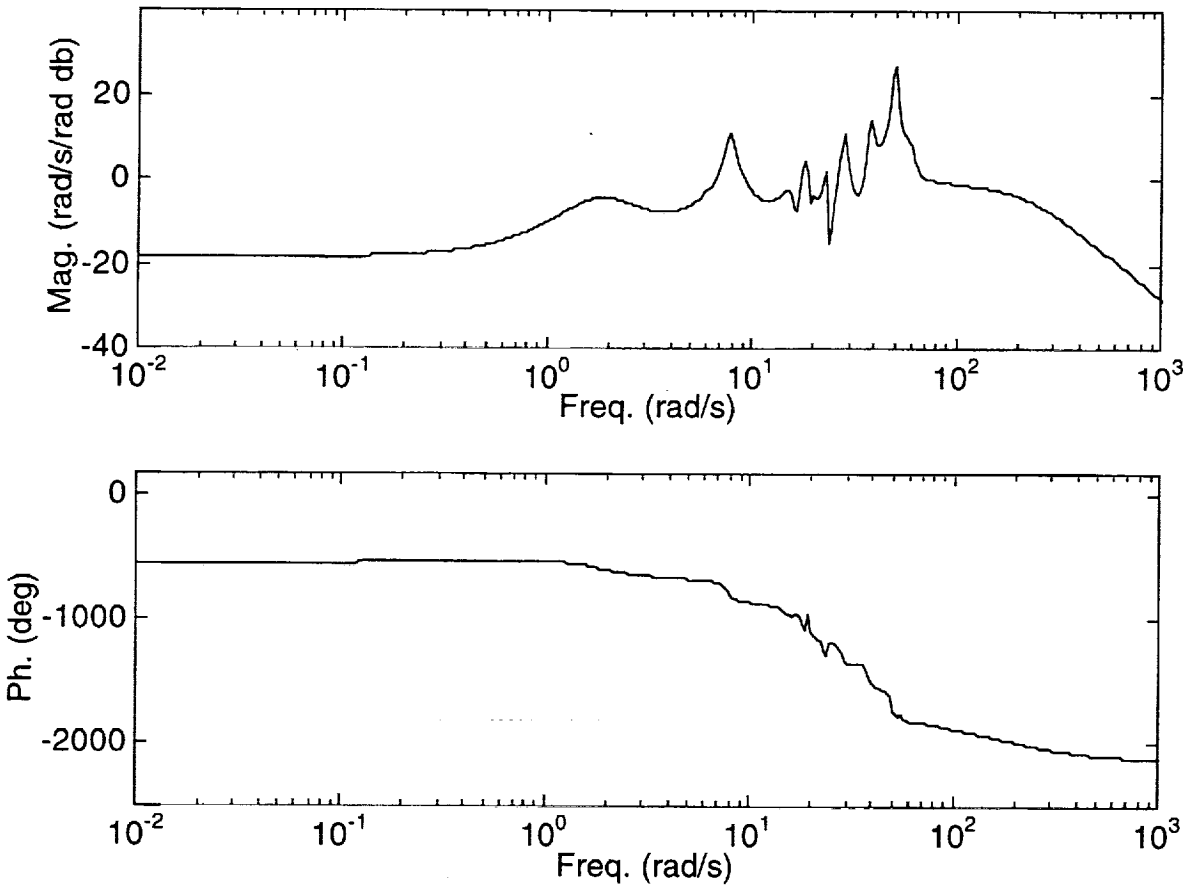

Figure 19. Frequency Response Of Langley Appendix C Model For 319 in Pitch Rate To Elevator Channel

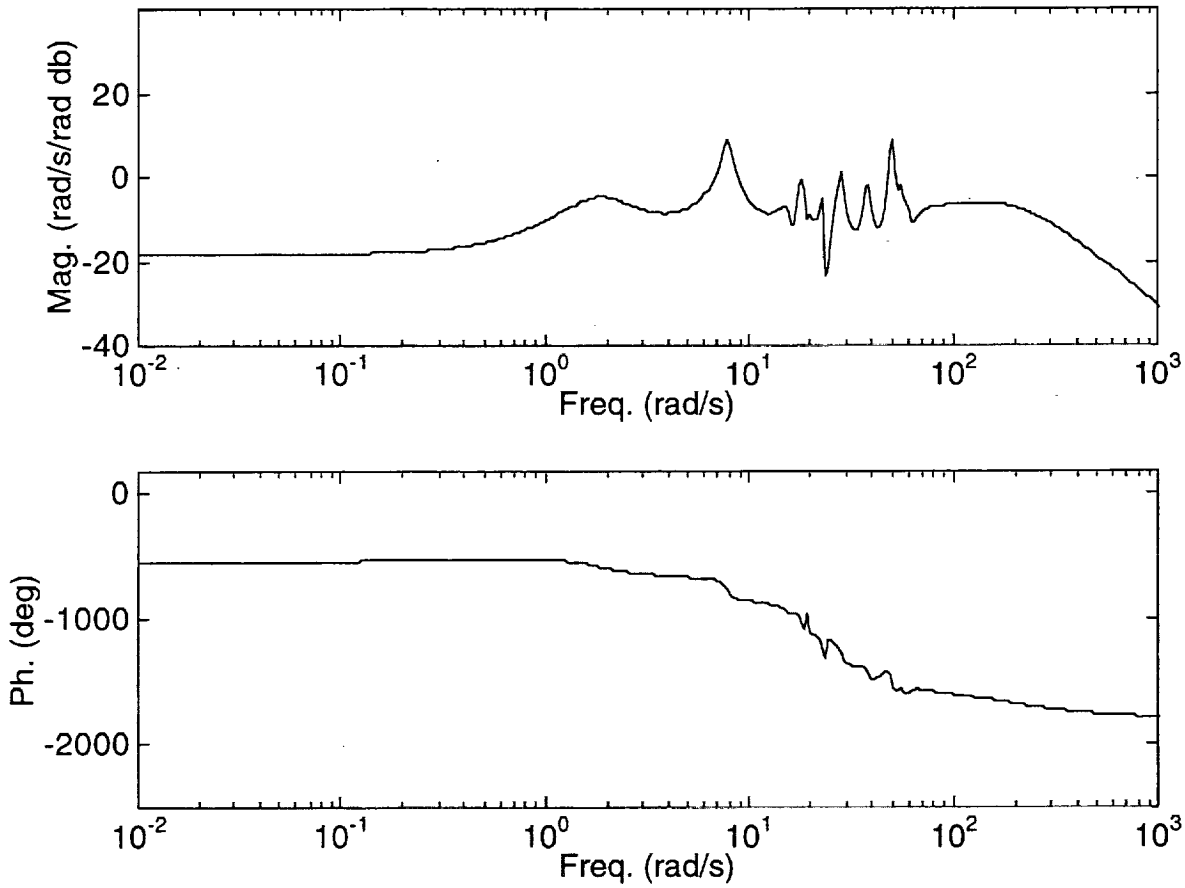

Figure 20. Frequency Response Of Langley Appendix C Model
For 778 in Pitch Rate To Elevator Channel

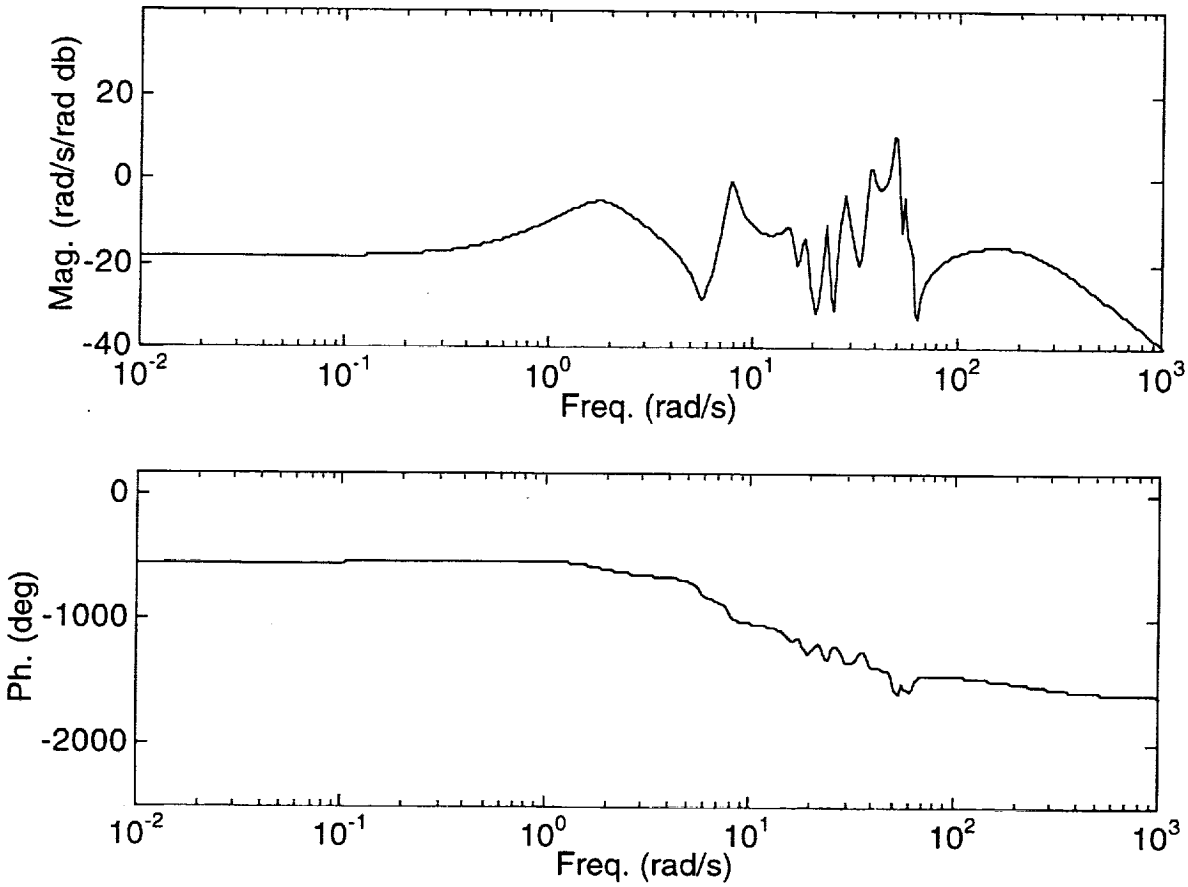

Figure 21. Frequency Response Of Langley Appendix C Model
For 2,115 in Pitch Rate To Elevator Channel

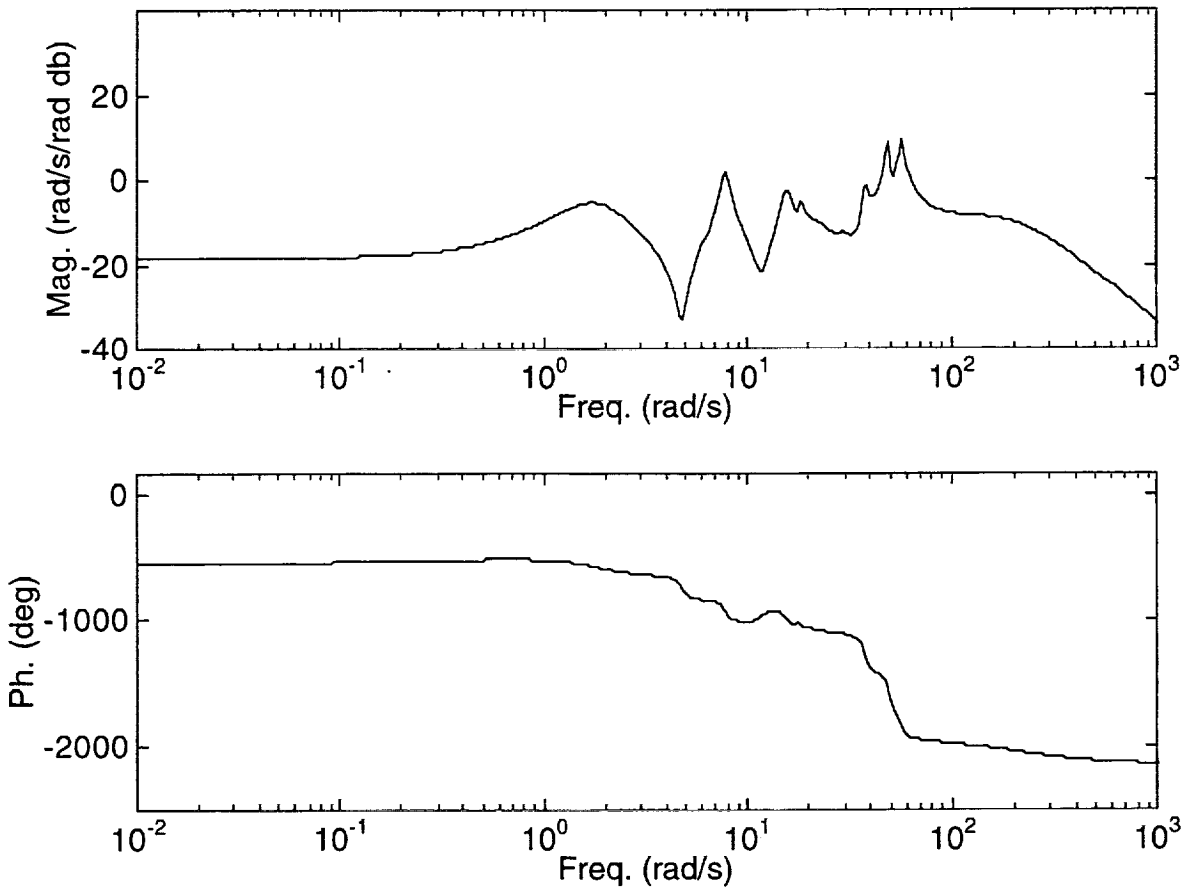

Figure 22. Frequency Response Of Langley Appendix C Model
For 2,525 in Pitch Rate To Elevator Channel

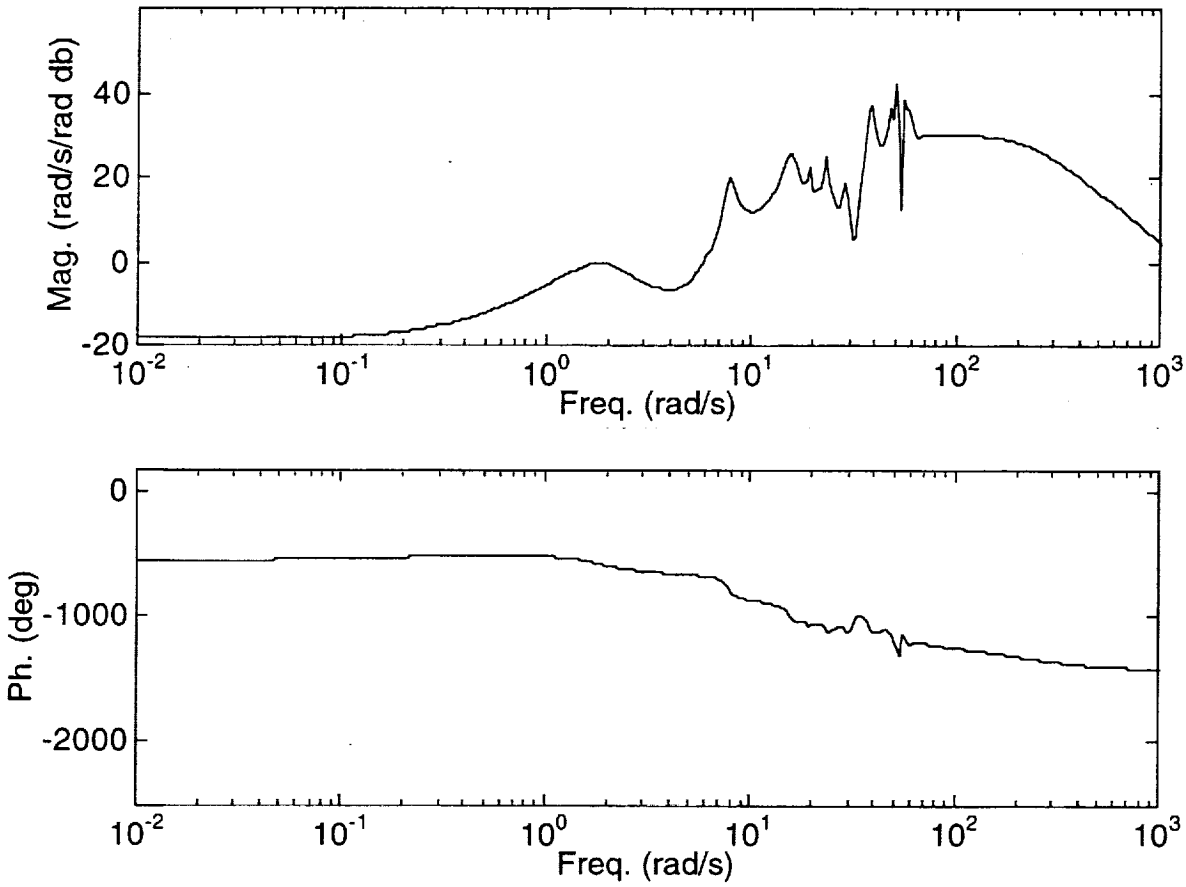

Figure 23. Frequency Response Of Langley Appendix C Model
For 3,157 in Pitch Rate To Elevator Channel

Examination of the poles in Tabs. 1 and 7 for the Boeing and Langley models reveals very good agreement, considering that one model does not have explicit unsteady aerodynamic states and the other model does. Aeroelastic pole numerical values match up well, with some departure beyond 40 rad/s noted. One conclusion that can be drawn from this observation is that the "A" matrix development, and hence the stability derivative computations can be looked upon with confidence. This result is a significant milestone in the model validation process and should not be taken lightly. Similar conclusions can not be reached, however, for the transfer function numerators.

Consider the frequency response plots for the 2,115 in rate gyro location in Figs. 11 and 21. The magnitude and phase curves are not similar below 0.1 rad/s. However, this difference can be attributed to the lack of a forward speed degree of freedom in the Langley model. In the 0.1 to 5 rad/s frequency region the frequency response curves have acceptable correlation. The magnitude and phase shapes are not at all alike in the aeroelastic frequency range, beyond 5 rad/s. Fig. 11 indicates virtually no aeroelastic activity in the Boeing model, whereas the Langley model displays severe aeroelastic motions. Further, the average attenuation characteristics are different. The aeroelastic zeros in the two transfer functions are fundamentally different, or the state space "B" and "C" matrices are in disagreement.

Factors which influence pitch rate to elevator numerator characteristics, other than stability derivatives, include the unsteady aerodynamic modeling differences, mode shapes/slopes at the elevator and rate gyro locations, and the control derivatives. In particular, control derivatives associated with the aeroelastic modes since the frequency responses agree within the 0.1 to 5 rad/s rigid-body frequency range. These factors are candidate sources of the model mismatch and are discussed below.

Recall the Boeing model has no explicit unsteady aerodynamic states where as the Langley model does. Careful examination of Tab. 10 reveals each real unsteady aerodynamic pole has an associated zero (not necessarily real) in rough proximity. One can reasonably conclude that the significant model differences are not driven by the explicit unsteady aerodynamic poles and

associated zeros. However, a significant difference due to the unsteady aerodynamic model does exist. Note that the noncausal inputs in Eq. (1.1) lead to a pair of zeros in each pitch rate transfer function. These noncausal zeros are primarily, but not completely, determined by the quadratic term $B''s^2+B's+B$. The third order actuator returns the familiar rate-to-force attenuation characteristics. In the Boeing model, these zeros are located well beyond the frequency region of interest, as expected if the B' and B" matrices are small. Therefore, the actuator poles attenuate well before the noncausal zeros amplify. Such is not the case with the Langley model. With some uncertainty as to the labeling of the zeros, the noncausal zeros fall within the frequency range of interest. In fact, the zeros are well inside the actuator bandwidth. The noncausal zeros amplify before the actuator poles attenuate. The noncausal terms B' and B" are thus the source of the attenuation differences between the two models.

The differences in the amount of aeroelastic dynamics superimposed upon the average attenuation is another issue. By deductive reasoning, the probable source of this mismatch feature lies with either the mode shapes/slopes or aeroelastic control derivatives. The aeroelastic control derivative $F_{i_{\delta_E}}$ is a function of the aerodynamic characteristics at each structural node due to elevator deflections $c_{i_{\delta_E}}$, as well as the mode shape ϕ_i and mode mass m_i, or

$$F_{i_{\delta_E}} = \frac{\sum_i \bar{q}_i \bar{S}_i \phi_i \, c_{i_{\delta_E}}}{m_i} \tag{1.8}$$

Comparison of model differences at this level is beyond the scope of the limited data made available to the contractors, and will not be pursued further. However, since measured pitch rate is the response of interest here, the mode slopes can be compared quite easily. The pitch rate is given by

$$q_{xs} = q - \sum_i \phi_i' \ddot{\eta}_i \tag{1.9}$$

Note the nonzero elements of the state space "C" matrix (except for the element associated with q) correspond to the negative of the mode slopes evaluated at the sensor location. Direct comparison between the mode slope values does not lead to a match. No match could be achieved with scaling either. With these facts laid out, it is reasonably safe to conclude that at least some of the

"aeroelastic" model mismatch is due to computation of the mode slope values, integration of the mode slopes into the dynamic model, or different modal data sets. Further conclusions can not be drawn until the modal/aeroelastic control derivative data from both modeling sources and how they are generated and used is compared one for one. The major implication here is that, at this time in the HSCT program, any and all dynamic aeroelastic models should be used with caution.

Based upon the contractor's experience with other aeroelastic models of large, high-speed vehicles (B-1, SCRA), the Appendix B and C models have several peculiar characteristics. Concerning the Boeing model, it is rather unrealistic to expect, with a highly elastic vehicle, all aeroelastic modes have coincident anti-nodes at 2,115 in. In other words, lessening of aeroelastic contamination in the feedback signal by careful sensor placement has taken care of all 15 modes (see Figs. 6 and 11). Also note in Figs. 4-8 that nonminimum phase aeroelastic zeros rarely occur for drastic changes in the sensor location. Especially note the 1st aeroelastic zeros become nonminimum phase for aft sensor locations. This behavior violates the "physics" of a 1st fuselage bending mode shape. Finally observe how the 1st aeroelastic zeros migrate horizontally, rather than vertically, as the sensor is moved from fore to aft. This behavior is atypical.[8,10]

Now focusing on the Langley model, attenuation characteristics of the magnitude frequency response in Fig. 21 are quite puzzling. Typically with aeroelastic models, attenuation characteristics are a gradual (-20 db/dec) roll off due to the fundamental rigid-body physics of rate-to-force transfers with aeroelastic peaks and troughs superimposed, not necessarily small. Here, the -20 db/dec attenuation behavior is missing in the 10 to 100 rad/s frequency range, and it has been traced to the noncausal zeros. This behavior leads to enormous aeroelastic peaks. Further, this model corresponds to mass case M5. Trend studies have revealed that the M5 data set is a "$+3\sigma$ data point," going against the data set trends.[17]

C. Cycle 1 Simulation/ISAC Aggregate Model

Despite these modeling concerns, one model made available to the contractor was deemed sufficiently accurate for use in control design studies. Appendix D contains the description of this

Langley generated model. Disturbing features similar to those associated with the Appendix B and C models are not present. Qualitative characteristics are consistent with other large, elastic, high-speed vehicles the contractors have experience with.

The one feature lacking in the original model is the missing forward speed degree of freedom. Before moving ahead with control design studies, it was considered prudent to include this degree of freedom, especially since the rigid-body modes are expected to be atypical, i.e., relaxed static stability with the unstable real axis mode significantly participating in the forward speed degree of freedom.

Therefore, an aggregate model was constructed using the original ISAC model augmented with the missing u stability derivatives computed from the rigid-body Cycle 1 Simulation data base.[16] The state space "A" and "B" matrices for a rigid aircraft are

$$A = \begin{bmatrix} X_u & X_w & X_q & -\cos(\Theta)G \\ Z_u & Z_w & U+Z_q & -\sin(\Theta)G \\ M_u & M_w & M_q & 0 \\ 0 & 0 & 1 & 0 \end{bmatrix}, \quad B = \begin{bmatrix} X_{\delta_E} & \ldots X_{\delta_{TEi}} \ldots \\ Z_{\delta_E} & \ldots Z_{\delta_{TEi}} \ldots \\ M_{\delta_E} & \ldots M_{\delta_{TEi}} \ldots \\ 0 & \ldots 0 \ldots \end{bmatrix} \tag{1.10}$$

The missing terms include X_u, X_w, X_q, $-\cos(\Theta)G$, X_{δ_E}, $X_{\delta_{TEi}}$, Z_u, and M_u. Tables 13 and 14 list the numerical values for the Cycle 1 Simulation model and a rigidized (residualized) ISAC model. Note the very good agreement between the stability and control derivatives associated with the w and θ degrees of freedom. This accuracy raises confidence in the aggregate model in Appendix D.

Table 15 lists the poles of the airframe-actuator model. At this low-speed, low-altitude condition, the HSCT inherent pitch instability is clearly present. Rigid-body modes consist of the so called third oscillatory mode and two real axis modes, one fast and stable, the other slow and unstable. Aeroelastic mode frequencies include the 1st and 2nd mode values at 7.7 and 12.8 rad/s all the way up to a value of 65.1 rad/s for the 17th mode with unsteady aerodynamic modes throughout this frequency range. Unsteady aerodynamic modes have reciprocal time constants ranging from 0.64 to 29.4 1/s. Damping ratios for the aeroelastic modes are again extremely light, as expected.

Tables 16 and 17 contain the gains and zeros for measured pitch rate to elevator transfer functions at two key locations along the fuselage centerline, 1,850 and 2,500 in. These positions correspond to the anti-nodes of the 1st and 3rd aeroelastic modes. Note the 1st aeroelastic zeros are virtually at the same location in the complex plane as the 1st aeroelastic poles for the rate gyro located at 1,850 in. For 2,500 in, this feature can be said for the 3rd mode, as well as for modes 2 and 4-7. Figs. 24-27 show the corresponding pole/zero patterns graphically, as well as the frequency responses. In Figs. 26-27, observe the 1st and 3rd aeroelastic modes being activated/deactivated by the sensor placement. Finally, these trends can be correlated with the structural vibration mode shapes for the fuselage centerline shown in Fig. 28. x_s and z_s denote typical structural axes with x_s pointing aft, z_s pointing up, and origin located at the nose.

Table 13. Rigid A Matrix Elements For Cycle 1 Simulation Model And Langley Appendix D Model			
Element	(unit)	Cycle 1 Simulation	"Rigid" Langley App D
Xu	(1/s)	5.9489e-04	×
Xw	(1/s)	2.1308e-02	×
Xq	(ft/s)	-4.1438e+01	×
Zu	(1/s)	-1.4249e-01	×
Zw	(1/s)	-6.1833e-01	-4.8406e-01
U+Zq	(ft/s)	2.3746e+02	2.4120e+02
Mu	(1/ft s)	-1.5018e-04	×
Mw	(1/ft s)	8.0241e-04	2.5688e-05
Mq	(1/s)	-2.6115e-01	-9.8561e-02
-cos(Θ)G	(ft/s^2)	-3.1782e+01	×
-sin(Θ)G	(ft/s^2)	-5.0058e+00	0

Table 14. Rigid B Matrix Elements For Cycle 1 Simulation Model And Langley Appendix D Model			
Element	(unit)	Cycle 1 Simulation	"Rigid" Langley App D
XδE	(ft/s^2)	-4.2796e-01	×
XδTE1	(ft/s^2)	2.8499e-01	×
XδTE2	(ft/s^2)	5.2052e-01	×
XδTE3	(ft/s^2)	1.9609e+00	×
XδTE4	(ft/s^2)	1.1745e+00	×
ZδE	(ft/s^2)	-6.2738e+00	-7.1797e+00
ZδTE1	(ft/s^2)	-1.1006e+01	-8.6090e+00
ZδTE2	(ft/s^2)	-1.0385e+01	-9.4398e+00
ZδTE3	(ft/s^2)	-1.1537e+01	-1.1421e+01
ZδTE4	(ft/s^2)	-6.8446e+00	-8.3454e+00
MδE	(1/s^2)	-1.7116e-01	-1.9649e-01
MδTE1	(1/s^2)	1.7074e-02	-4.7314e-04
MδTE2	(1/s^2)	-1.7297e-02	-3.7642e-02
MδTE3	(1/s^2)	-5.1701e-02	-6.7087e-02
MδTE4	(1/s^2)	-2.2460e-02	-6.5308e-02

Table 15. Poles Of Langley Appendix D Model			
Root Location (1/s)	Freq. (rad/s)	Damping (-)	Description
1.3391e-01	1.3391e-01	-1.0000e+00	Slow
-9.6820e-02+ 1.2764e-01i	1.6021e-01	6.0435e-01	Mid Period (3rd Osc)
-9.6820e-02- 1.2764e-01i	1.6021e-01	6.0435e-01	Mid Period (3rd Osc)
-6.4296e-01	6.4296e-01	1.0000e+00	Fast
-7.4206e-01	7.4206e-01	1.0000e+00	Unsteady Aero 1
-1.3593e+00	1.3593e+00	1.0000e+00	Unsteady Aero 2
-4.2575e+00	4.2575e+00	1.0000e+00	Unsteady Aero 3
-2.6896e-01+ 7.7327e+00i	7.7373e+00	3.4761e-02	Aeroelastic 1
-2.6896e-01- 7.7327e+00i	7.7373e+00	3.4761e-02	Aeroelastic 1
-8.3151e+00	8.3151e+00	1.0000e+00	Unsteady Aero 4
-9.3206e+00+ 3.1314e-01i	9.3258e+00	9.9944e-01	Unsteady Aero 5
-9.3206e+00- 3.1314e-01i	9.3258e+00	9.9944e-01	Unsteady Aero 6
-1.1153e+01	1.1153e+01	1.0000e+00	Unsteady Aero 7
-7.3473e-01+ 1.2797e+01i	1.2818e+01	5.7322e-02	Aeroelastic 2
-7.3473e-01- 1.2797e+01i	1.2818e+01	5.7322e-02	Aeroelastic 2
-1.3489e+01	1.3489e+01	1.0000e+00	Unsteady Aero 8
-1.0793e+00+ 1.6939e+01i	1.6973e+01	6.3589e-02	Aeroelastic 3
-1.0793e+00- 1.6939e+01i	1.6973e+01	6.3589e-02	Aeroelastic 3
-1.8737e-01+ 1.7264e+01i	1.7265e+01	1.0852e-02	Aeroelastic 4
-1.8737e-01- 1.7264e+01i	1.7265e+01	1.0852e-02	Aeroelastic 4
-1.8328e+01	1.8328e+01	1.0000e+00	Unsteady Aero 9
-3.1011e-01+ 1.9562e+01i	1.9565e+01	1.5850e-02	Aeroelastic 5
-3.1011e-01- 1.9562e+01i	1.9565e+01	1.5850e-02	Aeroelastic 5
-2.0000e+01	2.0000e+01	1.0000e+00	Trail Edge 1 Actuator
-2.6467e-01+ 2.0843e+01i	2.0845e+01	1.2697e-02	Aeroelastic 6
-2.6467e-01- 2.0843e+01i	2.0845e+01	1.2697e-02	Aeroelastic 6
-2.1000e+01	2.1000e+01	1.0000e+00	Trail Edge 2 Actuator
-2.2000e+01	2.2000e+01	1.0000e+00	Elevator Actuator
-2.3000e+01	2.3000e+01	1.0000e+00	Trail Edge 3 Actuator
-2.4000e+01	2.4000e+01	1.0000e+00	Trail Edge 4 Actuator
-2.9903e-01+ 2.4280e+01i	2.4282e+01	1.2315e-02	Aeroelastic 7
-2.9903e-01- 2.4280e+01i	2.4282e+01	1.2315e-02	Aeroelastic 7
-1.9528e+00+ 2.9249e+01i	2.9314e+01	6.6617e-02	Aeroelastic 8
-1.9528e+00- 2.9249e+01i	2.9314e+01	6.6617e-02	Aeroelastic 8
-2.9351e+01	2.9351e+01	1.0000e+00	Unsteady Aero 10
-3.3864e-01+ 3.5663e+01i	3.5665e+01	9.4951e-03	Aeroelastic 9
-3.3864e-01- 3.5663e+01i	3.5665e+01	9.4951e-03	Aeroelastic 9
-9.1256e-01+ 4.2395e+01i	4.2405e+01	2.1520e-02	Aeroelastic 10
-9.1256e-01- 4.2395e+01i	4.2405e+01	2.1520e-02	Aeroelastic 10
-6.9046e-01+ 4.6607e+01i	4.6612e+01	1.4813e-02	Aeroelastic 11
-6.9046e-01- 4.6607e+01i	4.6612e+01	1.4813e-02	Aeroelastic 11
-9.0145e-01+ 5.3632e+01i	5.3640e+01	1.6806e-02	Aeroelastic 12
-9.0145e-01- 5.3632e+01i	5.3640e+01	1.6806e-02	Aeroelastic 12
-7.4028e-01+ 5.6048e+01i	5.6053e+01	1.3207e-02	Aeroelastic 13
-7.4028e-01- 5.6048e+01i	5.6053e+01	1.3207e-02	Aeroelastic 13
-8.8230e-01+ 6.0403e+01i	6.0410e+01	1.4605e-02	Aeroelastic 14
-8.8230e-01- 6.0403e+01i	6.0410e+01	1.4605e-02	Aeroelastic 14
-3.2257e+00+ 6.1401e+01i	6.1486e+01	5.2462e-02	Aeroelastic 15
-3.2257e+00- 6.1401e+01i	6.1486e+01	5.2462e-02	Aeroelastic 15
-8.4985e-01+ 6.2380e+01i	6.2386e+01	1.3622e-02	Aeroelastic 16
-8.4985e-01- 6.2380e+01i	6.2386e+01	1.3622e-02	Aeroelastic 16
-7.2286e-01+ 6.5084e+01i	6.5088e+01	1.1106e-02	Aeroelastic 17
-7.2286e-01- 6.5084e+01i	6.5088e+01	1.1106e-02	Aeroelastic 17
-1.4140e+02+ 1.4144e+02i	2.0000e+02	7.0710e-01	Trail Edge 1 Actuator
-1.4140e+02- 1.4144e+02i	2.0000e+02	7.0710e-01	Trail Edge 1 Actuator

Table 15. Continued			
Root Location (1/s)	Freq. (rad/s)	Damping (-)	Description
-1.4845e+02+ 1.4854e+02i	2.1000e+02	7.0710e-01	Trail Edge 2 Actuator
-1.4845e+02- 1.4854e+02i	2.1000e+02	7.0710e-01	Trail Edge 2 Actuator
-1.5555e+02+ 1.5558e+02i	2.2000e+02	7.0710e-01	Elevator Actuator
-1.5555e+02- 1.5558e+02i	2.2000e+02	7.0710e-01	Elevator Actuator
-1.6265e+02+ 1.6261e+02i	2.3000e+02	7.0710e-01	Trail Edge 3 Actuator
-1.6265e+02- 1.6261e+02i	2.3000e+02	7.0710e-01	Trail Edge 3 Actuator
-1.6970e+02+ 1.6971e+02i	2.4000e+02	7.0710e-01	Trail Edge 4 Actuator
-1.6970e+02- 1.6971e+02i	2.4000e+02	7.0719e-01	Trail Edge 4 Actuator

Table 16. Zeros Of Langley Appendix D Model For 1,850 in Pitch Rate To Elevator Channel			
Gain = 2.5580e+01 rad/s/rad			
Root Location (1/s)	Freq. (rad/s)	Damping (-)	Description
0	0	-1.0000e+00	Pitch "Rate"
-5.4727e-03	5.4727e-03	1.0000e+00	Tau Theta 1
-4.6146e-01	4.6146e-01	1.0000e+00	Tau Theta 2
-7.2514e-01	7.2514e-01	1.0000e+00	Unsteady Aero 1
-1.3603e+00	1.3603e+00	1.0000e+00	Unsteady Aero 2
-4.3256e+00	4.3256e+00	1.0000e+00	Unsteady Aero 3
-7.3652e+00	7.3652e+00	1.0000e+00	Unsteady Aero 4
-8.9169e-02+ 7.5482e+00i	7.5488e+00	1.1812e-02	Aeroelastic 1
-8.9169e-02- 7.5482e+00i	7.5488e+00	1.1812e-02	Aeroelastic 1
-8.5780e+00	8.5780e+00	1.0000e+00	Unsteady Aero 5
-9.5036e+00	9.5036e+00	1.0000e+00	Unsteady Aero 6
-1.1117e+01	1.1117e+01	1.0000e+00	Unsteady Aero 7
-1.1891e+00+ 1.3929e+01i	1.3980e+01	8.5061e-02	Aeroelastic 2
-1.1891e+00- 1.3929e+01i	1.3980e+01	8.5061e-02	Aeroelastic 2
-1.4660e+01	1.4660e+01	1.0000e+00	Unsteady Aero 8
-1.7234e-01+ 1.7263e+01i	1.7263e+01	9.9827e-03	Aeroelastic 4
-1.7234e-01- 1.7263e+01i	1.7263e+01	9.9827e-03	Aeroelastic 4
-7.0980e-01+ 1.8793e+01i	1.8806e+01	3.7743e-02	Aeroelastic 5
-7.0980e-01- 1.8793e+01i	1.8806e+01	3.7743e-02	Aeroelastic 5
-1.4522e+01+ 1.1952e+01i	1.8808e+01	7.7213e-01	Unsteady Aero 9
-1.4522e+01- 1.1952e+01i	1.8808e+01	7.7213e-01	Aeroelastic 3
1.9553e+01	1.9553e+01	-1.0000e+00	Aeroelastic 3
-2.0266e-01+ 1.9689e+01i	1.9690e+01	1.0293e-02	Aeroelastic 6
-2.0266e-01- 1.9689e+01i	1.9690e+01	1.0293e-02	Aeroelastic 6
-2.0012e+01	2.0012e+01	1.0000e+00	Unsteady Aero 10
-2.0000e+01	2.0000e+01	1.0000e+00	Trail Edge 1 Actuator
-2.1000e+01	2.1000e+01	1.0000e+00	Trail Edge 2 Actuator
-2.3000e+01	2.3000e+01	1.0000e+00	Trail Edge 3 Actuator
-2.4000e+01	2.4000e+01	1.0000e+00	Trail Edge 4 Actuator
-3.0156e-01+ 2.4429e+01i	2.4431e+01	1.2344e-02	Aeroelastic 7
-3.0156e-01- 2.4429e+01i	2.4431e+01	1.2344e-02	Aeroelastic 7
-1.9915e-01+ 3.0671e+01i	3.0671e+01	6.4931e-03	Aeroelastic 8
-1.9915e-01- 3.0671e+01i	3.0671e+01	6.4931e-03	Aeroelastic 8
-4.8083e-01+ 4.0999e+01i	4.1002e+01	1.1727e-02	Aeroelastic 10
-4.8083e-01- 4.0999e+01i	4.1002e+01	1.1727e-02	Aeroelastic 10
1.0673e+01+ 4.3969e+01i	4.5246e+01	-2.3590e-01	Aeroelastic 11
1.0673e+01- 4.3969e+01i	4.5246e+01	-2.3590e-01	Aeroelastic 11
-3.9908e+01+ 2.2893e+01i	4.6008e+01	8.6742e-01	Aeroelastic 9
-3.9908e+01- 2.2893e+01i	4.6008e+01	8.6742e-01	Aeroelastic 9
-6.3404e+00+ 4.6931e+01i	4.7358e+01	1.3388e-01	Aeroelastic 12
-6.3404e+00- 4.6931e+01i	4.7358e+01	1.3388e-01	Aeroelastic 12
-7.2607e-01+ 5.6473e+01i	5.6478e+01	1.2856e-02	Aeroelastic 13
-7.2607e-01- 5.6473e+01i	5.6478e+01	1.2856e-02	Aeroelastic 13
-5.5008e-01+ 5.8838e+01i	5.8840e+01	9.3487e-03	Aeroelastic 14
-5.5008e-01- 5.8838e+01i	5.8840e+01	9.3487e-03	Aeroelastic 14
-3.6642e+00+ 6.1143e+01i	6.1253e+01	5.9821e-02	Aeroelastic 15
-3.6642e+00- 6.1143e+01i	6.1253e+01	5.9821e-02	Aeroelastic 15
-8.5473e-01+ 6.2321e+01i	6.2327e+01	1.3714e-02	Aeroelastic 16
-8.5473e-01- 6.2321e+01i	6.2327e+01	1.3714e-02	Aeroelastic 16
-1.4712e+00+ 6.7569e+01i	6.7585e+01	2.1768e-02	Aeroelastic 17
-1.4712e+00- 6.7569e+01i	6.7585e+01	2.1768e-02	Aeroelastic 17
4.0164e+01+ 7.9640e+01i	8.9194e+01	-4.5030e-01	Noncausal Rate
4.0164e+01- 7.9640e+01i	8.9194e+01	-4.5030e-01	Noncausal Acceleration
-1.4142e+02+ 1.4142e+02i	2.0000e+02	7.0710e-01	Trail Edge 1 Actuator

Table 16. Continued			
Root Location (1/s)	Freq. (rad/s)	Damping (-)	Description
-1.4142e+02- 1.4142e+02i	2.0000e+02	7.0710e-01	Trail Edge 1 Actuator
-1.4849e+02+ 1.4849e+02i	2.1000e+02	7.0710e-01	Trail Edge 2 Actuator
-1.4849e+02- 1.4849e+02i	2.1000e+02	7.0710e-01	Trail Edge 2 Actuator
-1.6263e+02+ 1.6263e+02i	2.3000e+02	7.0710e-01	Trail Edge 3 Actuator
-1.6263e+02- 1.6263e+02i	2.3000e+02	7.0710e-01	Trail Edge 3 Actuator
-1.6970e+02+ 1.6970e+02i	2.4000e+02	7.0710e-01	Trail Edge 4 Actuator
-1.6970e+02- 1.6970e+02i	2.4000e+02	7.0710e-01	Trail Edge 4 Actuator

Table 17. Zeros Of Langley Appendix D Model For 2,500 in Pitch Rate To Elevator Channel			
Gain = 2.6427e+02 rad/s/rad			
Root Location (1/s)	Freq. (rad/s)	Damping (-)	Description
0	0	-1.0000e+00	Pitch "Rate"
-6.2261e-03	6.2261e-03	1.0000e+00	Tau Theta 1
-4.5351e-01	4.5351e-01	1.0000e+00	Tau Theta 2
-7.2021e-01	7.2021e-01	1.0000e+00	Unsteady Aero 1
-1.3600e+00	1.3600e+00	1.0000e+00	Unsteady Aero 2
-4.2576e+00	4.2576e+00	1.0000e+00	Unsteady Aero 3
-1.5720e-01+ 5.0101e+00i	5.0125e+00	3.1362e-02	Aeroelastic 1
-1.5720e-01- 5.0101e+00i	5.0125e+00	3.1362e-02	Aeroelastic 1
-8.2077e+00+ 2.0126e-01i	8.2102e+00	9.9970e-01	Unsteady Aero 4
-8.2077e+00- 2.0126e-01i	8.2102e+00	9.9970e-01	Unsteady Aero 5
-1.0345e+01	1.0345e+01	1.0000e+00	Unsteady Aero 6
-1.1254e+01	1.1254e+01	1.0000e+00	Unsteady Aero 7
-6.6200e-01+ 1.2910e+01i	1.2927e+01	5.1211e-02	Aeroelastic 2
-6.6200e-01- 1.2910e+01i	1.2927e+01	5.1211e-02	Aeroelastic 2
-1.3746e+01	1.3746e+01	1.0000e+00	Unsteady Aero 8
-9.8399e-01+ 1.6972e+01i	1.7000e+01	5.7882e-02	Aeroelastic 3
-9.8399e-01- 1.6972e+01i	1.7000e+01	5.7882e-02	Aeroelastic 3
-1.9122e-01+ 1.7265e+01i	1.7266e+01	1.1075e-02	Aeroelastic 4
-1.9122e-01- 1.7265e+01i	1.7266e+01	1.1075e-02	Aeroelastic 4
-1.7938e+01	1.7938e+01	1.0000e+00	Unsteady Aero 9
-3.1371e-01+ 1.9548e+01i	1.9550e+01	1.6046e-02	Aeroelastic 5
-3.1371e-01- 1.9548e+01i	1.9550e+01	1.6046e-02	Aeroelastic 5
-2.0000e+01	2.0000e+01	1.0000e+00	Trail Edge 1 Actuator
-2.0950e-01+ 2.0693e+01i	2.0694e+01	1.0124e-02	Aeroelastic 6
-2.0950e-01- 2.0693e+01i	2.0694e+01	1.0124e-02	Aeroelastic 6
-2.1000e+01	2.1000e+01	1.0000e+00	Trail Edge 2 Actuator
-2.3000e+01	2.3000e+01	1.0000e+00	Trail Edge 3 Actuator
-2.4000e+01	2.4000e+01	1.0000e+00	Trail Edge 4 Actuator
-2.9619e-01+ 2.4319e+01i	2.4321e+01	1.2178e-02	Aeroelastic 7
-2.9619e-01- 2.4319e+01i	2.4321e+01	1.2178e-02	Aeroelastic 7
2.7297e+01	2.7297e+01	-1.0000e+00	Aeroelastic 8
-2.3867e+01+ 1.7217e+01i	2.9429e+01	8.1100e-01	Aeroelastic 8
-2.3867e+01- 1.7217e+01i	2.9429e+01	8.1100e-01	Unsteady Aero 10
-2.0004e-02+ 3.6076e+01i	3.6076e+01	5.5450e-04	Aeroelastic 9
-2.0004e-02- 3.6076e+01i	3.6076e+01	5.5450e-04	Aeroelastic 9
-4.2886e+01+ 1.1462e+01i	4.4392e+01	9.6609e-01	Noncausal Rate
-4.2886e+01- 1.1462e+01i	4.4392e+01	9.6609e-01	Noncausal Acceleration
-8.4489e-01+ 4.4456e+01i	4.4464e+01	1.9002e-02	Aeroelastic 10
-8.4489e-01- 4.4456e+01i	4.4464e+01	1.9002e-02	Aeroelastic 10
7.6615e+00+ 4.7419e+01i	4.8034e+01	-1.5950e-01	Aeroelastic 12
7.6615e+00- 4.7419e+01i	4.8034e+01	-1.5950e-01	Aeroelastic 12
-6.8888e+00+ 5.1597e+01i	5.2055e+01	1.3234e-01	Aeroelastic 11
-6.8888e+00- 5.1597e+01i	5.2055e+01	1.3234e-01	Aeroelastic 11
-6.7375e-01+ 5.5338e+01i	5.5343e+01	1.2174e-02	Aeroelastic 13
-6.7375e-01- 5.5338e+01i	5.5343e+01	1.2174e-02	Aeroelastic 13
-1.0367e+00+ 5.8612e+01i	5.8621e+01	1.7685e-02	Aeroelastic 14
-1.0367e+00- 5.8612e+01i	5.8621e+01	1.7685e-02	Aeroelastic 14
-3.5283e+00+ 6.1399e+01i	6.1500e+01	5.7371e-02	Aeroelastic 15
-3.5283e+00- 6.1399e+01i	6.1500e+01	5.7371e-02	Aeroelastic 15
-8.4270e-01+ 6.2356e+01i	6.2362e+01	1.3513e-02	Aeroelastic 16
-8.4270e-01- 6.2356e+01i	6.2362e+01	1.3513e-02	Aeroelastic 16
-6.5371e-01+ 6.5084e+01i	6.5088e+01	1.0044e-02	Aeroelastic 17
-6.5371e-01- 6.5084e+01i	6.5088e+01	1.0044e-02	Aeroelastic 17
-1.4142e+02+ 1.4142e+02i	2.0000e+02	7.0710e-01	Trail Edge 1 Actuator

Table. 17 Continued			
Root Location (1/s)	Freq. (rad/s)	Damping (-)	Description
-1.4142e+02- 1.4142e+02i	2.0000e+02	7.0710e-01	Trail Edge 1 Actuator
-1.4849e+02+ 1.4849e+02i	2.1000e+02	7.0710e-01	Trail Edge 2 Actuator
-1.4849e+02- 1.4849e+02i	2.1000e+02	7.0710e-01	Trail Edge 2 Actuator
-1.6263e+02+ 1.6263e+02i	2.3000e+02	7.0710e-01	Trail Edge 3 Actuator
-1.6263e+02- 1.6263e+02i	2.3000e+02	7.0710e-01	Trail Edge 3 Actuator
-1.6970e+02+ 1.6970e+02i	2.4000e+02	7.0710e-01	Trail Edge 4 Actuator
-1.6970e+02- 1.6970e+02i	2.4000e+02	7.0710e-01	Trail Edge 4 Actuator

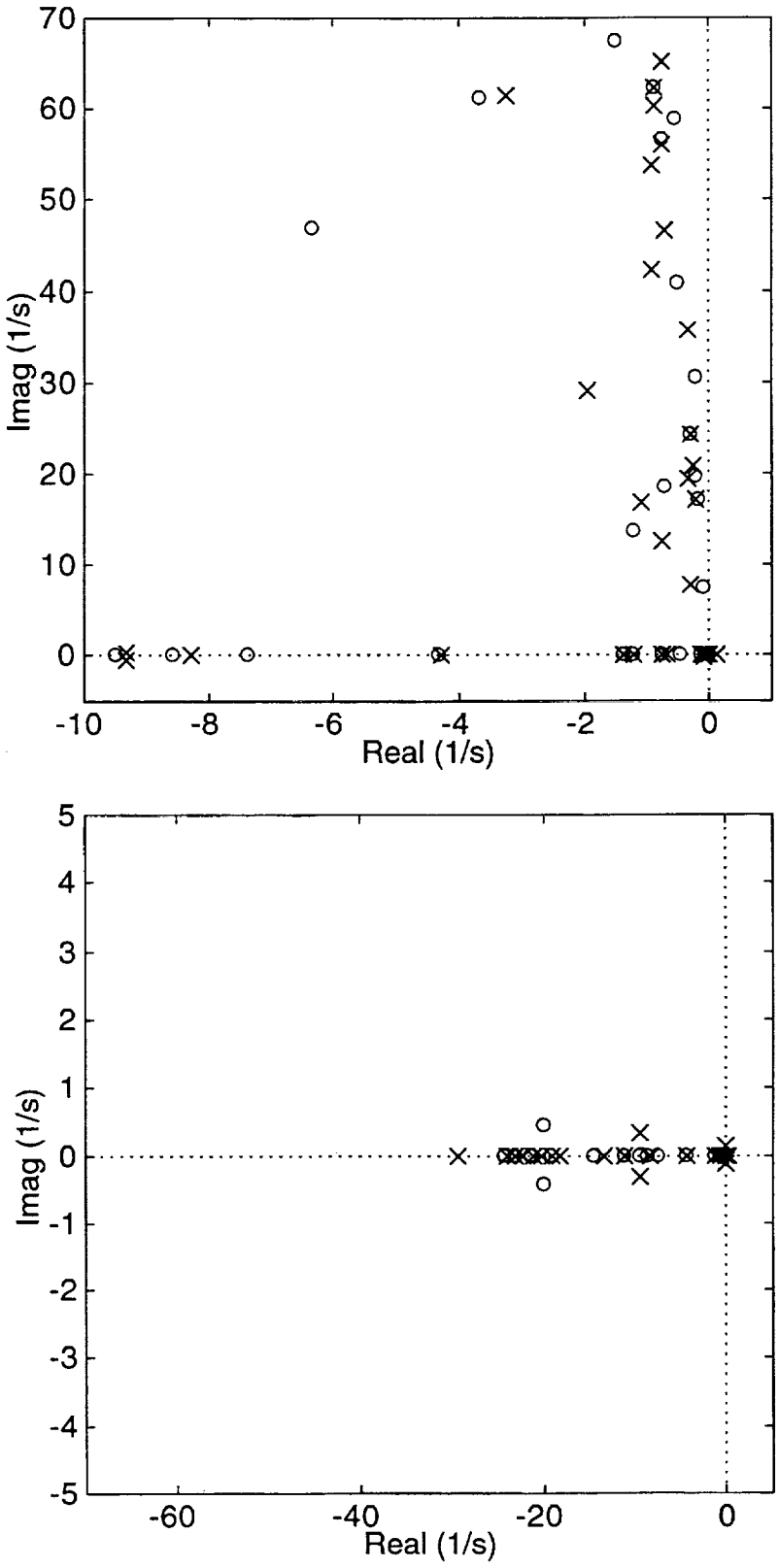

Figure 24. Pole-Zero Pattern Of Langley Appendix D Model For 1,850 in Pitch Rate To Elevator Channel

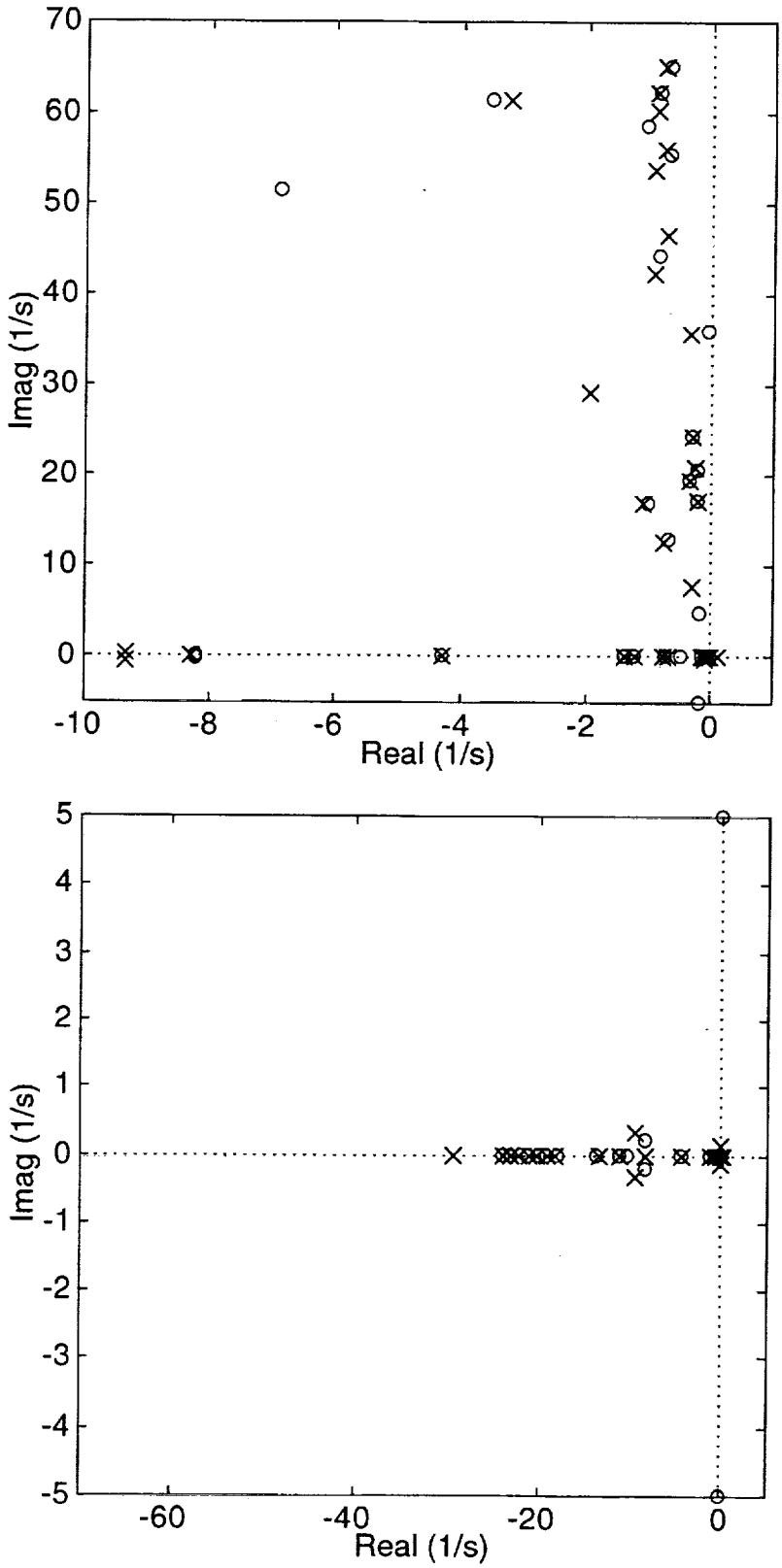

Figure 25. Pole-Zero Pattern Of Langley Appendix D Model For 2,500 in Pitch Rate To Elevator Channel

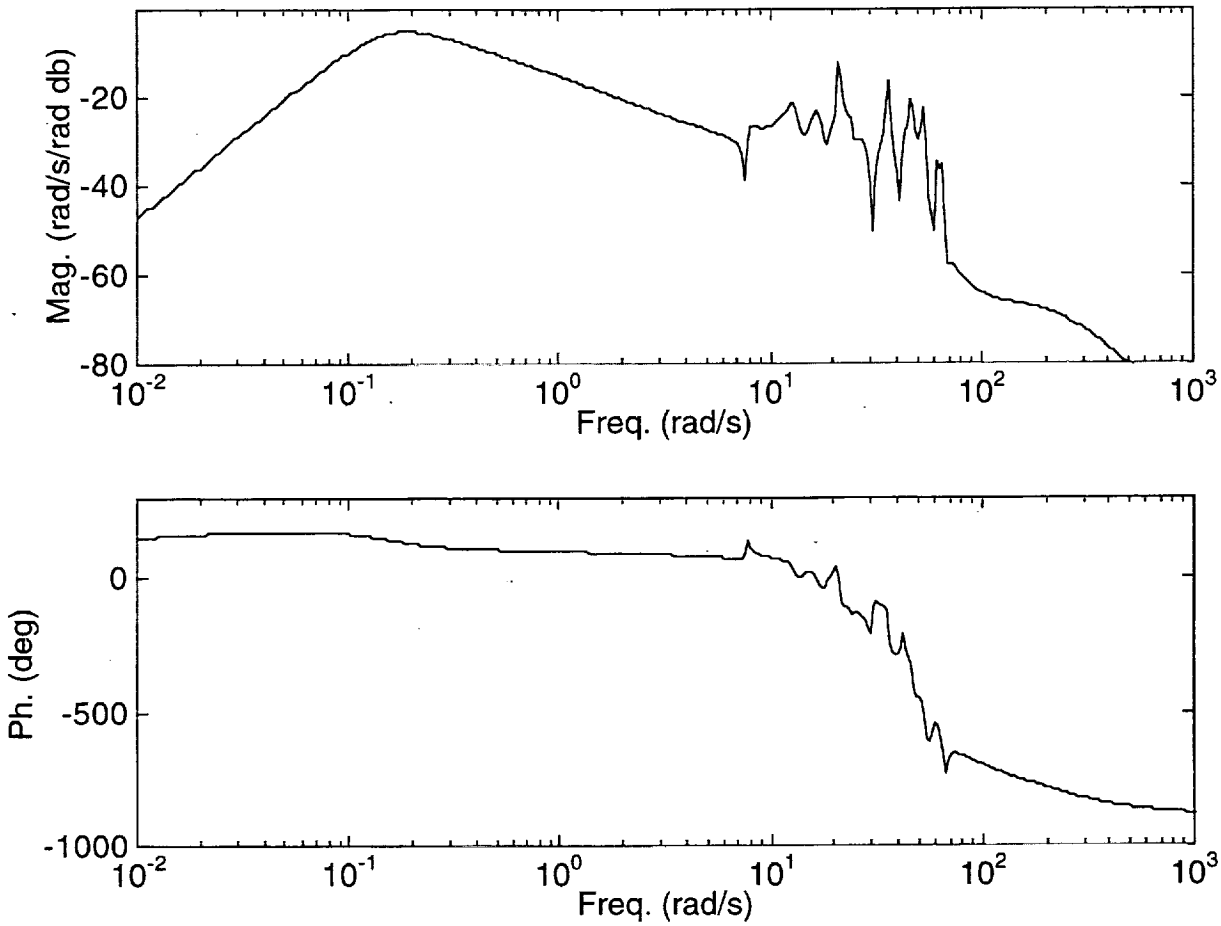

Figure 26. Frequency Response Of Langley Appendix D Model
For 1,850 in Pitch Rate To Elevator Channel

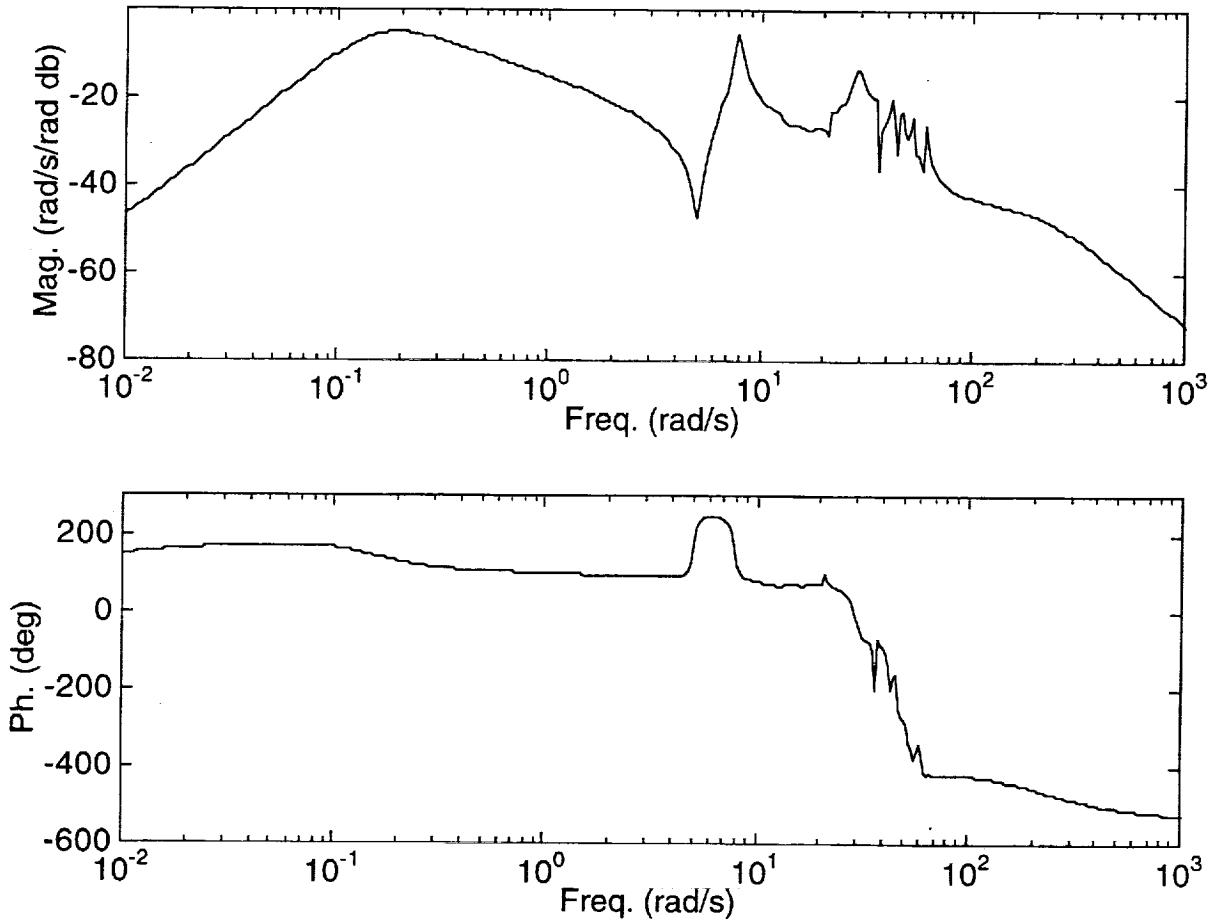

Figure 27. Frequency Response Of Langley Appendix D Model
For 2,500 in Pitch Rate To Elevator Channel

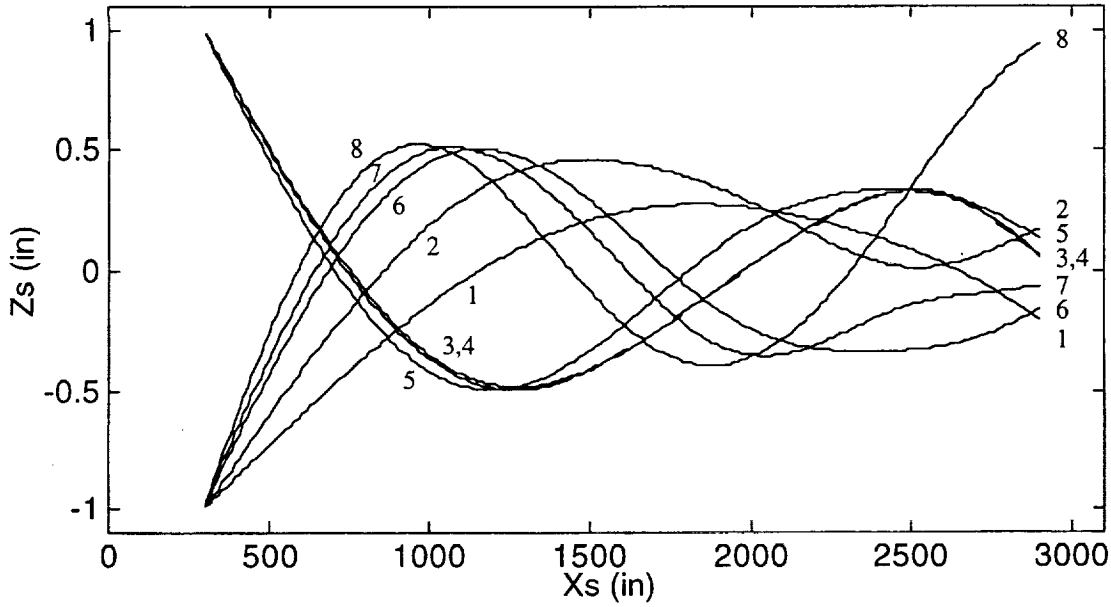

Figure 28. Structural Mode Shape Data - Mass Case M3A

Section III
Application of Previous Design Milestones to HSCT

A. Single-Sensor/Single-Surface Design With Forward Sensor

The objectives of the inner loop flight control system (FCS) are to 1) artificial supply the stability inherently lacking in the airframe, 2) augment the key pilot/passenger centered responses with crisp, well damped behavior according to the relevant flying quality metrics, and 3) suppress aeroelastic motions in the responses. If the above objectives can be accomplished with minimal FCS architecture, then burdens associated with implementation of multiply redundant channels requiring scheduling with flight condition and modification during test and development are lessened, and reliability/maintainability is enhanced. The feasibility of achieving these goals with a Single-Sensor/Single-Surface (SS/SS) inner loop arrangement are addressed next.

Consider the block diagram in Fig. 29 where K(s), A(s) and G(s) denote the transfer functions of the compensation, actuator, and vehicle for the SS/SS inner loop. Elevator deflection will serve as the control input, and measured pitch rate is selected as the feedback signal. Pitch rate has been an effective feedback signal for stability augmentation systems, and this effectiveness is true here as well. Examination of the pitch rate-to-elevator pole/zero pattern for a relaxed static stability flight vehicle reveals that proportional plus integral feedback of pitch rate, or

$$K(s) = \frac{k(s+z)}{s} \tag{3.1}$$

results in 1) stabilization by driving the real axis slow and fast poles into the $\tau_{\theta 1}$ and $\tau_{\theta 2}$ zeros and 2) augmentation by moving the mid period roots such that a dominate, well damped pitch behavior results (i.e., the superaugmented pitch loop).[18] Of concern is the ability of the loop to provide sufficient rigid-body stabilization and augmentation before expending gain/phase margins, as well as avoiding destabilization of, or increasing the contamination from, aeroelastic modes.

As a first strategy, the rate gyro is to be placed such that the participation of the 1st aeroelastic mode is minimized in the feedback signal. Mounting of the rate gyro at the anti-node of

the 1st aeroelastic mode, or where the mode slope has a value of zero, will achieve the desired effect. A sensor so placed will provide the best possibility of achieving the flight control objectives with gain stabilization in the high frequency region (i.e., the loop transfer is below 0 db beyond the rigid-body crossover range).

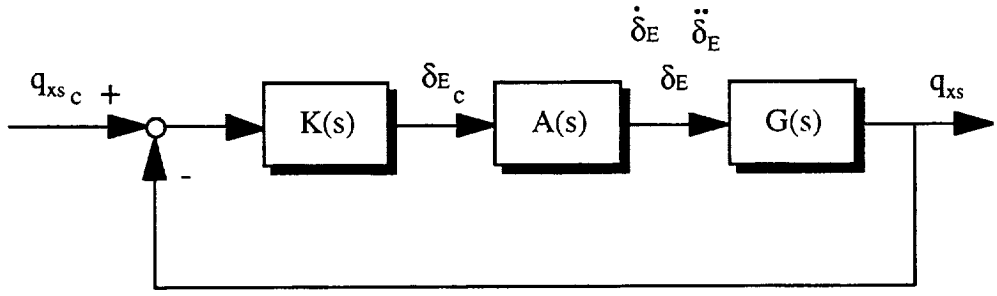

Figure 29. Single-Sensor/Single-Surface Feedback Loop

Consider the Evans plot behavior for a rate gyro located at 1,850 in along the fuselage centerline shown in Fig. 30 with z = 2 1/s. This station is forward of the center of mass located at 2,153 in. Observe how the unstable real axis pole is driven into $1/\tau_{\theta 1}$, which resides slightly in the left-half plane, and how the mid period mode moves out to become the dominate pitch mode. As expected, the 1st aeroelastic pole is accompanied by a closely spaced zero, canceling this mode in the signal as it travels around the loop, regardless of the loop gain. At the higher frequency aeroelastic modes, the 1,850 in location is not conducive to a good feedback signal. Note the 1,850 in rate gyro leads to "out of phase" pick-up of the 2nd, 3rd, and 6th modes. As the loop gain is increased, these modes lose damping and foretell hard instabilities. These characteristics noted in Fig. 30 correlate with the mode slopes in Fig. 28

The closed-loop poles in Fig. 30 are highlighted for two values of the compensator gain, k = -2.36 and -4.03 rad/rad/s. Figs. 31 and 32 show the corresponding Bode plots for these two gains. For k = -2.36 rad/rad/s, the real axis instability is just stabilized, as indicated by the dc gain of 0 db in Fig. 31 and the closed-loop pole at the origin in Fig. 30. Observe the rigid-body gain

crossover frequency occurs at 0.95 rad/s (see Fig. 31), which will be shown as insufficient for pitch damping, frequency, and phase margin requirements. Also note from the Bode the dangerous aeroelastic peak occurring at 20 rad/s, which also corresponds to the augmented 6th aeroelastic pole approaching the imaginary axis in the Evans plot. On the other hand, with k = -4.03 rad/rad/s, the 6th aeroelastic mode is just destabilized. The peak just touches the 0 db level and the closed-loop root is on the jω axis. Gain crossover is better at 1.3 rad/s, but still insufficient. Finally, note the real axis instability is fully stabilized.

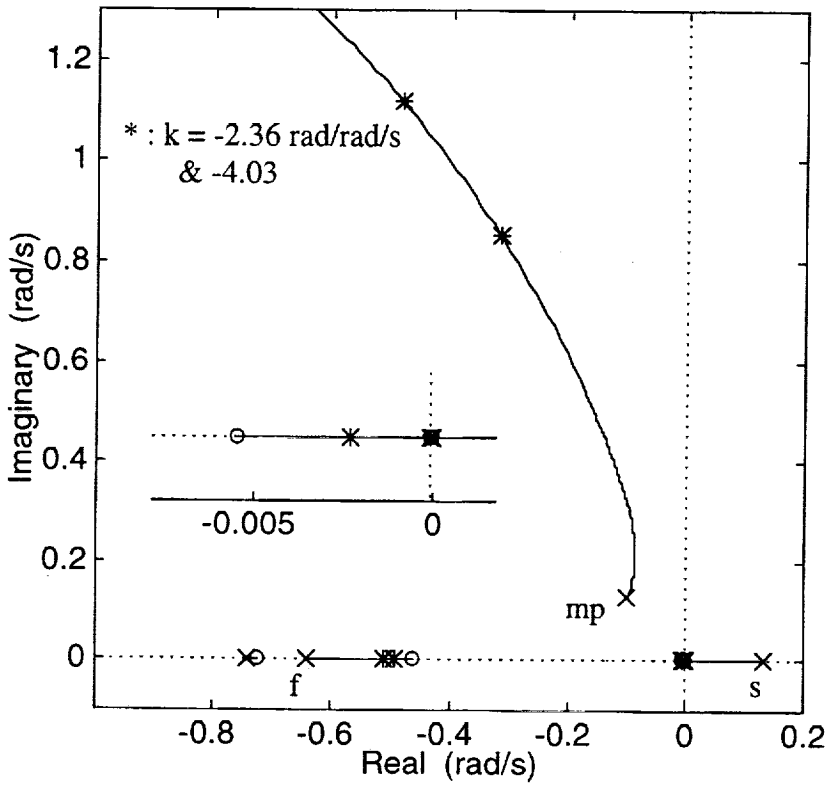

Figure 30. Evans Plot For 1,850 in Pitch Rate To Elevator Without Filtering

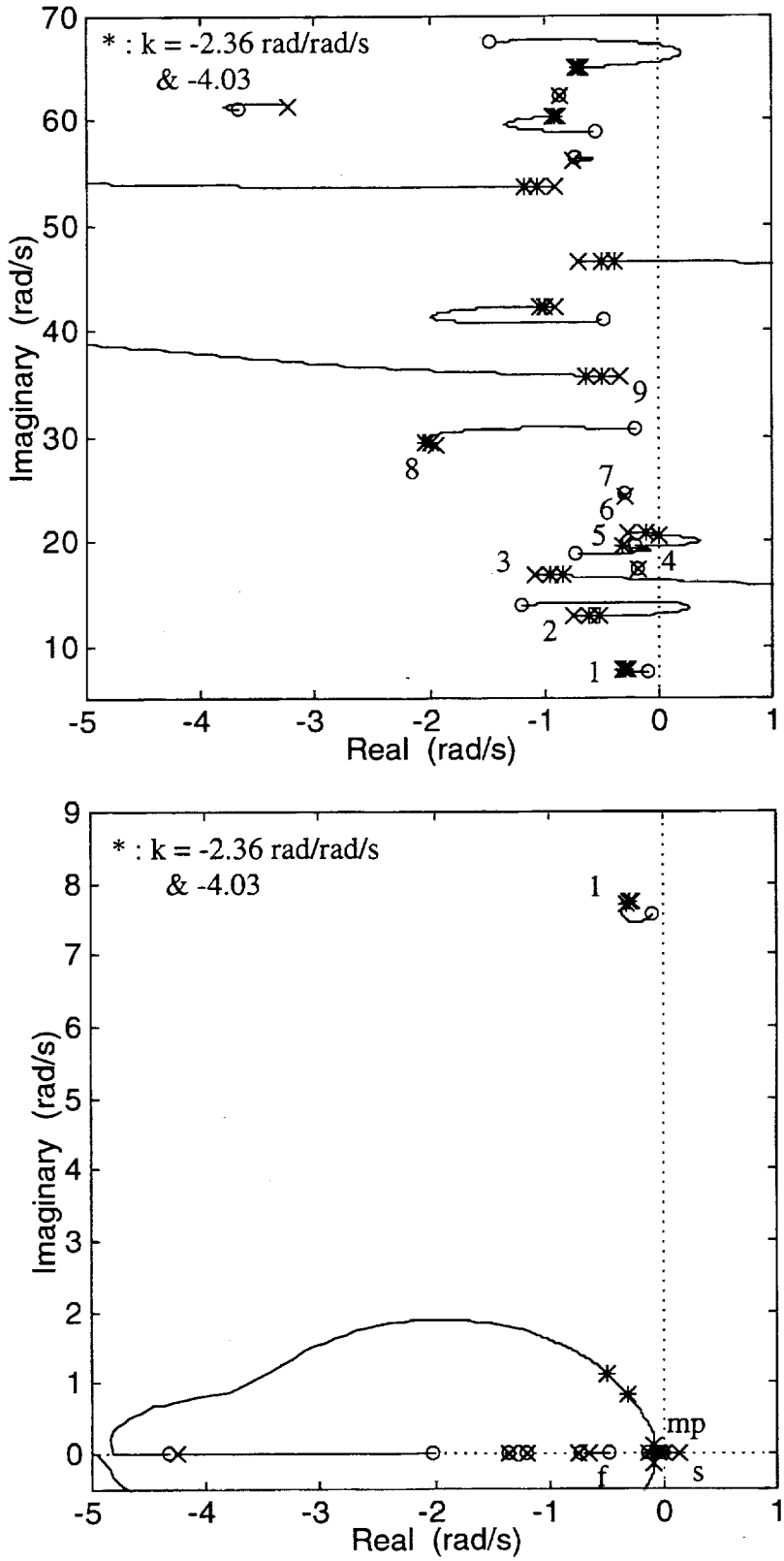

Figure 30. Continued

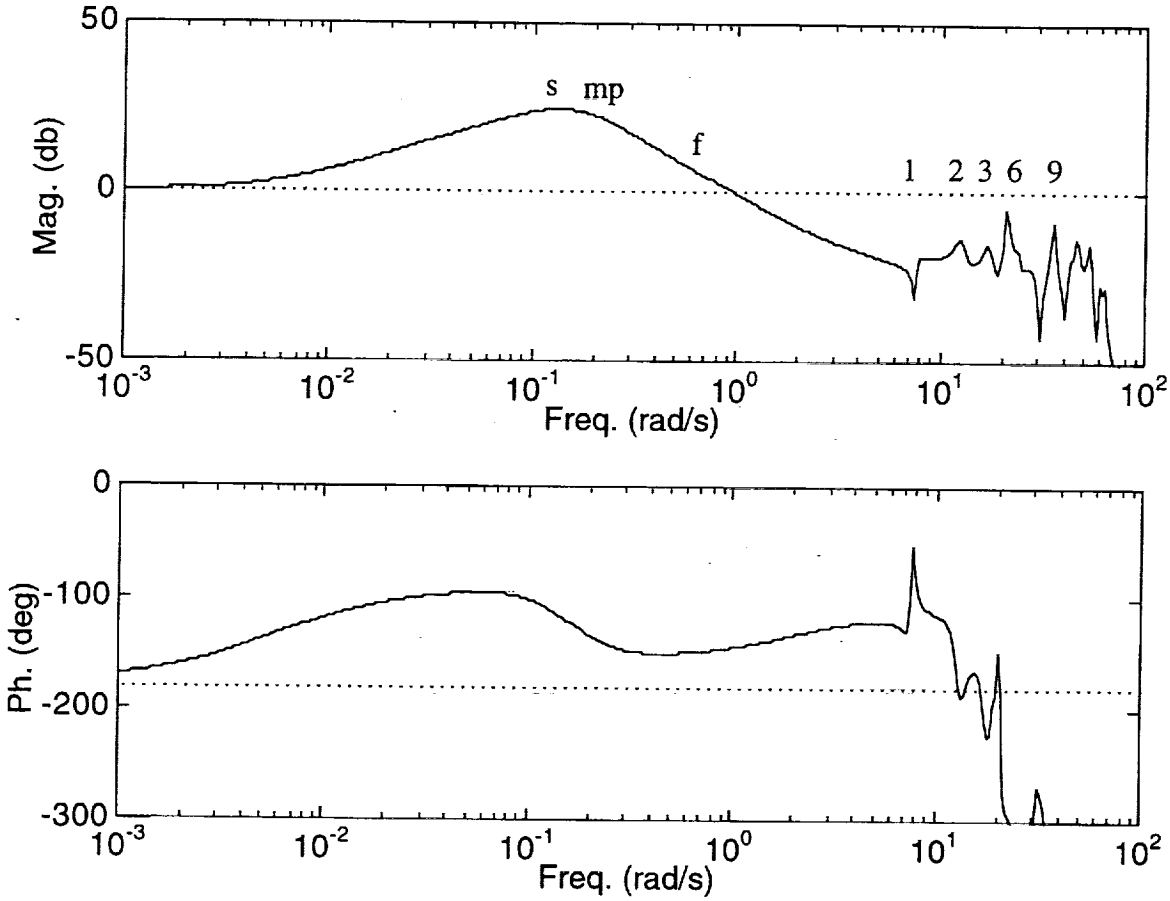

Figure 31. Bode Plot For 1,850 in Pitch Rate To Elevator Without Filtering, k = -2.36 rad/rad/s

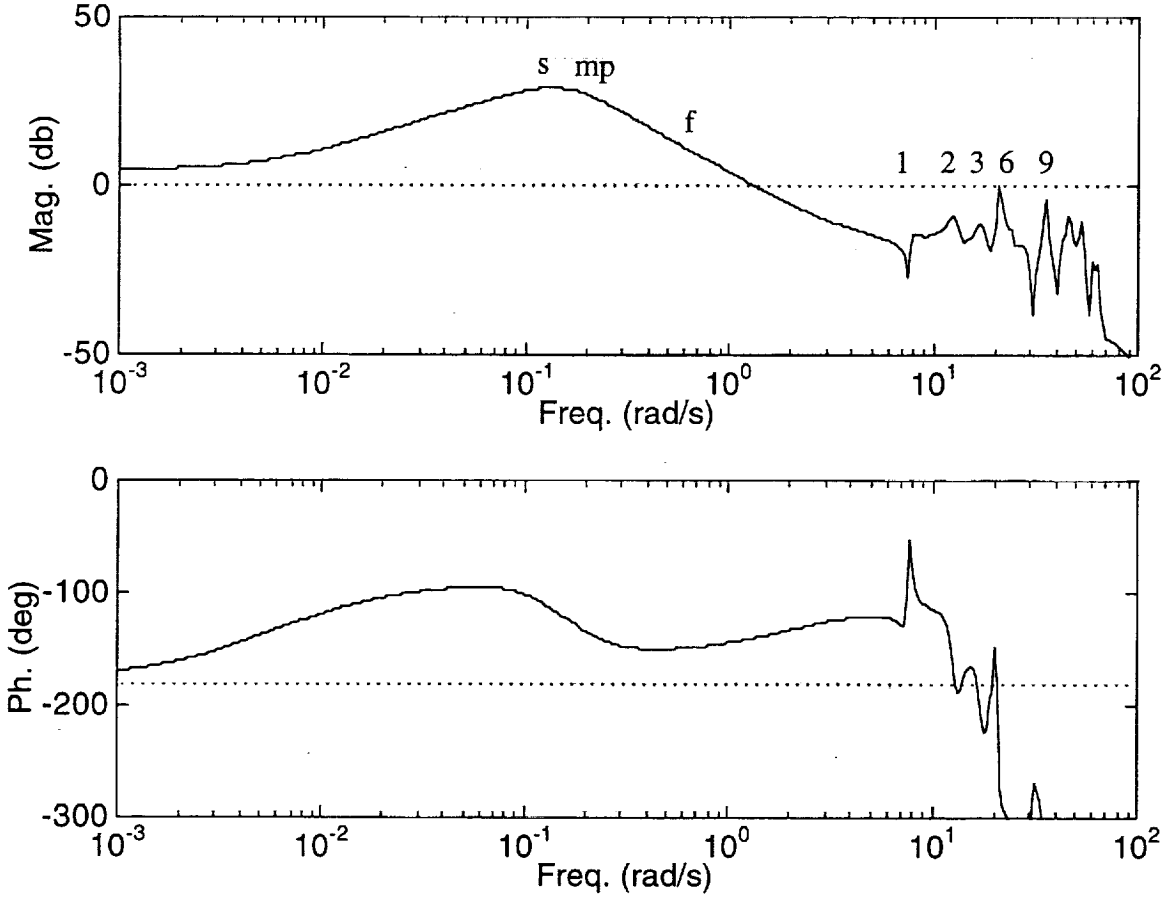

Figure 32. Bode Plot For 1,850 in Pitch Rate To Elevator Without Filtering, k = -4.03 rad/rad/s

These Evans and Bode features give a qualitative perspective of the severe tradeoffs between rigid-body and aeroelastic characteristics that confront the flight control engineer. For a quantitative description of the tradeoffs, consider Tab. 18 which indicates compliance or non-compliance with several flying quality requirements and metrics, as pure loop gain is adjusted with no filtering. Performance metrics include the rigid pitch frequency, damping, control anticipation, and omega-tau, while stability metrics consist of the rigid low frequency gain margin, rigid high frequency phase margin, and the aeroelastic mode 6 gain margin. Shaded boxes indicate noncompliance with the requirement. Before starting the discussion, a few comments are in order. The flying quality data base was not developed, and has never been validated, for highly flexible vehicles. Nevertheless, there is little else to base flight control decisions on, short of costly piloted simulation tests. Therefore, the requirements are used here, but only to seek ballpark estimates of flying quality levels, not definitive answers. Because of the uncertainty involved, the equivalent systems approach was not considered. Therefore, the numbers in Tab. 18 were calculated by using numbers taken directly from the full order model, not an equivalent number from a reduced order model. In computing $\omega_{sp}\tau_{\theta 2}$, z was substituted for $\tau_{\theta 2}$. Further, the requirements correspond to Class III vehicles in Category C flight.

Table 18. System Characteristics With Gain Adjustment For 1,850 in Pitch Rate To Elevator Without Filtering

-k (r/r/s)	ω_{sp} ≥0.7 (r/s)	ζ_{sp} ≥0.35 (-)	CAP ≥0.16 ($1/gs^2$)	$\omega_{sp}\tau_{\theta 2}$ ≥1.3 (-)	$GM_{<.38}$ ≥4.5 (db)	$PM_{>.38}$ ≥45. (deg)	GM_6 ≥8. (db)
0.92	0.54	0.30	0.018	0.27	-8.17	31.1	12.93
2.36	0.91	0.35	0.050	0.46	0.00	35.7	4.74
4.03	1.22	0.40	0.089	0.61	4.66	40.3	0.00
5.95	1.51	0.45	0.14	0.76	8.03	44.6	-3.29
7.94	1.76	0.50	0.19	0.88	10.54	48.3	-5.80
10.01	2.00	0.55	0.24	1.00	12.55	51.3	-7.81
12.20	2.22	0.60	0.30	1.11	14.27	53.9	-9.53
14.54	2.44	0.65	0.36	1.22	15.79	56.1	-11.05
17.02	2.65	0.70	0.42	1.33	17.18	57.7	-12.42

The entries in Tab. 18 correspond to 0.05 increments in rigid pitch damping, and note that two entries correspond to the gains previously discussed. Level 1 short period damping,

frequency, control anticipation, and phase margin can be reached, but not without an unacceptable trade with aeroelastic mode 6 gain margin. Note that as loop gain is increased, the aeroelastic mode 6 gain margin violates the requirement well before the relaxed static stability pole is even stabilized (negative gain margin entries imply a margin deficiency beyond neutral stability). Fig. 32 illustrates the situation further. These plots show the CAP vs. ζ and $\omega_{sp}\tau_{\theta 2}$ vs. ζ predicted pilot ratings with aeroelastic gain margin as the parameterization. The $6^{\underline{th}}$ aeroelastic mode is driven unstable well before moderate rigid-body flying qualities are approached.

To lessen the higher frequency aeroelastic mode sensitivity to loop gain variations, a proportional plus integral compensator with filtering must be considered. Insufficient frequency separation exists between the rigid-body modes and mode 6 to obtain significant attenuation of mode 6 from a simple low pass filter. Here, notching the $6^{\underline{th}}$ aeroelastic mode is necessary. An attenuation of 13 db is used to reduce the peak to the level of mode 2. However, this alone is not sufficient filtering to allow loop gain increases. Observe in Fig. 32 the aeroelastic mode 9 peak at 36 rad/s, and the other peaks lying beyond this frequency. Even though mode 9 would be considered phase stable for increased loop gain, it is highly desirable to have gain stabilization in this frequency range where model uncertainty is large. The mode 9/rigid-body separation is sufficient to allow low pass filtering with a break frequency of 10 rad/s to drag the peak down. The notch and first order filters add roughly 0.5 and 10 deg phase loss at the gain crossover. To recover this loss, an additional lead-lag filter is added. With this filtering in place, loop gain is again increased until aeroelastic mode 2 is near the gain margin requirement.

The final compensator is

$$K(s) = \frac{-5(s+2)}{s}\,\frac{1.6(s+1.1)}{1.1(s+1.6)}\,\frac{10}{(s+10)}\,\frac{s^2+2(0.013)(20.7)s+(20.7)^2}{s^2+2(0.06)(20.7)s+(20.7)^2} \qquad (3.2)$$

and Tab. 19 summarizes the design. Also, Figs. 34 and 35 show the final Bode and Evans features. Exploiting the inserted filtering, rigid-body gain crossover is up to 1.8 rad/s as seen in Fig. 34. Short period frequency and damping meet Level 1 requirements, however, control anticipation and omega-tau still indicate marginal flying qualities at best (see Tab. 19). Rigid-body

high frequency phase margin and aeroelastic mode 2 gain margin are right at the requirement limits preventing any further performance increments. In Fig. 35 the desensitized higher frequency aeroelastic modes due to the filtering can be clearly seen. Finally, Fig. 36 shows the pitch rate response for a unit pitch rate command step input. Rise time and overshoot look acceptable, and aeroelastic contamination, although present, is reduced due to the sensor placement.

Table 19. Design Summary With 1,850 in Pitch Rate To Elevator

Spec.	Level 1	(unit)	Design
ω_{sp}	≥0.7	(rad/s)	1.59
ζ_{sp}	≥0.35	(-)	0.56
CAP	≥0.16	($1/gs^2$)	0.15
$\omega_{sp}\tau_{\theta 2}$	≥1.3	(-)	0.80
$GM_{<.38}$	≥4.5	(db)	6.54
$PM_{>.38}$	≥45.	(deg)	45.0
GM_2	≥8.	(db)	9.66

Do not perceive this to be an acceptable inner loop design. There are significant risks and concerns with this gain stabilized system. First, gain stabilization could not be achieved with first order low pass filters. To achieve gain stabilization, the system relies upon significant notching just to achieve marginal flying qualities. Even more notching would be required to achieve Level 1 performance. The FCS may be highly vulnerable to modeling inaccuracies in the notched 6th aeroelastic mode. Attenuation filters eat up a significant fraction of the phase margin that must be restored with additional filtering. Finally, the 1st aeroelastic mode damping is not being augmented. Responses due to gusts may experience significantly more aeroelastic contamination than in Fig. 36. Because of these drawbacks, the contractors feel conventional gain stabilization for this vehicle is not feasible. For the given SS/SS architecture with filtering and closely spaced modes, there are few remaining design freedoms. One exception is the location of the pitch sensor.

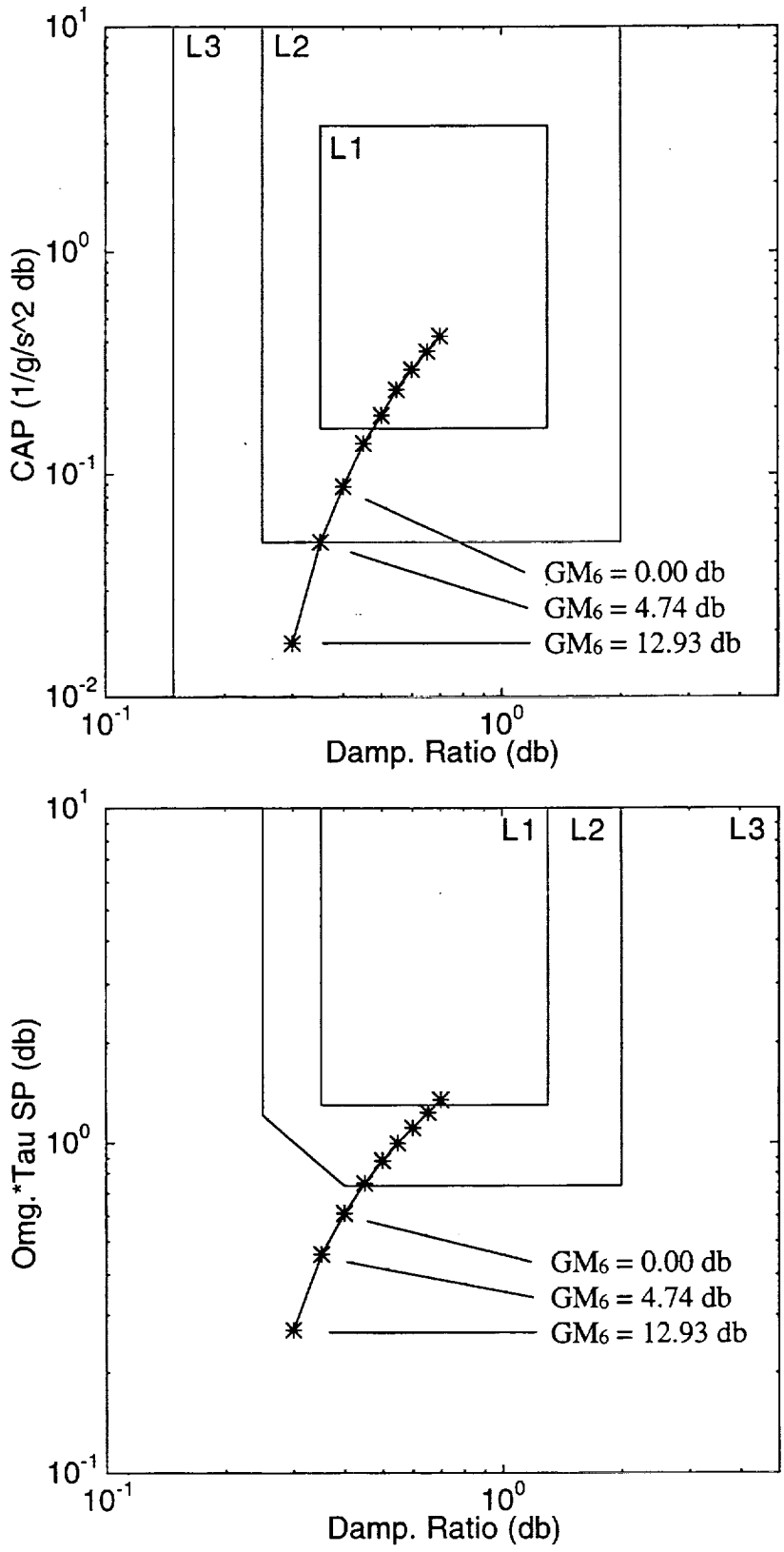

Figure 33. Control Anticipation & Omega-Tau vs. Damping
For 1,850 in Pitch Rate To Elevator Without Filtering

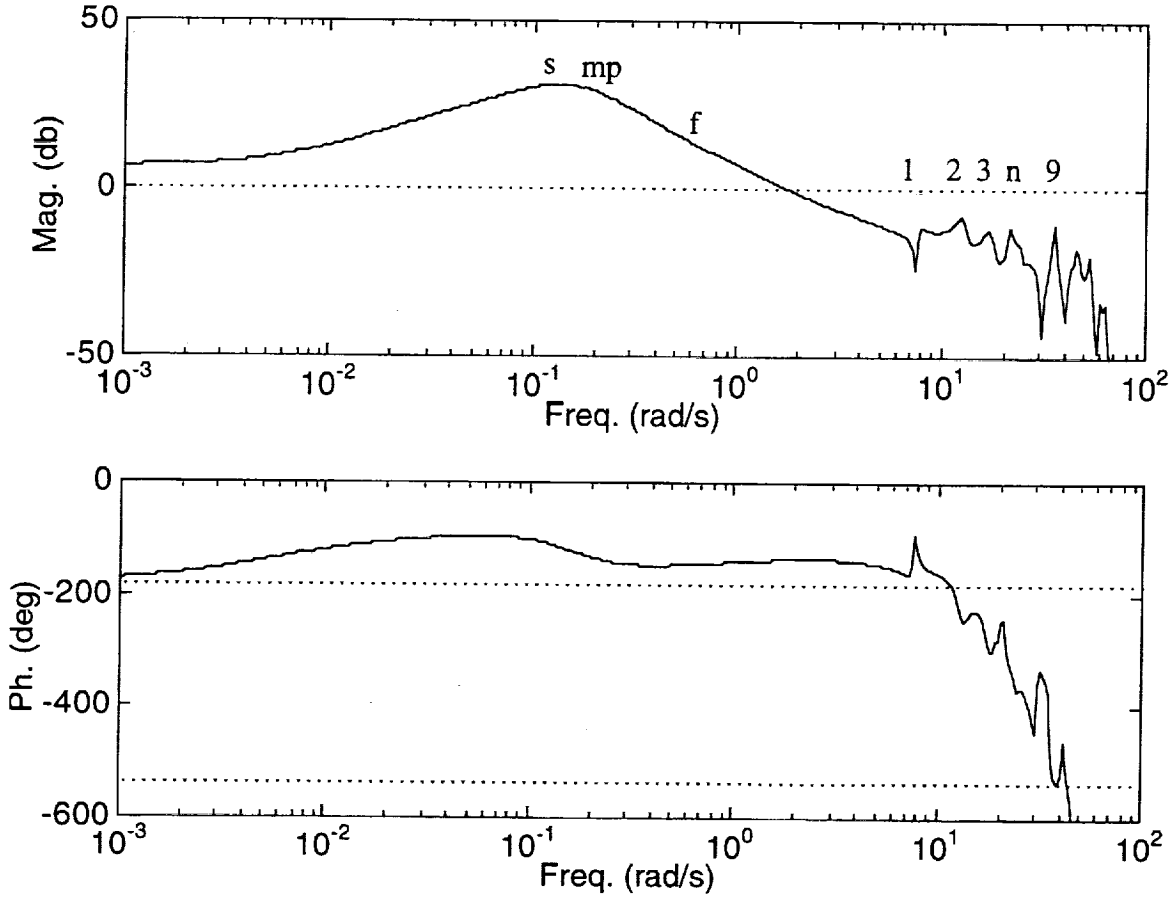

Figure 34. Bode Plot For 1,850 in Pitch Rate To Elevator With Filtering, k = -5.00 rad/rad/s

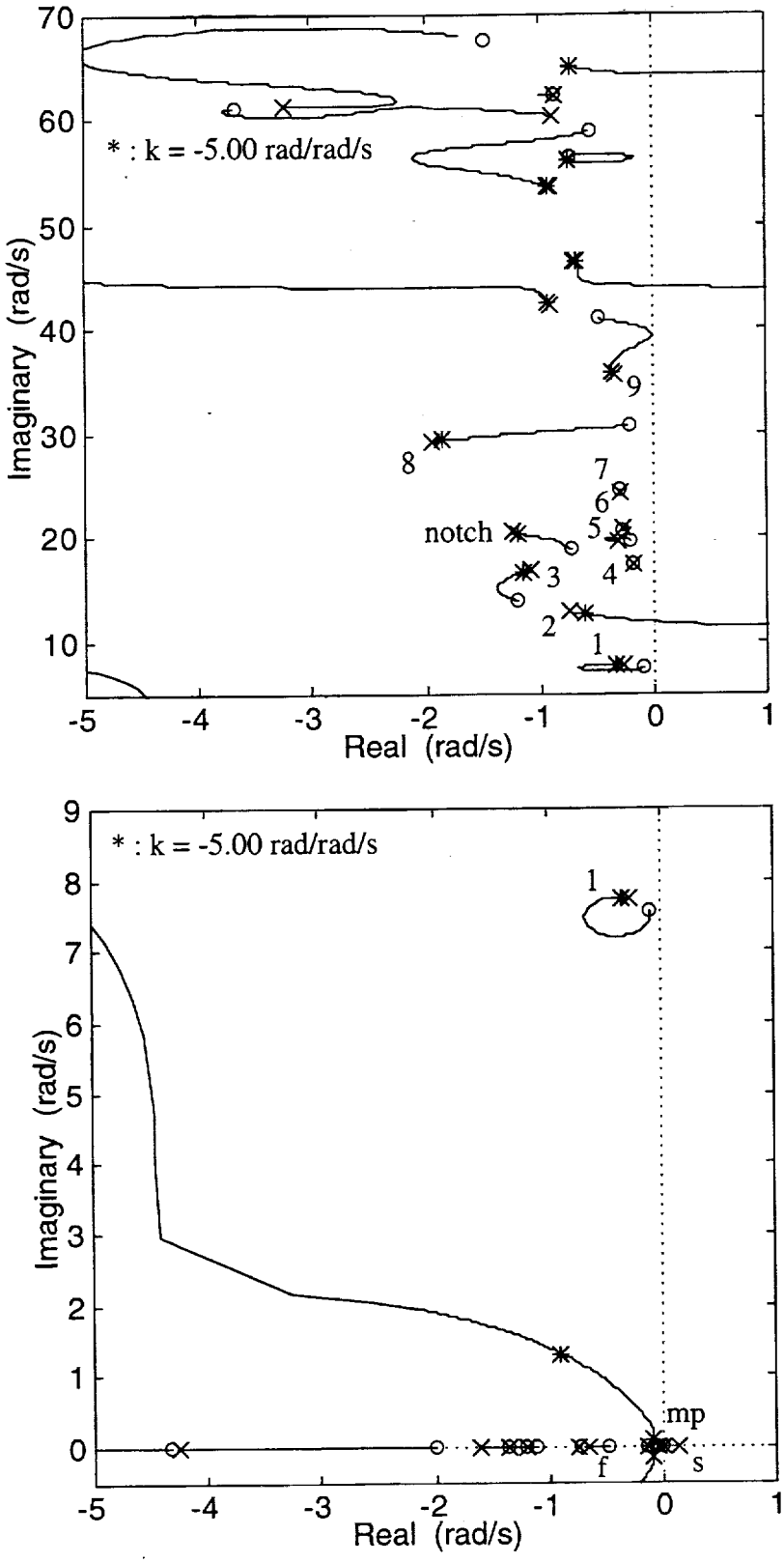

Figure 35. Evans Plot For 1,850 in Pitch Rate To Elevator With Filtering

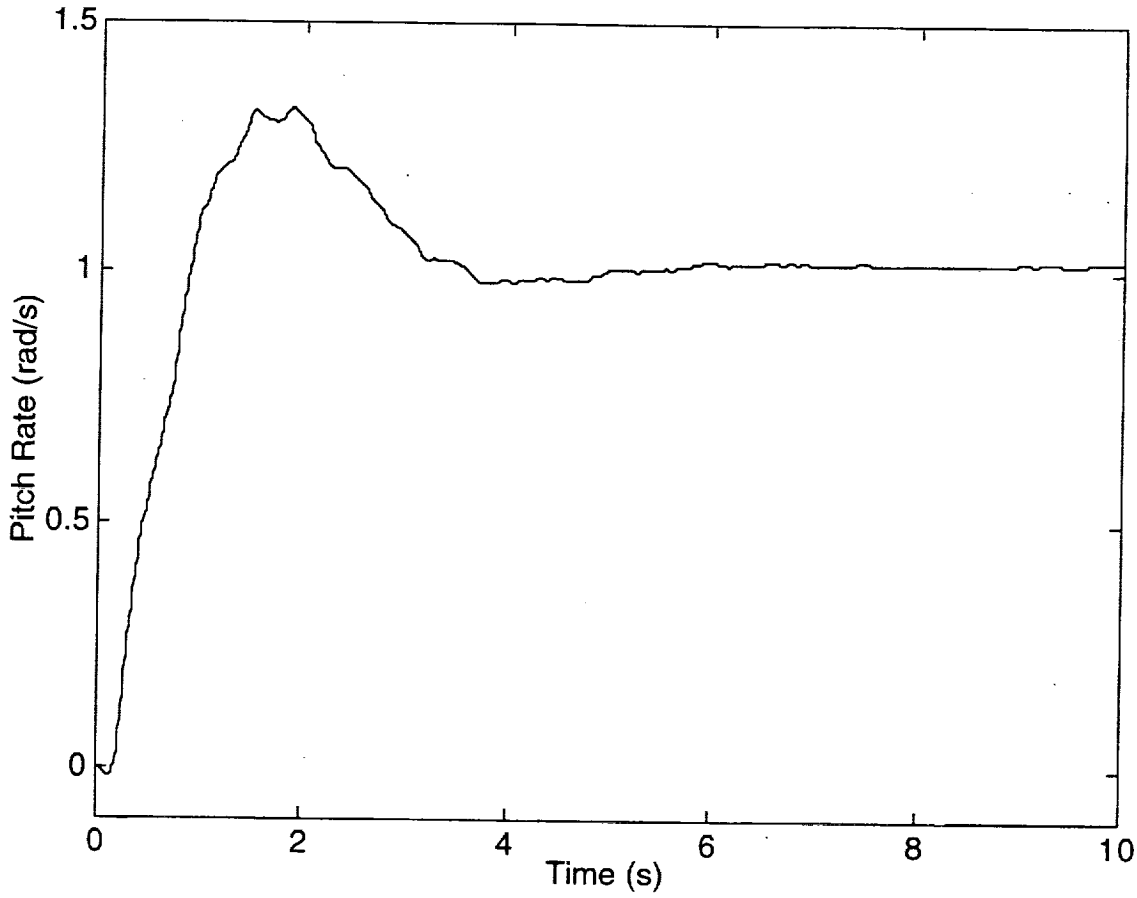

Figure 36. Closed-Loop 1,850 in Pitch Rate Time Response
Due To Unit Step Pitch Rate Command

B. Single-Sensor/Single-Surface Design With Aft Sensor

Reconsider the SS/SS inner loop in Fig. 29 and the proportional plus integral compensation of pitch rate with z = 2 1/s as in Eq. (3.1), but now with an aft mounted sensor. Examination of the mode shapes in Fig. 28 reveals a coincident anti-node for aeroelastic modes 2, 3, 5, and 6 at 2,500 in, which is aft of the center of mass. This station is a good opportunity for alleviating some of the troublesome characteristics with the forward mounting scenario in Fig. 30 due to these same modes. However, note that the rate gyro will now be well displaced from the 1st aeroelastic anti-node. The rate gyro will at least pick up "in phase" pitch motions from mode 1.

Consider the Evans plot behavior for a rate gyro located at 2,500 in along the fuselage centerline shown in Fig. 37. The difficulties with aeroelastic modes 2, 3, 5, and 6 have been eliminated. These modes are now accompanied by closely spaced zeros, preventing the closed-loop locus from penetrating the instability region, or even tending towards that direction. Potential closed-loop aeroelastic instability problems have been pushed out to a higher frequency range (i.e., mode 8). Note the 1st aeroelastic dipole structure has opened up considerably, with the zero migrating down towards the origin. This dipole structure is conducive to damping augmentation of the 1st aeroelastic mode with loop gain adjustment. At lower frequencies, the unstable real axis pole again moves into $1/\tau_{\theta 1}$, and the mid period mode moves out to become the dominate pitch mode. However, with the aft sensor, the mid period mode does not wrap around the compensator zero towards the real axis, but moves instead towards the 1st aeroelastic zeros. Note the limited amount of damping that can be added to the mid period mode due to the loci initially moving out radially from the origin. A clear tradeoff exists between the fore and aft sensor locations and the closed-loop damping of the rigid-body pitch and 1st aeroelastic modes.

The closed-loop poles in Fig. 37 are highlighted for two values of the compensator gain, k = -2.08 and -4.80 rad/rad/s. Figs. 38 and 39 show the corresponding Bode plots for these two gains. For k = -2.08 rad/rad/s, the real axis instability is just stabilized (dc gain of 0 db in Fig. 38 and closed-loop pole at the origin in Fig. 37). Rigid-body gain crossover frequency occurs at 0.88 rad/s, which is again insufficient for pitch damping, frequency, and phase margin requirements.

From the Bode, the 1st aeroelastic peak occurring at 7.7 rad/s may at first look ominous for stability. Closer examination shows that there is ample phase buffer from -180 deg at this magnitude crossover. Here, the 1st aeroelastic mode is phase stable (i.e., the loop transfer pierces the unit circle, but away from -180 deg). This feature corresponds to the augmented 1st aeroelastic pole moving away from the imaginary axis in the Evans plot. The aeroelastic peak occurring at 29 rad/s (i.e., mode 8) is a real danger for high frequency instability. In contrast, with k = -4.80 rad/rad/s, the 8th aeroelastic mode is just destabilized. The peak just touches the 0 db level and the closed-loop root is on the jω axis. Gain crossover is better at 1.4 rad/s, but still insufficient. Finally, note the real axis instability is fully stabilized.

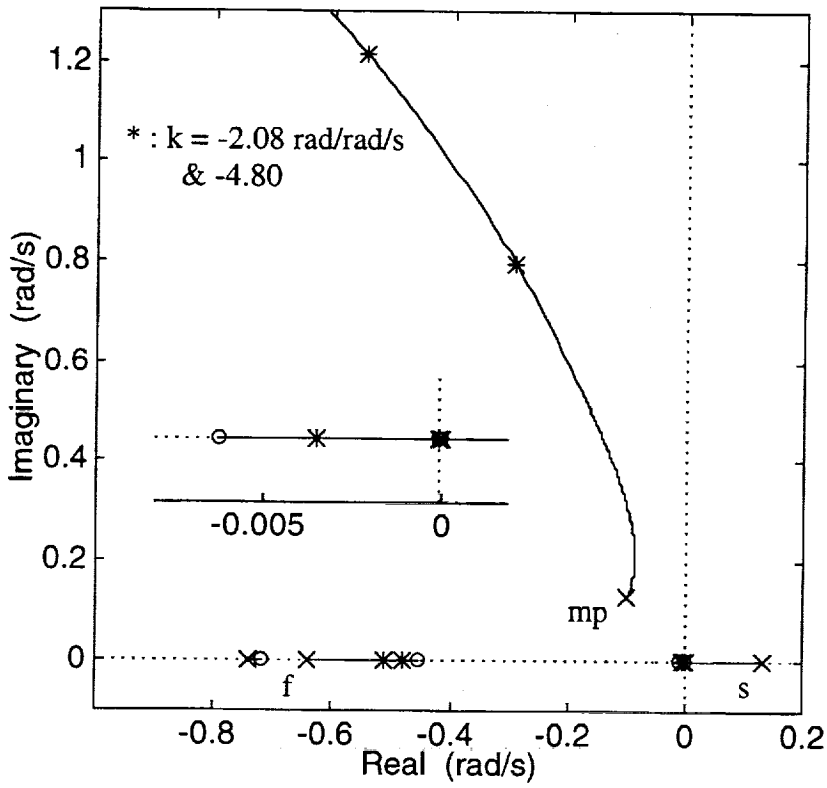

Figure 37. Evans Plot For 2,500 in Pitch Rate To Elevator Without Filtering

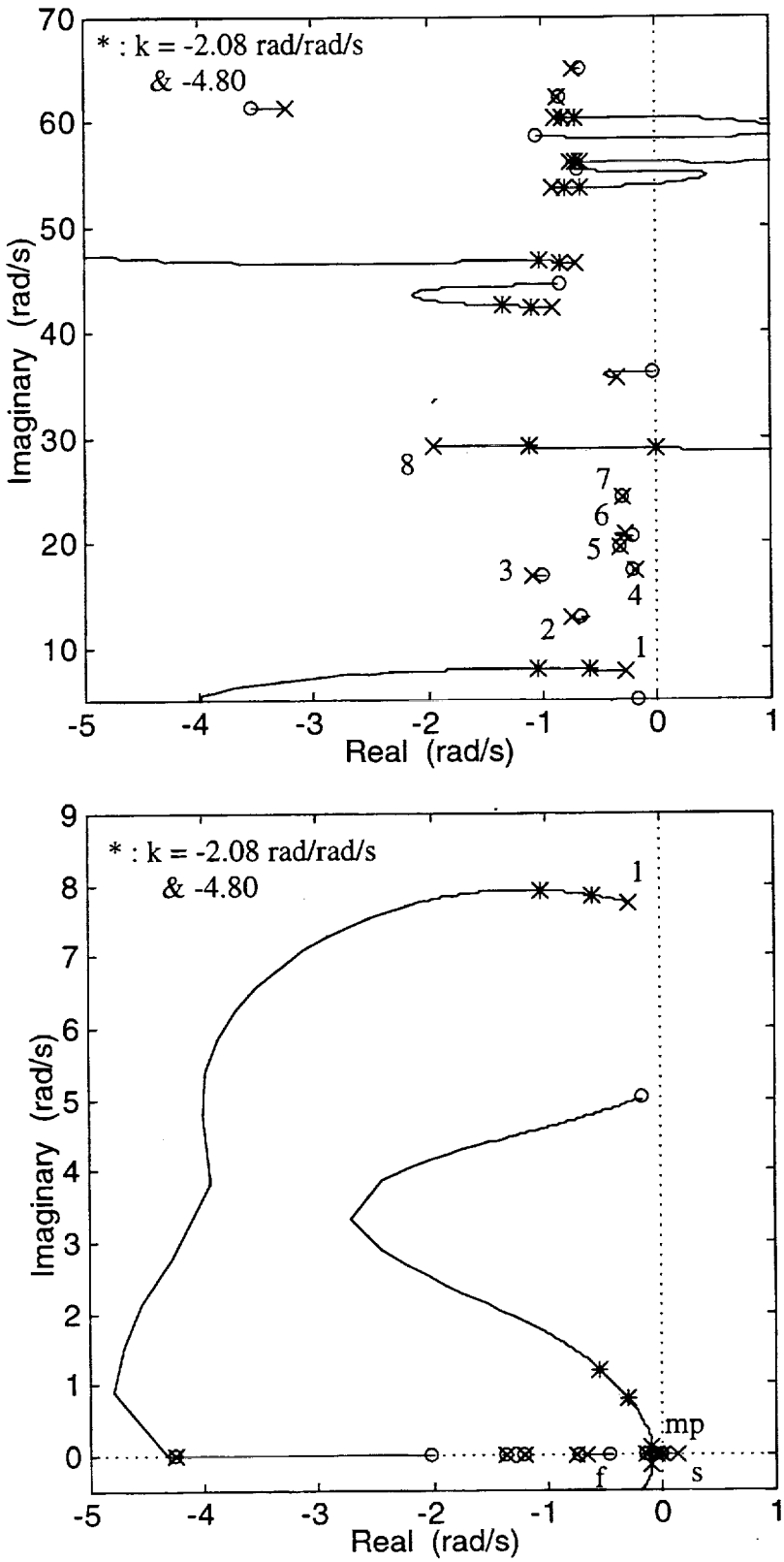

Figure 37. Continued

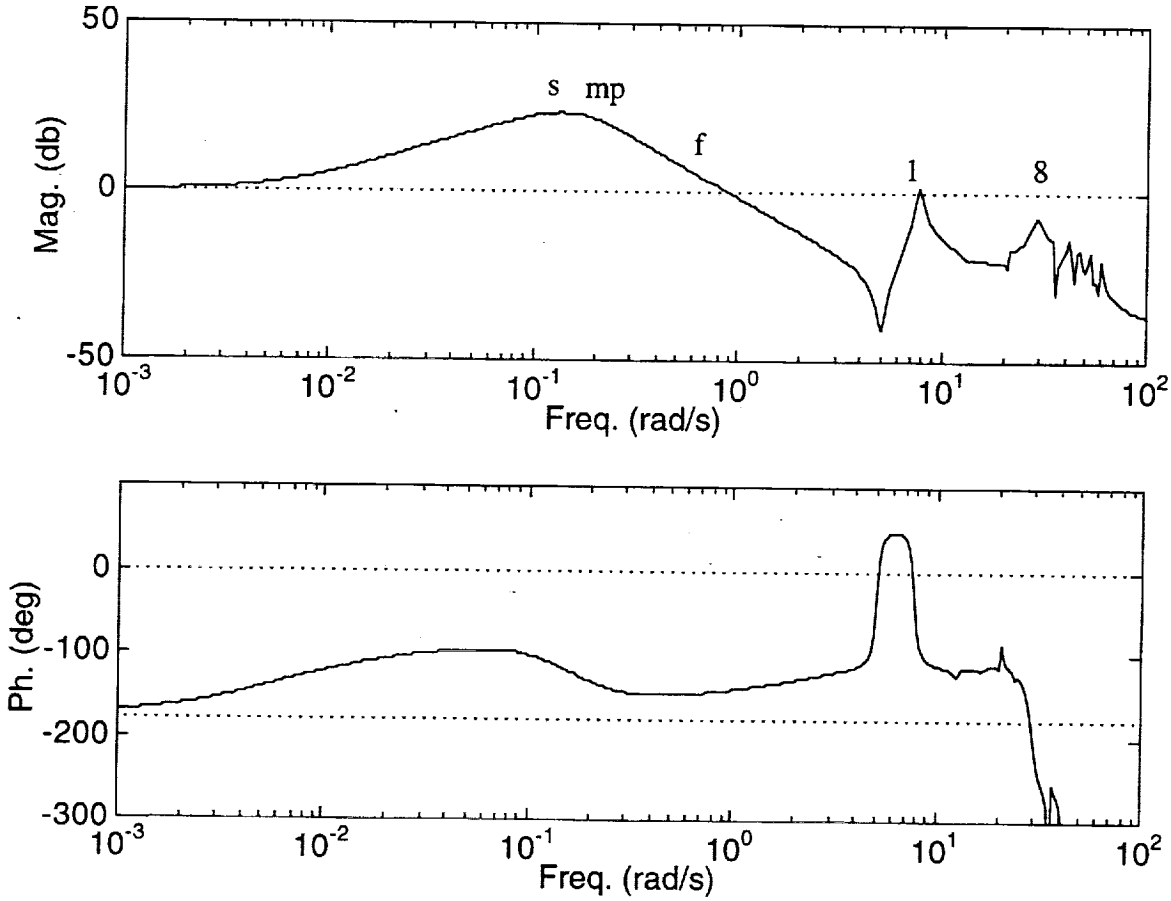

Figure 38. Bode Plot For 2,500 in Pitch Rate To Elevator Without Filtering, k = -2.08 rad/rad/s

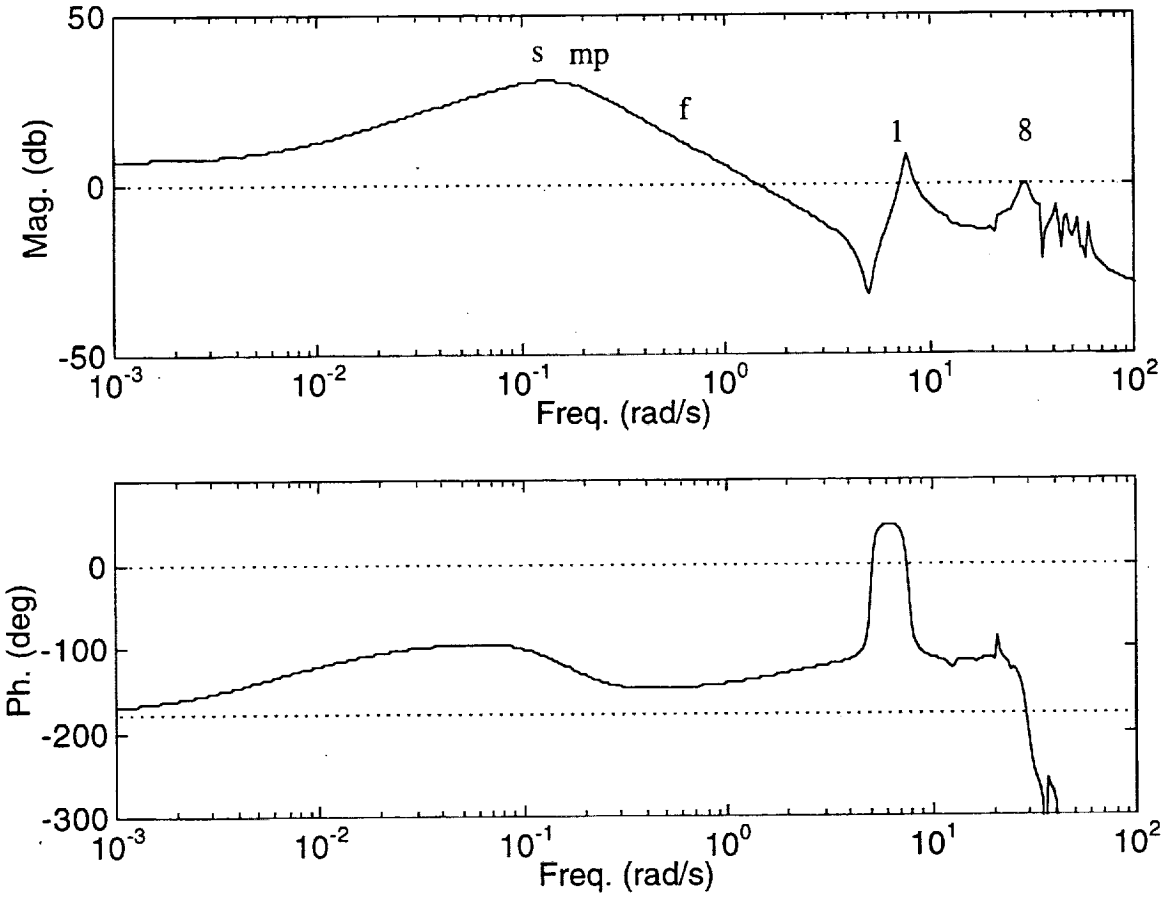

Figure 39. Bode Plot For 2,500 in Pitch Rate To Elevator Without Filtering, k = -4.80 rad/rad/s

Solid numbers for these features are given in Tab. 20. As pure loop gain is adjusted with no filtering, the table again shows compliance or non-compliance with flying quality requirements. Note that two entries in the table correspond to the gains previously discussed. One entry corresponds to a 0.05 damping reduction from k = -2.08 rad/rad/s. Other entries in Tab. 20 correspond to the same closed-loop rigid pitch frequency values appearing in Table 18 (observe the reduced dampings at equivalent frequencies for the aft sensor). Level 1 short period damping, frequency, control anticipation, and phase margin can again be reached, but not without intolerable trades with aeroelastic mode 8 gain margins. As loop gain is increased, aeroelastic mode 8 gain margin violates the requirement slightly before the relaxed static stability pole is even stabilized. Fig. 40 illustrates the situation further. These plots show the CAP vs. ζ and $\omega_{sp}\tau_{\theta 2}$ vs. ζ predicted pilot ratings with aeroelastic gain margin as the parameterization. The 8th aeroelastic mode is driven unstable just as moderate rigid-body flying qualities are being approached. As a final comment, note that Tab. 20 does not list the phase margins for the 1st aeroelastic mode. In every case except k = -15.36 rad/rad/s, the phase margin was above the 60 deg requirement.

Table 20. System Characteristics With Gain Adjustment For 2,500 in Pitch Rate To Elevator Without Filtering

-k (r/r/s)	ω_{sp} ≥0.7 (r/s)	ζ_{sp} ≥0.35 (-)	CAP ≥0.16 ($1/gs^2$)	$\omega_{sp}\tau_{\theta 2}$ ≥1.3 (-)	$GM_{<.38}$ ≥4.5 (db)	$PM_{>.38}$ ≥45. (deg)	GM_8 ≥8. (db)
0.69	0.46	0.30	0.013	0.23	-9.55	31.5	16.94
2.08	0.85	0.35	0.043	0.43	0.00	36.0	7.35
4.80	1.33	0.41	0.11	0.66	7.29	43.2	0.00
6.06	1.51	0.43	0.14	0.75	9.32	45.8	-1.93
8.01	1.76	0.47	0.19	0.88	11.74	49.0	-4.36
10.02	2.00	0.50	0.24	1.00	13.69	51.7	-6.30
11.90	2.22	0.53	0.29	1.11	15.18	53.8	-7.80
13.73	2.44	0.56	0.36	1.22	16.42	55.4	-9.04
15.36	2.65	0.58	0.42	1.33	17.40	56.6	-10.01

To again reduce the sensitivity of the higher frequency aeroelastic modes as loop gain is increased to meet lower frequency requirements, a proportional plus integral compensator with filtering must be considered. Because of phase stabilization of mode 1 and the coincident anti-node of modes 2, 3, 5, and 6, sufficient frequency separation exists to insert a simple low pass filter

between the rigid-body modes and mode 8 in order to obtain measurable attenuation of mode 8. Notching is not required for the aft sensor. A break frequency of 18 rad/s is used for the low pass. The filter adds roughly 5 deg phase loss at the gain crossover. To recover this loss, an additional lead-lag filter is added. With this filtering in place, loop gain is increased until aeroelastic mode 8 reaches the gain margin requirement.

The final compensator is

$$K(s) = \frac{-5.33(s+2)}{s} \frac{1.6(s+1.35)}{1.35(s+1.6)} \frac{18}{(s+18)} \tag{3.3}$$

and Tab. 21 summarizes the design. Figs. 41 and 42 also show the final Bode and Evans plots. Filtering has allowed the rigid-body gain crossover to be boosted to 1.6 rad/s as seen in Fig. 41. Short period frequency and damping meet Level 1 requirements, however, control anticipation and omega-tau are still below values that are considered appropriate for good flying qualities (see Tab. 21). Note that for roughly the same closed-loop rigid pitch frequency, the aft design has less damping relative to the forward case. Rigid-body high frequency phase margin and aeroelastic mode 8 gain margin are right at the requirement limits preventing any further performance increments (for the given filter break frequency). In Fig. 42 the effect of the filter in desensitizing the higher frequency aeroelastic modes is clearly seen. Finally, Fig. 43 shows the pitch rate response for a unit pitch rate command step input. Rise time and overshoot look acceptable, but aeroelastic contamination looks quite severe.

Table 21. Design Summary With 2,500 in Pitch Rate To Elevator

Spec.	Level 1	(unit)	Design
ω_{sp}	≥0.7	(rad/s)	1.49
ζ_{sp}	≥0.35	(-)	0.47
CAP	≥0.16	($1/gs^2$)	0.13
$\omega_{sp}\tau_{\theta 2}$	≥1.3	(-)	0.75
$GM_{<.38}$	≥4.5	(db)	8.20
$PM_{>.38}$	≥45.	(deg)	45.0
GM_8	≥8.	(db)	9.65

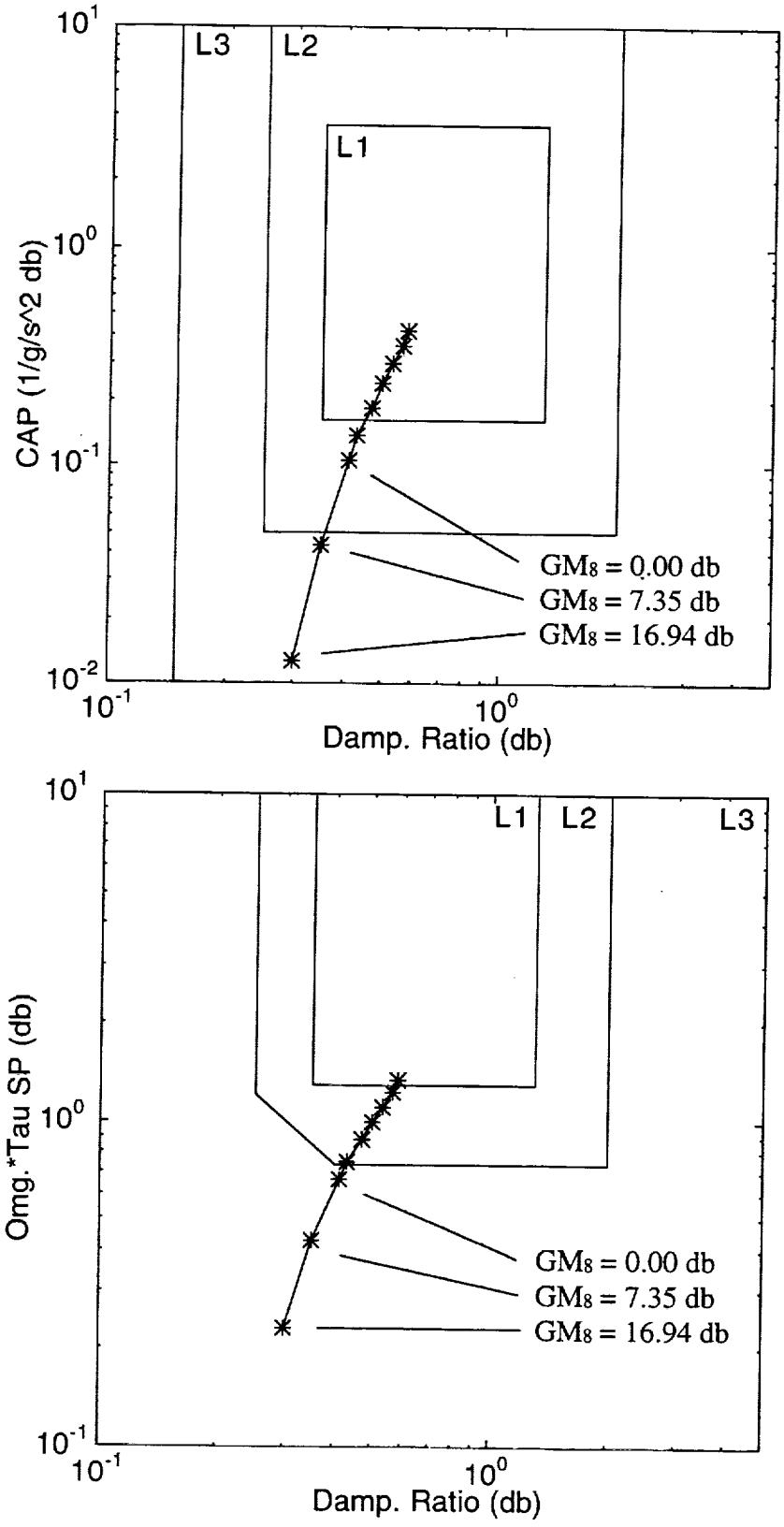

Figure 40. Control Anticipation & Omega-Tau vs. Damping
For 2,500 in Pitch Rate To Elevator Without Filtering

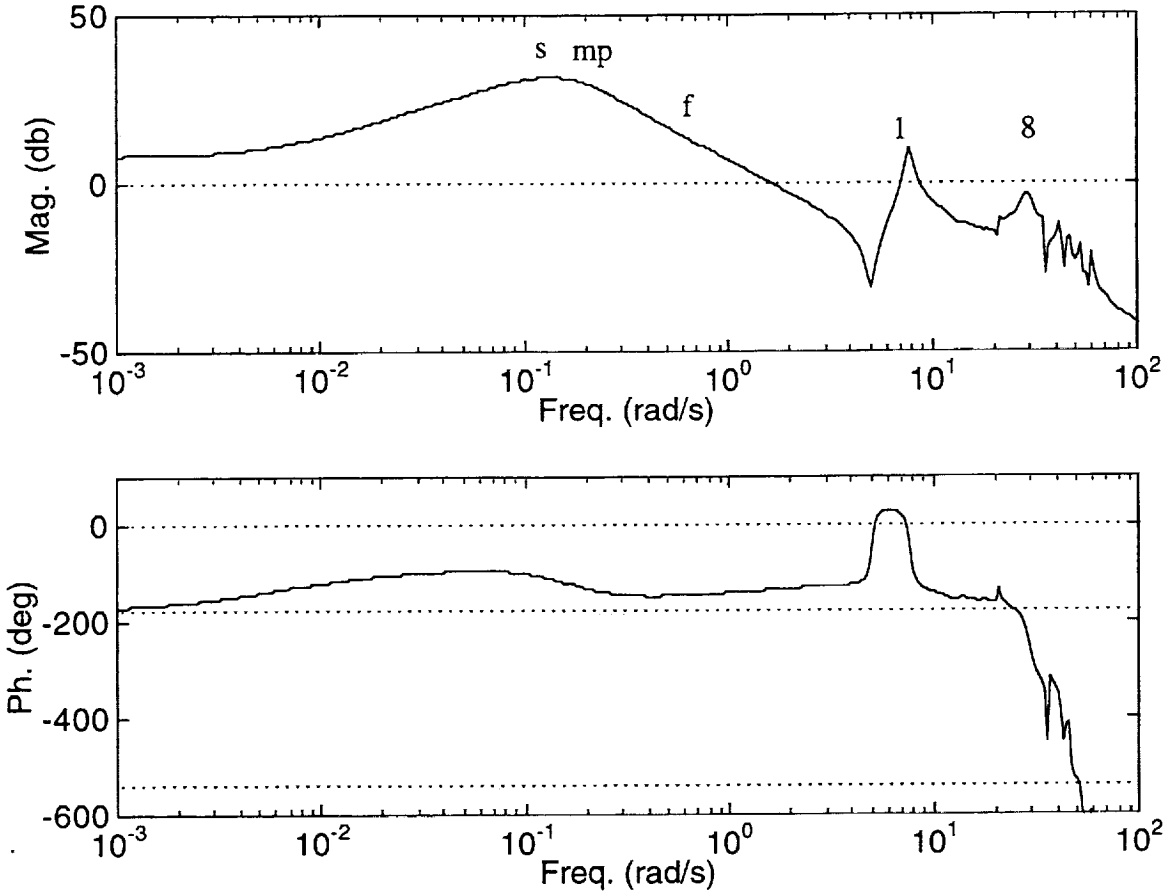

Figure 41. Bode Plot For 2,500 in Pitch Rate To Elevator With Filtering, k = -5.33 rad/rad/s

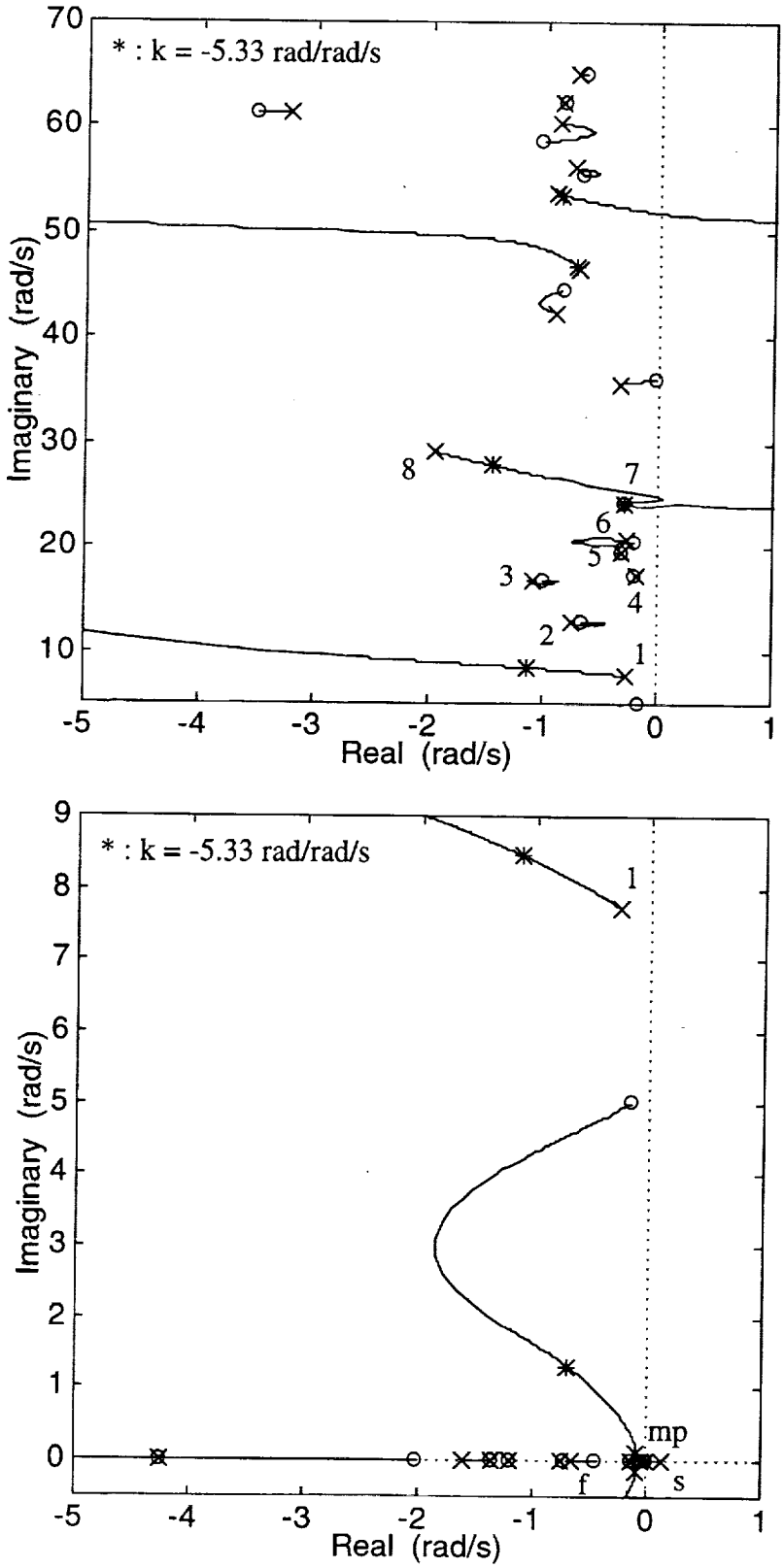

Figure 42. Evans Plot For 2,500 in Pitch Rate To Elevator With Filtering

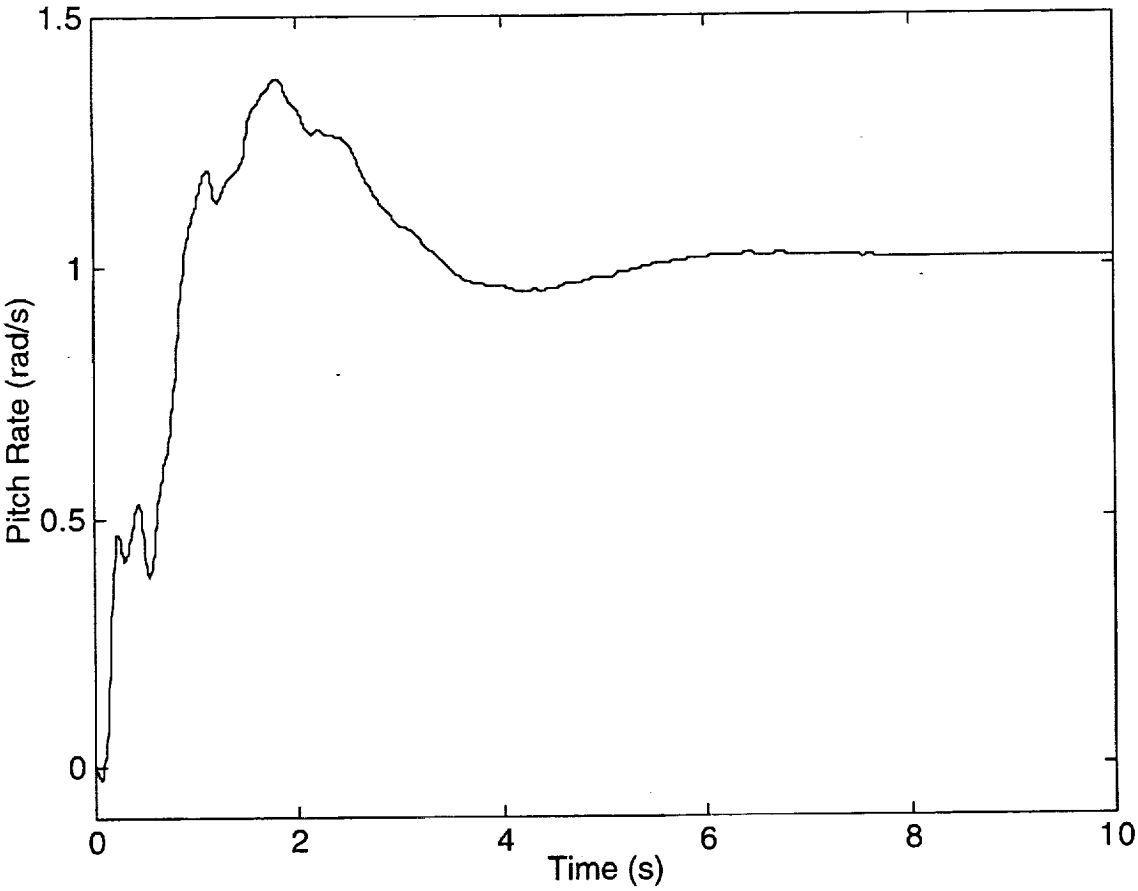

Figure 43. Closed-Loop 2,500 in Pitch Rate Time Response
Due To Unit Step Pitch Rate Command

A few comments concerning the forward and aft sensor designs are appropriate before moving on with the discussion. The designs are comparable based on the observation that closed-loop rigid pitch frequencies are roughly equal, rigid-body phase margin and aeroelastic gain margin are roughly at the requirement limits, each uses a low pass filter roughly 10 rad/s below the critical aeroelastic peak requiring attenuation, and both are predicted to have marginal flying qualities. Each design could use more aggressive filter attenuation to obtain further performance benefits, or to skew the advantages of one design over the other. This misrepresentation of the facts was intentionally avoided.

This phase stabilized system is by no means the final answer to the inner loop FCS. Significant concerns exist here also. At first glance, phase stabilization may appear as less of a risk since the Nyquist trace would be away from the critical -1 point when lying outside the unit circle. However, an aeroelastic mode which lies outside the unit circle is a significant risk in itself if the model is inaccurate. The FCS may be vulnerable to modeling inaccuracies in the phase stabilized 1st aeroelastic mode. Another point to note is that even though the 1st aeroelastic mode damping has increased relative to the forward sensor design, the aeroelastic contamination in the time response has gotten worse. The "loose" dipole structure leads to increased mode 1 participation in the input-output channel, which swamps the damping increase. Pilot opinion ratings of this high frequency contamination are expected to be lacking. Finally, recall that the rigid pitch control anticipation and omega-tau characteristics are still marginal. Because of these drawbacks, the contractors feel the non-conventional phase stabilized strategy for this vehicle is also probably not feasible.

C. Multi-Sensor/Single-Surface Design With Forward & Aft Sensors

The investigations thus far point to the conclusion that the SS/SS architecture is probably not sufficient to meet the design objectives for the highly flexible Ref. H HSCT vehicle, and more design freedom is required. A specific strategy, which surpasses the SS/SS architecture capabilities, but falls short of being a truly multivariable FCS, is addressed next. Consider the

Multi-Sensor/Single-Surface (MS/SS) architecture depicted in Fig. 44. Here, the feedback signal q_b consists of a blend of two rate gyro signals q_{xs1} and q_{xs2}, where $H_1(s)$ and $H_2(s)$ denote blending filters. This technique is an old strategy often overlooked in the modern control era.[8,11] Ref. 11 uses the MS/SS logic to achieve phase stable aeroelastic dipole structures. A different perspective is taken here.

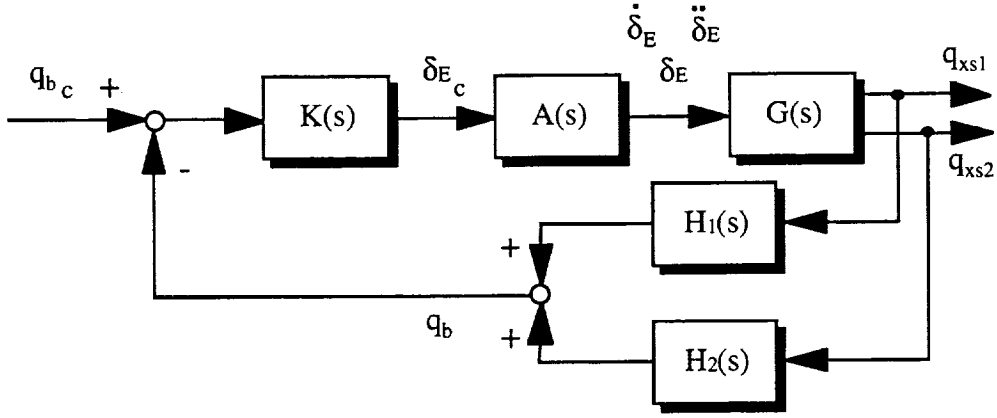

Figure 44. Multi-Sensor/Single-Surface Feedback Loop

The methodology is to blend the desirable features of the fore and aft sensor designs and avoid the undesirable features. For a specific blending strategy, reconsider the loci behavior in Figs. 30 and 37. For the forward sensor, observe the desirable low frequency characteristics below 10 rad/s (relaxed stability stabilization, pitch damping augmentation, and aeroelastic mode 1 cancellation), while above this frequency undesirable behavior is present (aeroelastic destabilization). Note the opposite trend with the aft sensor; undesirable features reside below 10 rad/s (limited pitch damping augmentation), while desirable characteristics are present above 10 rad/s (aeroelastic mode cancellations), until 30 rad/s is reached. Therefore, below 10 rad/s the 1,850 in sensor signal will be used, above 10 rad/s but below 30 rad/s the 2,500 in sensor signal is to be used, and above 30 rad/s attenuation of all feedback signals is enforced. Fig. 45 shows the blending filter frequency responses where $H_1(s)$ and $H_2(s)$ are low pass and band pass (with break frequencies not precisely at 10 and 30 rad/s after manual tuning), or

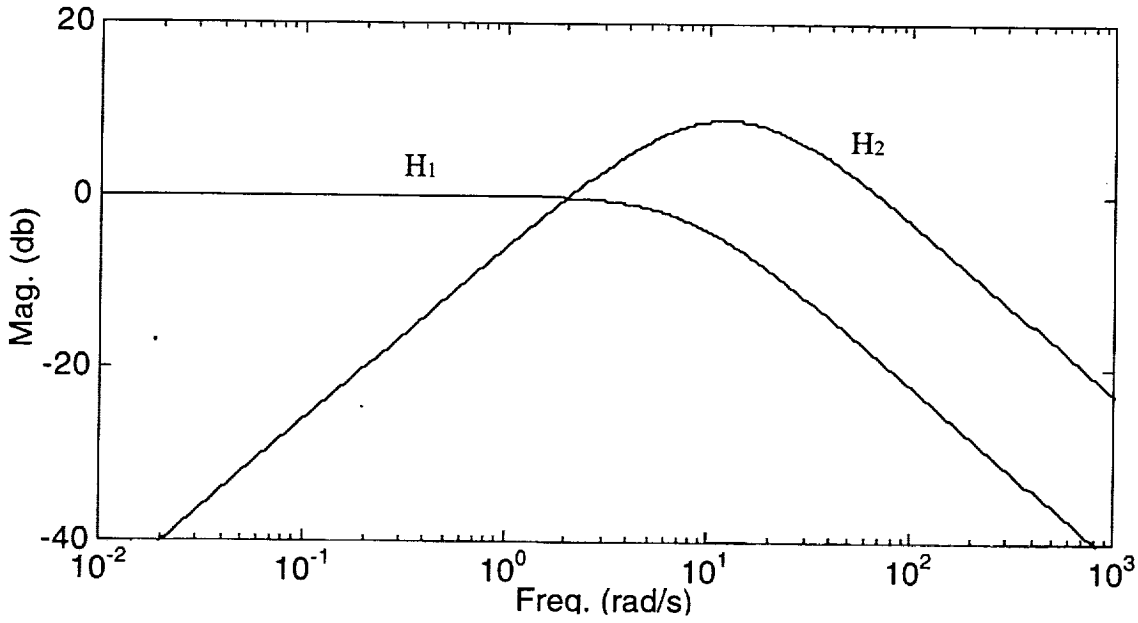

Figure 45. Low And Band Pass Blending Filter Frequency Responses

$$H_1(s) = \frac{8}{(s+8)} \qquad (3.4)$$

$$H_2(s) = 4\,\frac{s}{(s+8)}\,\frac{18}{(s+18)}$$

The MS/SS Evans behavior is shown in Fig. 46, and the results correlate with the objectives and intentions of the flight control engineer, but with some offending features. For frequencies below 10 rad/s, the closed-loop dynamics correlate with the forward SS/SS design in Fig. 30. A conventional, well damped rigid pitch mode is present. With the aft-to-fore signal weighted 4-to-1, the 1st aeroelastic dipole is unfortunately no tighter than in the SS/SS aft design in Fig. 37. An aft-to-fore ratio of 1-to-4 would similarly lead to problems with the location of aeroelastic mode 6 zeros as in Fig. 30. For frequencies in the band between 10 rad/s and 30 rad/s, the closed-loop dynamics match the aft SS/SS design. The aeroelastic modes are generally canceled due to the coincident anti-nodes.

Examination of the closed-loop transfer function consistent with Fig. 44 reveals the blending filters result in an extra first order over second order factor with roots at -1.7, -8,, and -20. 1/s, respectively. Impacts from this new factor on the flying qualities is unknown, but not

expected to be good. More troublesome is the 1st aeroelastic zeros having been pushed slightly to nonminimum phase. Mode 1 will no longer be phase stable, limiting rigid-body performance increments by loop gain adjustment. Fig. 47 shows the corresponding Bode plot with the loop gain set to just stabilize the real axis instability. Note aeroelastic mode 8 is already in violation of the gain/phase margin requirements of 8 db and 60 deg. Due to these deficiencies, the contractors also feel the MS/SS architecture with the specific blending filters in Eq. (3.4), although demonstrating some advantages over SS/SS scenarios, is probably not feasible for this vehicle.

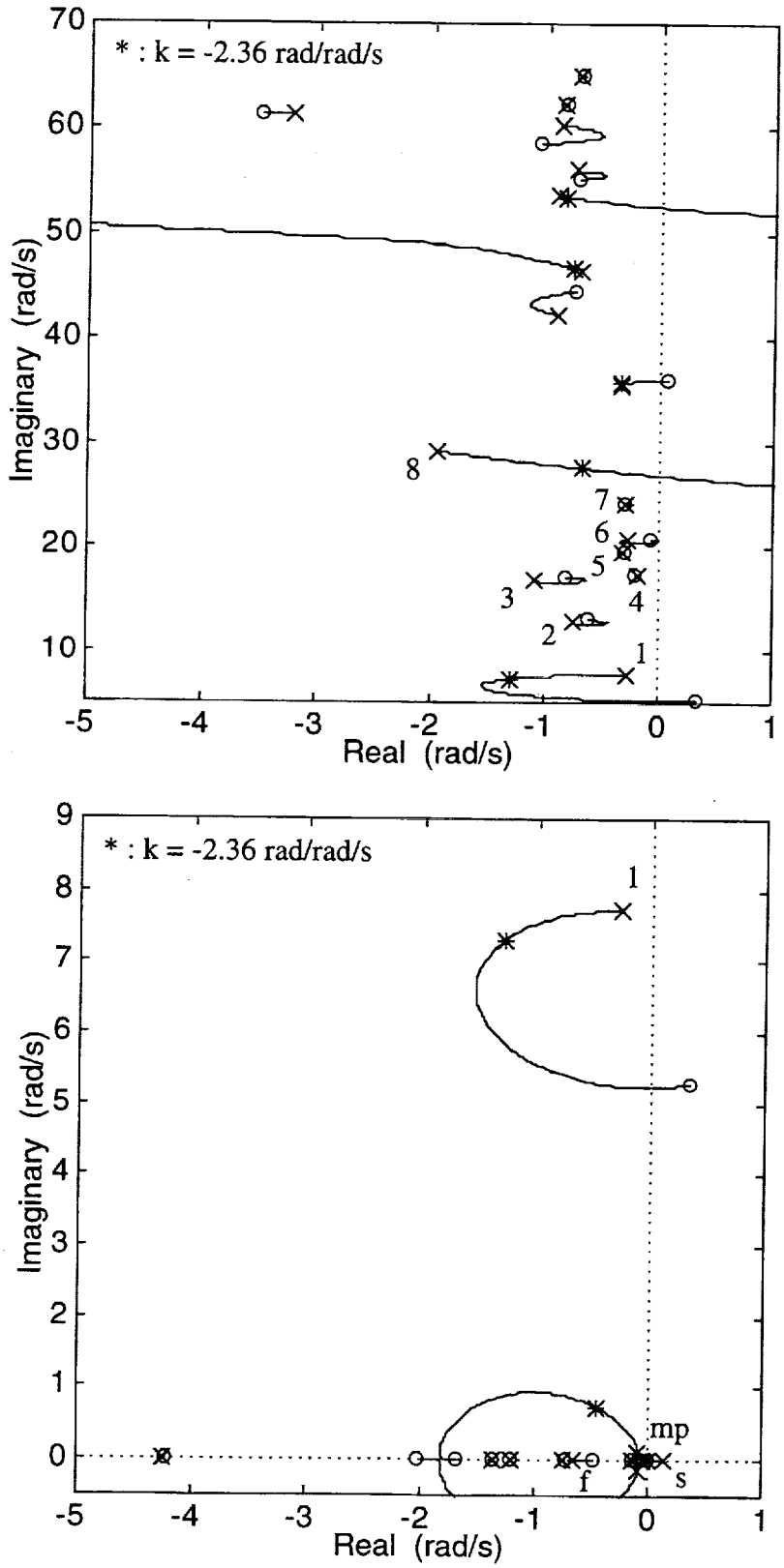

Figure 46. Evans Plot For Blend Of Low Pass 1,850 in And Band Pass 2,500 in Pitch Rate To Elevator

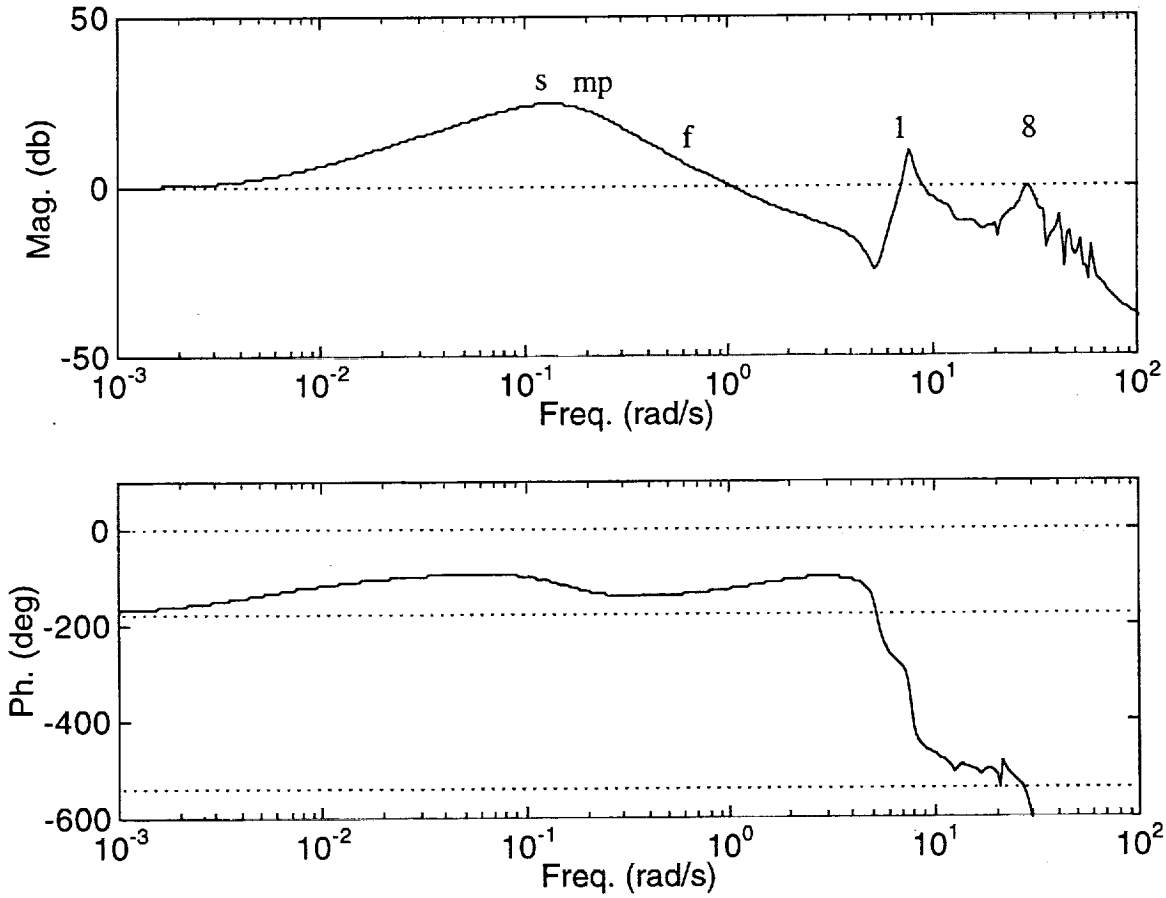

Figure 47. Bode Plot For Blend Of Low Pass 1,850 in
And Band Pass 2,500 in Pitch Rate To Elevator, k = -2.36 rad/rad/s

Section IV
Expanded Look at Multi-Sensor/Single-Surface Design Strategies

A. Optimal Sensor Placement

MS/SS architectures indicate some potential for improved closed-loop properties, relative to the SS/SS systems. However, the MS/SS loop is not without it's own difficulties. Specifically, nonminimum phase 1st aeroelastic zeros and their effect of bounding the usable loop gain is of concern. Selection of the blending filters and sensor locations for the MS/SS design in Section III-C was completed manually, based upon insight and familiarity with the vehicle dynamics. This approach has served well in laying a solid foundation to build upon. The question to be addressed now is whether a formal optimization search can squeeze any remaining benefits from the concept by reducing, or fully eliminating, the nonminimum phase characteristic of mode 1, without degrading other features. Success here would make the MS/SS architecture a more viable FCS.

Existing techniques appearing in the literature[19-22] for optimal sensor placement on flexible structures offer little assistance here. Most all reported studies have focused on either

1. Open-loop criteria like controllability/observability of the vehicle alone,
2. Closed-loop criteria employing control methodologies which have seen limited use in practice,
3. Large space structure vehicles (i.e., 2nd order systems with symmetric matrices), and
4. Vibration suppression (i.e., no allowance for rigid-body motion or control).

These studies appear to lack key aspects of our problem. Control design methodologies considered here are conventional based, not contemporary based. Open-loop criteria based upon key features from the Evans/Bode plots are of interest, rather than state space metrics. Further, the dynamic systems of interest have airflow pressures as the single most important load influencing the motion. Finally, our closed-loop objectives of rigid-body control and aeroelastic suppression are inherently integrated and can not be considered separately, without introducing large errors.

Criteria for optimal sensor placement must incorporate or address the critical aspects of the FCS design if success is to be achieved.

The single most important feature determining how the aeroelastic dynamics are augmented, as the proportional plus integral control law in Eq. (3.1) works the rigid-body pitch characteristics, are the dipole structures. Consider Fig. 48 which describes the structure of an aeroelastic dipole. The i^{th} aeroelastic dipole consists of a pole and zero denoted as p_i and $\tilde{z}_i$. Vector δ_i locates the aeroelastic zero in the complex plane, relative to the aeroelastic pole. The vector can be broken down into a magnitude and phase as

$$\delta_i = |\delta_i| e^{j \angle(\delta_i)} \tag{4.1}$$

To cancel the effects of the aeroelastic mode from the input-output channel, minimization of $|\delta_i|$ is appropriate. For typical aircraft pitch rate to elevator transfer functions, the dipole root locus has a stabilizing behavior if the zero lies below the pole.[8] Consequently, if damping augmentation of the aeroelastic mode is the objective, then minimization of $|\angle(\delta_i) - (-\pi/2)|$ is a logical criteria to consider.

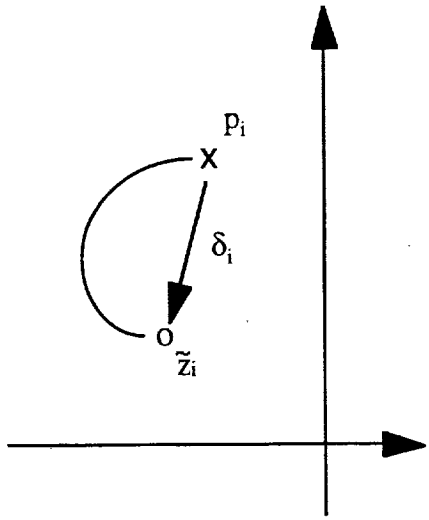

Figure 48. Aeroelastic Dipole Structure

A general cost functional includes both objectives, or

$$f(x_{s1},x_{s2},a,b,c,h_1,h_2) = \ldots + w_i|\delta_i| + w_i'|\angle(\delta_i) - (-\pi/2)| + \ldots \tag{4.2}$$

where w_i and w_i' are weights to be selected by the engineer. Note the dependency of f on the independent variables: sensor locations x_{s1}, x_{s2} and blending filter parameters a, b, c, h_1, h_2 where

$$H_1(s) = h_1 \frac{a}{(s+a)} = \frac{n_{H1}}{d_{H1}} \tag{4.3}$$

$$H_2(s) = h_2 \frac{s}{(s+b)} \frac{c}{(s+c)} = \frac{n_{H2}}{d_{H2}}$$

The functional dependency of δ_i upon the sensor locations and filter parameters is rather complex, highly nonlinear, and awkward to express mathematically. The sensor locations first determine the individual vehicle transfer function zeros as described in Section II-A and is represented here as

$$\begin{bmatrix} q_{xs1} \\ q_{xs2} \end{bmatrix} = \frac{1}{d_G} \begin{bmatrix} n_{G1} \\ n_{G2} \end{bmatrix} \delta_E \tag{4.4}$$

Secondly, according to Fig. 44, the filters use this information to construct the blended vehicle transfer function zeros, or

$$q_b = \frac{n_{G1}n_{H1}d_{H2} + n_{G2}n_{H2}d_{H1}}{d_G d_{H1} d_{H2}} \delta_E \tag{4.5}$$

After factoring the numerator and denominator of q_b/δ_E, the plant poles and zeros are available, a subset of which is the aeroelastic poles and zeros. It is not sufficient to locate the nearest zero to the aeroelastic pole in computing δ_i. In an Evans plot, the poles do not always migrate towards the nearest zero, especially with modally dense aeroelastic vehicles. To determine which aeroelastic zero z_j pairs off with aeroelastic pole p_i to form $\tilde{z}_i$, a root locus calculation is necessary. With the compensator and actuator denoted as

$$K(s) = k \frac{n_K}{d_K} \tag{4.6}$$

$$A(s) = \frac{n_A}{d_A}$$

the open-loop poles and zeros and closed-loop poles are determined as

$$\begin{aligned} &kn_K n_A(n_{G1}n_{H1}d_{H2} + n_{G2}n_{H2}d_{H1}) = k'(s+z_1) \ldots (s+z_n) \\ &d_K d_A d_G d_{H1} d_{H2} + kn_K n_A(n_{G1}n_{H1}d_{H2} + n_{G2}n_{H2}d_{H1}) = (s+p_{cl\,1}) \ldots (s+p_{cl\,m}) \;\forall\; k \le 0 \end{aligned} \tag{4.7}$$

where

$$p_{cl\,i} = p_i \text{ for } k = 0$$
$$p_{cl\,i} = z_i \text{ or } \pm\infty \text{ for } k = -\infty \tag{4.8}$$

Use the root loci to determine which zero is associated with the aeroelastic pole, or

$$\tilde{z}_i = z_j \mid p_i \text{ migrates towards } z_j \text{ as } k : 0 \rightarrow -\infty \tag{4.9}$$

Finally, δ_i is given as

$$\delta_i = \tilde{z}_i - p_i \tag{4.10}$$

Although less computationally efficient, a steady and reliable first order gradient or steepest descent optimization algorithm was considered.[23] A flow chart for the algorithm is given in Fig. 49 where x denotes the vector of independent parameters and f(x) is the cost function. As developed above, the problem is classified as an unconstrained optimization problem. There are practical constraints that need to be enforced. These constraints include sensor locations lying between the vehicle nose and tail, and nonnegative, but bounded, filter parameters. If not constrained, the optimizer has, on occasion, exploited this freedom. The resulting closed-loop systems have been impractical. Rather than appending these inequality constraints to the cost function explicitly, they are implicitly included in the adaptive step algorithm as indicated by Fig. 49. Note the output solution in Fig. 49 is a local minimum which depends on the starting conditions. There are no easy answers to these issues, as always.

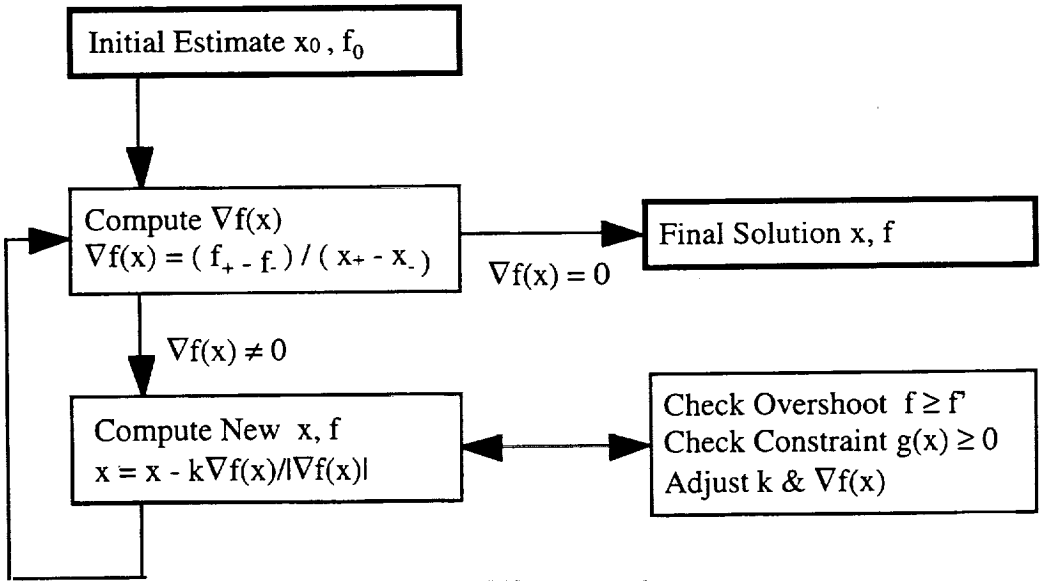

Figure 49. Steepest Descent Solution Algorithm

In the overall FCS design process, note the optimizer only provides the blended transfer function zeros. Rather than releasing all aspects of the solution to the optimizer, only a fraction was delegated to the optimizer. The engineer must still complete the design manually with the Evans/Bode plots by setting closed-loop poles, gain/phase margins, etc. This partitioning is intentional and considered to be a good strategy because optimization is a powerful tool, but if used blindly, optimization will almost invariably bite back with impractical results. It must be treated with caution and respect.

Due to the untimely nature in the delivery of valid aeroelastic models of the Ref. H HSCT to the contractors, insufficient time existed to exercise the optimal sensor placement scheme on the Ref. H configuration. Several runs were tested on the SCRA model, however. With high similarity between the previous SCRA studies and the current Ref. H HSCT studies, knowledge gained here should be directly transferable to the current vehicle of interest.

Ref. 10 contains a complete description of the SCRA design aspects and only the relevant features of the MS/SS architecture are recalled here. Fig. 50 shows the Evans features for the SCRA design which corresponds to Fig. 46 for the Ref. H design. Note the similarities. In the SCRA case, the fore and aft sensors are at 2,000 and 2,500 in. The tradeoff involves the 1st and 3rd aeroelastic modes. In the Ref. H case, mode 6, rather than mode 3, is critical. However, the essence of the problem is identical. Fig. 50 corresponds to the blending filters listed below. Note that h_2 is slightly different from that in Ref. 10.

$$H_1(s) = \frac{7}{(s+7)} \tag{4.11}$$

$$H_2(s) = 1.2\,\frac{s}{(s+7)}\,\frac{31}{(s+31)}$$

Consider a small subset of the overall optimal sensor placement scheme proposed. Filters parameters will be fixed and the dipole phase costs are ignored. Further, only the dipoles for modes 1 and 3 are considered. Under these restrictions, the cost functional becomes

$$f(x_{s1},x_{s2}) = w_1\left|\delta_1\right| + 1\left|\delta_3\right| \tag{4.12}$$

Only the sensor locations are allowed to vary. Filters are specified as in Eq. (4.11).

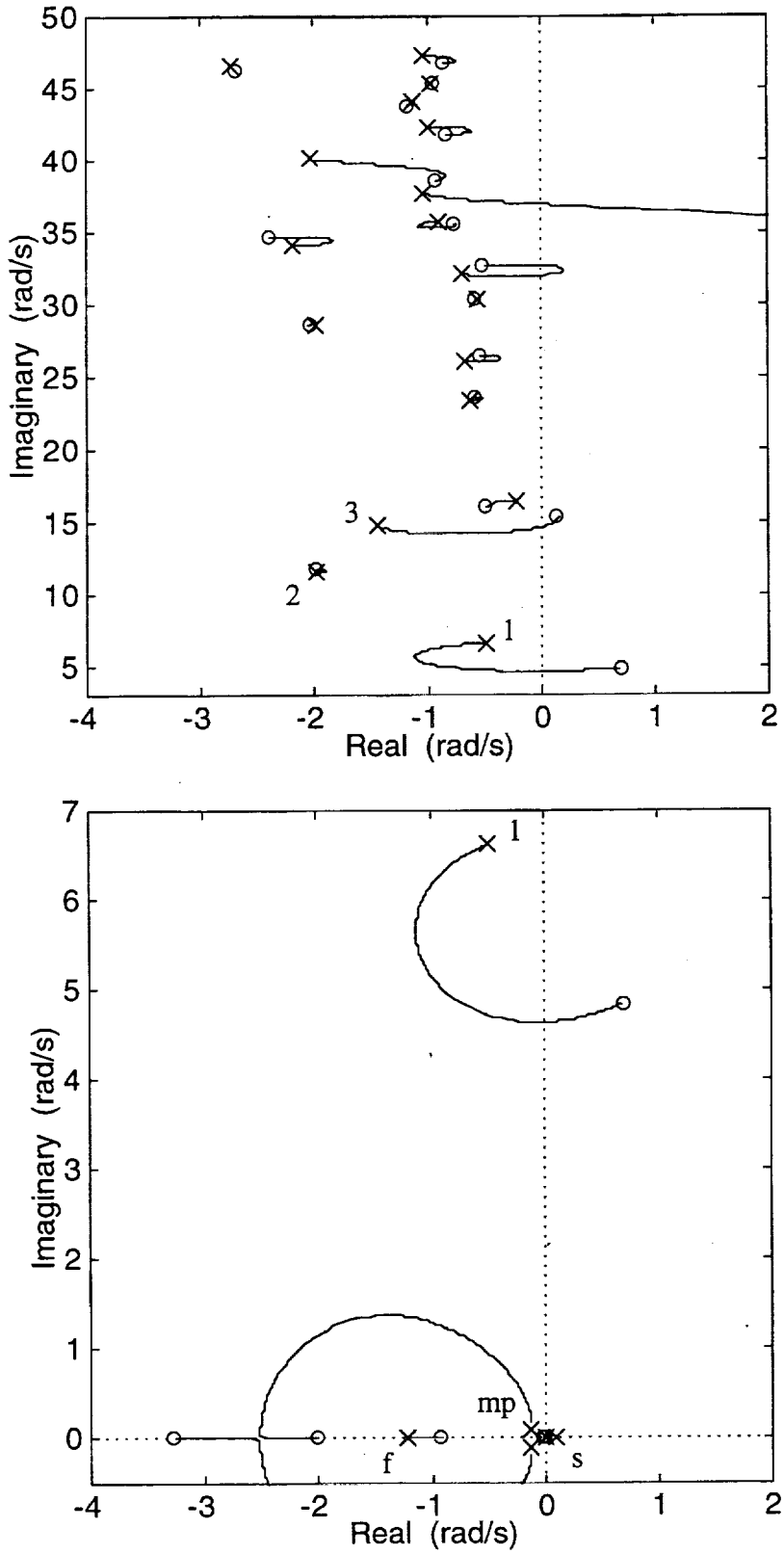

Figure 50. SCRA Evans Plot For Manual Sensor Placement

Figs. 51-53 contain the Evans plots corresponding to three runs made with different values for weight w_1. Algorithm starting values for sensor locations are 2,000 and 2,500 in. Convergence is achieved when the gradient is positive in all directions using a ± 1 in perturbation for the gradient calculation. There is a clear trade between concentrating on mode 1 vs. mode 3 in the cost function. For $w_1 = 2$ (see Fig. 51), the optimizer has improved dipole 3 at the expense of dipole 1. The opposite trend is found with $w_1 = 7$, as seen in Fig. 53. For the case $w_1 = 3$ displayed in Fig. 52, both mode 1 and 3 dipoles are considered better (i.e., tighter) than the manual design shown in Fig. 50. Further, nonminimum phase behavior is almost eliminated for mode 1 and completely eliminated for mode 3. Results for $w_1 = 4$, 5, and 6 are essentially unchanged from the $w_1 = 3$ case. This demonstrates the potential of the optimal sensor placement strategy.

The optimizer applied to the aeroelastic sensor placement problem has been found to be a temperamental tool. It can be sensitive to user specified tolerances or starting conditions. Further, convergence speed can be lacking. It will also exploit strange freedoms hidden within ill posed cost functions. However, with a properly posed cost, and with proper constraints on the independent parameters, the optimizer will perform as asked. The scheme has shown the capability to squeeze out further benefits from the MS/SS architecture that would possibly be overlooked in a manual approach.

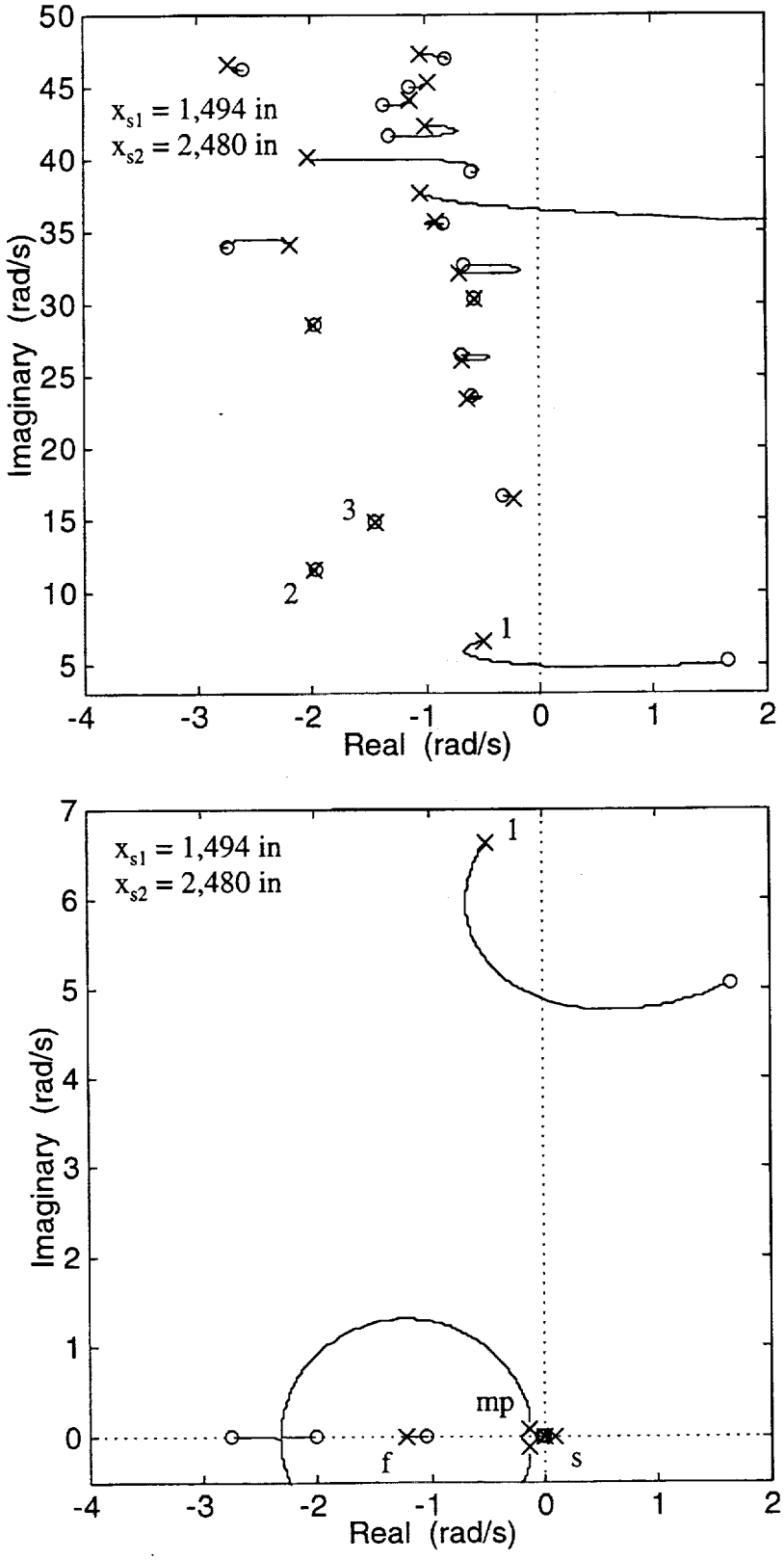

Figure 51. SCRA Evans Plot For Optimal Sensor Placement, Sensor Locations Free, $w_1 = 2$

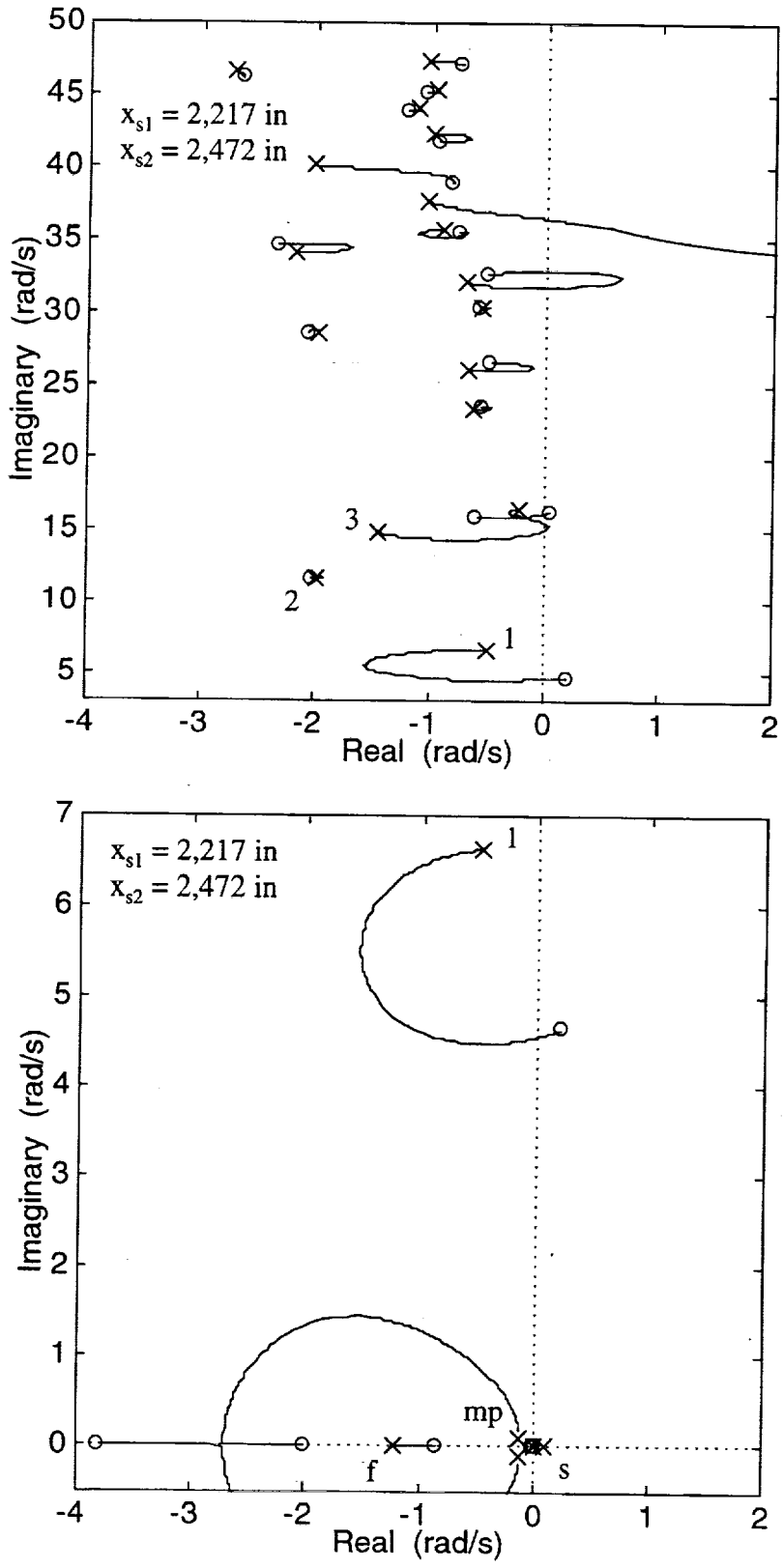

Figure 52. SCRA Evans Plot For Optimal Sensor Placement, Sensor Locations Free, $w_1 = 3$

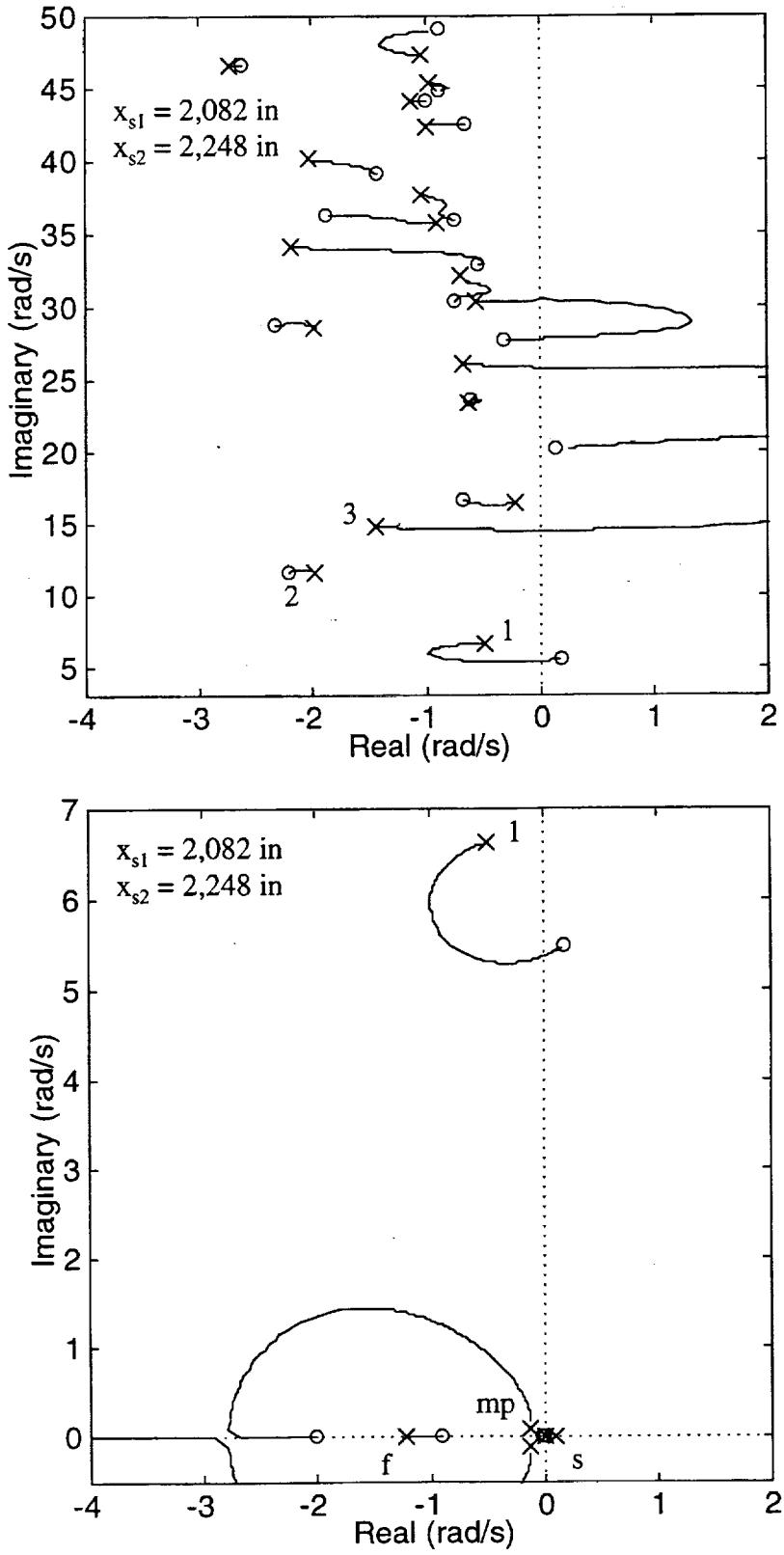

Figure 53. SCRA Evans Plot For Optimal Sensor Placement, Sensor Locations Free, $w_1 = 7$

B. Limitations of Low Pass/Band Pass Blending

Some strides have been made toward the elimination of the aeroelastic mode 1 nonminimum phase zeros with the optimal sensor placement technique. However, the characteristic still lingers and appears to be an inherent feature of the blended FCS strategy. Actually, the undesirable feature results from the specific low pass and band pass filters in Eq. (3.4), used to implement the MS/SS strategy, and this is discussed next.

Recall the q_b/δ_E transfer function in Eq. (4.5). Numerator dynamics consist of the addition of two terms originating from the two feedback signals in Fig. 44. The relative strength of the two channels determines the final zeros according to the root locus

$$1 + \frac{h_2}{h_1}\frac{18}{8}\frac{s}{(s+18)}\frac{n_{G2}}{n_{G1}} = 0 \tag{4.13}$$

where h_2/h_1 plays the role of parameterization variable. Note the blending filters act like an extra $s/(s+18)$ factor. For $h_2/h_1 = 0$, Eq. (4.13) indicates the q_b/δ_E zeros are coincident with the q_{xs1}/δ_E zeros and $s = -18$. For a large value of h_2/h_1, the q_b/δ_E zeros tend towards the q_{xs2}/δ_E zeros and $s = 0$. At intermediate values for h_2/h_1, the zeros follow loci according to the conventional rules. Fig. 54 shows this numerator root locus for the MS/SS design in Section III-C.

In Fig. 54, the symbol "x" represents the zeros of q_{xs1}/δ_E as found in Fig. 30, while symbol "o" denotes the q_{xs2}/δ_E zeros shown in Fig. 37. With the h_2-to-h_1 ratio set at a value of 4, the zeros are equivalent to those in Fig. 46 corresponding to the MS/SS design of Section III-C. There is a clear trade between the troublesome modes. As the mode 6 zero is slid down near the mode 6 pole, the mode 1 zero slides out into the right-half plane leading to the nonminimum phase behavior. Mode 1's zero immediately heads to the right-half plane as h_2/h_1 is increased from zero.

Consider the angle of departure relationship as applied to mode 1 in Eq. (4.13) and Fig. 54. Let θ_1 represent the phase angle of factor $s+z_1$ contained within n_{G1} where z_1 represents the aeroelastic mode 1 zero with imaginary part greater than zero. From Fig. 30 or Tab. 16, $z_1 = -0.089 + j7.5$. For a test point very near z_1, this relationship is

$$\theta_1 = \angle(s) - \angle(s+18) + \angle(n_{G2}) - \angle(n'_{G1}) - (2i+1)\pi \tag{4.14}$$

n'_{G1} denotes n_{G1} with the factor $s+z_1$ removed and i represents an integer. With $s = z_1$, the $s/(s+18)$ factor results in an additional contribution of 68 deg of phase to the departure angle from zero z_1. Without this contribution, the initial migration would point down towards the origin, avoiding the right-half plane and nonminimum phase behavior.

It can now be said with certainty the source of the 1st aeroelastic mode nonminimum phase characteristic in the MS/SS design in Section III-C is due to the width of the band pass filter differentiator and final break frequency. Insertion of the zero at the origin "pushes' the mode 1 loci out into the right-half plane. The low pass/band pass implementation of the blending idea is fundamentally flawed. A more gradual implementation of the rate gyro blend is needed.

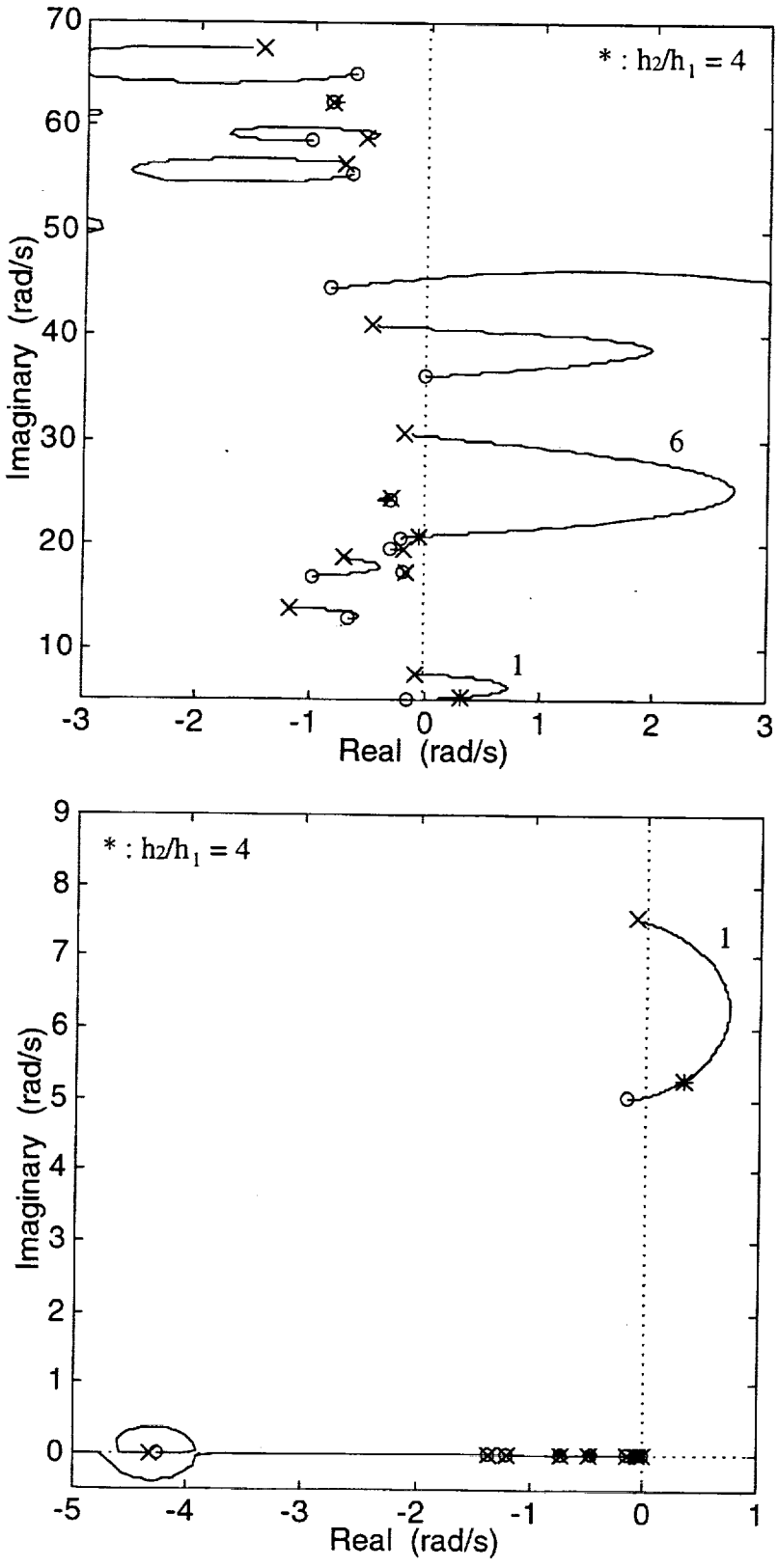

Figure 54. Numerator Root Locus For Low Pass 1,850 in And Band Pass 2,500 in Pitch Rate To Elevator MS/SS Design

C. Utilization of Lag-Lead/Lead-Lag Blending

Implementation of the blending strategy requires a more subtle tactic to avoid the aeroelastic mode 1 nonminimum phase characteristic associated with the low pass/band pass approach displayed in Fig. 46. Relying upon previous knowledge of the vehicle dynamics, use of the 1,850 in sensor signal below 10 rad/s and the 2,500 in sensor signal between 10 and 30 rad/s is still desirable. Therefore, consider a lag-lead factor for H_1 and a lead-lag factor for H_2 which transition in the critical frequency range. Attenuation is still needed for the higher frequency aeroelastic modes. This attenuation can be lumped into K for both signals or kept separate in H_1 and H_2. The latter was chosen. Further, lead-lag filters in both H_1 and H_2 are necessary to recover phase loss near magnitude crossover due to the attenuation factors.

The chosen filters are

$$H_1(s) = h_1 \frac{14}{16} \frac{(s+16)}{(s+14)} \frac{1.6(s+1.1)}{1.1(s+1.6)} \frac{10}{(s+10)} \tag{4.15}$$

$$H_2(s) = h_2 \frac{(s+14)}{(s+16)} \frac{1.6(s+1.35)}{1.35(s+1.6)} \frac{18}{(s+18)}$$

and Fig. 55 displays the corresponding frequency responses. Filtering used in the fore and aft SS/SS designs in Eqs. (3.2) and (3.3) are used in Eq. (4.15) with one exception. Notching in the forward design is not used here (i.e., one goal is to achieve an acceptable design without resorting to notching). Note the blending lag-lead and lead-lag factors in Eq. (4.15) are almost straight blending with break frequencies separated by only 2 1/s.

Fig. 56 shows the numerator root locus for the MS/SS design here. Similar to Eq. (4.13), the governing relationship is

$$1 + \frac{h_2}{h_1} \frac{16}{14} \frac{(s+14)^2}{(s+16)^2} \frac{1.1(s+1.35)}{1.35(s+1.1)} \frac{18(s+10)}{10(s+18)} \frac{n_{G2}}{n_{G1}} = 0 \tag{4.16}$$

where again h_2/h_1 is the parameterization variable. The blending filters act like an extra $(s+14)^2/(s+16)^2$ factor. Note the migration path for the 1st aeroelastic zero, although still slightly penetrating the right-half plane, ends up in the left-half plane and is much improved relative to Fig. 54. Zero locations for $h_2/h_1 = 4$ (as in Section III-C) are noted in Fig. 56. Lag-lead and lead-lag implementation has allowed tailoring of the zero characteristics so that both mode 1 and 6 are

nonminimum phase, and mode 1's dipole is tighter, relative to the other blending approach. Note from Fig. 56 the freedom still available in reducing h_2/h_1 to increase this tightness and still avoid nonminimum phaseness.

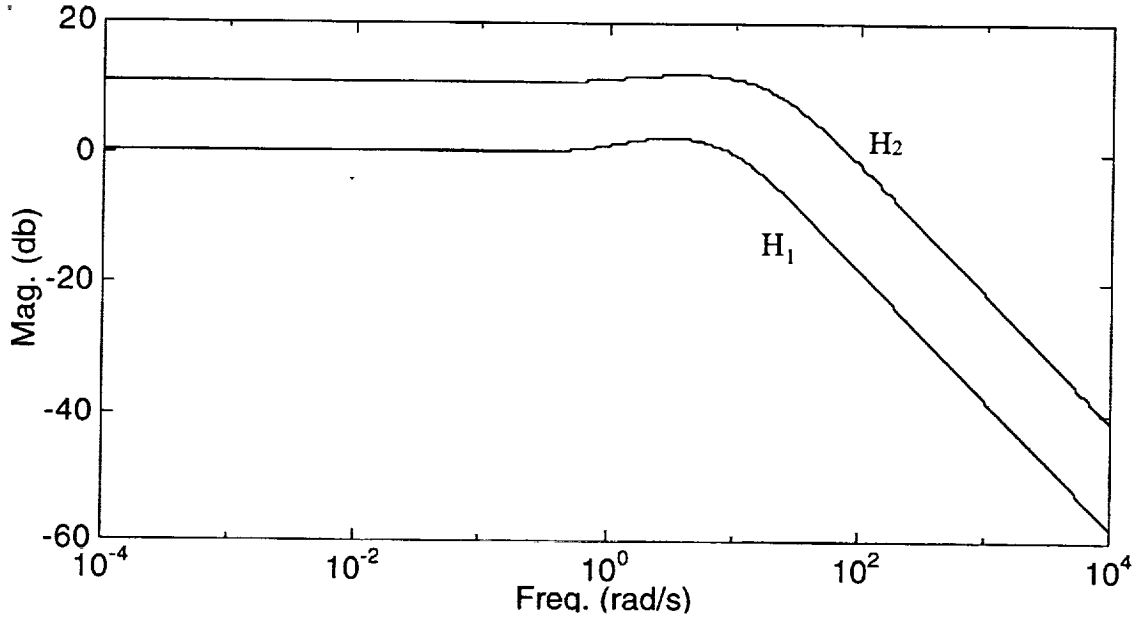

Figure 55. Modified Lag-Lead And Lead-Lag Blending Filter Frequency Responses

The MS/SS Evans behavior is shown in Fig. 57. Again, not that the objectionable nonminimum phase mode 1 behavior has been eliminated with the new filters. Unfortunately, the mid period roots switch their migration direction, from the case displayed in Fig. 46, to the 1st aeroelastic zeros. Recall this limits the effective rigid pitch damping augmentation per unit loop gain, but with a phase stable mode 1, the gain can be increased further. Thus, another clear tradeoff is present between the low pass/band pass and lag-lead/lead-lag strategies. However, this design does indicate limited improvement over the aft SS/SS design. Fig. 58 displays the Bode plot for k = -1.25 rad/rad/s and Tab. 22 lists the final closed-loop numbers. The loop gain has been increased until the rigid phase margin requirement is just met at 45 deg and the aeroelastic mode 8 gain margin is also at the requirement of 8 db. These numbers make a comparison with the aft SS/SS design in Tab. 21 possible. Note here a slight improvement in the achievable rigid pitch

frequency and damping values. However, these improvements are not sufficiently significant to claim a successful design has been achieved for the Ref. H HSCT vehicle.

Table 22. Design Summary With Lag-Lead 1,850 in And Lead-Lag 2,500 in Pitch Rate To Elevator

Spec.	Level 1	(unit)	Design
ω_{sp}	≥0.7	(rad/s)	1.58
ζ_{sp}	≥0.35	(-)	0.50
CAP	≥0.16	($1/gs^2$)	0.15
$\omega_{sp}\tau_{\theta 2}$	≥1.3	(-)	0.79
$GM_{<.38}$	≥4.5	(db)	8.44
$PM_{>.38}$	≥45.	(deg)	46.2
GM_8	≥8.	(db)	9.65

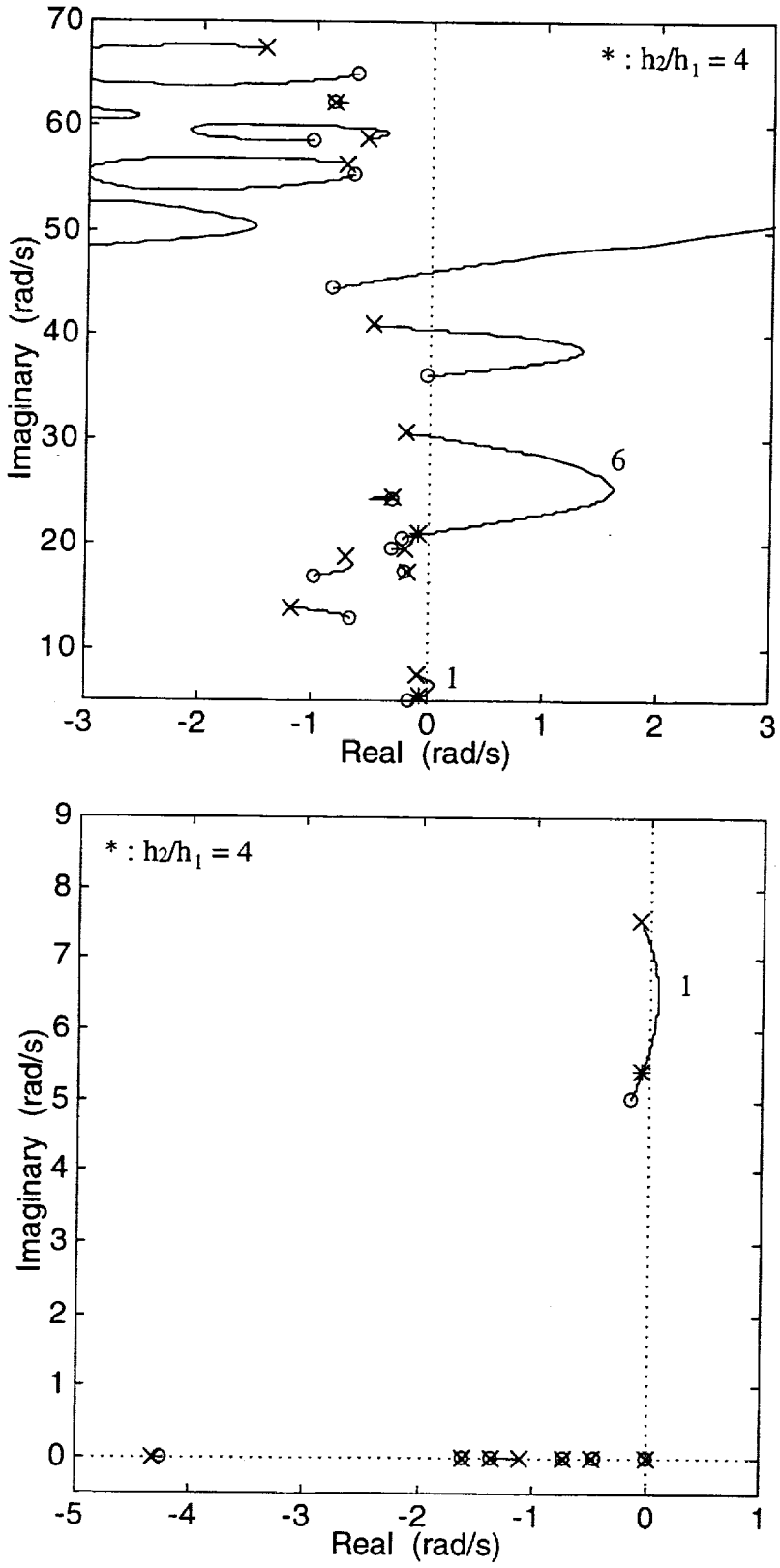

Figure 56. Numerator Root Locus For Lag-Lead 1,850 in And Lead-Lag 2,500 in Pitch Rate To Elevator MS/SS Design

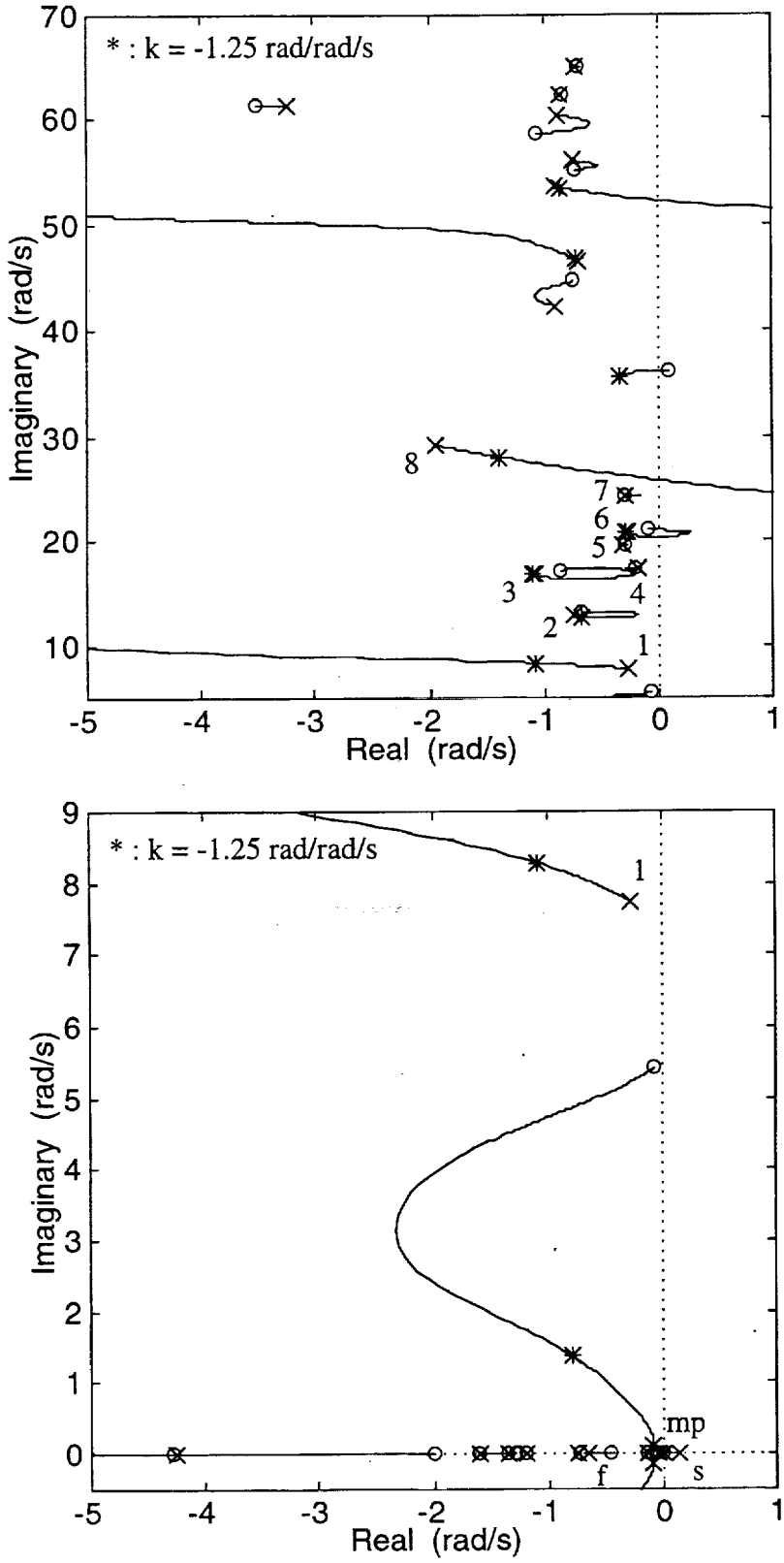

Figure 57. Evans Plot For Blend Of Lag-Lead 1,850 in And Lead-Lag 2,500 in Pitch Rate To Elevator

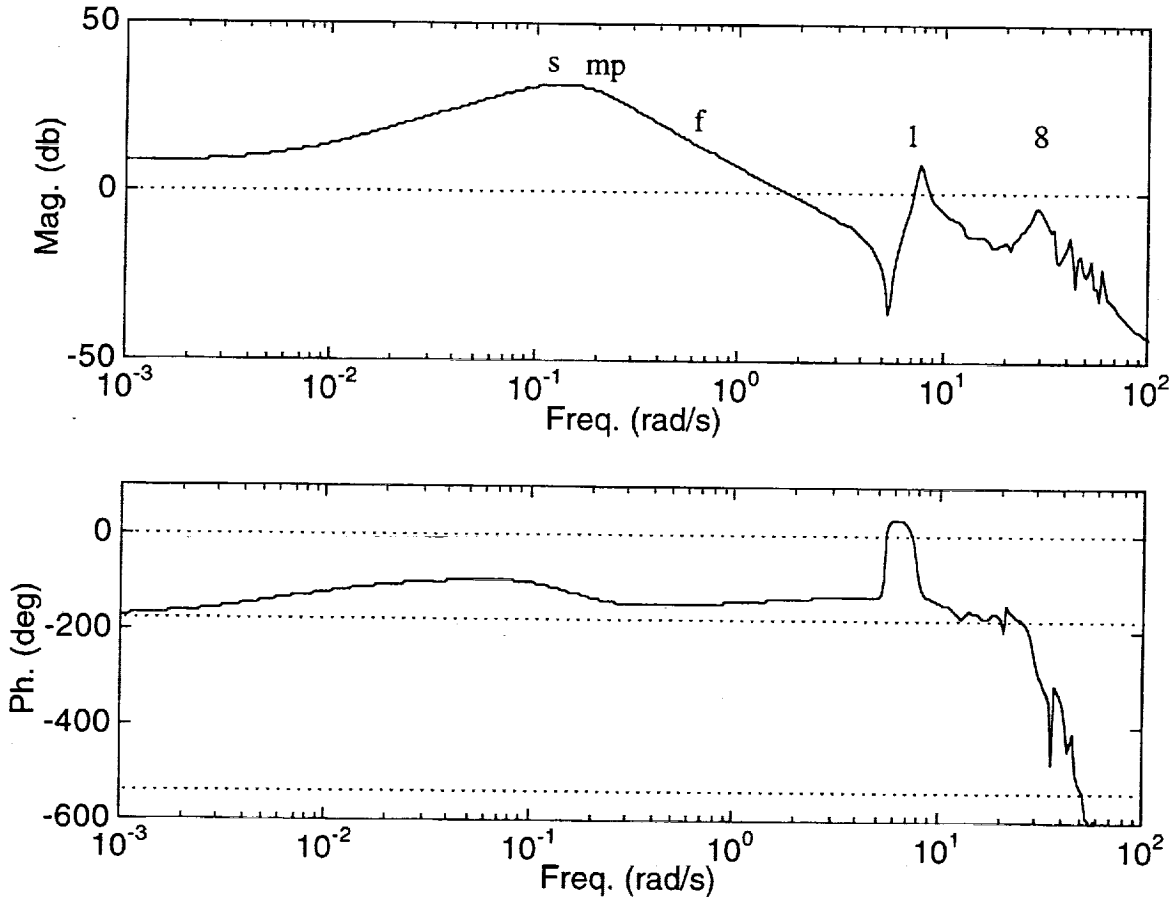

Figure 58. Bode Plot For Blend Of Lag-Lead 1,850 in
And Lead-Lag 2,500 in Pitch Rate To Elevator, k = -1.25 rad/rad/s

Section V
Preliminary Consideration of Multi-Sensor/Multi-Surface Design Strategies

A. Limitations To Influence Pilot Station Responses

Consider the feedback structure displayed in Fig. 59. This closed-loop system can represent either the SS/SS or MS/SS architectures previously considered. For example, q_{xs1} would denote the forward or aft single-sensor feedback variable (i.e., q_{xs} in Fig. 29), or possibly the multi-sensor feedback signal (i.e., q_b in Fig. 44). q_{xs2} is some other pitch rate signal of interest. Here, q_{xs2} will denote the output of a rate gyro placed at the cockpit station. More importantly, q_{xs2} is the pitch rate characteristics the pilot would sense while closing outer loops during manual augmented flight control, such as during the approach-to-land task.

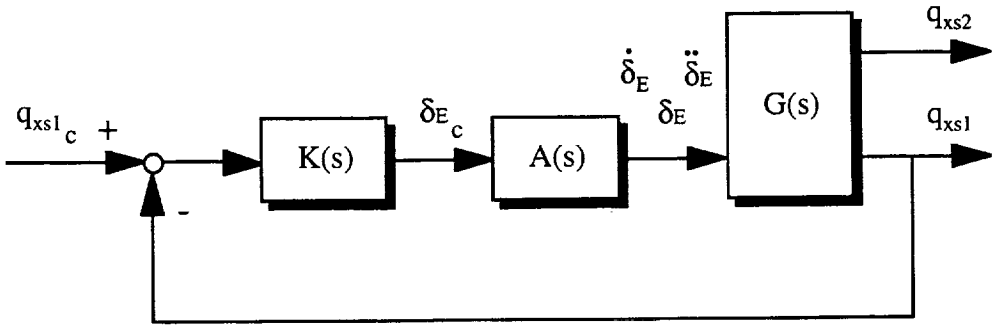

Figure 59. Feedback Loop With A Second Response

Fig. 60 shows the cockpit pitch rate time response for the 1,850 in forward sensor SS/SS design in Section III-A. A unit pitch rate command input signal is the excitation source. Aeroelastic contamination of the cockpit response is severe. Responses corresponding to the aft SS/SS design or the MS/SS design are equally bad. Note the high frequency ringing due to the lightly damped aeroelastic modes. Also note the vehicle initially responds in the wrong direction due to strong nonminimum phase features at this fuselage location. Even without an applicable

flying quality data base for flexible vehicles, the cockpit dynamics displayed in Fig. 60 are highly objectionable and totally unacceptable for manual loop closure, not to mention the severe ride discomfort associated with such dynamic motions.

The SS/SS and MS/SS designs have primarily concentrated upon tailoring the responses solely at the sensor by either augmentation of aeroelastic dampings or cancellation of aeroelastic poles/zeros, or a combination of both. Characteristics at stations far from the sensor, such as the cockpit, have been ignored. Why not place the sensor at the cockpit and redesign ? The 1,850 and 2,500 in stations were found to be the most promising for aeroelastic modification with feedback. Aeroelastic dipoles corresponding to the cockpit station are not appropriate for feedback control using only elevator inputs. Setting aside the difficulties noted in Section III in achieving the flight control objectives with the SS/SS and MS/SS architectures, the contractors do not feel the SS/SS and MS/SS loops will provide viable FCS for the Ref. H HSCT. These systems do not yield acceptable cockpit responses.

This conclusion is further demonstrated with Fig. 59. The vehicle is represented as

$$\begin{bmatrix} q_{xs1} \\ q_{xs2} \end{bmatrix} = \begin{bmatrix} G_1 \\ G_2 \end{bmatrix} \delta_E \tag{5.1}$$

and the control law is

$$\delta_{E_c} = K(q_{xs1_c} - q_{xs1}) \tag{5.2}$$

Using Eqs. (5.1)-(5.2), the closed-loop transfer functions in Fig. 59 correspond to

$$q_{xs1} = \frac{KG_1A}{1 + KG_1A} q_{xs1_c} \tag{5.3}$$

$$q_{xs2} = \frac{KG_2A}{1 + KG_1A} q_{xs1_c}$$

The closed-loop transfer function denominators are identical, but the numerators are distinct. Each numerator has it's respective vehicle transfer, either G_1 or G_2. Using the q_{xs1}/q_{xs1c} system, a combination of aeroelastic damping augmentation and pole/zero cancellation is achieved with careful selection of G_1 and K. Note that, while damping augmentation carries over to the q_{xs2}/q_{xs1c} channel, reliance upon cancellation for response tailoring does not. The zeros associated

with G_1 and G_2 are different. SS/SS or MS/SS architectures simply do not have the capacity to tailor responses at several points around the vehicle.

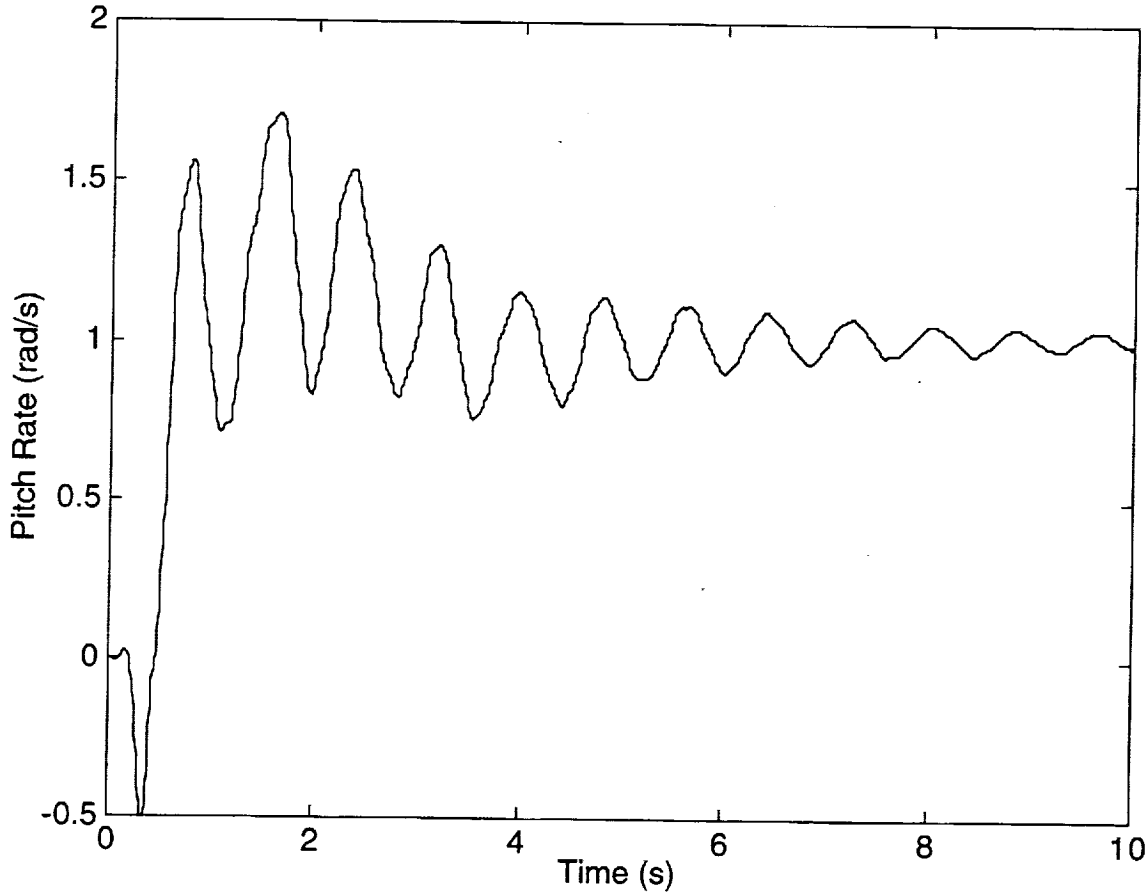

Figure 60. Closed-Loop 358 in Pitch Rate Time Response
Due To Unit Step Pitch Rate Command

B. Multi-Sensor/Multi-Surface Design With Elevator and Wing Trailing Edge

The single loop FCS previously considered as candidate inner loop architectures (i.e., SS/SS and MS/SS systems) appear to lack sufficient design freedoms to meet all flight control objectives simultaneously. Findings thus far point to the need for multi loop FCS. With this said, focus attention on Fig. 61 which shows a Multi-Sensor/Multi-Surface (MS/MS) feedback arrangement.

In Fig. 61, q_{xs1} and q_{xs2} denote two rate gyro feedback signals, perhaps representing cockpit (q_{xs2}) and aft (q_{xs1}) pitch rate responses, as in Fig. 59. The input u_2 represents the elevator deflection δ_E previously used as the sole means of control. The additional, new input available for control is u_1. Note a second input allows an additional feedback loop, as well as a crossfeed. Only one crossfeed is considered in this preliminary MS/MS investigation.

The Ref. H HSCT configuration has multiple devices distributed along the wing leading and trailing edges which are possible candidates for input u_1. Active control using the leading edge devices seems impractical due to the associated airflow disturbance over the wing and at the propulsion inlets, and the inherent one-directional motion (down only). Further, current aeroelastic modeling capabilities[9] preclude math models with leading edge inputs. Therefore, trailing edge surfaces are considered exclusively here.

Examination of the relative effectiveness of the trailing edge devices as force generators for the Langley Appendix D HSCT model in Tab. 14 reveals that trailing edge 3 is most effective and will be chosen as input u_1 in Fig. 61. Even though current planning recommends use of trailing edge 3 as a scheduled flap for high-lift generation, it is appropriate to consider this surface during feasibility studies of inner loop FCS.

From Fig. 61, the vehicle model is

$$\begin{bmatrix} y_1 \\ y_2 \end{bmatrix} = \begin{bmatrix} G_{11} & G_{12} \\ G_{21} & G_{22} \end{bmatrix} \begin{bmatrix} u_1 \\ u_2 \end{bmatrix} \tag{5.4}$$

Using sequential root locus concepts,[24] consider closing the y_1/u_1 loop first. The control law is

$$u_{1c} = K_{11}(y_{1c} - y_1) \tag{5.5}$$

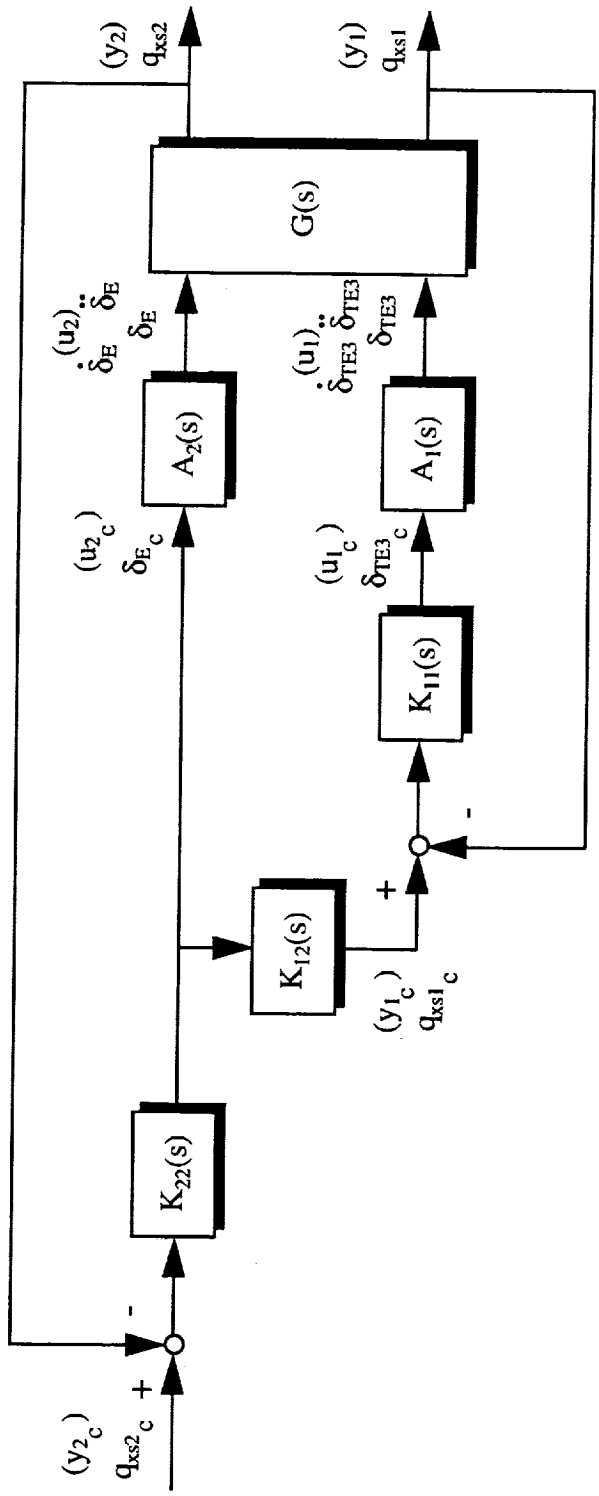

Figure 61. Multi-Sensor/Multi-Surface Feedback Loop

and the resulting intermediate system is

$$y_1 = \frac{K_{11}G_{11}A_1}{1+K_{11}G_{11}A_1} y_{1c} + \frac{G_{12}A_2}{1+K_{11}G_{11}A_1} u_{2c} \tag{5.6}$$

$$y_2 = \frac{K_{11}G_{21}A_1}{1+K_{11}G_{11}A_1} y_{1c} + \frac{G_{22}A_2+K_{11}\tilde{G}A_1A_2}{1+K_{11}G_{11}A_1} u_{2c}$$

$$\tilde{G} = G_{11}G_{22} - G_{12}G_{21}$$

where $\tilde{G}$ denotes the vehicle coupling transfer function leading to the coupling numerator[3] or transmission zero polynomial. As part of the synthesis, $1+K_{11}G_{11}A_1$ would be used to generate an Evans plot. This feedback loop represents a secondary loop dedicated to aeroelastic suppression.

Before closing the primary y_2/u_2 loop dedicated to rigid pitch stabilization and augmentation, note the coupling that exists between these two channels in Eq. (5.6). If this coupling is ignored, the loops can not be expected to operate properly. Therefore, consider a u_2-to-u_1 crossfeed, or

$$y_{1c} = K_{12}u_{2c} \tag{5.7}$$

which leads to a second intermediate system

$$y_1 = \frac{G_{12}A_2+K_{12}K_{11}G_{11}A_1}{1+K_{11}G_{11}A_1} u_{2c} \tag{5.8}$$

$$y_2 = \frac{G_{22}A_2+K_{11}\tilde{G}A_1A_2+K_{12}K_{11}G_{21}A_1}{1+K_{11}G_{11}A_1} u_{2c}$$

Introduction of the crossfeed alters the numerator characteristics. K_{12} can be used to reduce excitation of troublesome aeroelastic modes in both the y_1 and y_2 responses from the input u_{2c}. The relevant numerator root locus plots from Eq. (5.8) are based on $1+K_{12}\{K_{11}G_{11}A_1\}/\{G_{12}A_2\}$ and $1+K_{12}\{K_{11}G_{21}A_1\}/\{G_{22}A_2+K_{11}\tilde{G}A_1A_2\}$.

Finally, the y_2/u_2 loop is closed, or

$$u_{2c} = K_{22}(y_{2c} - y_2) \tag{5.9}$$

With this loop closed, the final augmented system is

$$y_1 = \frac{K_{22}(G_{12}A_2+K_{12}K_{11}G_{11}A_1)}{1+K_{11}G_{11}A_1+K_{22}\{G_{22}A_2+K_{11}\tilde{G}A_1A_2+K_{12}K_{11}G_{21}A_1\}} y_{2c} \tag{5.10}$$

$$y_2 = \frac{K_{22}\{G_{22}A_2+K_{11}\tilde{G}A_1+K_{12}K_{11}G_{21}A_1\}}{1+K_{11}G_{11}A_1+K_{22}\{G_{22}A_2+K_{11}\tilde{G}A_1A_2+K_{12}K_{11}G_{21}A_1\}} y_{2c}$$

Here, $1+K_{22}(G_{22}A_2+K_{11}\tilde{G}A_1A_2+K_{12}K_{11}G_{21}A_1\}/(1+K_{11}G_{11}A_1\}$ is the root locus of interest. Again, this feedback loop is the primary loop dedicated to stabilizing relaxed stability and augmenting the pitch damping behavior.

This feedback strategy applied to a highly flexible aircraft corresponds to the "physics" illustrated in Fig. 62 and discussed below. Suppose the pilot commands a nose down pitch motion with command signal q_{xs2c}. Initial elevator deflection will be down with rigid rotation indicated in the figure. The q_{xs2}/δ_E loop will stabilize this motion and provide good handling qualities. The up tail force will excite the aeroelastic dynamics and mode 1 will initially deform as shown. The elevator-to-trailing edge 3 crossfeed will lead to initial down deflection of trailing edge 3. This coordination hinders aeroelastic excitations from δ_E inputs. Superimposed on top of this two-surface deflection strategy, the q_{xs1}/δ_{TE3} loop acts to dampen aeroelastic motions that invariably squeak through.

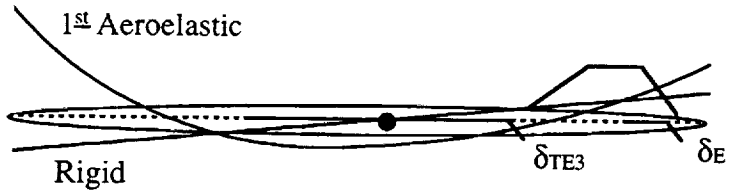

Figure 62. "Physics" Of The MS/MS Flight Control System

The quarter chord point along the mid span of the swept trailing edge 3 surface is located at 2,523 in. Therefore, a rate gyro near, but offset from, this station should prove effective in controlling aeroelastic mode 1 motions. The 2,600 in station is a particularly good spot. At this station, mode shape information from Fig. 28 indicates "in phase" sensing of not only mode 1, but several other higher frequency modes. Fig. 63 shows the Evans plot for the closed-loop poles corresponding to Eq. (5.6) using static compensation (i.e., $K_{11}(s) = k_{11}$). Recall only the y_1/u_1 loop is closed here. Observe the stable dipole loci for modes 1 and 2 and a perceived ability to influence dampings.

Closer examination reveals this loop is ineffective at aeroelastic suppression for the following reasons. Sensitivity of mode 1 damping to compensator gain k_{11} ($\partial\zeta_1/\partial k_{11} = 0.0072$ rad/s/rad) is low when compared with that for the aft SS/SS design in Section III-B ($\partial\zeta_1/\partial k_{11} =$ 0.022 rad/s/rad). The mode 1 loci in Fig. 63 has an optimum shape and initial direction, but it takes excessive gain to move along this loci. The source of this low sensitivity is the trailing edge 3 location relative to the characteristic deflection shape for mode 1. In Fig. 28, note trailing edge 3 is extremely close to the aft node for mode 1, and is thus not effective in controlling mode 1 by force. Trailing edge 3, or for that matter, all trailing edge devices, are in a poor spot for serving in the aeroelastic suppression role. Note the forward most wing leading edge flap suffers from the same ineffectiveness being somewhat close to the mode 1 forward node.

Another severe drawback when using trailing edge 3 as the additional second input with a nearby sensor can be seen from Fig. 63. The relaxed static stability pole at +0.13 1/s is further destabilized by this loop. The rigid pitch motion is "out of phase" with the local elastic pitch motion near the co-located actuator and sensor (see Fig. 28). Destabilization here will make the y_2/u_2 loop synthesis more difficult by requiring increased bandwidth for stabilization.

Despite the nonideal conditions surrounding the use of trailing edge 3 as the secondary input, a compensator gain of $k_{11} = 4$ rad/rad/s is chosen, and the design is carried one step further to demonstrate the potential of the two loop MS/MS architecture. Fig. 64 shows the numerator root locus plot for the y_2/u_{2c} transfer in Eq. (5.8) using static crossfeed compensation (i.e., $K_{12}(s) = k_{12}$). In this figure, "x" denotes the zeros of the y_2/u_{2c} transfer function before crossfeed insertion. Realize these roots no longer correspond to the numerator of $G_{22}A_2$ alone, but to $G_{22}A_2+K_{11}\tilde{G}A_1A_2$ due to the earlier y_1/u_1 loop closure. The symbol "o" denotes the cross channel zeros corresponding to $K_{11}G_{21}A_1$. The 1st aeroelastic mode loci from Fig. 63 has been superimposed upon the numerator root locus plot. Note the y_2/u_{2c} 1st aeroelastic zero path crosses the 1st aeroelastic pole path.

Tuning of this feature can lead to both suppression (pole/zero cancellation) of aeroelastic motions in the cockpit response, such as in the forward SS/SS design in Fig. 35, and aeroelastic

damping augmentation, as in the aft SS/SS design in Fig. 42. Further, with increased dampings, motions due to gust inputs will show an improvement. The contractors feel the MS/MS architecture in Fig. 61 demonstrates considerable potential as a practical candidate for the inner loop FCS. However, it can not be implemented with the wing trailing edge devices.

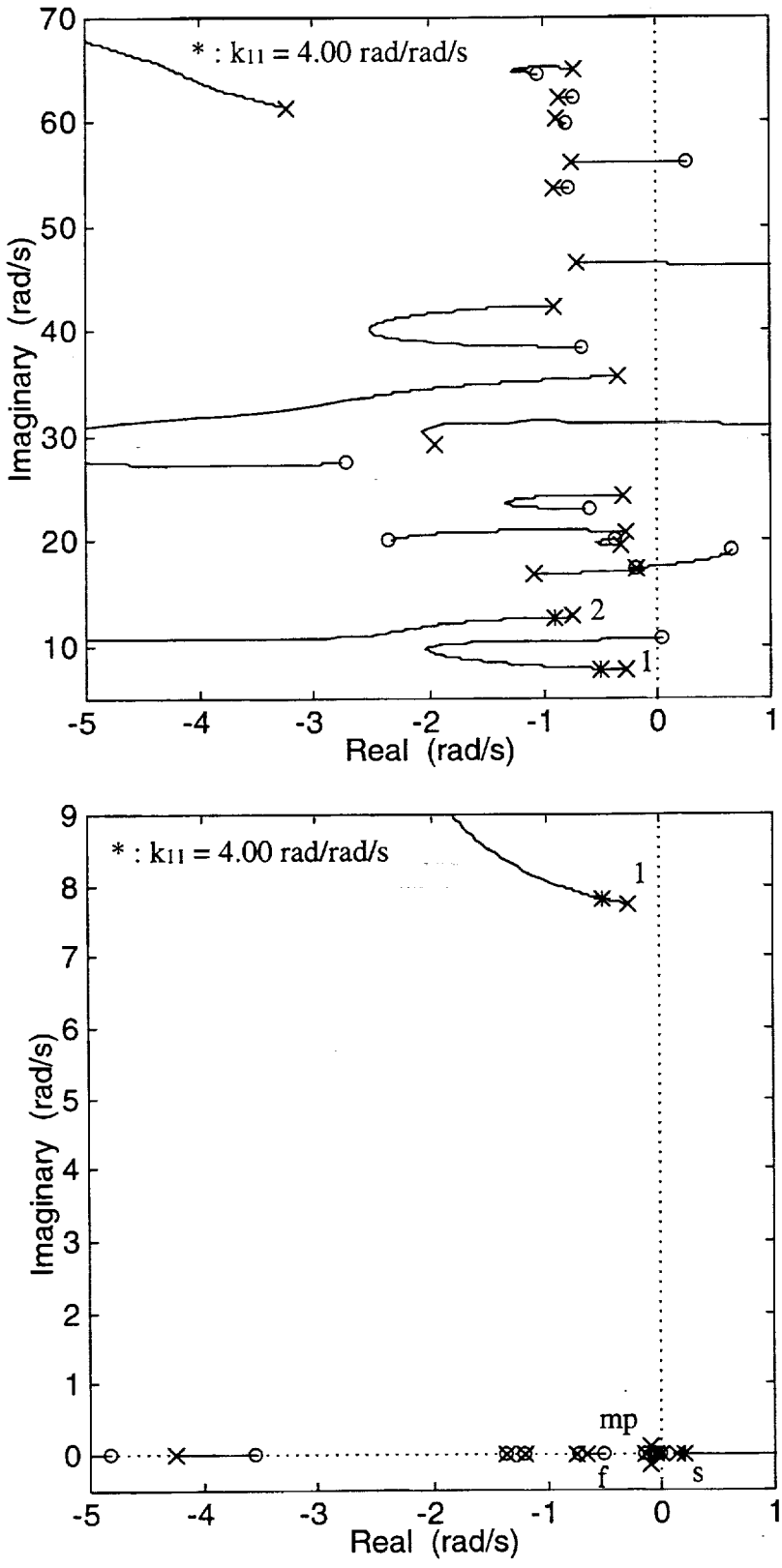

Figure 63. Evans Plot For 2,600 in Pitch Rate To Trailing Edge 3

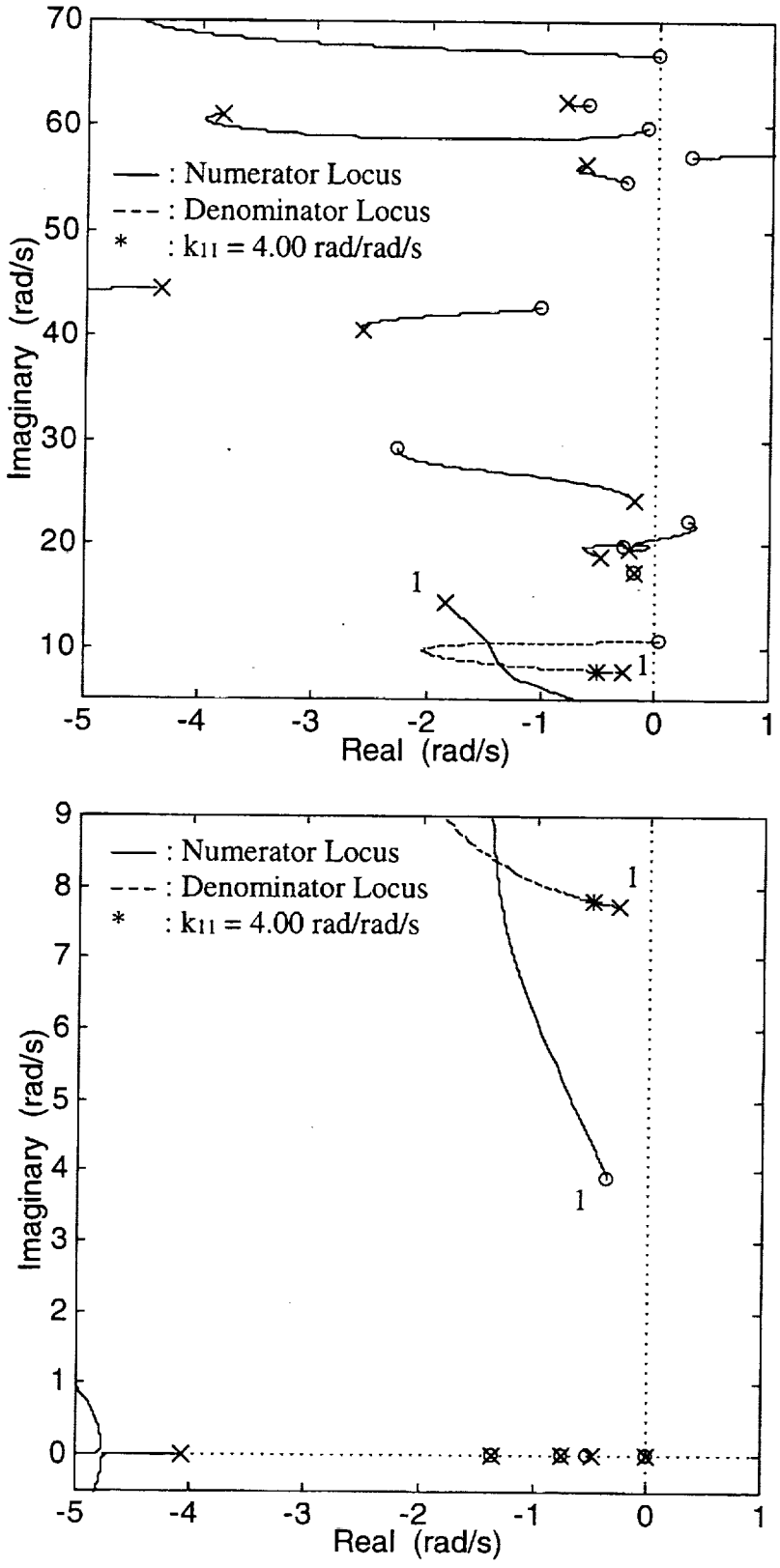

Figure 64. Numerator Root Locus Plot For 358 in Pitch Rate To Elevator

Section VI
Conclusions and Recommendations

One major conclusion is that, at this time in the HSCT program, any and all aeroelastic airframe dynamic models should be used with caution. In particular, applications such as piloted simulation, or flight control design, whose results will be used in major program decisions, are particularly critical. Requisite fidelity of supplied math models is the issue. Large discrepancies between two independently generated but similar aeroelastic vehicle models were discovered in the course of the contract activities. Further, both models have disturbing features which raise concerns during predictions of dynamic motions using these models. By deduction, model mismatch can be traced to transfer function numerator characteristics influenced by any or all of the following: noncausal unsteady input matrices, aeroelastic control derivatives, mode shape/slopes, and integration of this data into the overall vehicle model. Disturbing features include atypical attenuation characteristics and aeroelastic dipole features. Despite these findings, a third model was deemed sufficiently accurate to push ahead with flight control studies.

Another conclusion drawn from the contract findings is that traditional and nontraditional inner loop flight control strategies employing a single feedback loop do not appear sufficient for highly flexible HSCT class vehicles. Traditional gain stabilization logic implemented with a Single-Sensor/Single-Surface (SS/SS) architecture does not appear to be within reach. To achieve acceptable handling performance, the flight control system must resort to severe notching and/or rolling off of higher frequency aeroelastic modes. In this case, the closed-loop system becomes vulnerable to aeroelastic model uncertainty, and significant phase lead compensation near the rigid-body crossover region is necessary to restore stability margins. With sensor placement, the lowest frequency aeroelastic mode can be canceled, but only in the pilot command channel. Further, no damping augmentation in this mode takes place. Nontraditional phase stabilization logic implemented with a SS/SS architecture also does not appear within reach. The lowest frequency

aeroelastic mode damping is augmented, but without assistance from cancellation, the high frequency contamination of the vehicle pitch motions is severe. Further, rigid pitch damping augmentation has to be traded off to achieve this aeroelastic damping augmentation. A blended gain/phase stabilization approach using a Multi-Sensor/Single-Surface (MS/SS) architecture implemented with lag-lead and lead-lag filters did show some limited improvement, but not nearly enough to satisfy the stated objectives.

An associated conclusion is that, for a highly flexible HSCT vehicle, the inner loop FCS will, in all likelihood, require multiple interacting feedback loops. An overriding concern with the SS/SS and MS/SS architectures is their inability to influence the cockpit or pilot centered motions. These architectures do not have the capability to tailor responses at several locations within the vehicle. Multi-Sensor/Multi-Surface (MS/MS) architectures do. A preliminary investigation of a MS/MS closed-loop system shows the ability to simultaneously provide aeroelastic damping augmentation and pole/zero cancellation (not from compensation notching), at selected stations throughout the vehicle. An integral part of the MS/MS architecture will include finding suitable, or possibly the "best", locations for surface and sensor mountings.

A final conclusion is that the Ref. H HSCT configuration presents major challenges to designing acceptable closed-loop flight dynamics. The airframe is inherently unstable to begin with. The configuration is extremely flexible with lowest frequency structural mode lying close to the rigid-body modes. Further, the aeroelastic modes do not repeat along the imaginary axis at regularly spaced intervals, but rather are densely packed at irregular intervals. Severe coupling of rigid and aeroelastic modes, as well as between different aeroelastic modes, exists. Finally, secondary aerodynamic control surfaces are not in advantageous regions throughout the vehicle. This latter point is particularly critical because there is no forward surface to implement a secondary feedback loop dedicated to aeroelastic suppression within multi-loop architectures.

Recommendations for future activities which are most critical for development of workable inner loop flight control systems for large, high-speed, highly flexible vehicles are listed below.

1. Development of multivariable flight control design strategies which have the practical/insightful aspects of conventional approaches, as well as the potential of contemporary approaches. Techniques such as these will be needed to design and implement the inner loop control system.
2. Advancements in aeroelastic vehicle dynamics modeling capabilities incorporating large overall motions, structural vibrations, and unsteady airflow. Control of unsteady aeroelastic modally dense vehicles with limited control bandwidth will, to some extent, rely upon combinations of damping augmentation (phase stabilization) and pole/zero cancellation (gain stabilization). These designs are highly dependent upon accurate knowledge of aeroelastic dipole and unsteady pole/zero pair constellations.
3. Creation of a flying and ride qualities data base, applicable to flight vehicles exhibiting significant structural vibration motions, through moving-base piloted simulation test programs. Currently there are little, if any, guidelines and requirements for flight control design of such vehicles.
4. Integrated airframe design methodologies which allow the controls discipline to impact airframe design decisions up front. If constraints from the controls discipline are not passed to other disciplines, the resulting flight control design challenges may prove to be unrealistic.

References

1. U.S. Dept. of Defense, "Military Standard: Flying Qualities of Piloted Aircraft," MIL-STD-1797A, January, 1990.

2. Princen, N. H., Page, M. A., and Rossito, K. F., "High Speed Civil Transport Preliminary Controls Sizing and Flying Qualities Issues and Requirements," MDC Report 94K0269, NASA Contract NAS1-18763, Task No. 26, Long Beach, California, May, 1994.

3. McRuer, D., Ashkenas, I., and Graham, D., *Aircraft Dynamics and Automatic Control*, Princeton University Press, Princeton, New Jersey, 1973.

4. Ray, J. K., Carlin, C. M., and Lambregts, A. A., "High-Speed Civil Transport Flight - and Propulsion - Control Technological Issues," NASA-CR-186015, NASA Dryden Flight Research Facility, Edwards, California, March, 1992.

5. McCarty, C. A., Feather, J. B., Dykman, J. R., Page, M. A., Hodgkinson, J., "Design and Analysis Issues of Integrated Control Systems for High-Speed Civil Transports," NASA-CR-186022, Dryden Flight Research Facility, Edwards, California, May, 1992.

6. Deliverable Item No. 18, Contract NAS1-20220, Task Assignment No. 7, Flight Controls, Langley Research Center, Hampton, Virginia, June, 1995.

7. Zeiler, T., Informal Deliverable Item from Lockheed Martin Engineering & Sciences Co., HSR Program, Langley Research Center, Hampton, Virginia, June-August, 1995.

8. Ashkenas, I. L., Magdaleno, R. E., and McRuer, D. T., "Flight Control and Analysis Methods for Studying Flying and Ride Qualities of Flexible Transport Aircraft," NASA-CR-172201, Langley Research Center, Hampton, Virginia, August, 1983.

9. Adams, W. A. and Hoadley, S. T., "ISAC: A Tool for Aeroservoelastic Modeling and Analysis," NASA-TM-109031, NASA Langley Research Center, Hampton, Virginia, December, 1993.

10. Newman, B. and Buttrill, C., "Conventional Flight Control for an Aeroelastic, Relaxed Static Stability High-Speed Transport," *Proceedings Of The AIAA Guidance, Navigation, And Control Conference*, Baltimore, Maryland, August, 1995, pp. 717-726.

11. Chan, S. Y., Cheng, P. Y., Myers, T. T., Klyde, D. H., Magdaleno, R. E., and McRuer, D. T., "Advanced Aeroservoelastic Stabilization Techniques for Hypersonic Flight Vehicles," NASA-CR-189702, Langley Research Center, Hampton, Virginia, November, 1992.

12. Bisplinghoff, R. L. and Ashley, H., *Principles of Aeroelasticity*, Dover Publications, New York, New York, 1962.

13. Swaim, R. L. and Fullman, D. G., "Prediction of Elastic-Airplane Longitudinal Dynamics From Rigid-Body Aerodynamics," *Journal Of Aircraft*, Vol. 14, No. 9, September, 1977, pp. 868-873.

14. Waszak, M. R. and Schmidt, D. K., "Flight Dynamics of Aeroelastic Vehicles," *Journal Of Aircraft*, Vol. 25, No. 6, June, 1988, pp. 563-571.

15. Arbuckle, P. D., Buttrill, C. S., and Zeiler, T. A., "A New Simulation Model Building Process for Use in Dynamic Systems Interaction Research," *Proceedings Of The AIAA Flight Simulation Technologies Conference*, Monterey, California, August, 1987, pp. 96-106.

16. Sotack, R. A., Chowdhry, R. S., and Buttrill, C. S., "High Speed Civil Transport Aircraft Simulation: Reference H Cycle 1 - Matlab Implementation," NASA/TM-1999-209530, Langley Research Center, Hampton, Virginia, December, 1999.

17. Greiner, G. P. and Buttrill, C. S., "Quasi-Steady Aeroelastic Effects On The HSCT During Climb Out, Cruise, And Descent," Working Paper, Langley Research Center, Hampton, Virginia, June, 1995.

18. McRuer, D., Johnston, D., and Myers, T., "A Perspective On Superaugmented Flight Control Advantages And Problems," *Active Control Systems - Review, Evaluation And Projections, AGARD Conference Proceedings No. 384*, Toronto, Canada, October, 1984, pp. 3.1-3.16.

19. Juang, J. N. and Rodriguez, G., "Formulation and Application of Large Structure Sensor and Actuator Placement," *Proceedings Of The 2nd VPI&SU/AIAA Symposium on Dynamics and Control of Large Flexible Spacecraft*, Blacksburg, Virginia, June, 1979, pp. 247-262.

20. DeLorenzo, M. L., "Sensor and Actuator Selection for Large Space Structure Control," *Journal Of Guidance, Control, And Dynamics*, Vol. 13, No. 2, March-April, 1990, pp. 249-257.

21. Baruh, H. and Choe, K., "Sensor Placement in Structural Control," *Journal Of Guidance, Control, And Dynamics*, Vol. 13, No. 3, May-June, 1990, pp. 524-533.

22. Lim, K. B., "Method for Optimal Actuator and Sensor Placement for Large Flexible Structures," *Journal Of Guidance, Control, And Dynamics*, Vol. 15, No. 1, January-February, 1992, pp. 49-57.

23. Bryson, A. E. and Ho, Y. C., Applied Optimal Control Optimization, Estimation and Control, Hemisphere Publishing, Washington, District of Columbia, 1975.

24. Newman, B., "Multivariable Flight Control Design Using Root Locus Techniques," *Proceedings Of The AIAA Guidance, Navigation, And Control Conference*, Baltimore, Maryland, August, 1995, pp. 1157-1166.

Appendix A

Statement of Work for NAS-19858-71

Investigation of Inner Loop Flight Control Strategies for HSR

Objective: The High-Speed Civil Transport (HSCT) is projected to have a pitch divergence due to the relaxation of static stability at subsonic speeds. Further, significant interaction between rigid-body and aeroelastic degrees of freedom is expected. The objectives of an inner loop flight control system (FCS) for HSCT will be to artificially supply the stability inherently lacking in the airframe, augment the key responses with crisp, well damped behavior, and to suppress, or lessen, aeroelastic motions in the rigid-body responses. To lower costs associated with FCS development, validation, and modification, the attainment of multiple control objectives with minimal architecture is highly desirable. Here, the objective is to explore and/or assess candidate inner loop FCS strategies for the HSCT. This task shall be coordinated with the HSR Flight Controls Task (Task 7 on NAS1-20220), specifically, the subtask entitled "Ref. H Assessment."

Approach: Preliminary analysis of a conventional single-sensor/single-surface (ss/ss) FCS for an HSCT class vehicle indicates multiple conflicting constraints that can not be overcome with this architecture. Studies of a multi-sensor/single-surface (ms/ss) arrangement show promise and warrant further analysis. The first task is exercising these milestones on aeroelastic models of the HSCT, as they become available. The ss/ss and ms/ss strategies exploit specific vehicle dynamic characteristics such as modal frequency distribution and input-output participation. FCS tuned for configuration specific data may exploit new design freedoms, or be constrained from using existing freedoms. This task will support the benchmark assessment of the baseline configuration.

The second task is a more in-depth investigation of the ms/ss or blended sensor architecture. Mounting locations for sensors are critical to shaping the composite feedback signal so that undesirable aeroelastic characteristics are minimized. Formulation of metrics which capture the key desirable/undesirable FCS characteristics associated with fore, aft, and off center line candidate sensor locations are to be considered. Sensors may include both rate gyros and accelerometers. Consideration for actuator placement may also be investigated. Solutions are to be obtained by formal optimization search algorithms in the MATLAB environment.

Studies with ms/ss architectures, although showing promise, also indicate drawbacks. A third task is to explore the advantages of using a multi-sensor/multi-surface (ms/ms) architecture for achieving multiple closed-loop objectives. Studies may concentrate on existing baseline configuration surfaces such as leading and trailing edge devices. Addition of a small forward surface is a likely candidate also. Design freedoms that multiple surfaces offer are to be investigated from both a conventional (sequential loop closure) and modern (simultaneous loop closure) perspective.

Quantifying the merits and/or deficiencies of inner loop FCS strategies will be an integral part of the tasks. Metrics should address closed-loop features such as augmented damping increments, bandwidth requirements, controllability, robustness levels, modal frequency separations, and ride qualities. Data of this kind pertaining to the baseline HSCT configuration may prove invaluable in future configuration redesign decisions.

Deliverables:

- Feasibility assessment and recommendation of selected inner loop FCS architectures.
- Documentation of results and findings in an HSR controlled distribution report.
- Software used to perform analysis. Shall include documentation and preliminary user's guide. Software shall be well commented and legible.

Appendix B

Boeing M = 0.95 / h = 30,000 ft Model

This Appendix describes the Boeing M = 0.95, h = 30,000 ft model. All variables are expressed with feet, second, and radian units. Airframe states, inputs, and outputs are listed below.

$$x = \left[u\ w\ q\ \theta\ \dot{\eta}_1 \ldots \dot{\eta}_{15}\ \eta_1 \ldots \eta_{15} \right]^T$$

$$u = \delta_E$$

$$y = \left[q_{319}\ \ q_{778}\ \ q_{2,115}\ q_{2,525}\ \ q_{3,157} \right]^T$$

Actuator model data corresponding to Eq. (1.5) is tabulated below.

Actuator Data	p	ω	ζ
δ_E	22.	220.	0.7071

State space matrices listed below are defined in Eqs. (1.1)-(1.7).

A =

Columns 1 through 6

-9.0960e-03	4.6165e-02	-6.1650e+01	-3.2103e+01	7.6608e-17	2.3016e-16
-6.5816e-03	-6.1622e-01	9.2213e+02	-2.2156e+00	-6.8224e-03	2.7282e-02
-1.0784e-04	-1.4482e-03	-5.0640e-01	-4.6348e-04	-7.5540e-05	-6.6829e-06
0	0	1.0000e+00	0	0	0
0	-1.3107e+00	-1.6762e+03	8.1732e+00	-8.4348e-01	-2.0614e-01
0	3.5197e+00	1.9853e+02	-2.1947e+01	-5.9285e-01	-2.1045e+00
0	1.1224e+00	4.5483e+02	-6.9987e+00	1.1014e-01	-3.1696e-01
0	8.4788e+00	2.5760e+03	-5.2868e+01	7.4050e-01	-1.7123e+00
0	3.6938e+00	9.2515e+02	-2.3033e+01	1.5749e-01	-9.2079e-01
0	3.4465e+00	-1.1541e+03	-2.1491e+01	5.2950e-01	1.5119e+00
0	2.3376e+00	-2.3191e+02	-1.4575e+01	2.0612e-02	-4.1171e-01
0	-6.1496e+00	-1.4500e+03	3.8347e+01	-2.4045e-01	-1.5475e-01
0	-6.2588e+00	-4.7147e+03	3.9026e+01	-1.5363e+00	-1.5192e+00
0	4.7264e+01	6.1627e+03	-2.9471e+02	2.7195e+00	4.7729e-01
0	1.7675e+01	3.9613e+03	-1.1021e+02	1.0199e+00	7.2704e-01
0	-2.2208e+01	-3.6560e+03	1.3848e+02	-9.7373e-01	-3.2490e-01
0	5.5437e+00	7.7825e+02	-3.4568e+01	2.2794e-03	-2.8971e-01
0	-6.6522e+00	-9.2922e+02	4.1478e+01	-5.1971e-01	-4.9135e-01
0	-5.6348e+00	-6.9643e+02	3.5135e+01	-2.7875e-01	-1.7479e-01
0	0	0	0	1.0000e+00	0
0	0	0	0	0	1.0000e+00
0	0	0	0	0	0

0	0	0	0	0	0
0	0	0	0	0	0
0	0	0	0	0	0
0	0	0	0	0	0
0	0	0	0	0	0
0	0	0	0	0	0
0	0	0	0	0	0
0	0	0	0	0	0
0	0	0	0	0	0
0	0	0	0	0	0
0	0	0	0	0	0

Columns 7 through 12

-4.8200e-17	-1.4744e-16	-7.7308e-17	5.9955e-17	2.3439e-16	7.4475e-16
1.1867e-02	2.8954e-02	2.3658e-02	-3.5852e-02	-8.1960e-03	-2.0001e-02
1.7886e-05	5.0232e-05	3.3048e-05	-8.5160e-06	3.9806e-06	-1.8534e-05
0	0	0	0	0	0
2.9890e-02	1.0281e-01	4.0576e-02	5.6705e-02	-6.4250e-02	-3.0470e-01
-3.2860e-01	-8.4983e-01	-9.0626e-01	1.0696e+00	-5.0262e-01	-2.0347e-01
-4.2864e-01	-3.6533e-01	-3.1676e-01	2.7866e-01	-1.2772e-01	1.1936e-01
-7.4942e-01	-2.3542e+00	-1.7698e+00	1.4625e+00	-7.2700e-01	7.7789e-01
-3.2958e-01	-8.9562e-01	-1.1393e+00	7.4242e-01	-3.8074e-01	2.8202e-01
4.2486e-01	1.0796e+00	1.0712e+00	-1.7816e+00	4.9891e-01	-1.6287e-01
-9.2420e-02	-2.5137e-01	-2.7309e-01	2.8345e-01	-7.5557e-01	-3.4275e-02
1.3323e-01	4.0144e-01	2.7741e-01	-3.0703e-02	7.6443e-02	-1.2477e+00
-1.0769e-01	-3.3649e-01	-6.7111e-01	8.8317e-01	-1.1544e+00	-5.5679e-01
-5.7029e-01	-1.7547e+00	-1.3710e+00	6.5891e-01	-4.3791e-01	3.2479e+00
-8.5518e-02	-2.6106e-01	1.4653e-02	-5.0223e-01	2.9729e-01	5.3288e-01
2.0176e-01	6.1996e-01	4.1464e-01	5.1910e-02	1.5897e-01	-8.1093e-01
-1.2828e-01	-3.9370e-01	-4.1266e-01	2.8753e-01	-4.7672e-01	6.7299e-02
-4.3416e-02	-1.3142e-01	-2.5719e-01	3.4812e-01	-4.7502e-01	-3.9425e-01
1.4696e-02	4.6057e-02	-1.4149e-02	9.4084e-02	-1.1576e-01	-2.4737e-01
0	0	0	0	0	0
0	0	0	0	0	0
1.0000e+00	0	0	0	0	0
0	1.0000e+00	0	0	0	0
0	0	1.0000e+00	0	0	0
0	0	0	1.0000e+00	0	0
0	0	0	0	1.0000e+00	0
0	0	0	0	0	1.0000e+00
0	0	0	0	0	0
0	0	0	0	0	0
0	0	0	0	0	0
0	0	0	0	0	0
0	0	0	0	0	0
0	0	0	0	0	0
0	0	0	0	0	0

Columns 13 through 18

4.0799e-16	-4.7974e-16	2.3967e-17	1.1863e-17	2.2822e-17	4.4209e-17
-4.0242e-02	2.6623e-03	1.5349e-02	-1.2977e-03	-2.9299e-03	-5.6683e-03
-5.8603e-05	3.9436e-05	3.9504e-05	-1.2325e-05	1.3228e-06	-5.0054e-06
0	0	0	0	0	0
-1.9903e-01	2.1751e-01	2.4954e-01	-8.8016e-02	2.6255e-02	-5.7778e-03
-3.6178e-01	2.8032e-01	1.5146e-01	-4.7052e-02	-1.0492e-02	-4.6517e-02

1.4298e-02	-8.5824e-02	-3.9953e-02	1.6044e-02	-1.7303e-04	1.0267e-02
1.0886e-02	-5.9273e-01	-2.3434e-01	1.1834e-01	-2.3870e-02	3.6533e-02
-1.4037e-01	-2.2440e-01	-1.2098e-02	4.0244e-02	-2.5122e-02	-1.6485e-02
3.0793e-01	2.6393e-03	-2.3921e-01	4.9364e-02	2.8307e-03	3.6157e-02
-2.6208e-01	-7.4626e-02	1.0367e-01	1.4919e-02	-4.2200e-02	-6.2860e-02
-9.8713e-02	4.6248e-01	2.7548e-01	-1.2835e-01	3.5944e-02	-2.3047e-02
-3.6644e+00	4.3126e-01	1.9145e+00	-2.5536e-01	-3.0538e-01	-7.1765e-01
7.4126e-01	-4.7791e+00	-1.6902e+00	1.0177e+00	-3.2906e-01	1.6265e-01
1.6415e+00	-8.8376e-01	-2.5088e+00	4.7232e-01	2.0935e-02	3.7238e-01
-7.3163e-01	1.4756e+00	1.2765e+00	-1.3576e+00	1.5878e-01	-1.1383e-01
-6.8413e-01	-5.6599e-01	1.6414e-01	1.6441e-01	-1.0445e+00	-2.7107e-01
-1.1930e+00	1.7993e-01	9.0919e-01	-1.1866e-01	-1.6740e-01	-1.2464e+00
-4.4226e-01	2.8828e-01	4.4947e-01	-1.1764e-01	-2.7183e-02	-1.3889e-01
0	0	0	0	0	0
0	0	0	0	0	0
0	0	0	0	0	0
0	0	0	0	0	0
0	0	0	0	0	0
0	0	0	0	0	0
0	0	0	0	0	0
0	0	0	0	0	0
1.0000e+00	0	0	0	0	0
0	1.0000e+00	0	0	0	0
0	0	1.0000e+00	0	0	0
0	0	0	1.0000e+00	0	0
0	0	0	0	1.0000e+00	0
0	0	0	0	0	1.0000e+00
0	0	0	0	0	0

Columns 19 through 24

1.6321e-17	1.1045e-14	9.7901e-15	-6.5174e-15	-2.4560e-14	-1.5466e-14
-1.1594e-03	7.2086e-03	4.2136e-01	8.4373e-02	1.6169e-01	1.4788e-01
-2.0579e-06	1.5566e-03	1.1094e-03	1.9759e-04	3.5467e-04	3.9767e-04
0	0	0	0	0	0
-8.6024e-03	-4.8213e+01	2.9605e+00	7.2537e-01	1.5344e+00	1.4888e+00
-1.4133e-02	-2.1760e+01	-1.8200e+02	-1.1970e+01	-2.8258e+01	-2.6509e+01
3.7811e-03	1.7168e+00	-1.0992e+01	-2.1774e+02	-7.4372e+00	-6.8315e+00
2.0347e-02	8.0627e+00	-8.0968e+01	-2.0416e+01	-2.8286e+02	-4.7359e+01
1.5223e-03	-1.5231e+00	-4.5186e+01	-1.1398e+01	-2.8774e+01	-2.9392e+02
1.1995e-02	8.3528e+00	1.6750e+01	1.0190e+01	2.7978e+01	2.2908e+01
-1.0402e-02	-6.1037e+00	-2.6280e+01	-4.1880e+00	-9.9559e+00	-1.1376e+01
-2.0436e-02	-1.9435e+01	2.7686e+01	1.0278e+01	2.7669e+01	2.3019e+01
-1.8101e-01	-1.1152e+02	-2.4123e+02	-4.1608e+01	-1.0376e+02	-1.1082e+02
1.8602e-01	1.5719e+02	-1.5911e+02	-8.7085e+01	-2.3676e+02	-1.9259e+02
1.4090e-01	9.1100e+01	9.8228e+01	6.1270e+00	1.4019e+01	2.6732e+01
-1.0120e-01	-7.3307e+01	2.1518e+01	2.7196e+01	7.3719e+01	5.5395e+01
-3.5511e-02	-1.9218e+01	-1.0851e+02	-3.1557e+01	-8.2477e+01	-7.6971e+01
-1.0325e-01	-6.7221e+01	-1.1563e+02	-2.1394e+01	-5.4338e+01	-5.8740e+01
-9.2291e-01	-3.2612e+01	-2.9951e+01	-1.6271e+00	-3.2550e+00	-7.6759e+00
0	0	0	0	0	0
0	0	0	0	0	0
0	0	0	0	0	0
0	0	0	0	0	0
0	0	0	0	0	0
0	0	0	0	0	0
0	0	0	0	0	0
0	0	0	0	0	0

```
         0         0         0         0         0         0
         0         0         0         0         0         0
         0         0         0         0         0         0
         0         0         0         0         0         0
         0         0         0         0         0         0
         0         0         0         0         0         0
 1.0000e+00         0         0         0         0         0
```

Columns 25 through 30

```
 1.1945e-14   9.6961e-14   2.8151e-13   2.2005e-13  -1.7779e-13   3.1294e-13
-2.7227e-01   1.0058e-01   5.5307e-01  -4.8603e-02  -8.1447e-01  -3.2745e-01
-1.2174e-03  -1.7783e-04   2.4681e-04  -2.0019e-04  -1.3529e-03  -8.8804e-04
         0            0            0            0            0            0
-3.0016e+00   3.3896e-01   3.9228e+00  -1.5796e-01  -3.7592e+00  -4.4210e+00
 3.7874e+01  -7.4815e+00  -1.3273e+01   2.4749e+01   1.6433e+01  -1.1537e+01
 8.5339e+00  -2.1446e+00  -8.9858e-01   2.5472e+00   3.6776e+00  -1.1277e+00
 5.9272e+01  -1.5203e+01  -1.0108e+01   2.0469e+01   2.6505e+01  -1.0483e+01
 3.1696e+01  -8.7789e+00  -4.1176e+00   1.0569e+01   1.2588e+01  -5.9694e+00
-2.9782e+02   1.1618e+01  -1.2286e+01   4.8005e+00  -1.5191e+00  -1.2441e+00
 1.9085e+01  -4.1366e+02  -2.1898e+00   3.4438e+00   2.9282e+00  -2.2482e+00
-1.4106e+01   1.4688e+01  -6.7521e+02  -8.4382e+00  -5.9946e+00   8.5647e+00
 1.4262e+02  -6.1361e+01  -5.2076e+01  -1.0055e+03   3.5184e+01  -1.3325e+01
 1.5379e+02  -4.9975e+01   1.1905e+02   5.7262e+01  -1.3983e+03  -3.7662e+01
-4.0949e+01   3.5830e+01   2.6861e+01   5.1040e+01  -2.1005e+01  -1.4918e+03
-4.6500e+01  -1.7236e+00  -4.3916e+01  -4.6693e+01   1.6085e+01  -6.4921e+00
 8.8118e+01  -2.5673e+01   1.4188e+01   3.3035e+00  -1.2332e+00   1.6199e+01
 7.8117e+01  -3.1028e+01  -9.4022e+00  -2.4661e+01   7.1754e+00   1.9484e+01
 1.5566e+01  -8.6885e+00  -1.0936e+01  -1.4714e+01   4.8276e+00   6.6707e+00
         0            0            0            0            0            0
         0            0            0            0            0            0
         0            0            0            0            0            0
         0            0            0            0            0            0
         0            0            0            0            0            0
         0            0            0            0            0            0
         0            0            0            0            0            0
         0            0            0            0            0            0
         0            0            0            0            0            0
         0            0            0            0            0            0
         0            0            0            0            0            0
         0            0            0            0            0            0
         0            0            0            0            0            0
         0            0            0            0            0            0
```

Columns 31 through 34

```
-7.2460e-14  -1.3578e-14  -9.8812e-14  -2.5719e-14
 2.7019e-01  -1.4510e-01  -5.0288e-02   3.3076e-02
 5.1520e-04  -2.3162e-04  -2.7892e-05   7.2271e-05
         0            0            0            0
 1.7065e+00  -2.8039e-01   8.4142e-01   4.6168e-01
-2.4840e+00   5.5356e+00   8.3830e+00   1.5148e+00
-7.6384e-01   8.7978e-01   9.5889e-01   5.2028e-02
-4.3325e+00   5.4748e+00   6.1681e+00   3.8454e-01
-2.1070e+00   3.1639e+00   4.0454e+00   4.6529e-01
 2.8520e+00  -3.8112e+00  -5.2217e+00  -8.1326e-01
-1.1668e-01   7.1844e-01   1.3275e+00   3.0384e-01
```

-1.3924e+00	8.1381e-01	1.2121e+00	4.4122e-01
-2.2541e+00	7.0625e+00	1.3968e+01	3.8052e+00
1.4393e+00	3.0529e+00	4.2956e-01	-2.6818e+00
-5.3097e+00	3.5150e+00	-1.3810e-01	-1.8383e+00
-1.6103e+03	-7.3186e+00	-5.3016e+00	9.5312e-01
-8.9311e+00	-1.7160e+03	8.9331e+00	1.0159e+00
-7.2154e+00	5.8349e+00	-1.7985e+03	1.7556e+00
-1.5731e+00	9.3781e-01	1.7501e+00	-1.9147e+03
0	0	0	0
0	0	0	0
0	0	0	0
0	0	0	0
0	0	0	0
0	0	0	0
0	0	0	0
0	0	0	0
0	0	0	0
0	0	0	0
0	0	0	0
0	0	0	0
0	0	0	0
0	0	0	0

$\hat{A}$ =

1.0010e+00	-2.2660e-16	1.4413e-19
-1.1512e+01	1.5079e-02	6.1426e-05
-4.6416e-01	3.9272e-05	1.2749e-07
0	0	0
-2.2772e+00	1.9976e-01	5.3085e-04
-2.0526e+00	2.3101e-01	6.1988e-04
4.0702e-01	-5.3754e-02	-8.4299e-05
2.3944e+00	-3.3112e-01	-5.1322e-04
5.4725e-01	-7.3889e-02	-8.2414e-05
1.6825e-01	-1.0332e-01	-2.0492e-04
-2.0259e-01	5.6373e-02	8.3852e-05
5.0331e-01	2.6949e-01	1.4338e-04
7.2049e+00	1.1832e+00	7.4255e-05
-1.9454e+01	-1.8970e+00	1.1783e-03
-1.1027e+01	-9.7729e-01	7.7733e-04
1.1023e+01	8.8740e-01	-8.4357e-04
6.6005e-02	3.3216e-03	-5.4351e-05
7.1270e+00	5.0073e-01	-6.8652e-04
4.2221e+00	2.7762e-01	-4.1233e-04
0	0	0
0	0	0
0	0	0
0	0	0
0	0	0
0	0	0
0	0	0
0	0	0
0	0	0
0	0	0
0	0	0
0	0	0

```
            0            0            0
            0            0            0
            0            0            0
```

A_a =

```
            0   1.0000e+00            0
            0            0   1.0000e+00
  -1.0648e+06  -5.5245e+04  -3.3312e+02
```

B_a =

```
            0
            0
   1.0648e+06
```

C =

Columns 1 through 6

```
            0            0   1.0000e+00            0  -9.1508e-04   3.4994e-04
            0            0   1.0000e+00            0  -1.3961e-03   4.8712e-04
            0            0   1.0000e+00            0   2.4103e-04  -4.0003e-06
            0            0   1.0000e+00            0   6.2902e-04   1.6301e-04
            0            0   1.0000e+00            0   8.8314e-04   4.8206e-04
```

Columns 7 through 12

```
-1.5001e-04  -4.4995e-04  -2.3597e-04  -5.4803e-04  -6.1505e-04  -1.6961e-03
-1.8902e-04  -5.5711e-04  -2.8205e-04  -6.4507e-04  -6.4106e-04  -1.3411e-03
 3.0002e-05   9.1001e-05   5.3006e-05   1.0800e-04   6.3006e-05  -4.2010e-05
-4.3005e-05  -1.0100e-04  -3.7001e-05  -6.2012e-05  -6.6008e-05  -3.0805e-04
-1.4401e-04  -4.4000e-04  -2.0298e-04  -2.0508e-04   2.0298e-04   1.1210e-03
```

Columns 13 through 18

```
 2.5604e-04  -5.7596e-04   1.0510e-03  -3.4802e-04   2.6494e-04   2.9409e-04
 1.4202e-04  -1.8797e-04   2.7995e-04  -7.0005e-05   3.9008e-05   3.2009e-05
-1.3800e-04  -1.7001e-05   1.7001e-04  -6.5014e-05   6.7998e-05   9.7005e-05
-5.2308e-04   2.4295e-04  -1.4001e-04  -3.3999e-05   2.7000e-04   3.8397e-04
 1.0701e-03  -5.1208e-04  -3.4400e-04   2.7995e-05   7.0005e-06  -6.9010e-05
```

Columns 19 through 24

```
 4.0003e-05            0            0            0            0            0
 2.0001e-06            0            0            0            0            0
 1.7994e-05            0            0            0            0            0
 3.7996e-05            0            0            0            0            0
-5.7002e-05            0            0            0            0            0
```

Columns 25 through 30

```
            0            0            0            0            0            0
            0            0            0            0            0            0
            0            0            0            0            0            0
```

```
     0     0     0     0     0     0
     0     0     0     0     0     0
```

Columns 31 through 34

```
     0     0     0     0
     0     0     0     0
     0     0     0     0
     0     0     0     0
     0     0     0     0
```

Appendix C

Langley M = 0.88 / h = 20,000 ft Model

This Appendix describes the Langley M = 0.88, h = 20,000 ft model. All variables are expressed with feet, second, and radian units. Airframe states, inputs, and outputs are listed below

$$x = \left[w\ q\ \theta\ \dot{\eta}_1 \ldots \dot{\eta}_{17}\ \eta_1 \ldots \eta_{17}\ z_1 \ldots z_{10} \right]^T$$

$$u = \delta_E$$

$$y = \left[q_{319}\ \ q_{778}\ q_{2,115}\ q_{2,525}\ q_{3,157} \right]^T$$

Actuator model data corresponding to Eq. (1.5) is tabulated below.

Actuator Data	p	ω	ζ
δ_E	22.	220.	0.7071

State space matrices listed below are defined in Eqs. (1.1)-(1.7).

A =

Columns 1 through 6

-1.1502e+00	8.3396e+02	0	5.1390e-03	-1.6404e-03	1.7995e-03
-6.6120e-02	-2.5634e+00	0	2.3173e-04	-7.5725e-05	8.0027e-05
0	1.0000e+00	0	0	0	0
-7.2076e+02	-2.7320e+04	0	2.8253e+00	-1.3258e+00	1.8421e+00
-4.4932e+02	-2.7915e+02	0	8.7082e-01	-3.5070e+00	-1.3163e+00
1.3004e+03	3.7944e+04	0	-3.9986e+00	-2.0847e+00	-4.1738e+00
-2.4263e+02	-7.0134e+03	0	7.2514e-01	4.4376e-01	8.2230e-01
-1.9476e+02	-3.6914e+02	0	1.2204e+00	-1.3825e+00	-1.5297e+00
1.2123e+02	1.8226e+03	0	-8.0194e-01	3.8023e-01	4.3737e-01
-2.9799e+02	-4.1654e+03	0	1.3317e+00	-7.2855e-01	-1.6863e-01
4.6223e+02	1.9727e+04	0	-2.0967e+00	-1.1257e+00	6.7161e-01
6.8064e+02	1.4876e+04	0	-4.0691e+00	1.9402e+00	-1.2252e+00
-1.3178e+03	-3.1835e+04	0	4.8674e+00	1.3830e+00	3.3157e-01
-2.7996e+02	3.3003e+03	0	2.0391e+00	7.5912e-01	5.9029e-01
-1.1986e+03	-3.0175e+04	0	7.1623e+00	3.6138e-01	6.2992e-01
-4.8460e+02	-2.2289e+04	0	1.4917e+00	-9.4041e-01	7.0051e-01
2.0104e+02	5.0625e+03	0	-1.6674e+00	6.6946e-01	9.7891e-02
-6.5503e+02	-1.8445e+04	0	1.6993e+00	7.3983e-01	-8.5297e-02
-4.1791e+02	-1.2148e+04	0	1.8178e+00	6.6076e-01	5.7403e-01
-3.5908e+02	-7.7330e+03	0	1.3920e+00	2.9847e+00	1.6179e+00
0	0	0	1.0000e+00	0	0
0	0	0	0	1.0000e+00	0

0	0	0	0	0	1.0000e+00
0	0	0	0	0	0
0	0	0	0	0	0
0	0	0	0	0	0
0	0	0	0	0	0
0	0	0	0	0	0
0	0	0	0	0	0
0	0	0	0	0	0
0	0	0	0	0	0
0	0	0	0	0	0
0	0	0	0	0	0
0	0	0	0	0	0
0	0	0	0	0	0
0	0	0	0	0	0
1.5759e-01	-3.8778e+01	0	1.1312e-01	2.5785e-02	5.3072e-02
-1.2180e+00	3.4839e+02	0	-3.1361e-01	1.0779e-01	-7.0383e-02
-7.4149e+01	5.3115e+02	0	-3.0548e+00	-5.8131e-01	-3.3688e+00
7.8764e+02	6.4988e+04	0	-7.0577e+00	7.5884e+00	3.8551e+00
-4.5985e+02	-4.8423e+04	0	-6.2839e+00	-8.0183e+00	-1.0589e+01
-1.2694e+02	3.7571e+03	0	1.5324e+00	3.4568e+00	4.9819e+00
-3.5440e+02	-8.7212e+04	0	7.7020e+00	-8.2604e+00	-3.1657e+00
-2.2802e+02	1.2517e+04	0	1.9938e+00	3.9841e+00	3.0764e+00
3.0855e+03	1.1200e+05	0	-3.3955e+01	1.0958e+01	-9.0923e+00
-3.0955e+04	-6.7866e+05	0	1.4945e+02	3.9565e+01	2.7150e+01

Columns 7 through 12

-3.1130e-04	2.5588e-04	-1.3587e-04	-1.1373e-04	1.0110e-03	1.3387e-03
-1.6226e-05	-2.1712e-05	-1.8184e-05	-1.3538e-05	2.1358e-05	1.2064e-04
0	0	0	0	0	0
-3.7883e-01	-5.1550e-01	-3.9872e-01	-2.1833e-01	-5.0272e-01	2.6352e+00
2.6607e-01	-1.3693e+00	1.8031e-01	-8.9718e-01	-8.3176e-01	2.9849e+00
8.9553e-01	-9.5369e-01	8.7184e-01	2.5077e-02	1.1682e+00	-1.8341e+00
-1.7944e-01	1.8000e-01	-1.7751e-01	-5.7323e-03	-2.5823e-01	3.4798e-01
2.8400e-01	-1.5560e+00	5.5695e-02	-4.5449e-01	-8.0428e-02	4.9907e-01
-9.8077e-02	1.8496e-01	-7.9871e-02	3.1469e-02	-4.4533e-01	3.7122e-02
3.1980e-02	-5.2517e-01	1.6607e-02	-5.2324e-01	6.7132e-02	1.4139e+00
-1.2714e-01	1.7293e-01	5.3560e-02	-1.8853e-01	-1.5415e+00	3.3771e+00
2.3711e-01	8.9340e-01	2.1677e-01	6.8355e-01	1.6399e+00	-8.3096e+00
-1.0229e-01	-3.2146e-01	-2.5221e-01	-3.1206e-01	9.8299e-01	-1.1468e+00
-2.0225e-01	-6.1067e-02	-4.6825e-01	3.6660e-01	-8.7459e-01	-1.0421e-01
-1.6389e-01	-9.2900e-01	-3.8751e-01	-1.4601e-01	6.8340e-01	8.2848e-01
-1.6287e-01	-1.9150e-01	-2.1202e-01	3.1730e-02	2.7336e-01	-1.1385e+00
-4.8321e-02	5.0913e-02	-8.2303e-02	-5.4345e-02	-2.1273e-01	-8.9496e-01
6.4518e-03	4.6007e-02	-8.0831e-02	-1.6450e-03	8.4662e-01	-1.7372e+00
-1.2227e-01	-1.0786e-01	-1.2235e-01	-1.9891e-01	2.7387e-01	3.1017e-01
-4.4659e-01	-7.9264e-01	-7.1096e-01	-5.1847e-01	-5.4153e-01	-3.3597e-01
0	0	0	0	0	0
0	0	0	0	0	0
0	0	0	0	0	0
1.0000e+00	0	0	0	0	0
0	1.0000e+00	0	0	0	0
0	0	1.0000e+00	0	0	0
0	0	0	1.0000e+00	0	0
0	0	0	0	1.0000e+00	0
0	0	0	0	0	1.0000e+00
0	0	0	0	0	0

0	0	0	0	0	0
0	0	0	0	0	0
0	0	0	0	0	0
0	0	0	0	0	0
0	0	0	0	0	0
0	0	0	0	0	0
0	0	0	0	0	0
7.2875e-04	-1.7727e-01	-3.5064e-02	8.5265e-02	3.6696e-01	-9.9601e-02
-1.9137e-02	3.4352e-01	1.0812e-02	-1.4173e-01	-1.0524e+00	3.2540e-01
8.7835e-01	3.6322e+00	2.2464e+00	-2.8940e+00	-2.8015e+00	-1.1852e+00
-1.1624e+00	-1.4149e-01	-1.6703e+00	-1.7782e-01	-1.4012e+01	-7.4496e+00
3.0262e+00	5.4962e+00	6.1438e+00	-4.3052e+00	1.3814e+01	3.6155e-01
-1.0764e+00	6.2980e-01	-7.8313e-01	-1.6303e+00	-3.0726e+00	-9.4203e+00
1.0123e+00	7.7883e-01	1.9290e+00	-5.9404e-01	8.9870e+00	6.5398e+00
-6.7787e-01	-3.3314e-01	-6.3968e-01	-9.1635e-01	-2.7448e+00	-1.0573e+00
1.6606e+00	5.3570e+00	1.6549e+00	-1.2556e+00	-9.0011e+00	6.6107e+00
-7.4499e+00	-1.9551e+01	-1.6458e+01	-2.5255e+00	7.0427e+00	4.3565e+00

Columns 13 through 18

-4.0870e-06	3.6726e-04	-5.2490e-04	-4.6346e-04	3.7970e-05	2.5547e-04
2.5645e-05	-1.4538e-06	-4.0632e-05	-2.1719e-05	1.3080e-05	2.4475e-05
0	0	0	0	0	0
1.8832e-01	-2.3227e-01	-2.7421e-01	3.8747e-01	4.0430e-02	4.3843e-01
4.2370e-01	3.1864e-01	-1.7496e-01	5.0717e-01	9.1809e-01	4.1644e-01
-1.4122e+00	1.1125e+00	3.0390e-01	-5.8710e-01	3.8439e-01	-1.4247e+00
2.8481e-01	-2.5943e-01	-5.0872e-02	1.2380e-01	-1.0146e-01	2.8254e-01
-7.6227e-02	9.7172e-01	-6.3992e-01	2.0239e-01	3.4868e-01	-1.4742e-01
2.1454e-01	-3.5658e-01	1.1558e-01	2.9791e-02	-2.1369e-01	7.7767e-02
-1.1085e-01	5.7110e-01	-6.1535e-01	2.1256e-01	2.8531e-01	9.4279e-02
1.8356e-01	-1.1535e+00	2.1648e-01	4.5854e-01	-6.6784e-02	1.5552e-01
-1.8676e+00	-3.3332e-01	1.1926e+00	-2.2005e+00	-1.0940e+00	-6.7470e-01
-9.4059e-01	1.4851e+00	-7.9061e-01	-1.6847e-02	2.2957e-01	4.2701e-01
1.2246e+00	-1.9276e+00	1.4224e+00	3.7102e-01	-5.7293e-01	7.6390e-01
-4.5720e-01	1.2775e+00	-1.9315e+00	1.9027e-01	3.2882e-01	2.0633e-01
-3.9798e-01	-1.1959e-01	3.3991e-01	-3.0040e+00	-1.0874e+00	-2.1071e+00
2.4524e-01	-3.5842e-01	1.3897e-01	-4.9470e-01	-1.0351e+00	-7.6452e-01
-3.4060e-01	3.3632e-01	-1.9148e-01	-5.1816e-01	-7.3074e-01	-1.7474e+00
-3.3301e-01	1.0401e+00	-1.1345e+00	1.2362e-01	3.1320e-02	2.5741e-02
4.6212e-01	8.6748e-01	-2.3790e+00	-1.0633e-01	-1.8789e+00	3.2935e-01
0	0	0	0	0	0
0	0	0	0	0	0
0	0	0	0	0	0
0	0	0	0	0	0
0	0	0	0	0	0
0	0	0	0	0	0
0	0	0	0	0	0
0	0	0	0	0	0
0	0	0	0	0	0
1.0000e+00	0	0	0	0	0
0	1.0000e+00	0	0	0	0
0	0	1.0000e+00	0	0	0
0	0	0	1.0000e+00	0	0
0	0	0	0	1.0000e+00	0
0	0	0	0	0	1.0000e+00
0	0	0	0	0	0
0	0	0	0	0	0
1.3344e-02	5.6583e-01	-4.2751e-01	-9.4806e-02	2.4419e-01	-1.6524e-01

6.6744e-01	-9.3826e-01	8.3512e-01	5.9896e-01	-2.5288e-01	1.0773e+00
-5.6373e-01	6.1998e+00	3.5272e+00	1.1231e+00	6.1690e-01	-1.0019e+00
4.6682e+00	5.9296e+00	5.1383e+00	2.2557e+00	-7.6146e+00	-3.5895e+00
-1.1579e+01	9.7714e+00	-1.3416e+00	-8.1140e+00	7.7541e+00	-7.5910e+00
-4.7265e+00	6.6426e+00	-7.6751e-02	-2.5629e+00	-3.3210e+00	-5.1209e+00
-5.2141e+00	-6.1704e+00	-1.2717e+00	3.1647e+00	5.0339e+00	5.0110e+00
-1.0873e+00	6.8524e+00	-2.5420e+00	2.8952e-01	2.9514e-01	-2.0155e+00
1.7182e+01	-1.5168e+01	-5.5538e-01	3.3040e+01	3.2416e+00	2.5484e+01
1.4270e+01	2.0227e+01	-3.6203e+01	2.2801e+01	1.4532e+01	2.7006e+01

Columns 19 through 24

-3.3082e-04	-1.8417e-03	-5.0418e-02	9.5143e-02	1.2007e-01	-3.4690e-02
-2.4813e-05	-9.4753e-05	-4.1899e-04	7.1712e-05	3.0094e-03	-7.4019e-04
0	0	0	0	0	0
-2.5574e-01	-1.2607e+00	-6.0969e+01	-1.6484e+01	2.7097e+01	-5.6952e+00
-6.0373e-02	1.1927e+00	1.1229e+01	-2.5055e+02	-6.4296e+01	1.8951e+01
2.4558e-01	3.8325e+00	2.2337e+01	-5.4464e+01	-3.5426e+02	2.1619e+01
-4.4970e-02	-7.9958e-01	-3.7015e+00	8.6899e+00	1.4990e+01	-2.8873e+02
-6.6351e-01	1.6486e-01	1.1113e+01	-6.1513e+01	-7.5264e+01	1.9397e+01
7.8678e-02	-3.7423e-01	-1.9998e+00	-4.9232e-01	-9.5422e-01	3.0484e-01
-4.9656e-01	-3.9046e-01	4.8042e+00	-9.0199e+00	-9.8860e-01	6.6347e-01
4.0521e-01	8.0881e-01	1.9630e+01	-2.0855e+01	-2.3783e+00	2.1524e+00
5.5098e-01	1.8413e-01	5.3188e+00	-3.1494e+01	3.5130e+00	1.1711e+00
-1.1698e+00	-2.1841e+00	-2.0153e+01	2.5391e+01	3.4231e+01	-9.0886e+00
1.0106e+00	-1.2465e+00	1.3421e+01	-5.1683e+01	-6.4631e+01	1.8088e+01
-1.6639e+00	-3.1732e+00	-2.0348e-01	3.0595e+01	1.4242e+01	-5.2395e+00
-2.4722e-03	-1.1312e+00	-3.8597e+00	-4.0425e+01	3.1025e+01	-5.5702e+00
-1.0376e-01	-2.0063e+00	5.0867e+00	-3.5509e+01	-1.8600e+01	6.2245e+00
-2.5551e-01	-6.9261e-01	-1.0548e+01	9.9180e+00	3.1631e+01	-7.7437e+00
-1.1582e+00	-2.1973e+00	-6.5538e+00	2.6551e+01	2.7977e+01	-7.7185e+00
-2.7077e+00	-1.0854e+01	1.1610e+01	-3.6941e+01	-3.6360e+01	9.6933e+00
0	0	0	0	0	0
0	0	0	0	0	0
0	0	0	0	0	0
0	0	0	0	0	0
0	0	0	0	0	0
0	0	0	0	0	0
0	0	0	0	0	0
0	0	0	0	0	0
0	0	0	0	0	0
0	0	0	0	0	0
0	0	0	0	0	0
0	0	0	0	0	0
0	0	0	0	0	0
0	0	0	0	0	0
1.0000e+00	0	0	0	0	0
0	1.0000e+00	0	0	0	0
-1.2606e-01	9.5788e-01	0	0	0	0
2.9436e-01	-2.0735e+00	0	0	0	0
8.2717e-02	5.2394e+00	0	0	0	0
-1.0801e+00	-1.7587e+01	0	0	0	0
5.2791e-01	3.7956e+01	0	0	0	0
-2.3310e+00	-5.5179e+00	0	0	0	0
2.3410e+00	1.4555e+01	0	0	0	0
-2.8501e+00	-1.7664e+00	0	0	0	0
4.7220e+00	-7.5170e+00	0	0	0	0

-2.8904e+01	-7.9209e+01	0	0	0	0

Columns 25 through 30

-4.3701e-02	-6.5150e-02	4.6291e-02	-1.3420e-01	1.3168e-01	1.6872e-01
-9.4638e-04	-1.0802e-03	3.0234e-05	-3.7799e-03	1.1736e-02	4.9702e-03
0	0	0	0	0	0
3.3700e-01	-3.1273e+00	-1.6859e+01	-7.0707e+01	1.9983e+02	7.7419e+01
-1.0488e+01	3.6989e+01	-5.5430e+01	-8.7229e+00	2.7867e+02	6.0831e+00
-3.1272e+01	2.7281e+01	-9.0453e+00	9.6074e+01	-1.2130e+02	-1.5921e+02
6.7309e+00	-4.3144e+00	1.0825e+00	-1.7600e+01	2.4037e+01	2.9024e+01
-3.6253e+02	3.2991e+01	-3.7218e+01	1.8866e+01	6.2134e+01	-6.3667e+01
9.6532e+00	-3.7925e+02	-3.0960e+00	-1.1973e+01	8.1640e+00	7.8200e+00
-1.4278e+01	-1.1398e+00	-5.4501e+02	1.2174e+01	5.3237e+01	9.7970e+00
-7.2824e+00	2.5923e+00	8.0538e+00	-7.7655e+02	7.7370e+01	-5.9725e+00
6.2984e+00	7.6626e+00	-1.2145e+01	1.8524e+01	-9.6711e+02	-3.8513e+01
-3.1646e+00	-1.3336e+01	-5.8617e+00	-4.8485e+01	6.8056e+01	-1.3654e+03
1.7497e+01	3.1378e+01	-1.5223e+01	3.1251e+01	-1.9104e+01	-3.2448e+01
-8.0844e-01	-1.2657e+01	1.6096e+01	7.4188e+00	-9.7204e+01	-1.4373e+01
-7.9972e-01	1.2891e+00	-3.4705e+01	-8.6254e+01	2.9352e+02	8.6120e+01
3.2788e+00	1.3111e+01	-1.6704e+01	-3.6838e+00	7.7319e+01	1.8401e+00
4.5527e-01	-9.3805e+00	-3.6709e+00	-3.5206e+01	7.6739e+01	4.9430e+01
5.9074e-01	-1.3395e+01	1.0399e+01	-1.6019e+01	-1.4370e+01	2.7118e+01
1.0559e+00	1.3933e+01	-1.0422e+01	1.2801e+01	1.3411e+01	-1.9554e+01
0	0	0	0	0	0
0	0	0	0	0	0
0	0	0	0	0	0
0	0	0	0	0	0
0	0	0	0	0	0
0	0	0	0	0	0
0	0	0	0	0	0
0	0	0	0	0	0
0	0	0	0	0	0
0	0	0	0	0	0
0	0	0	0	0	0
0	0	0	0	0	0
0	0	0	0	0	0
0	0	0	0	0	0
0	0	0	0	0	0
0	0	0	0	0	0
0	0	0	0	0	0
0	0	0	0	0	0
0	0	0	0	0	0
0	0	0	0	0	0
0	0	0	0	0	0
0	0	0	0	0	0
0	0	0	0	0	0
0	0	0	0	0	0
0	0	0	0	0	0
0	0	0	0	0	0
0	0	0	0	0	0

Columns 31 through 36

-2.5904e-01	-2.2586e-02	1.3616e-01	-7.4097e-02	2.0966e-01	3.1669e-02
-5.6586e-03	-2.6524e-03	9.6770e-03	2.8572e-03	1.0127e-02	-1.3086e-05
0	0	0	0	0	0
-4.0997e+01	-3.0954e+01	1.8005e+02	6.6702e+01	1.6561e+02	-2.4008e+00

1.6207e+02	-1.3864e+02	2.2644e+02	2.0543e+02	1.2253e+02	-8.0122e+01
2.0306e+02	-3.0478e+01	-1.5060e+02	2.4757e+01	-2.3765e+02	-7.0160e+01
-3.6344e+01	6.5582e+00	2.9293e+01	-2.5445e+00	4.5287e+01	1.3787e+01
1.4794e+02	-5.5700e+01	4.3298e+01	9.9417e+01	-2.7407e+01	-6.8514e+01
-9.3120e+00	1.1973e+01	1.1594e+01	9.4102e-01	1.6181e+01	1.0540e+01
1.5980e+01	-4.4498e+01	5.0581e+01	3.8975e+01	4.0583e+01	-2.7934e+01
-8.4679e+00	-4.2602e+01	8.7811e+01	8.1332e+01	1.1171e+02	6.0837e+00
1.4672e+01	5.5053e+01	-1.9377e+02	-1.0061e+02	-2.7195e+02	2.9520e+01
-2.0747e+01	-1.5497e+01	1.4745e+01	-4.3225e+01	4.8482e+00	-2.0764e+01
-1.4416e+03	3.7951e+01	-3.6660e+00	6.5638e+01	-1.0358e+01	1.6873e+01
-3.0596e+01	-2.4452e+03	-4.2524e+01	-5.8753e+01	-4.3224e+00	-2.1014e+01
-3.5123e+01	-2.6576e+01	-2.4144e+03	3.6148e+01	4.9971e+01	-1.4511e+00
4.1139e+01	-2.4460e+01	3.1818e+01	-3.0240e+03	6.7595e+00	-3.0455e+00
-4.5700e+01	-7.5948e+00	3.9312e+01	-1.1484e+01	-3.1667e+03	-2.1406e+00
-5.3353e+01	4.6433e+00	-3.2092e+00	-3.2057e+01	1.8690e+01	-3.7475e+03
5.2814e+01	-1.4445e+01	-7.3341e+00	3.9101e+01	-8.3237e+00	-2.8249e+01
0	0	0	0	0	0
0	0	0	0	0	0
0	0	0	0	0	0
0	0	0	0	0	0
0	0	0	0	0	0
0	0	0	0	0	0
0	0	0	0	0	0
0	0	0	0	0	0
0	0	0	0	0	0
0	0	0	0	0	0
0	0	0	0	0	0
0	0	0	0	0	0
0	0	0	0	0	0
0	0	0	0	0	0
0	0	0	0	0	0
0	0	0	0	0	0
0	0	0	0	0	0
0	0	0	0	0	0
0	0	0	0	0	0
0	0	0	0	0	0
0	0	0	0	0	0
0	0	0	0	0	0
0	0	0	0	0	0
0	0	0	0	0	0
0	0	0	0	0	0
0	0	0	0	0	0
0	0	0	0	0	0

Columns 37 through 42

-4.5648e-01	-7.0749e-03	-1.8265e-02	1.0246e-02	-8.9841e-03	-4.3752e-04
-6.4980e-03	-3.6445e-04	-2.8274e-04	-1.4638e-04	1.1476e-04	-1.2458e-05
0	0	0	0	0	0
-4.4534e+01	-4.5176e+00	-1.6909e+00	-7.3020e+00	2.5657e+00	1.6948e+00
3.0708e+02	1.0884e-01	4.8080e+00	-6.6963e+00	1.2763e+01	3.3603e+00
3.2341e+02	4.4978e+00	7.8122e+00	-7.0447e+00	7.6348e+00	6.9936e+00
-5.5108e+01	-8.3900e-01	-1.2646e+00	1.1567e+00	-1.2856e+00	-1.3923e+00
2.3635e+02	-1.3234e+00	4.5527e+00	-5.6703e+00	5.7427e+00	5.9648e-01
-2.2836e-01	-4.4114e-01	-2.7604e-02	-4.0970e-01	1.0313e+00	-6.9531e-01
1.0868e+01	7.4279e-01	7.2234e-01	1.3077e+00	-1.2376e+00	-2.7567e-01
1.1613e+02	1.9510e+00	3.9128e+00	4.7802e+00	1.1399e+00	-1.1480e+00
9.4772e+01	-3.8489e+00	-4.3459e-01	-5.5994e+00	1.1676e+01	6.2527e+00

-1.9212e+02	-8.2826e-01	-5.9589e+00	2.2420e+00	-7.9246e+00	-1.9926e+00
1.9938e+02	5.4745e-01	6.3762e+00	-9.5079e+00	2.7872e+00	2.1889e+00
-1.9892e+02	-4.0969e+00	-3.1453e+00	-1.5597e+00	-1.0590e+01	-1.2597e+00
-7.2510e+00	-7.1145e+00	-3.3428e+00	-1.1227e+01	1.2399e+01	6.7578e+00
1.0007e+02	-1.2790e-01	2.5954e+00	-3.6244e+00	7.2583e+00	1.1101e+00
-1.0588e+02	-4.4753e+00	-5.1591e+00	-1.1241e-01	1.5752e-01	3.3787e-01
-1.3867e+02	-5.7010e-01	-2.7781e+00	2.7290e+00	-4.2156e+00	-2.0390e+00
-3.8838e+03	4.9842e-02	4.7445e+00	-4.4074e+00	4.7113e+00	-2.6164e+00
0	0	0	0	0	0
0	0	0	0	0	0
0	0	0	0	0	0
0	0	0	0	0	0
0	0	0	0	0	0
0	0	0	0	0	0
0	0	0	0	0	0
0	0	0	0	0	0
0	0	0	0	0	0
0	0	0	0	0	0
0	0	0	0	0	0
0	0	0	0	0	0
0	0	0	0	0	0
0	0	0	0	0	0
0	0	0	0	0	0
0	0	0	0	0	0
0	-2.2932e+00	0	0	0	0
0	0	-4.5863e+00	0	0	0
0	0	0	-1.5288e+01	0	0
0	0	0	0	-2.6754e+01	0
0	0	0	0	0	-3.0576e+01
0	0	0	0	0	0
0	0	0	0	0	0
0	0	0	0	0	0
0	0	0	0	0	0
0	0	0	0	0	0

Columns 43 through 47

-1.3379e-02	-1.8350e-02	2.9546e-02	4.3805e-03	-1.7610e-03
-4.5833e-04	-1.6686e-04	1.2636e-03	2.1162e-04	-1.6523e-04
0	0	0	0	0
-5.9626e+00	-7.5425e-01	1.4412e+01	2.8757e+00	-1.7551e+00
-1.2799e+01	1.4992e+01	2.7701e+01	-2.1273e-01	-1.6300e+00
4.8042e+00	3.4355e+00	-1.2735e+01	-6.0914e-01	4.0255e+00
-7.6075e-01	-5.5355e-01	1.6242e+00	8.5403e-02	-7.5161e-01
-1.1497e-01	6.1434e+00	2.8185e+00	3.9429e-01	-8.8343e-01
2.6189e-01	1.3959e+00	-3.8432e+00	-4.3086e-01	3.9979e-01
-1.8243e+00	-9.3172e-01	5.7901e+00	1.0775e+00	-8.7815e-01
-2.3379e+00	1.0939e+00	-3.4121e+00	2.4247e+00	2.0484e+00
5.1905e+00	-3.1131e+00	-3.8206e+01	-9.5204e+00	2.2011e+00
2.6528e-01	-5.8592e+00	8.0065e+00	-2.7552e+00	-4.7942e+00
2.2648e+00	6.5930e+00	9.0829e-01	1.6667e+00	-1.4329e+00
6.4419e+00	-8.7845e+00	9.4515e+00	6.6589e+00	-3.5660e+00
-4.4305e+00	1.7162e+00	-2.6618e-01	-6.6649e-01	-7.0954e-01
-5.5589e-01	3.1178e+00	-1.4835e+01	-3.0147e+00	7.0350e-01
-2.7043e+00	-3.1033e+00	5.4463e+00	-3.6091e+00	-2.2536e+00
1.3576e+00	-4.0944e+00	-1.5374e+00	7.6116e-01	-1.1465e+00
6.1829e+00	-7.3231e-01	-3.9097e+01	-1.5392e-01	-5.0539e-01

0	0	0	0	0
0	0	0	0	0
0	0	0	0	0
0	0	0	0	0
0	0	0	0	0
0	0	0	0	0
0	0	0	0	0
0	0	0	0	0
0	0	0	0	0
0	0	0	0	0
0	0	0	0	0
0	0	0	0	0
0	0	0	0	0
0	0	0	0	0
0	0	0	0	0
0	0	0	0	0
0	0	0	0	0
0	0	0	0	0
0	0	0	0	0
-3.4398e+01	0	0	0	0
0	-3.8220e+01	0	0	0
0	0	-4.5863e+01	0	0
0	0	0	-6.4973e+01	0
0	0	0	0	-9.9371e+01

$\hat{A}$ =

-3.6026e+01	1.0918e+00	-3.3026e-02
-2.3315e+00	1.9467e-01	1.1421e-04
0	0	0
-4.0650e+04	2.0486e+03	6.7301e+00
-4.8081e+04	5.7651e+03	-7.7248e+01
4.0398e+04	-9.5397e+03	1.0818e+02
-7.8055e+03	1.8235e+03	-1.9952e+01
-6.4808e+03	1.3580e+03	1.4072e+01
-3.0922e+03	-4.1747e+02	4.7074e+00
-1.3647e+04	1.5361e+03	-2.2694e+01
-3.4703e+04	-5.3553e+03	2.3030e+01
8.0598e+04	3.2944e+03	-4.0411e+01
1.1194e+04	1.3249e+04	-1.3621e+02
-1.6751e+03	2.4724e+03	-2.1910e+00
4.0077e+03	9.0363e+02	5.9992e+01
-1.3873e+04	3.3918e+03	5.9853e+00
-2.9656e+03	2.1272e+03	-2.9222e+01
-3.3237e+03	8.0987e+03	-8.3042e+01
-2.6443e+02	1.9216e+03	-1.2899e+01
6.4933e+02	3.5121e+03	-1.4251e+01
0	0	0
0	0	0
0	0	0
0	0	0
0	0	0
0	0	0
0	0	0

```
         0              0              0
         0              0              0
         0              0              0
         0              0              0
         0              0              0
         0              0              0
         0              0              0
         0              0              0
         0              0              0
         0              0              0
         0   1.1311e+02              0
         0  -3.1944e+02              0
         0  -1.3116e+03              0
         0   8.5331e+03              0
         0  -1.0315e+04              0
         0   1.7100e+04              0
         0  -1.0202e+04              0
         0   9.2279e+03              0
         0   3.6187e+04              0
         0   2.6440e+05              0
```

A_a =

```
         0   1.0000e+00              0
         0              0   1.0000e+00
-1.0648e+06  -5.5244e+04  -3.3310e+02
```

B_a =

```
         0
         0
 1.0648e+06
```

C =

Columns 1 through 6

```
         0   1.0000e+00              0  -2.3102e-04   7.7219e-05  -1.9976e-04
         0   1.0000e+00              0  -1.9643e-04   5.2614e-05  -1.2363e-04
         0   1.0000e+00              0   5.5175e-05  -2.6413e-05   6.3330e-05
         0   1.0000e+00              0   7.9851e-05   5.2375e-05  -3.0868e-05
         0   1.0000e+00              0  -6.6751e-04   1.7121e-03  -1.5745e-03
```

Columns 7 through 12

```
 4.0723e-05   2.2454e-04   1.0235e-04  -1.7981e-04  -6.0123e-04  -2.2699e-04
 2.4650e-05   1.2755e-04   5.6999e-05  -8.5524e-05  -2.0717e-04  -6.6005e-05
-1.1770e-05  -2.9085e-05  -1.1251e-05  -2.1128e-05  -1.0967e-04  -3.0318e-05
 5.0179e-06   1.1984e-05   4.6995e-06  -1.6127e-05  -4.0219e-05   9.4572e-05
 2.8864e-04  -1.3179e-04  -1.2818e-04   8.4077e-04  -2.4897e-04   1.6004e-03
```

Columns 13 through 18

```
 3.3140e-04   4.8043e-04   4.8334e-04   1.5906e-04  -1.4649e-04   2.9317e-05
 4.1354e-05   4.6476e-05  -5.7167e-05  -2.0641e-05   3.1515e-05  -6.4589e-06
```

```
-5.9589e-05   2.8917e-05  -7.8092e-05  -1.4839e-05   3.9293e-05   7.4950e-07
-2.8744e-05   1.3363e-05   7.8693e-05  -2.1823e-04   2.4606e-05   1.9208e-04
 5.0436e-03   5.0751e-03  -6.0008e-04  -6.8638e-03   4.1590e-03   2.7566e-03

Columns 19 through 24

 1.2711e-05  -3.2786e-04            0            0            0            0
-3.2377e-06   9.1743e-05            0            0            0            0
 4.2067e-06   2.5320e-05            0            0            0            0
-1.4749e-05  -2.2995e-05            0            0            0            0
-1.3088e-03   7.5969e-03            0            0            0            0

Columns 25 through 30

         0            0            0            0            0            0
         0            0            0            0            0            0
         0            0            0            0            0            0
         0            0            0            0            0            0
         0            0            0            0            0            0

Columns 31 through 36

         0            0            0            0            0            0
         0            0            0            0            0            0
         0            0            0            0            0            0
         0            0            0            0            0            0
         0            0            0            0            0            0

Columns 37 through 42

         0            0            0            0            0            0
         0            0            0            0            0            0
         0            0            0            0            0            0
         0            0            0            0            0            0
         0            0            0            0            0            0

Columns 43 through 47

         0            0            0            0            0
         0            0            0            0            0
         0            0            0            0            0
         0            0            0            0            0
         0            0            0            0            0
```

Appendix D

Langley M = 0.24 / h = 0 ft Model

This Appendix describes the Langley M = 0.24, h = 0 ft model. All variables are expressed with feet, second, and radian units except structural axes coordinates and mode shape/slope deflections which utilize inch. Airframe states, inputs, and outputs are listed below.

$$x = \left[u\ w\ q\ \theta\ \dot{\eta}_1 \ldots \dot{\eta}_{17}\ \eta_1 \ldots \eta_{17}\ z_1 \ldots z_{10} \right]^T$$

$$u = \left[\delta_E\ \delta_{TE1}\ \delta_{TE2}\ \delta_{TE3}\ \delta_{TE4} \right]^T$$

$$y = \left[\ldots q_{xs} \ldots \right]^T$$

Measured pitch rates are calculated from

$$q_{xs} = q - \sum_{i=1}^{17} \phi_i'(x_s)\dot{\eta}_i$$

$$\phi_i'(x_s) = \frac{d\,\phi_i(x_s)}{dx_s}$$

$$\phi_i(x_s) = C_{\phi_i}\bar{x}_s$$

where $C_{\phi i}$ is the $i^{\underline{th}}$ row of C_ϕ and

$$\bar{x}_s = [x_s^{10}\ x_s^9 \cdots x_s\ 1]^T$$

C_ϕ represents a polynomial curve fit to the mode shapes which allows pitch rates to be computed at any point along the fuselage centerline. The state space C matrix can be easily constructed from the above description. Actuator model data corresponding to Eq. (1.5) is tabulated below.

Actuator Data	p	ω	ζ
δ_E	22.	220.	0.7071
δ_{TE1}	20.	200.	0.7071
δ_{TE2}	21.	210.	0.7071
δ_{TE3}	23.	230.	0.7071
δ_{TE4}	24.	240.	0.7071

State space matrices defined in Eqs. (1.1)-(1.7) and C_ϕ are listed below.

A =

Columns 1 through 6

5.9489e-04	2.1308e-02	-4.1438e+01	-3.1782e+01	0	0
-1.4249e-01	-1.0721e+00	2.4930e+02	0	5.3729e-04	-2.2968e-03
-1.5018e-04	-1.8599e-02	-3.1355e-02	0	-4.5619e-06	-1.4275e-05
0	0	1.0000e+00	0	0	0
0	-4.4139e+01	-2.2403e+03	0	-1.6894e-01	8.7569e-01
0	-7.1775e+01	-4.3776e+03	0	5.3115e-01	-1.2258e+00
0	-1.4749e+02	5.5858e+02	0	-4.4209e-02	-1.0684e+00
0	-4.9584e+01	6.6759e+01	0	-8.0959e-03	-3.6329e-01
0	2.5259e+01	2.2349e+03	0	-1.2638e-01	3.8536e-01
0	-2.0751e+01	-8.1567e+03	0	4.1638e-01	-2.8163e-01
0	-3.5676e+01	-4.3653e+03	0	1.8139e-01	1.0144e-01
0	5.4516e+00	-2.5686e+03	0	-6.7514e-02	1.9907e-01
0	-4.1838e+01	3.6544e+03	0	-7.9658e-02	-7.1520e-01
0	2.5353e+02	6.8818e+03	0	-5.3516e-02	3.3174e-01
0	-1.1372e+02	-5.1944e+03	0	-3.0425e-01	5.4338e-01
0	2.5037e+02	6.8620e+03	0	8.6741e-02	-3.7957e-01
0	1.0228e+01	4.4531e+03	0	2.6974e-01	-5.5910e-01
0	7.9047e+00	-2.9758e+03	0	-4.8364e-02	-1.4033e-01
0	1.4316e+01	4.1789e+02	0	-4.4431e-03	2.6953e-01
0	-9.6461e+01	-3.8370e+03	0	3.3366e-01	-3.1288e-01
0	1.7867e+01	2.8637e+03	0	-2.2241e-01	1.5869e-01
0	0	0	0	1.0000e+00	0
0	0	0	0	0	1.0000e+00
0	0	0	0	0	0
0	0	0	0	0	0
0	0	0	0	0	0
0	0	0	0	0	0
0	0	0	0	0	0
0	0	0	0	0	0
0	0	0	0	0	0
0	0	0	0	0	0
0	0	0	0	0	0
0	0	0	0	0	0
0	0	0	0	0	0
0	0	0	0	0	0
0	0	0	0	0	0
0	5.0274e-01	-8.4015e+00	0	1.0870e-02	1.9733e-02
0	8.6196e-01	3.2999e+02	0	-1.6020e-01	-3.7630e-01
0	-6.1473e+01	-7.0734e+02	0	-1.0947e-01	3.0905e-01
0	2.8760e+02	3.7594e+03	0	4.9659e-01	-3.6739e-01
0	-1.8644e+02	4.0003e+03	0	2.2756e-01	-1.2203e+00
0	-3.5938e+02	-6.7843e+03	0	5.4455e-01	-1.2685e-01
0	-1.2347e+02	-2.3769e+03	0	5.1268e-01	7.2126e-01
0	-7.9291e+02	-2.6798e+04	0	3.6005e+00	-1.1180e+00
0	-2.6492e+02	-7.1313e+04	0	3.9221e+00	4.8925e+00
0	-2.6749e+03	9.3293e+02	0	4.8022e+00	2.2209e-01

Columns 7 through 12

0	0	0	0	0	0
-1.0818e-03	-4.8790e-04	5.0216e-04	2.4977e-04	3.5022e-04	1.7135e-02
-7.2402e-06	-3.9869e-06	2.9077e-06	7.0115e-07	-2.5169e-06	3.8738e-04

```
         0         0         0         0         0         0
-1.4369e-01 -3.0074e-02 -1.4779e-01  2.7682e-01 -1.4413e-01 -1.1772e+00
-1.2725e+00 -4.8926e-01  4.5995e-01  1.4925e-02  4.0226e-01  2.0149e+00
-1.7458e+00 -5.3294e-01  5.6936e-01 -2.0847e-01  1.4261e-01  1.0916e+00
-4.9877e-01 -5.3565e-01  2.0094e-01 -7.1752e-02  5.4390e-02  3.7886e-01
 5.6219e-01  2.0827e-01 -6.1123e-01  7.3426e-02 -1.4368e-01 -2.1899e-01
-5.9684e-01 -2.0793e-01  1.9994e-01 -4.7091e-01  1.9538e-01  2.6697e-01
 2.2007e-02  1.4927e-02 -6.0054e-02  1.3323e-01 -5.9947e-01 -5.0828e-02
-3.1196e-01 -1.0650e-01 -5.5209e-02  4.0050e-01  9.5328e-03 -3.8663e+00
 5.7705e-02  2.6892e-03  2.2788e-02  7.3971e-02  1.3355e-01  1.0712e+00
 4.9468e-01  1.7801e-01 -5.8103e-02 -2.7437e-01  2.0155e-01 -1.3917e+00
 1.2734e-01  5.8566e-02 -4.0672e-02 -8.4425e-02 -2.0138e-01 -4.0199e-02
 2.2718e-01  7.5731e-02  2.0112e-02 -1.6334e-01  1.2466e-01 -1.3121e+00
-1.3084e-01 -5.4351e-02  1.0142e-01 -1.0275e-01  1.2892e-01  1.3986e+00
-2.7915e-01 -1.0049e-01  7.0614e-02  5.1077e-02 -1.0376e-01 -1.1455e+00
 1.5424e-01  7.0800e-02 -3.7289e-02 -1.4471e-01 -3.2611e-02 -9.3735e-02
-8.1182e-01 -2.4861e-01  2.9184e-01 -5.0360e-01 -1.4312e-01  6.5847e-02
 4.5654e-01  1.4892e-01 -1.3837e-01  1.3279e-01  6.4090e-02  3.3065e-01
         0         0         0         0         0         0
         0         0         0         0         0         0
 1.0000e+00         0         0         0         0         0
         0  1.0000e+00         0         0         0         0
         0         0  1.0000e+00         0         0         0
         0         0         0  1.0000e+00         0         0
         0         0         0         0  1.0000e+00         0
         0         0         0         0         0  1.0000e+00
         0         0         0         0         0         0
         0         0         0         0         0         0
         0         0         0         0         0         0
         0         0         0         0         0         0
         0         0         0         0         0         0
         0         0         0         0         0         0
         0         0         0         0         0         0
         0         0         0         0         0         0
-6.4576e-02 -2.3055e-02 -4.6117e-03  4.6993e-02  3.3040e-02 -5.1215e-02
 5.2193e-01  1.6784e-01  4.6369e-02 -1.6794e-01  2.1601e-01  1.0131e+00
 3.1263e-01  1.3671e-01  6.1207e-02 -6.2795e-01 -1.0173e+00 -1.0026e+00
-1.0992e+00 -3.9282e-01 -3.8935e-01  1.9763e+00  2.6149e+00  6.6115e+00
 6.7413e-01  1.5754e-01  1.5947e-01 -1.1183e+00 -2.9486e-01  9.9624e+00
 6.6493e-01  2.1482e-01  2.2968e-01 -1.5844e+00 -1.4616e+00  1.0493e+00
-1.8519e-01 -3.0157e-02 -4.1860e-03  5.5422e-02 -5.2063e-01 -2.1455e+00
 1.1693e+00  3.3250e-01  2.6711e-01 -4.3147e+00 -1.7979e+00  7.7710e+00
-2.8950e+00 -8.6880e-01 -1.6836e-01  1.6101e+00 -9.6289e-01 -2.0033e+00
-1.7876e-01 -2.2370e-01 -4.6449e-03 -6.6874e-01 -1.0274e+00  8.9590e+01

Columns 13 through 18

         0         0         0         0         0         0
 1.0980e-02 -2.6660e-05 -1.8693e-03 -5.1695e-05  1.3192e-03 -4.5828e-04
 2.5177e-04  1.3490e-05 -4.0504e-05 -5.2607e-06  6.4290e-06 -7.6733e-06
         0         0         0         0         0         0
-4.3223e-01 -3.6306e-01  5.1029e-01 -7.2835e-01 -6.8122e-01  1.8109e-01
 1.6999e+00 -7.8445e-01 -1.1919e+00  2.0684e-01  1.1235e+00  1.1997e-01
 1.4418e+00 -1.5355e+00 -6.9388e-01 -3.5625e-01  6.3811e-01  6.5220e-01
 5.1226e-01 -5.6469e-01 -2.6615e-01 -1.2486e-01  2.3145e-01  2.4323e-01
-2.7178e-01  4.5415e-01  3.5298e-01 -5.2562e-02 -3.1895e-01 -2.0991e-01
-1.1534e-01  2.5259e-02 -3.8410e-01  3.0466e-01  3.2213e-01  4.7882e-02
```

-3.9969e-01	3.1749e-01	2.0526e-01	-4.9406e-03	-1.1395e-01	-1.7271e-01
-1.6163e+00	-1.8155e+00	1.8037e+00	-2.0466e+00	-1.3311e+00	5.4156e-01
-1.4728e-01	-6.5258e-02	7.0487e-01	-3.6569e-01	-1.2941e-01	-2.4688e-01
-8.2260e-01	-1.9287e+00	-1.6795e-02	-2.6678e-01	-4.4803e-01	8.0974e-01
-2.4905e-02	-8.2627e-02	-1.4225e+00	5.0925e-01	8.7760e-02	3.6897e-01
-1.0902e+00	-1.7191e-01	3.9275e-01	-1.7452e+00	-5.2304e-01	4.1281e-01
6.5677e-01	3.3534e-01	9.6512e-02	-3.7960e-01	-1.4874e+00	5.6834e-02
-6.0126e-01	3.3416e-02	1.4962e-01	6.7803e-02	3.6094e-01	-1.6248e+00
-2.2163e-01	7.3268e-02	-6.3764e-02	1.8832e-01	-3.7657e-01	3.3380e-01
-5.1705e-01	9.5091e-01	3.9262e-01	2.1726e-01	-9.3839e-01	-2.0848e-02
5.1631e-01	-4.0300e-01	-1.2683e-01	-1.0556e-01	1.2593e-01	2.1452e-01
0	0	0	0	0	0
0	0	0	0	0	0
0	0	0	0	0	0
0	0	0	0	0	0
0	0	0	0	0	0
0	0	0	0	0	0
0	0	0	0	0	0
0	0	0	0	0	0
1.0000e+00	0	0	0	0	0
0	1.0000e+00	0	0	0	0
0	0	1.0000e+00	0	0	0
0	0	0	1.0000e+00	0	0
0	0	0	0	1.0000e+00	0
0	0	0	0	0	1.0000e+00
0	0	0	0	0	0
0	0	0	0	0	0
0	0	0	0	0	0
4.3539e-02	-4.2040e-02	-3.8771e-02	-5.0614e-02	-1.0846e-02	-1.2448e-02
3.0797e-02	-1.3013e-01	2.1032e-02	6.1924e-01	5.9149e-01	3.1094e-02
-1.0921e+00	5.9243e-01	3.7703e-01	-2.4342e-01	-6.8003e-01	5.2032e-01
4.9573e+00	1.2436e+00	-1.3153e-02	4.3299e-01	1.2582e+00	-2.8783e+00
6.9899e+00	-2.5719e+00	-4.6741e-01	-5.4233e-01	9.0328e-01	7.0160e-02
2.6866e-01	-1.4613e+00	-1.7574e-01	-1.1025e-01	-5.6022e-01	1.1310e+00
-1.9129e+00	8.1748e-01	7.3412e-02	-3.7964e-02	3.5500e-02	-4.1469e-01
6.5650e+00	-1.7105e+00	-1.7710e+00	-7.4774e-01	-1.7037e+00	-2.9915e-02
-2.8062e+00	4.7038e-01	-1.1856e-01	-9.3840e-01	-1.9088e+00	2.1388e-01
5.5113e+01	4.2794e+00	-7.1330e+00	-2.1585e+00	2.6753e+00	-5.3698e+00

Columns 19 through 24

0	0	0	0	0	0
1.6854e-03	1.1107e-02	-3.1535e-03	-1.0345e-02	-2.2086e-02	-6.9142e-03
1.6407e-05	1.5402e-04	-3.8463e-05	-7.9892e-06	3.6196e-05	-1.2968e-06
0	0	0	0	0	0
-1.6916e-01	-9.4386e-01	2.1272e-01	-5.8408e+01	5.4562e+00	2.1584e+00
2.6992e-01	4.1973e+00	-1.4870e+00	6.8081e-01	-1.6088e+02	-5.3423e+00
-2.2077e-02	3.8146e+00	-1.4879e+00	-1.3953e+00	-7.0903e+00	-2.8777e+02
-2.2539e-02	1.3629e+00	-5.4209e-01	-4.2259e-01	-2.2291e+00	-2.0160e-01
6.0137e-02	-1.2271e+00	5.5330e-01	3.1980e-01	2.1284e+00	2.2784e+00
-2.7545e-02	7.6339e-01	-4.1336e-01	-5.6000e-01	-2.9455e+00	-7.2962e+00
2.1376e-01	-9.5585e-02	1.0405e-01	-4.3335e-01	-1.1376e+00	-2.9584e+00
4.9556e-02	4.7510e-02	-1.8154e-01	1.0084e+00	-1.8506e+00	1.8335e+00
5.7455e-01	1.0359e+00	-1.0300e-01	-8.6864e-01	-5.4735e+00	-1.4340e+00
-1.1474e+00	-1.9837e+00	6.7507e-02	2.2646e+00	6.6152e+00	7.3502e+00
-5.8814e-01	-1.1017e+00	9.7463e-02	-1.1173e+00	3.7086e+00	2.2967e+00
1.2575e-02	-2.4971e-01	-8.7250e-02	2.6285e-01	-2.7125e+00	2.5258e+00
1.7284e-01	6.3673e-02	-2.5538e-02	1.6969e-01	-6.3345e+00	-3.1695e+00

4.5235e-01	9.2668e-01	4.7253e-02	-1.3338e+00	-2.2801e+00	-2.2451e+00
-2.0149e+00	-2.3126e+00	4.5115e-01	2.9416e-01	2.5796e-02	-3.0148e-01
-8.0120e-01	-6.1744e+00	1.5028e+00	-1.4039e+00	-1.6682e+01	-1.6534e+01
-3.5151e-03	1.0427e+00	-1.7874e+00	5.3484e-01	6.0088e+00	7.9210e+00
0	0	0	0	0	0
0	0	0	0	0	0
0	0	0	0	0	0
0	0	0	0	0	0
0	0	0	0	0	0
0	0	0	0	0	0
0	0	0	0	0	0
0	0	0	0	0	0
0	0	0	0	0	0
0	0	0	0	0	0
0	0	0	0	0	0
0	0	0	0	0	0
0	0	0	0	0	0
0	0	0	0	0	0
1.0000e+00	0	0	0	0	0
0	1.0000e+00	0	0	0	0
0	0	1.0000e+00	0	0	0
1.9768e-02	1.2190e-01	-7.5640e-02	0	0	0
1.7947e-01	1.0697e+00	-1.8981e-01	0	0	0
-5.4807e-01	-2.7616e+00	1.1847e+00	0	0	0
1.2436e+00	1.0950e+00	2.9058e-01	0	0	0
1.3966e+00	8.0582e+00	-2.8129e+00	0	0	0
-2.8869e-03	2.5204e+00	-1.6530e+00	0	0	0
-1.5214e-01	-2.8884e+00	1.3550e+00	0	0	0
8.1616e-01	4.8504e+00	-3.5551e+00	0	0	0
-1.0261e+00	-8.9203e-01	-1.2996e+00	0	0	0
3.8606e+00	2.2522e+01	-2.7545e+00	0	0	0

Columns 25 through 30

0	0	0	0	0	0
-4.4162e-03	-4.5325e-04	3.1884e-02	3.0162e-02	3.8986e-01	3.7500e-01
-8.7077e-06	-1.1970e-05	1.5021e-05	-6.0777e-05	8.8743e-03	7.2401e-03
0	0	0	0	0	0
1.1485e+00	3.2600e-01	-8.5110e+00	-1.0457e+01	-1.1202e+00	-8.4121e+00
-2.3444e+00	3.6399e-01	6.1893e+00	1.9786e+00	2.2200e+01	4.5652e+01
-7.2617e-01	1.3380e+00	2.0358e+00	1.4126e+00	3.7567e+01	3.4225e+01
-2.9959e+02	4.2144e-01	5.7418e-01	2.8786e-01	1.2895e+01	1.1443e+01
9.8103e-01	-3.8456e+02	-3.6745e+00	-2.2108e+00	-1.2481e+00	-6.3645e+00
-2.8848e+00	-3.7859e-01	-4.3185e+02	7.8191e+00	-9.4985e+00	6.5667e+00
-1.1493e+00	-2.6765e-01	6.2164e+00	-5.8937e+02	6.2756e-01	4.2068e+00
6.2705e-01	4.3489e-01	-9.6740e-01	2.7792e+00	-8.6402e+02	9.1643e+00
-1.0339e+00	1.0047e+00	2.6592e+00	4.3442e+00	4.5594e+01	-1.2490e+03
3.3269e+00	-2.1020e+00	-8.5158e+00	-6.3413e+00	-1.1263e+01	-3.6523e+01
1.2190e+00	-1.3064e+00	-1.5125e+00	-5.6206e+00	-1.2892e+01	-2.3099e+01
8.8401e-01	2.4110e-02	-6.4541e-01	5.0533e+00	-2.2451e+01	-2.1999e+01
-1.6101e+00	1.3951e+00	3.3621e+00	6.0647e+00	2.8097e+01	3.9138e+01
-9.8570e-01	1.1636e+00	1.3116e+00	1.4368e+00	-2.0167e+01	-1.5017e+01
-1.7530e-02	-3.3512e-01	9.5172e-03	-1.0048e+00	-1.4338e+00	-9.7646e+00
-6.8611e+00	5.5555e+00	8.1793e+00	7.4380e+00	3.1418e+00	1.3474e+01
3.1969e+00	-2.2054e+00	-5.0643e+00	-5.5069e+00	4.7236e+00	3.2067e+00
0	0	0	0	0	0
0	0	0	0	0	0
0	0	0	0	0	0

```
            0            0            0            0            0            0
            0            0            0            0            0            0
            0            0            0            0            0            0
            0            0            0            0            0            0
            0            0            0            0            0            0
            0            0            0            0            0            0
            0            0            0            0            0            0
            0            0            0            0            0            0
            0            0            0            0            0            0
            0            0            0            0            0            0
            0            0            0            0            0            0
            0            0            0            0            0            0
            0            0            0            0            0            0
            0            0            0            0            0            0
            0            0            0            0            0            0
            0            0            0            0            0            0
            0            0            0            0            0            0
            0            0            0            0            0            0
            0            0            0            0            0            0
            0            0            0            0            0            0
            0            0            0            0            0            0
            0            0            0            0            0            0
            0            0            0            0            0            0
            0            0            0            0            0            0

Columns 31 through 36

            0            0            0            0            0            0
  -3.1819e-02  -3.5480e-02  -6.5990e-02   9.2163e-02  -3.0315e-02  -1.6696e-02
   1.5166e-03   2.0467e-05  -1.4138e-03   6.4452e-04  -1.2836e-03   3.1345e-04
            0            0            0            0            0            0
   7.8217e+00   2.6401e+01  -2.5931e+01  -2.9311e+01  -9.7821e+00   4.7607e+00
  -2.7606e+01  -4.9016e+01  -1.1352e+00   2.3878e+01   2.2822e+01  -3.5920e+01
  -3.4278e+01  -1.7306e+01  -6.5832e+00   1.7299e+01   2.5942e+01  -2.0402e+01
  -1.0846e+01  -5.7679e+00  -2.3087e+00   5.1388e+00   8.8023e+00  -7.3302e+00
   9.0569e+00   7.8689e+00   1.3051e+00  -8.0542e+00  -5.2470e+00   5.8680e+00
  -1.2134e+01  -1.2395e+01  -2.6644e+00   1.5209e+01  -2.9734e+00  -1.9726e+00
  -1.2486e+01  -1.9352e+00  -1.1449e+00   5.1994e+00  -1.3956e+00  -3.7480e+00
  -2.1261e+00   1.0349e+01  -2.7149e+01  -1.7192e+01   5.3046e+00  -1.2584e+00
  -1.8359e+01  -3.7239e+01  -5.6005e+00   2.7277e+01   5.6311e+00  -8.2634e+00
  -1.8017e+03   1.6306e+01   3.1335e+01  -2.2950e+01  -3.1212e+01   4.1826e+01
   7.7882e+00  -2.1740e+03  -3.7363e+01  -3.6361e+01  -2.6121e+01   3.3354e+01
   2.1611e+01  -2.2136e+01  -2.8823e+03   5.0198e+01  -1.3020e+01  -1.1255e+01
  -4.6826e+00  -3.7132e+01   4.5255e+01  -3.1283e+03  -2.7609e+01   6.2453e+00
  -3.1978e+01  -7.8441e+00  -1.5334e+01  -1.8878e+01  -3.6425e+03  -3.6194e+01
   2.8447e+01   2.3307e+01  -6.7673e+00  -3.1464e+00  -3.2074e+01  -3.8428e+03
  -1.4462e+01   3.4718e+00  -2.0462e+01   3.9872e+01  -2.2117e+01   8.2912e+01
   1.9018e+01   9.8254e+00   8.1256e+00  -6.2376e+00  -2.0638e+01  -4.6730e+00
            0            0            0            0            0            0
            0            0            0            0            0            0
            0            0            0            0            0            0
            0            0            0            0            0            0
            0            0            0            0            0            0
            0            0            0            0            0            0
            0            0            0            0            0            0
            0            0            0            0            0            0
            0            0            0            0            0            0
            0            0            0            0            0            0
```

```
            0            0            0            0            0            0
            0            0            0            0            0            0
            0            0            0            0            0            0
            0            0            0            0            0            0
            0            0            0            0            0            0
            0            0            0            0            0            0
            0            0            0            0            0            0
            0            0            0            0            0            0
            0            0            0            0            0            0
            0            0            0            0            0            0
            0            0            0            0            0            0
            0            0            0            0            0            0
            0            0            0            0            0            0
            0            0            0            0            0            0
            0            0            0            0            0            0
            0            0            0            0            0            0
            0            0            0            0            0            0

  Columns 37 through 42

            0            0            0            0            0            0
   3.9415e-01  -3.1250e-02   2.0562e-02   4.8222e-03   1.6083e-02   8.3086e-03
   7.7253e-03  -5.5355e-04   1.8273e-05   9.4965e-06   5.1030e-05  -1.0831e-06
            0            0            0            0            0            0
  -1.4879e+01   1.4274e+01  -2.7659e+00  -6.9369e-01  -2.2084e+00  -1.0263e+00
   2.7923e+01  -2.7996e+01   2.9115e+00   4.6823e-01   3.6769e+00   3.4577e+00
   7.4329e+01  -2.9523e+01   3.5738e+00   7.3409e-01   3.4500e+00   1.7810e+00
   2.4159e+01  -9.9847e+00   1.1582e+00   2.3382e-01   1.1415e+00   6.1367e-01
  -1.9272e+01   1.1216e+01  -1.5378e+00  -2.9736e-01  -1.4871e+00  -1.1140e+00
   2.8704e+01  -1.7473e+01   3.5149e+00   7.0550e-01   3.1679e+00   2.7649e+00
  -5.3820e+00  -1.8524e+00   1.9291e+00   4.1944e-01   1.5066e+00   8.8431e-01
  -1.6863e+00   1.1413e+00   6.5375e-01   1.6810e-01   3.6752e-01   3.1831e-02
   4.6466e+01  -6.0134e+00   1.9946e+00   4.4964e-01   2.3934e+00   1.9587e+00
  -3.5821e+01   1.8871e+01  -4.7307e+00  -1.0461e+00  -4.1723e+00  -2.5150e+00
  -3.8609e+00   2.6517e+01  -1.4154e+00  -2.5825e-01  -1.7044e+00  -1.1763e+00
  -4.6940e+01   9.0763e+00  -7.6622e-01  -1.7965e-01  -6.1444e-01  -5.6377e-01
   7.3640e+01  -6.6907e+00   2.6348e+00   5.2032e-01   2.9923e+00   1.8493e+00
  -2.7349e+01  -2.6146e+01   1.3361e+00   2.8428e-01   8.1134e-01   5.2798e-01
   7.2380e+01  -2.2029e+00  -4.3622e-01  -7.4722e-02  -4.8939e-01  -2.4212e-01
  -3.8178e+03  -7.8378e+01   5.2022e+00   1.0501e+00   5.1680e+00   3.7717e+00
  -7.8848e+01  -4.2202e+03  -2.7467e+00  -5.6801e-01  -2.3795e+00  -1.7435e+00
            0            0            0            0            0            0
            0            0            0            0            0            0
            0            0            0            0            0            0
            0            0            0            0            0            0
            0            0            0            0            0            0
            0            0            0            0            0            0
            0            0            0            0            0            0
            0            0            0            0            0            0
            0            0            0            0            0            0
            0            0            0            0            0            0
            0            0            0            0            0            0
            0            0            0            0            0            0
            0            0            0            0            0            0
            0            0            0            0            0            0
            0            0            0            0            0            0
            0            0            0            0            0            0
            0            0            0            0            0            0
```

0	0	-6.7336e-01	0	0	0
0	0	0	-1.3467e+00	0	0
0	0	0	0	-4.4891e+00	0
0	0	0	0	0	-7.8559e+00
0	0	0	0	0	0
0	0	0	0	0	0
0	0	0	0	0	0
0	0	0	0	0	0
0	0	0	0	0	0
0	0	0	0	0	0

Columns 43 through 48

0	0	0	0	0	0
1.1200e-03	2.7831e-03	5.0904e-04	1.3465e-03	1.0151e-03	-8.2236e-03
1.8267e-04	-2.6077e-04	8.1015e-05	1.4817e-05	6.3773e-05	-1.8647e-04
0	0	0	0	0	0
6.1435e-01	-1.8146e+00	-1.6549e+00	-3.9037e-01	-7.9864e-01	-1.2346e-01
-1.6888e+00	6.9104e+00	-1.5351e+00	-1.0870e+00	-1.4987e+00	-6.0223e-01
-3.7467e-01	9.7934e-02	-2.6455e-01	9.1193e-01	5.3330e-01	-9.5197e-01
-1.2510e-01	8.5173e-02	-9.2806e-02	2.8242e-01	1.4408e-01	-3.2673e-01
8.3281e-01	-2.0644e+00	5.5602e-01	7.5977e-02	5.2132e-01	5.4102e-02
-2.4821e+00	6.6097e+00	-1.7202e+00	-6.5545e-01	-2.0624e+00	1.7392e-01
-9.2786e-01	2.0037e+00	-1.2708e+00	-9.0678e-02	-8.9967e-01	4.2727e-03
-4.5097e-01	4.4784e-01	3.9444e-04	2.9611e-01	-5.6234e-01	6.9888e-02
-4.2818e-01	3.0087e+00	-4.6460e-01	-3.4844e-01	1.0591e+00	-7.2473e-01
1.4487e+00	-1.2655e+00	3.3452e+00	-6.7198e-01	6.4075e-01	9.4682e-01
3.7387e-01	-3.5960e+00	-3.0577e+00	3.3900e-01	-1.0266e-01	-2.6610e-01
-7.3597e-01	2.5314e+00	3.1765e+00	-6.3651e-02	2.8685e-01	1.2162e+00
-7.0397e-01	3.8158e+00	6.2640e-01	-2.1016e-01	3.9537e-01	-3.8339e-01
-9.2785e-01	7.3645e-01	1.4110e-01	4.1424e-01	-7.8393e-01	4.1845e-01
1.6878e-01	-2.8363e-01	4.5730e-01	-3.4596e-02	8.2093e-04	5.3745e-02
-2.8909e+00	6.0539e+00	-4.8953e-01	2.9469e-01	-1.4472e+00	-9.9552e-02
1.5586e+00	-3.2025e+00	3.8394e-02	-1.4643e-01	9.6796e-01	-1.6995e-01
0	0	0	0	0	0
0	0	0	0	0	0
0	0	0	0	0	0
0	0	0	0	0	0
0	0	0	0	0	0
0	0	0	0	0	0
0	0	0	0	0	0
0	0	0	0	0	0
0	0	0	0	0	0
0	0	0	0	0	0
0	0	0	0	0	0
0	0	0	0	0	0
0	0	0	0	0	0
0	0	0	0	0	0
0	0	0	0	0	0
0	0	0	0	0	0
0	0	0	0	0	0
0	0	0	0	0	0
0	0	0	0	0	0
0	0	0	0	0	0
0	0	0	0	0	0
-8.9782e+00	0	0	0	0	0
0	-1.0100e+01	0	0	0	0
0	0	-1.1223e+01	0	0	0

0	0	0	-1.3467e+01	0	0
0	0	0	0	-1.9079e+01	0
0	0	0	0	0	-2.9179e+01

$\hat{A}$ =

Columns 1 through 6

-4.2796e-01	0	0	2.8499e-01	0	0
-2.1582e+00	2.1105e-02	-1.2991e-03	-7.2392e+00	-8.2180e-02	-8.6334e-03
-7.0595e-02	-1.2823e-03	-2.2137e-05	1.9046e-02	1.1132e-02	-2.0913e-04
0	0	0	0	0	0
-4.0604e+03	-1.3613e+02	-1.2154e+00	2.2386e+03	2.3225e+02	-1.2552e+00
2.5850e+03	8.5826e+01	8.9500e-01	-1.1406e+03	1.2703e+02	-6.7353e+00
-2.0286e+03	-5.5991e+01	-9.3193e-01	7.7170e+02	7.7893e+01	2.8020e+00
-6.8974e+02	-1.9360e+01	-3.0839e-01	2.7788e+02	3.1669e+01	8.0396e-01
-3.4643e+02	-1.3904e+01	-9.3009e-02	4.9169e+02	-1.5562e+01	1.4263e+00
1.8715e+03	6.6480e+01	6.7954e-01	-1.8882e+03	1.9397e+01	-5.6312e+00
-1.9086e+02	-5.8778e+00	3.7657e-02	-3.9015e+02	6.5101e+01	-2.4882e+00
-1.0736e+04	-4.3033e+02	-2.9172e+00	-3.5020e+02	6.6446e+01	-2.7240e+00
-1.8711e+03	-9.2314e+01	-6.7493e-01	-2.2351e+03	-1.2986e+02	-1.4544e+00
-3.1457e+02	-9.7201e+01	4.5704e-01	-1.2966e+03	-1.5998e+02	-4.1089e+00
-1.0017e+03	5.3107e+01	-5.2362e-01	2.0641e+03	9.7938e+01	3.7692e+00
1.8563e+03	-8.6922e+01	4.0814e-01	-1.3780e+03	-1.5029e+02	-1.9263e+00
1.7076e+03	-4.0999e+01	4.5612e-02	-1.6814e+03	-6.5638e+01	-2.9720e+00
-5.9616e+02	3.4254e+01	2.1683e-01	7.7960e+02	5.2839e+01	2.5710e+00
1.5631e-01	1.4049e+00	1.5519e-02	1.5133e+02	2.5919e-01	3.8916e-01
-9.1487e+01	9.4009e+00	-1.9353e-01	-8.8359e+02	6.9505e+01	-1.5553e+00
-7.2696e+01	-2.6935e+01	-1.7156e-01	-7.7078e+01	-6.6315e+01	-2.3912e-01
0	0	0	0	0	0
0	0	0	0	0	0
0	0	0	0	0	0
0	0	0	0	0	0
0	0	0	0	0	0
0	0	0	0	0	0
0	0	0	0	0	0
0	0	0	0	0	0
0	0	0	0	0	0
0	0	0	0	0	0
0	0	0	0	0	0
0	0	0	0	0	0
0	0	0	0	0	0
0	0	0	0	0	0
0	0	0	0	0	0
0	0	0	0	0	0
0	-4.9040e+00	0	0	3.9549e-01	0
0	2.8501e+01	0	0	-1.6690e+02	0
0	2.7036e+01	0	0	3.7286e+02	0
0	3.4873e+01	0	0	-1.5309e+03	0
0	-1.4355e+02	0	0	9.2491e+02	0
0	-1.2306e+02	0	0	1.6019e+03	0
0	2.6433e+01	0	0	2.7383e+02	0
0	-2.3578e+02	0	0	2.2656e+03	0
0	-1.6747e+02	0	0	2.9876e+03	0
0	-1.8617e+02	0	0	3.2261e+03	0

Columns 7 through 12

5.2052e-01	0	0	1.9609e+00	0	0
-8.5714e+00	-4.3036e-01	-2.0833e-03	-1.1227e+01	-6.4748e-01	4.7392e-03
-2.5598e-02	-3.1459e-03	4.5311e-05	-6.4816e-02	-9.7806e-03	1.4992e-04
0	0	0	0	0	0
1.5597e+03	1.3899e+02	-1.0965e+00	1.6811e+03	6.5352e+01	1.1726e-02
-1.5629e+03	-1.4659e+01	-2.9598e+00	-3.9684e+03	-1.4001e+02	-1.3610e+00
7.9804e+01	4.2448e+01	4.2586e-01	-2.6962e+03	-7.8968e+01	-6.6889e-01
4.1765e+01	1.4827e+01	7.6001e-02	-9.1718e+02	-2.8195e+01	-2.2857e-01
3.7391e+02	-2.4418e+01	1.1579e+00	9.4301e+02	6.0879e+00	6.7198e-01
-1.0589e+03	7.3080e+01	-3.7597e+00	-1.0825e+03	2.9867e+01	-1.1129e+00
-5.1334e+02	4.8132e+01	-2.2376e+00	-9.0076e+02	-1.1838e+01	-8.4242e-01
-1.7167e+02	2.5337e+01	-1.1577e+00	-2.0218e+02	5.0292e+00	-4.2391e-01
-1.5751e+03	-1.5271e+02	2.3832e+00	-2.1007e+03	-1.0126e+02	5.0248e-01
1.3166e+03	-5.7471e+01	2.4052e+00	4.6252e+03	1.2702e+02	2.1743e+00
9.6929e+02	8.6333e+01	-4.7846e-01	2.4563e+03	1.1150e+02	-3.6144e-02
1.0218e+02	-4.6918e+01	3.3187e-01	-1.2113e+02	-1.4502e+01	-5.6176e-02
-1.3376e+03	-9.7264e+01	-2.5673e-01	-5.8265e+02	-1.2080e+01	7.4863e-01
-1.1666e+01	5.6951e+01	-9.2590e-01	-2.0813e+03	-5.2593e+01	-1.4294e+00
1.3600e+02	-9.3455e-01	2.4027e-01	3.0506e+03	1.5093e+02	1.3018e+00
-8.8664e+02	1.0220e+02	-3.1564e+00	3.1126e+03	3.4856e+02	4.3892e-01
1.0540e+02	-7.4108e+01	1.3755e+00	2.3937e+02	-7.4531e+01	5.9945e-01
0	0	0	0	0	0
0	0	0	0	0	0
0	0	0	0	0	0
0	0	0	0	0	0
0	0	0	0	0	0
0	0	0	0	0	0
0	0	0	0	0	0
0	0	0	0	0	0
0	0	0	0	0	0
0	0	0	0	0	0
0	0	0	0	0	0
0	0	0	0	0	0
0	0	0	0	0	0
0	0	0	0	0	0
0	0	0	0	0	0
0	0	0	0	0	0
0	0	0	0	0	0
0	-5.3967e+00	0	0	-1.3196e+01	0
0	-5.4493e+01	0	0	3.0614e+01	0
0	2.1684e+02	0	0	1.4709e+02	0
0	-5.7079e+02	0	0	-7.5019e+01	0
0	-6.6675e+01	0	0	-4.3512e+02	0
0	4.2541e+02	0	0	-9.9051e+01	0
0	2.2883e+02	0	0	1.9513e+02	0
0	-7.8010e+01	0	0	-3.7738e+02	0
0	1.7989e+03	0	0	3.1772e+02	0
0	-8.1832e+01	0	0	-1.4980e+03	0

Columns 13 through 15

1.1745e+00	0	0
-9.7098e+00	-5.7291e-01	8.6043e-03
-7.4839e-02	-1.1051e-02	2.0932e-04
0	0	0
1.4906e+03	1.4335e+01	6.5570e-01

-6.9989e+03	-1.9132e+02	-2.8576e-01
-8.0365e+03	-1.9535e+02	-1.3855e+00
-2.8656e+03	-7.1253e+01	-4.6108e-01
3.0622e+03	6.3547e+01	6.6244e-01
-2.4984e+03	-3.8472e+01	-3.4850e-01
7.1890e+02	2.3546e+01	1.6708e-01
-5.6733e+00	6.0565e+00	-1.5176e-01
-1.1955e+02	-1.2584e+01	4.6692e-01
8.7547e+02	7.5503e+00	1.9811e-01
3.5405e+02	-6.2431e+00	-9.3328e-02
1.2123e+02	4.0260e+01	-8.8277e-01
-8.0219e+01	1.4753e+01	4.3266e-01
-1.0293e+03	5.3974e+00	-8.8670e-01
1.8674e+03	6.6142e+01	4.4658e-01
3.0995e+03	2.5728e+02	-2.4674e-01
-2.6548e+02	-7.8450e+01	4.7595e-01
0	0	0
0	0	0
0	0	0
0	0	0
0	0	0
0	0	0
0	0	0
0	0	0
0	0	0
0	0	0
0	0	0
0	0	0
0	0	0
0	0	0
0	0	0
0	0	0
0	0	0
0	0	0
0	-1.1973e+01	0
0	4.8211e+01	0
0	9.4618e+01	0
0	5.1442e+01	0
0	-4.5660e+02	0
0	-2.2550e+02	0
0	1.4187e+02	0
0	-5.8025e+02	0
0	-1.3681e+02	0
0	-1.8836e+03	0

A_a =

Columns 1 through 6

0	1.0000e+00	0	0	0	0
0	0	1.0000e+00	0	0	0
-1.0648e+06	-5.5244e+04	-3.3310e+02	0	0	0
0	0	0	0	1.0000e+00	0
0	0	0	0	0	1.0000e+00
0	0	0	-8.0000e+05	-4.5656e+04	-3.0280e+02
0	0	0	0	0	0
0	0	0	0	0	0
0	0	0	0	0	0

```
         0         0         0         0         0         0
         0         0         0         0         0         0
         0         0         0         0         0         0
         0         0         0         0         0         0
         0         0         0         0         0         0
         0         0         0         0         0         0
```

Columns 7 through 12

```
         0         0         0         0         0         0
         0         0         0         0         0         0
         0         0         0         0         0         0
         0         0         0         0         0         0
         0         0         0         0         0         0
         0         0         0         0         0         0
         0    1.0000e+00         0         0         0         0
         0         0    1.0000e+00         0         0         0
-9.2610e+05 -5.0336e+04 -3.1790e+02         0         0         0
         0         0         0         0    1.0000e+00         0
         0         0         0         0         0    1.0000e+00
         0         0         0 -1.2167e+06 -6.0380e+04 -3.4830e+02
         0         0         0         0         0         0
         0         0         0         0         0         0
         0         0         0         0         0         0
```

Columns 13 through 15

```
         0         0         0
         0         0         0
         0         0         0
         0         0         0
         0         0         0
         0         0         0
         0         0         0
         0         0         0
         0         0         0
         0         0         0
         0         0         0
         0         0         0
         0    1.0000e+00         0
         0         0    1.0000e+00
-1.3824e+06 -6.5745e+04 -3.6340e+02
```

B_a =

```
         0         0         0         0         0
         0         0         0         0         0
 1.0648e+06         0         0         0         0
         0         0         0         0         0
         0         0         0         0         0
         0 8.0000e+05         0         0         0
         0         0         0         0         0
         0         0         0         0         0
         0         0 9.2610e+05         0         0
         0         0         0         0         0
         0         0         0         0         0
         0         0         0 1.2167e+06         0
```

0	0	0	0	0
0	0	0	0	0
0	0	0	0	1.3824e+06

C_ϕ =

Columns 1 through 3

2.619643071928745e-33	-3.662650064675893e-29	2.171734143039691e-25
1.061288371044740e-32	-1.720227533889429e-28	1.201235819613770e-24
-4.822716539318745e-33	8.273174222453042e-29	-6.076639042214411e-25
-1.446171975537073e-33	2.517790263018709e-29	-1.872383666904238e-25
1.015163796411903e-33	-1.484015282068149e-29	9.294357513382509e-26
-1.140524488826204e-32	1.730290663042760e-28	-1.130878727637102e-24
-1.980367703556376e-32	3.108924392893731e-28	-2.106205976793113e-24
4.172508147557280e-33	-6.521185294955085e-29	4.353513654916478e-25
9.496651290316193e-33	-1.694840607437875e-28	1.324769948323528e-24
-1.857082653372436e-32	2.833288154248727e-28	-1.861110973239443e-24
-3.199761081603517e-32	4.634846316474403e-28	-2.822601698709337e-24
-5.442445729553661e-32	8.219901485478656e-28	-5.327589328216484e-24
1.811371863499419e-32	-2.717742991394453e-28	1.753116378242865e-24
-2.643500366746380e-32	3.887573148499687e-28	-2.503650741486426e-24
-8.892490650019221e-33	1.441106236880430e-28	-9.849831220522667e-25
-3.069269545240876e-33	6.523061807723121e-29	-5.992626043135658e-25
-1.330768565359461e-33	8.133323861929407e-29	-1.026862887086196e-24

Columns 4 through 6

-7.102853734506066e-22	1.389645729819991e-18	-1.632978014064453e-15
-4.735458894644195e-21	1.160457534098140e-17	-1.835459359776141e-14
2.503083978253761e-21	-6.361808463646208e-18	1.035322672408983e-14
7.792332607737115e-22	-1.997154231659607e-18	3.272441310747364e-15
-3.282322937426889e-22	7.265931574159426e-19	-1.059851889124187e-15
4.186200641532230e-21	-9.716677823450091e-18	1.476499126384620e-14
8.085538239714672e-21	-1.942404887048516e-17	3.038876718746611e-14
-1.617936279660515e-21	3.665896995464928e-18	-5.265229667098711e-15
-5.931519290974930e-21	1.663867482220715e-17	-2.996331264256791e-14
6.906611500051563e-21	-1.598128625971362e-17	2.402548023546252e-14
9.415422726859322e-21	-1.891416820055840e-17	2.406558398770335e-14
1.948484289707208e-20	-4.462317928831169e-17	6.726937381846504e-14
-6.395912550317892e-21	1.463229717567974e-17	-2.200283280938736e-14
9.430933158323044e-21	-2.339707595203532e-17	4.018004209599058e-14
3.685665326504614e-21	-8.198341401243104e-18	1.103613145646011e-14
3.092615345635300e-21	-9.795658494488476e-18	1.958087108214280e-14
5.977122761306204e-21	-1.941808404420912e-17	3.756502140743908e-14

Columns 7 through 9

1.074096485108769e-12	-3.281839209447257e-10	-1.764031636869905e-08
1.887004653664311e-11	-1.243158844997728e-08	4.978098248197266e-06
-1.088693652092254e-11	7.338692551835055e-09	-2.989466049092692e-06
-3.461301646864357e-12	2.345978854832657e-09	-9.599118647968261e-07
1.025130809298564e-12	-6.242826620863745e-10	2.372991787568142e-07
-1.475816868166181e-11	9.379548467869470e-09	-3.676107880247640e-06
-3.109464516642467e-11	2.026559808758404e-08	-8.093227585171751e-06
4.942957553758776e-12	-3.126833624294042e-09	1.173066494216409e-06
3.419935917375025e-11	-2.398117502534028e-08	1.034258163481368e-05

```
-2.371543581996922e-11     1.511940699768860e-08    -5.872083215264353e-06
-2.031724136434099e-11     1.160321452888763e-08    -3.659523323397660e-06
-6.796542737011697e-11     4.494770620855398e-08    -1.761409662288230e-05
 2.204972729158325e-11    -1.436822155982120e-08     5.570355443044361e-06
-4.729462984499309e-11     3.545988667727973e-08    -1.450168822995220e-05
-8.867503713099941e-12     4.315072054493550e-09    -1.641460201934930e-06
-2.446707979053089e-11     1.820408283324094e-08    -7.166767300510724e-06
-4.352183928486075e-11     2.881128457176598e-08    -9.393061309888366e-06

Columns 10 through 11

 2.356809431278060e-04    -2.135518639968848e-01
-9.172887710064263e-04    -3.709229434708460e-02
 4.913096386977278e-04     5.772378485942669e-02
 1.575840676049128e-04     1.860930532238502e-02
-9.877029221943447e-05     3.578469913092890e-02
 1.088499013141565e-03    -2.547371138208678e-01
 2.047749160777185e-03    -3.205794283648200e-01
-3.061798242369468e-05    -8.979695586887435e-02
-3.063501661704725e-03     5.393813309916287e-01
 1.198769590667727e-03    -8.762669858695393e-02
-4.756499086655450e-05     2.302674909428932e-01
 3.163448768491699e-03    -1.010322469064967e-01
-1.034212390234211e-03     4.846870624833456e-02
 2.205881754512442e-03     6.755304067032704e-02
 6.570528034738893e-04    -1.390139557459541e-01
 1.063244100510320e-03     2.515741882888601e-02
 7.366995244902247e-04     1.765274997635236e-01
```

REPORT DOCUMENTATION PAGE

Form Approved
OMB No. 0704-0188

1. AGENCY USE ONLY *(Leave blank)*	2. REPORT DATE	3. REPORT TYPE AND DATES COVERED
	December 1999	Contractor Report

4. TITLE AND SUBTITLE
Investigation of Inner Loop Flight Control Strategies for High-Speed Research

5. FUNDING NUMBERS
C NAS1-19858
TA 71
WU 537-07-24-01

6. AUTHOR(S)
Brett Newman and Ayman Kassem

7. PERFORMING ORGANIZATION NAME(S) AND ADDRESS(ES)
Old Dominion University
Department of Aerospace Engineering
Norfolk, VA 23529

8. PERFORMING ORGANIZATION REPORT NUMBER

9. SPONSORING/MONITORING AGENCY NAME(S) AND ADDRESS(ES)
National Aeronautics and Space Administration
Langley Research Center
Hampton, VA 23681-2199

10. SPONSORING/MONITORING AGENCY REPORT NUMBER
NASA/CR-1999-209522

11. SUPPLEMENTARY NOTES
Langley Technical Monitor: Carey S. Buttrill

12a. DISTRIBUTION/AVAILABILITY STATEMENT
Unclassified–Unlimited
Subject Category 08 Distribution: Nonstandard
Availability: NASA CASI (301) 621-0390

12b. DISTRIBUTION CODE

13. ABSTRACT ***(Maximum 200 words)***

This report describes the activities and findings conducted under contract NAS1-9858-71 with NASA Langley Research Center. Subject matter is the investigation of suitable flight control design methodologies and solutions for large, flexible high-speed vehicles. Specifically, methodologies are to address the inner control loops used for stabilization and augmentation of a highly coupled airframe system possibly involving rigid-body motion, structural vibrations, unsteady aerodynamics, and actuator dynamics. Techniques considered in this body of work are primarily conventional-based, and the vehicle of interest is the High-Speed Civil Transport (HSCT). Major findings include 1) current aeroelastic vehicle modeling procedures require further emphasis and refinement, 2) traditional and nontraditional inner loop flight control strategies employing a single feedback loop do not appear sufficient for highly flexible HSCT class vehicles, 3) inner loop flight control systems will, in all likelihood, require multiple interacting feedback loops, and 4) Ref. H HSCT configuration presents major challenges to designing acceptable closed-loop flight dynamics.

14. SUBJECT TERMS
High-Speed Civil Transport; High-speed research; Inner loop; Stability augmentation; Handling qualities; Aeroelastic; Modeling

15. NUMBER OF PAGES
171

16. PRICE CODE
A08

17. SECURITY CLASSIFICATION OF REPORT	18. SECURITY CLASSIFICATION OF THIS PAGE	19. SECURITY CLASSIFICATION OF ABSTRACT	20. LIMITATION OF ABSTRACT
Unclassified	Unclassified	Unclassified	UL